Government of **Western Australia**
Department of **Mines and Petroleum**

RECORD 2015/9

REGOLITH CHEMISTRY OF THE BALANGGARRA AREA, NORTH KIMBERLEY

by
PA Morris, AJ Scheib, and N de Souza Kovacs



Geological Survey
of Western Australia

BALANGGARRA RANGERS

Government of Western Australia
Department of Mines and Petroleum

Record 2015/9

REGOLITH CHEMISTRY OF THE BALANGGARRA AREA, NORTH KIMBERLEY

by
PA Morris, AJ Scheib, and N de Souza Kovacs

Perth 2015

Geological Survey of
Western Australia

REFERENCE
The recommended reference for this publication is:

Morris PA, Scheib AJ and de Souza Kovacs N 2015, Regolith chemistry of the Balanggarra area, north Kimberley: Geological Survey of Western Australia, Record 2015/9, 142p.

National Library of Australia Card Number and ISBN 978-1-74168-641-8

Grid references in this publication refer to the Geocentric Datum of Australia 1994 (GDA94). Locations mentioned in the text are referenced using Map Grid Australia (MGA) coordinates, Zone 52. All locations are quoted to at least the nearest 100 m.

Published 2015 by Geological Survey of Western Australia
This Record is published in digital format (PDF) and is available online at <www.dmp.wa.gov.au/GSWApublications>.

Further details of geological products and maps produced by the Geological Survey of Western Australia are available from:
Information Centre
Department of Mines and Petroleum
100 Plain Street
EAST PERTH WESTERN AUSTRALIA 6004
Telephone: +61 8 9222 3459 Facsimile: +61 8 9222 3444
www.dmp.wa.gov.au/GSWApublications

Contents

Appendices

Appendices 1–4 (MS Excel spreadsheets of sample duplicate data) are provided separately on USB accompanying the printed Record, and as downloadable files accessed at <www.dmp.wa.gov.au/ebookshop>.

Plate

Plate 1. Interpreted regolith–landform geology of the Balanggarra area, north Kimberley

Figures

Bubble plot figures

Tables

Regolith chemistry of the Balanggarra area, north Kimberley

by

PA Morris, AJ Scheib, and N de Souza Kovacs

Abstract

Combined regolith sampling and regolith–landform mapping has shown that, unlike other areas of Western Australia, regolith is subordinate in volume to bedrock in the Balanggarra area of the north Kimberley. This, and the dominance of colluvium in the transported regolith component, means that regolith composition largely reflects that of the parent rock. For mafic volcanic rocks of the Carson Volcanics, comparison of regolith found in areas of outcrop with fresh bedrock shows that breakdown of phenocrysts results in the loss of labile components such as Mg, Na, K, Ba and Ni. Conversely, the enrichment in resistate phases such as rutile, zircon, monazite, and secondary oxide and sulfide minerals is reflected in enrichments of Th, Zr, Hf, Ti, As and Sb. Conversion of feldspar to clay minerals means that Si and Al can be conserved. These changes are less apparent for quartz-rich siliciclastic sedimentary rocks due to their chemical maturity.

When the effects of chemical weathering are understood, variations in bedrock chemistry can be tracked using the chemistry of regolith. This approach has identified changes in magma chemistry within the Carson Volcanics, whereby higher Mg, Cr, As and Ni in regolith from the base of the unit reflects eruption of less fractionated magma. Elevated rare earth elements in regolith from adjacent to regional linear structures could reflect post-regolith hydrothermal alteration, whereas strike-parallel regolith samples with elevated Zr and Hf in parts of the Pentecost Sandstone indicate derivation from a zircon-rich bedrock unit. A statistical analysis of regolith chemistry of samples from sedimentary rocks shows the higher level of chemical maturity of the oldest unit (King Leopold Sandstone), and the relative heterogeneity of units overlying the Carson Volcanics. This is interpreted in terms of a more local provenance of younger sedimentary units.

The chemistry of in situ and transported duricrust samples details the formation of bauxitic regolith at the tops of profiles over the Carson Volcanics at two localities. Transported duricrust units (ferricretes) found over sandstone units result from erosion of the Carson Volcanics and mixing with sandstone detritus, shown by variations in Th, Nb, Ti and V, and contrasting rare earth element (REE) patterns. The distribution of ferricrete indicates that it represents remnants of a sheet that extended over an area of >700 km^2.

KEYWORDS: geochemistry, rare earth elements, regolith, statistical analysis, stratigraphy, weathering

Introduction

The composition of regolith reflects the combined effects of parent rock composition and the extent of physical and chemical weathering, which are in turn affected by the distance of regolith transport (e.g. Eggleton, 2001; Scott and Pain, 2008; GSWA, 2013). In many parts of Western Australia, such as the Archean Yilgarn Craton, regolith forms a thick and contiguous cover, and far exceeds in area that of bedrock (Anand and Butt, 2010). In these areas, the physical and chemical characteristics of regolith show that, in the majority of cases, it has been transported and is genetically unrelated to the underlying bedrock. Thus, regolith is of limited use in predicting either the composition of the bedrock, or any bedrock-hosted mineralization.

In other areas, where chemical weathering and the distance of regolith transport is more limited, regolith retains more compositional information about the underlying bedrock, and in these cases, regolith is a useful sample medium to detect bedrock-hosted mineralization (e.g. Carver et al., 1987; Cornelius et al., 2008; Morris and Verren, 2001; Morris, 2013) and trace the distribution of underlying rock units (Morris, 2013). An important byproduct of understanding the extent of physical and chemical weathering responsible for the generation of regolith is a better understanding of climatic conditions under which regolith formed.

On the Kimberley Plateau of northern Western Australia, regolith is usually thin and found as isolated patches between areas of outcrop. Compositional changes in

regolith can be accounted for by changes in bedrock lithology: for example, quartz-rich sandy regolith is found on or close to siliciclastic sedimentary rocks; red-brown, more clay-rich regolith is found in areas of mafic igneous rocks. Thus, this area is well suited to examining the early stages of regolith formation and, with an understanding of these processes, how regolith chemistry can be used as a proxy for bedrock composition.

In June 2010, the Western Australia State government initiated the Kimberley Science and Conservation Strategy (KSCS), a five-year, multi-agency program to provide a better understanding of the Kimberley region, including the evolution of the Kimberley landscape, and the distribution of different soil (regolith) types. The Kimberley area is ideal to study regolith–bedrock relations, due to the close spatial relationship of regolith and bedrock and the small amount of regolith that has been transported any significant distance. An understanding of the composition and distribution of regolith in relation to parent rock not only contributes to knowledge of landscapes, but also provides information related to vegetation distribution. This in turn contributes to an understanding of weed and feral animal distribution, and helps with fire management. Accordingly, the Department of Mines and Petroleum (DMP) formulated a regolith sampling program in 2010, comprising compilation of an interpretive regolith–landform map showing the distribution of different regolith–landform units, and the collection and analysis of regolith from sites at a nominal density of one sample per 25 square kilometres. Over the 88 000 km^2 area of the KSCS, this equated to approximately 3500 samples. At the conclusion of the program in June 2014, a 1:100 000-scale interpreted regolith–landform map had been compiled (GSWA, 2014), and samples from 1019 sites have been collected from four sampling programs (Fig. 1). This record discusses the results from the first of these programs, carried out on part of Balanggarra country in the north Kimberley during August and September 2013.

Location and access

The Balanggarra project area (Fig. 2) lies in the northern part of the ASHTON[1] 1:250 000-scale (SE52-9) map sheet and the southern part of the DRYSDALE–LONDONDERRY 1:250 000-scale map sheet (SD52-9 and part of SD52-5). The largest permanent settlement in the project area is at Kalumburu, which has a population of about 400. Three smaller communities are found to the north of Kalumburu, at Honeymoon Beach, Pago, and McGowan Island. Carson River station is uninhabited.

Vehicle access to Kalumburu is via the unsealed Gibb River – Kalumburu Road, which is passable in the April–November dry season, but frequently flooded and inaccessible during the wet season from December to March. Supplies to Kalumburu are transported by road and by a fortnightly barge service from Darwin. There is also an airstrip suitable for light aircraft.

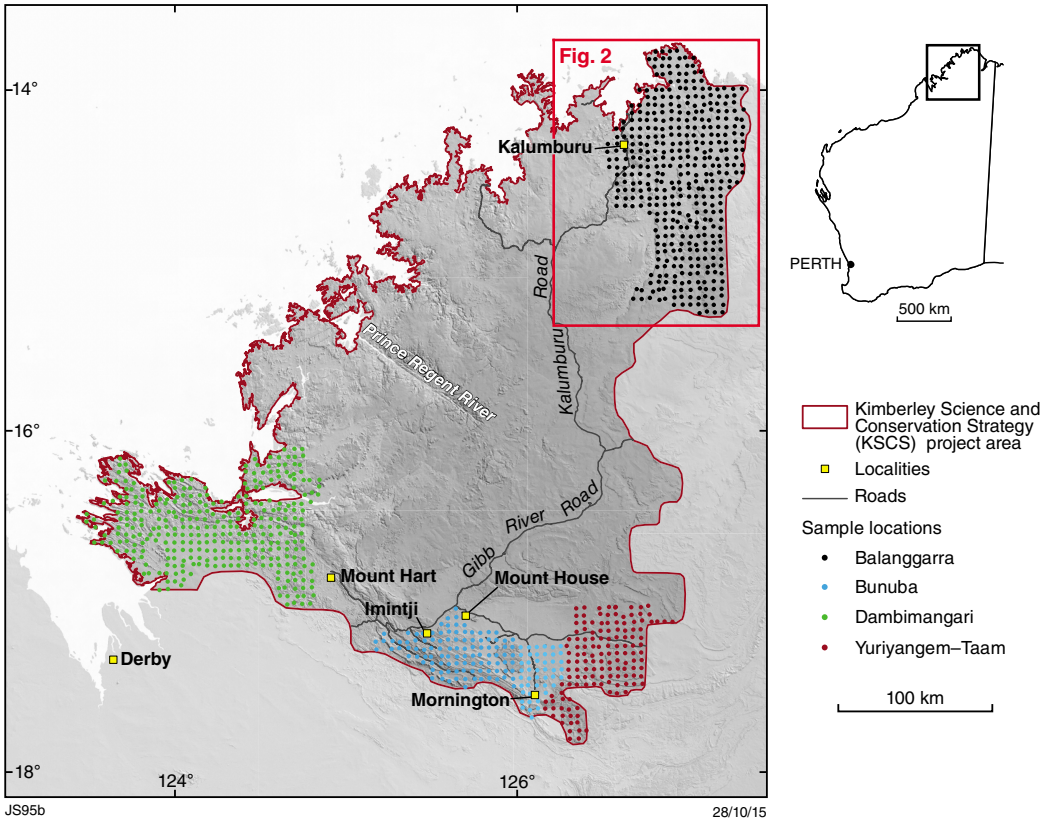

Figure 1. Locations of the four regolith sampling programs (Balanggarra, Bunuba, Yuriyangem–Taam, Dambimangari) carried out by GSWA as part of the Kimberley Science and Conservation Strategy (KSCS) program

1 Map names in small capitals refer to 1:250 000-scale Geological Series maps, unless otherwise specified.

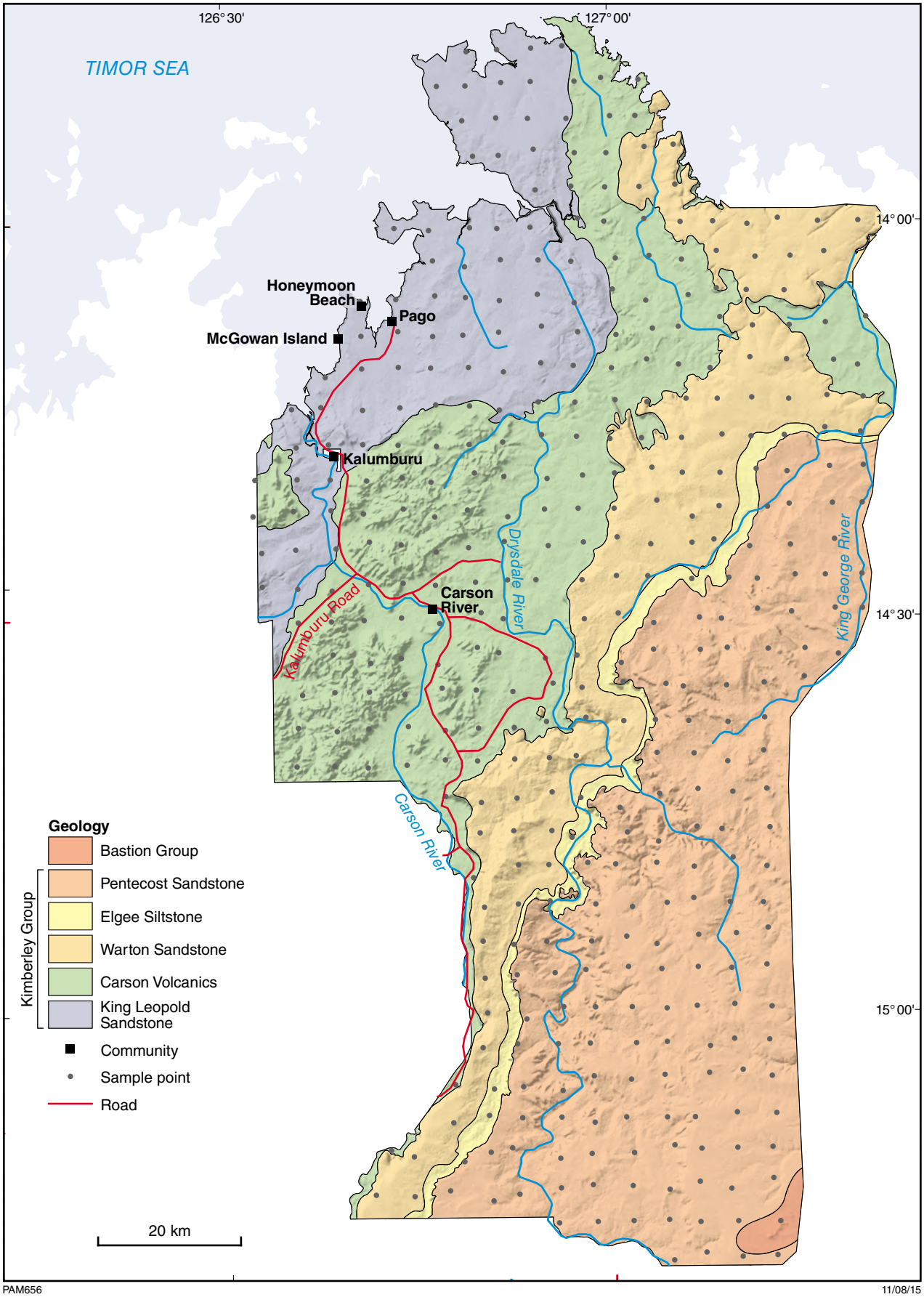

Figure 2. Extent of the Balanggarra regolith sampling program, showing the 407 sample sites, and 1:500 000-scale interpreted bedrock geology (GSWA, 2014) overlain on a digital elevation model (DEM)

Climate and vegetation

Bureau of Meteorology <www.bom.gov.au> climate data for the period 1941–2005 for Kalumburu show an average maximum temperature of 34.3°C, and an average minimum temperature of 20.7°C. November has the highest average maximum temperature of 37.1°C, and July the lowest average minimum temperature of 14.1°C. The average annual rainfall is 1209 mm, with most (average of 310 mm) falling in January.

Vegetation is in large part controlled by geology. The project area is characterized by grassy areas with scattered trees. Of the two eucalypt associations discussed by Gellatly and Sofoulis (1969), *Eucalyptus tectifolia* and *Eucalyptus grandifolia* are found on more iron- and magnesium-rich soils derived from volcanic rocks, whereas *Eucalyptus tetrodonta* and *Eucalyptus miniata*, along with Cypress pine (*Callitropsis intratropica*) and soft spinifex (*Triodia pungens*), are found on more silica-rich sandy soils over sandstones. Both associations have areas of cane grass, and drainages support pandanus, paperbarks, and boabs. Estuaries and mudflats have stands of mangroves (Derrick, 1968).

Geomorphology

On the Kimberley Plateau, the topography from the central part of the north Kimberley area in the vicinity of Mt Hann (Fig. 1) slopes gently northwards, but the drainage is broadly radial, although joints — such as the NW–SE joint system that controls the course of the Prince Regent River (Fig. 1) — faults and folds, along with rock hardness, strongly influence the drainage pattern. The geomorphology of the north Kimberley area has been discussed in detail by Stewart et al. (1960) who identified six geomorphological units, three of which are found over areas of volcanic rocks, two over areas of sandstone, and one corresponding to recent depositional plains along the coast. Speck (1960) discussed the broader Kimberley area in terms of land systems.

The three geomorphological units of Stewart et al. (1960) over areas of mafic volcanic rocks are found in the central part of the Balanggarra project area. Lateritic plains and cappings (corresponding to Speck's (1960) Foster land system) are remnants of an extensive immature laterite surface, which was elevated in the late Cenozoic or Pleistocene and then dissected. Rounded hills with little laterite cover make up more-dissected plateaus developed on volcanic rocks, and comprise the second geomorphic division. These are areas of more advanced erosion, and dendritic drainage is common (e.g. Napier land system). Continued erosion has resulted in even more subdued topography, characterized by low hills. This third geomorphic division — erosional plains on volcanic rocks — represents complete removal of the Cenozoic land surface, and has resulted in the development of thicker more mature soils (e.g. Barton, Kennedy and Isdell land systems).

One of the two geomorphic units recognized over sedimentary rocks — dissected sandstone plateaus formed on well-jointed and weakly folded sandstone — has been divided into three subunits by Stewart et al. (1960). These are similar to the three geomorphic units over volcanic rocks described above. The first subunit consists of gently undulating undissected plateaus (e.g. Pago land system) which are similar to areas of laterite on volcanic rocks, but the quartz-rich composition of the sandstone means that laterite is less well developed. The second subunit results from erosion along joint plains and removal of any laterite, producing mature dissected sandstone plateaus, often with steep gorges (Buldiva land system). The third subunit is erosional plains, on which Conzoic cover has been completely removed by erosion. The second geomorphic unit includes cuestas and structural plateaus (also part of the Pago land system) which are developed on gently dipping sandstones and shales (e.g. Warton Sandstone).

Less common are depositional plains typical of the Carpentaria land system, which are confined to coastal areas.

Stewart et al. (1960) have argued that the once-continuous laterite surface of the north Kimberley is equivalent to the Australian surface of King (1949) or the Miocene surface of David (1950), although the precise age of laterite is unknown. In a number of places, dissection of this surface to the bottom of some gorges is close to 200 m, indicating significant structural control on landscape development. When dissection had almost reached its greatest expression, an episode of submergence occurred, resulting in drowning of valleys and formation of a highly indented coastline.

Bedrock geology

The Balanggarra project area is composed of Paleoproterozoic sedimentary and volcanic rocks of the Kimberley Group, with limited outcrop of the overlying Bastion Group (Fig. 2; Table 1). The Kimberley Group is a conformable succession which strikes roughly north-northeast and dips at about five degrees to the east-southeast. The geology of the Kimberley Group in the Balanggarra area was first described in detail by Derrick (1968) on Ashton, and by Gellatly and Sofoulis (1969) on Drysdale–Londonderry. Kimberley Group siliciclastic sedimentary rocks are dominated by quartz-rich sandstones, with subordinate siltstone (locally calcareous), mudstone, and conglomerate. The majority of the units are current bedded, providing information on provenance direction (Derrick, 1968; Gellatly and Sofoulis, 1969; Sheppard et al., 2012; Hollis et al., 2014).

The King Leopold Sandstone, the lowest unit in the Kimberley Group, is a medium- to coarse-grained, poorly bedded, quartz-rich sandstone with thin units of pebbly quartz sandstone (Derrick, 1968). It covers 1559 km^2 or 15% of the project area (Table 1). On Ashton, Derrick (1968) discussed a thin, more mica-rich unit containing accessory amounts of tourmaline and zircon, along with epidote and feldspar. Gellatly and Sofoulis (1969) noted a southwards decrease in grain size of this unit. Current bedding indicates a provenance from the north and northwest. The unit forms dissected plateaus where drainage lines are in part controlled by joints in the bedrock (Fig. 3).

Table 1. Summary of stratigraphy of the Balanggarra project area in terms of lithologies, and thickness and area of lithological units. Also shown is the number of regolith samples from each unit. Thickness of King Leopold Sandstone is a minimum

Unit	*Lithology*	*Maximum thickness (metres)*	*Area (square kilometres)*	*No. of regolith samples*	*Reference*
BASTION GROUP	Siltstone and mudstone, with less common quartz sandstone and feldspathic sandstone	20	52	1	Derrick (1968)
KIMBERLEY GROUP					
Pentecost Sandstone	Dominantly quartz sandstone, but divided lithologically into three members (lower quartz sandstone; middle glauconitic, quartz and feldspathic sandstone; upper quartz sandstone). Cross-bedding common	760	3488	141	Derrick (1968); Gellatly and Sofoulis (1969); Sheppard et al. (2012)
Elgee Siltstone	Siltstone, mudstone and shale with interbedded quartz and quartz and feldspathic sandstone. Siltstones are calcareous	135	320	10	Derrick (1968); Gellatly and Sofoulis (1969); Sheppard et al. (2012)
Warton Sandstone	Quartz sandstone and less common feldspathic sandstone and conglomerate. Commonly cross-bedded	525	1850	73	Derrick (1968); Gellatly and Sofoulis (1969); Sheppard et al. (2012)
Carson Volcanics	Fine grained, weakly porphyritic, locally amygdaloidal, mafic volcanic and volcaniclastic rocks; rare pillow lava. Local sandstone beds. Locally epidotized	580	2896	116	Derrick (1968); Gellatly and Sofoulis (1969); Sheppard et al. (2012)
King Leopold Sandstone	Well-sorted, thick-bedded quartz sandstone; less common conglomerate and silty sandstone	1070 (base not exposed)	1559	66	Derrick (1968); Gellatly and Sofoulis (1969); Sheppard et al. (2012)

The Carson Volcanics, which overlies the King Leopold Sandstone, covers an area of about 2896 km^2, or 28% of the project area. The unit is dominated by fine-grained, blue to dark-grey, weakly porphyritic mafic volcanic rocks. Some flow units are columnar jointed, but pillow basalt and peperite are locally developed. Intercalated volcaniclastic and sandstone units, up to 9 m thick, are found on DRYSDALE–LONDONDERRY (Derrick, 1968). Some flow units are epidotized, and amygdales contain calcite, quartz, zeolite, and chalcopyrite. Macroscopic features of this unit indicate dominantly subaerial eruption, but pillow lavas and the close spatial association with stromatolite horizons are consistent with localized submarine eruption.

The overlying Warton Sandstone is mainly medium- to coarse-grained, light-coloured, well-sorted quartz-rich sandstone. It occupies an area of 1850 km^2 or 18% of the project area. Towards the base and top of the unit, the sandstone is more feldspathic (Gellatly and Sofoulis, 1969). The unit is commonly cross-bedded, indicating derivation from the west and northwest, although a provenance from the northeast is indicated for lower parts of the succession. Derrick (1968) discussed intraformational conglomerate on ASHTON, consisting of sandstone and siltstone clasts in a muscovite-bearing sandstone matrix.

The Elgee Siltstone is a thin unit of 320 km^2 (3% by area). Quartz-rich rocks are subordinate to red-brown siltstone, mudstone, and shale, although sandstone is more common towards the top of the unit (Gellatly and Sofoulis, 1969). Derrick (1968) noted that the unit is locally calcareous on ASHTON. Current bedding in sandstone units indicates a provenance from the northwest, and the ratio of siltstone to sandstone decreases westwards. The occurrence of mud cracks, probable high ferric iron content, rain drop impressions, and calcareous horizons are consistent with a shallow water or intertidal setting.

The Pentecost Sandstone is the most extensive unit within the project area, covering almost 3500 km^2 or 34%. On ASHTON, Derrick (1968) divided the unit into a lower, middle and upper part. The lower part (400 m thick on DRYSDALE–LONDONDERRY; Gellatly and Sofoulis, 1969) is composed of medium-grained quartz sandstone that is massive and cross-bedded, and locally overturned. The middle division (335 m thick on DRYSDALE–LONDONDERRY) is also composed of massive quartz sandstone, with interbeds of feldspathic sandstone. At the base of this division are Cu-rich chloritic, and glauconitic sandstone and siltstone. Current bedding indicates a general provenance from the north. On DRYSDALE–LONDONDERRY, the transition from the middle to the upper division is marked by a change from medium- to coarse-grained sandstone. This division reaches a thickness of approximately 30 m (Gellatly and Sofoulis, 1969).

The Bastion Group unconformably overlies the Kimberley Group in the south of the project area, where it occupies about 52 km^2. According to Derrick (1968), the Bastion Group on ASHTON comprises the lowermost Mendena Formation, a poorly exposed siltstone and mudstone.

Hollis et al. (2014) have summarized the depositional setting of the Kimberley Group in terms of a shallow, partly enclosed sea. Sedimentary structures within siliciclastic units, and evidence for both submarine and subaerial eruption along with units of stromatolites in the Carson Volcanics, indicate shallow water (tidal) conditions.

PAM679 11.08.15

Figure 3. Subhorizontal King Leopold Sandstone on the north coast of the Balanggarra project area. Note the joint control on drainage

Geochronology

A SHRIMP U–Pb age for a felsic volcanic rock in the underlying Speewah Group (Page and Sun, 1994) provides a maximum depositional age for the Kimberley Group of 1834 ± 3 Ma. This age is in agreement with a SHRIMP U–Pb zircon age of 1835 ± 3 Ma for the underlying Valentine Siltstone (Speewah Group) reported by Sheppard et al. (2012). The Hart Dolerite intrudes the Kimberley Group up to the Warton Sandstone, providing a minimum depositional age for the lower part of the succession. A weighted mean age of 1797 ± 11 Ma for zircon and baddeleyite from the Hart Dolerite (Sheppard et al., 2012) is a good estimate of the timing of crystallization. However, as Sm–Nd isotope data for the upper part of the Hart Dolerite are different to samples from lower in the unit, it is uncertain if this 1797 Ma age can be applied for the whole unit, or those age data can be reliably used to constrain the timing of deposition of the whole Kimberley Group. Recent work by Orth (2015) has identified mafic sills within the upper part of the Kimberley Group, although whether these sills are part of the Hart Dolerite or another intrusive event (e.g. the c. 500 Ma Kalkarinji Large Igneous Province [LIP]; Hanley and Wingate, 2000) is currently unknown. A U–Pb zircon age of 1740 ± 6 Ma for the Wotjulum Porphyry provides an upper limit for Kimberley Group deposition (Sheppard et al., 2012). Based on this age, the upper part of the Kimberley Group may be about 50 Ma younger (Hollis et al., 2014).

U–Pb dating of detrital zircons from the Warton Sandstone (McNaughton et al., 1999) produced a maximum depositional age of 1786 ± 14 Ma. The same authors also reported SHRIMP U–Pb ages for xenotime in the Warton and Pentecost Sandstones respectively of 1704 ± 7 and 1704 ± 14 Ma, respectively. Their assertion that the xenotime was diagenetic implied a break of about 85 Ma between the lower and upper parts of the Kimberley Group (Sheppard et al., 2012). McNaughton et al. (1999) also reported a range of $^{207}Pb/^{206}Pb$ xenotime ages ranging from 1721 to 1459 Ma, which Sheppard et al. (2012) interpreted as indicating either open-system behaviour or crystallization over a long time period (i.e. post-depositional). Thus, these phosphate dates cannot be reliably used to assess the timing of deposition of the Kimberley Group.

The age of the Bastion Group is poorly constrained. It overlies the Hart Dolerite, which provides a maximum depositional age of 1797 Ma, and underlies the Kalkarinji LIP (Hanley and Wingate, 2000), which provides a minimum age of c. 500 Ma.

Mineralization

There are currently no operating mines in the Balanggarra project area, but several mineral deposits and prospects are recorded in DMP's MINEDEX database <www.dmp.wa.gov/minedex>. Copper mineralization has been recorded at Londonderry near the basal contact of the Carson Volcanics with King Leopold Sandstone, and lead mineralization at Couchman Range (Fig. 4) is near the contact of the Carson Volcanics and Warton Sandstone. Diamond occurrences are found in the Warton and Pentecost Sandstones, and the Elgee Siltstone. The area has been explored for bauxite, which is mostly found on plateaus overlying the Carson Volcanics.

Copper mineralization is known from parts of the Carson Volcanics, Elgee Siltstone and Pentecost Sandstone in the project area (Derrick, 1968; Marston, 1979; Gellatly and Sofoulis, 1969), as well as the Warton Sandstone and Hart Dolerite elsewhere in the Kimberley region (Marston, 1979). Most occurrences are stratiform, with less common mineralization in quartz veins (Marston, 1979). Chalcopyrite is found in vesicles in the Carson Volcanics (Derrick, 1968), and malachite and copper sulfides are found in veins, fractures and along bedding planes in sedimentary rocks (Marston, 1979). Derrick (1968) reported that copper mineralization is more prominent in the lower part of the Carson Volcanics, and Marston (1979) noted that copper sulfides and carbonates were found in the lower basaltic flows.

In the Warton Sandstone, copper mineralization is related to chert and siltstone, as disseminated malachite and ferruginous nodules. Fine-grained, chlorite-rich sedimentary rocks of the Elgee Siltstone and Pentecost Sandstone contain malachite (Derrick, 1968) associated with graphite, a single assay of which returned 0.36% copper. The bulk of known copper mineralization in the Elgee Siltstone is found towards the base of the unit (Teronis Member; Marston, 1979), although this unit has not been recorded on Drysdale–Londonderry. Copper concentrations reach between 200 and 350 ppm in this unit, and are of syngenetic or diagenetic origin according to Marston (1979). Copper mineralization in the Pentecost Sandstone is also found in shales and siltstones, as malachite on bedding planes and fractures.

Bauxite is found on plateaus overlying the Carson Volcanics. Some deposits are up to 4 m thick and are characterized by gibbsite, boehmite, kaolinite, hematite and goethite (Derrick, 1968; Gellatly and Sofoulis, 1969).

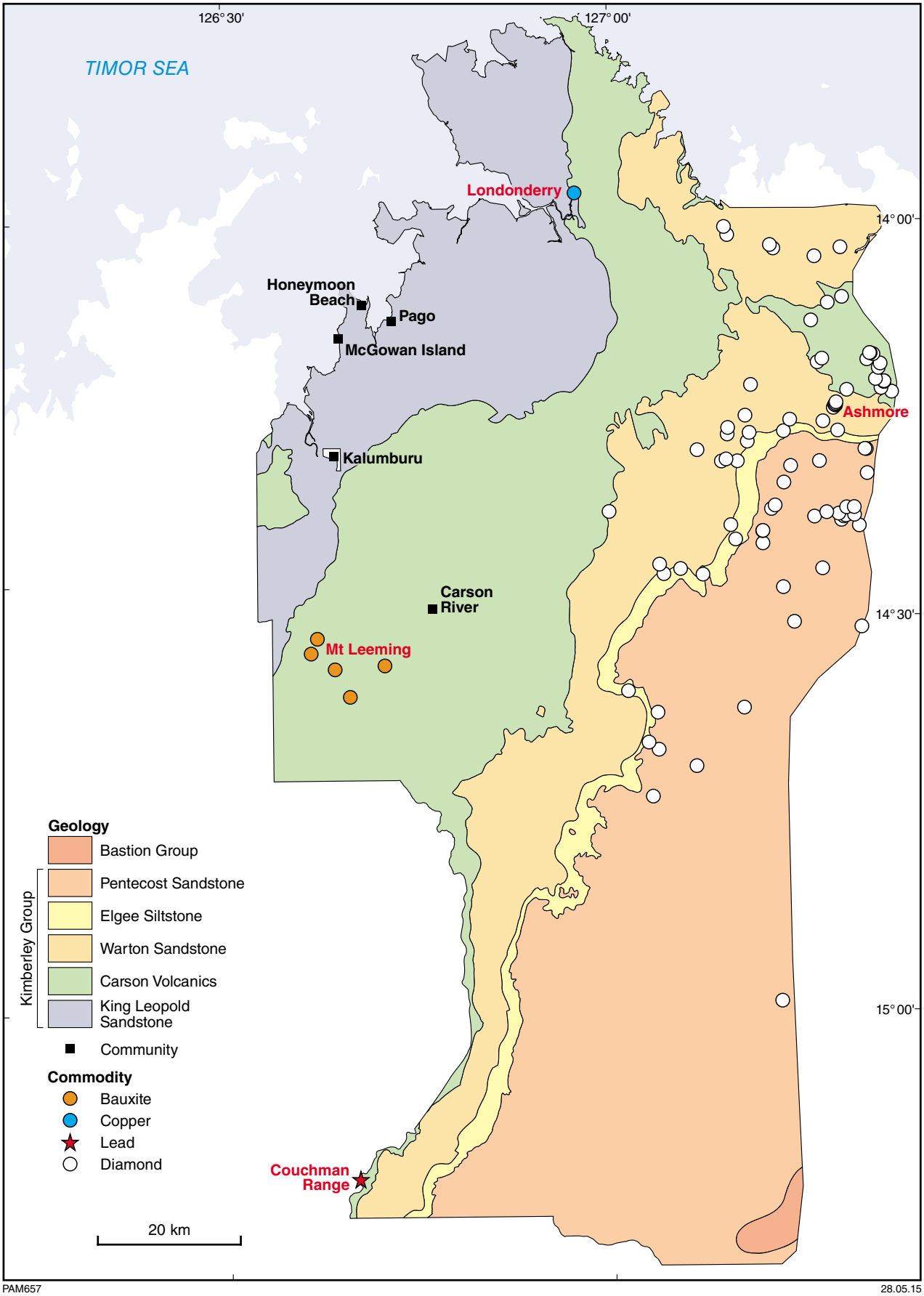

Figure 4. Bauxite, copper, and lead mineralization, and diamond occurrences, from DMP's MINEDEX database

Samples have up to 63% available alumina with low contents of TiO_2 (3.7 wt%) and reactive silica (3.12 wt%; Derrick, 1968). Field observations, chemistry, and the occurrence of ferruginous cores to pisolites in bauxite deposits indicate that bauxite resulted from chemical weathering of the Carson Volcanics. Gellatly and Sofoulis (1969) noted that in some areas of bauxite mineralization, the high iron content of duricrust in the southwest of DRYSDALE–LONDONDERRY could be examined in terms of iron ore, with up to 45 wt% Fe recorded in some laterite.

The Couchman Range bauxite deposit was discovered by an AMAX subsidiary in 1965 (Ruddock, 2003), but deposits were found to be subeconomic. Exploration for bauxite has been carried out at the Mt Leeming prospect, south of Kalumburu (Fig. 4). BHP noted high available Al_2O_3 (28–49%) and high reactive silica (12–37%), but the project was discontinued (Ruddock, 2003). Summers (2005) reported an indicated resource of 7.2 million tonnes @ 29.9 wt% available Al_2O_3 and 10.8 wt% reactive SiO_2 using a 25 wt% Al_2O_3 cut-off grade.

Eighty-four diamond occurrences are recorded in the MINEDEX database, most of which are alluvial (Ruddock, 2003). These are in the Warton Sandstone, Elgee Siltstone, and Pentecost Sandstone in the northeast of the project area. The only extant mining lease in the project area is approximately 70 km east of Kalumburu (Fig. 4). Here, North Australian Diamonds Ltd described a kimberlite-related diamond resource, referred to as the Ashmore Diamond Project (Kammermann, 2008), comprising diamond-bearing kimberlite pipes intruding the Warton Sandstone, although Kammermann (2008) argued that the 'pipes' represented erupted parts of a regional dyke suite. Diamond indicator minerals in the sedimentary infill of the pipes are consistent with the weathering of buried kimberlite (Kammermann, 2008). A combined inferred resource of 2 458 600 tonnes grading at 6.8 cpht for a total of 166 800 carats was estimated from four pipes.

Regolith–landform mapping

The Balanggarra 1:100 000-scale interpreted regolith–landform map is part of a map layer compiled for the Kimberley Science and Conservation Strategy (GSWA, 2014). The Balanggarra regolith–landform map (Fig. 5; see also Plate 1) shows the distribution of different regolith types in a landform context, utilizing the GSWA classification scheme and approach to regolith mapping (GSWA, 2013). This scheme, which is based on the RED (residual, erosional, depositional) scheme of Anand et al. (1993), uses a primary code to identify the landform, a secondary code for regolith composition, and a tertiary code for the parent rock, or cement type. Each of the primary regolith regime codes (*R* – residual or relict, *X* – exposed rock (thin regolith; corresponds to the 'E' of Anand et al., 1993), *D* – depositional), and secondary and tertiary codes can be further subdivided using a series of subscripts. Due to the diversity of depositional regolith types, it has been subdivided further into nine codes.

Identification of different regolith–landform units was carried out using published geological maps (Derrick, 1968; Gellatly and Sofoulis, 1969), remotely sensed data, ground observations from GSWA's WAROX database, and site observations made during the regolith sampling program. Primary (landform) codes were determined using orthophotos, Google Earth imagery, and digital elevation models (DEM). Secondary and tertiary codes (those related to regolith composition) were determined using existing 1:250 000-scale geological maps (Gellatly and Sofoulis, 1969; Derrick, 1968), Landsat TM, radiometric, aeromagnetic, and ASTER imagery.

Residual–relict regime regolith (*R*)

In the GSWA regolith classification scheme, the primary code *R* corresponds to either regolith developed in situ by weathering of the underlying bedrock (residual regolith), or the eroded remnants of a previously more extensive regolith unit (relict regolith). The latter represents regolith that may be in situ, but more likely has been transported from elsewhere and deposited. If this is the case, then regolith is genetically unrelated to the underlying bedrock.

Remotely sensed data are particularly useful in terms of mapping the type and extent of residual and relict units, especially when different kinds of images are used concurrently. Residual regolith units have elevated responses for Th and U in a ternary KTU (K – potassium, T – thorium, U – uranium) image, and in Th imagery, due to both Th and U being found in higher concentration in resistate minerals such as monazite. The extent of residual units can be further checked using the AGSO Landsat image, where iron- and silica-rich regolith appear in shades of green and blue, respectively. The ASTER ferric oxide content image can separate ferruginous and aluminous duricrust, as the latter appears more blue due to a lower iron content.

In the Balanggarra project area, residual regolith is more abundant (approximately 10% by area) compared to relict units (<1%; Table 2). The majority of both residual and relict units are found over siliciclastic sedimentary rocks. Residual sand (*Rs*, 6% by area) results from the in situ weathering of quartz-rich sedimentary rocks (Plate 1). Less common residual iron-rich material over sandstone units (R_rfs) consists of iron-rich lag and ferruginized sandstone fragments, covering about 2% of the project area and accounting for two samples. This unit could be derived by weathering of the underlying sandstone, but is more likely to be related to a more extensive area of ferruginous indurated gravel or ferricrete coded as R_tf (four samples). The presence of variably weathered and ferruginized sandstone clasts in an iron-rich matrix is consistent with R_tf being a transported unit, with the iron-rich component derived from the adjacent Carson Volcanics. This unit occupies an area of about 100 km^2 on the King Leopold Sandstone north of Kalumburu.

Residual regolith over mafic volcanic rocks of the Carson Volcanics can be subdivided into ferruginous (R_rfv_b; eight samples) and aluminous ($R_rx_av_b$; 1 sample) varieties, both of which are usually found as mesas and cappings

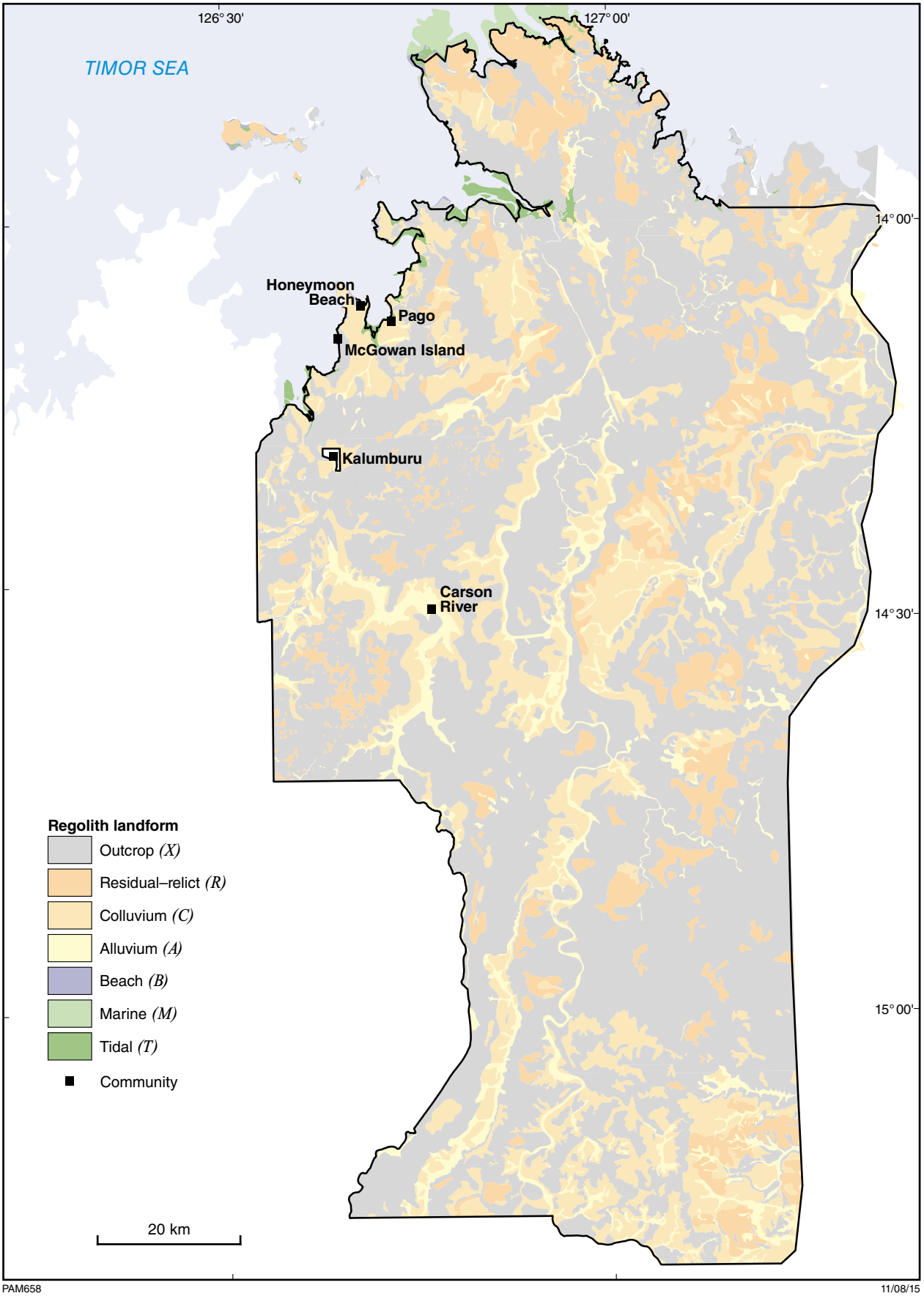

Figure 5. Interpreted regolith–landform map of the Balanggarra project area. To display the coverage at this scale, only primary regolith–landform units are shown. A more detailed version of the map is available as GSWA (2014) and included as Plate 1.

on hills. $R_r fv_b$ is red-brown, nodular, iron-rich material typically containing ferruginized mafic clasts, whereas $R_r x_a v_b$, commonly found in the uppermost part of regolith profiles, is characterized by gibbsite-rich layers up to three metres thick composed of nodular pisoliths in a yellow-brown goethite and siliceous matrix.

Exposed regime regolith (*X*)

Regolith in areas of outcrop (Fig. 5) is termed exposed regime regolith (*X*) in the GSWA regolith classification scheme. It forms a thin and discontinuous cover, and accounts for 60% of the Balanggarra project area, and 282 or 69% of regolith samples (Table 2). This regolith type is generally poorly sorted, with angular to subangular clasts of the underlying bedrock (some of which may be ferruginized) in a sandy matrix, although over the Carson Volcanics, the regolith is more clay rich.

Regolith derived from siliciclastic sedimentary rocks (Xqs_s) is the most common type, accounting for 42% by area and 196 samples (Table 2). Finer grained and more micaceous regolith ($Xx_i s_m$) is found over the Elgee Siltstone and Bastion Group, but it is of limited extent (<1% by area and only three samples). Exposed regime regolith derived from ferromagnesian rocks of the Carson Volcanics (Xmv_b) accounts for 18% of the area and 83 samples.

Depositional regime regolith (*D*)

Colluvium (*C*)

Colluvium is found throughout the project area, accounting for 21% of the area and 66 samples (Table 2). Quartz-rich colluvium derived from siliciclastic sedimentary rocks (Cqs) is the most common type, found in 16% of the project area and accounting for 46 samples. Typically, it is grey-brown to yellow-orange brown, fine- to medium-grained quartz-rich sand, supporting sandstone clasts, some of which are ferruginized. It forms on low-angle slopes and occupies topographic depressions. Small areas of mica-rich colluvium ($Cx_i s$) derived from siltstones and fine-grained sandstones occupy less than 1% by area and two samples. It comprises grey-yellow to red-brown silty sand found downslope from outcrops of the Elgee Siltstone and Bastion Group.

Iron- and magnesium-rich colluvium derived from the Carson Volcanics (Cmv_b) accounts for approximately 5% of the project area and 18 samples. It is found on very low angle slopes and pediplains, as red-brown to yellow-brown silty clay and sand with ferruginous nodules and pisoliths.

Alluvial/fluvial regolith (*A*)

Alluvial/fluvial regolith is found in or adjacent to drainages. It covers approximately 7% of the project area and accounts for 20 samples. Two types have been mapped: an undivided alluvium (*A*), and black soil, also known as gilgai ($A_a c_b$). Undivided alluvium (*A*) accounts for almost all of the mapped alluvial/fluvial regolith and for all regolith samples (Table 2). It consists of varying proportions of locally derived clay, sand and gravel. Alluvium in areas of sandstone is composed of quartz-rich sand, gravel, and lithic fragments, whereas alluvial deposits in areas of basalt comprise variable amounts of gravel, sand, silt and clay, ferruginous pisoliths, duricrust fragments, and basalt clasts.

Gilgai ($A_a c_b$), consists of grey, swelling and cracking smectitic clay derived by weathering of mafic rocks. It is found on floodplains on or near to the Carson Volcanics. Although this unit is common elsewhere in the Kimberley area, in the Balanggarra project area, it covers only four square kilometres (Table 2; Plate 1), which in part reflects the difficulty in depicting the unit at 1:100 000 scale. No samples were collected from this unit.

Coastal wave-dominated (*B*), coastal tide-dominated (*T*), and marine regolith (*M*)

Coastal wave-dominated (*B*), coastal tide-dominated (*T*) and marine (*M*) regolith–landform units are restricted to the north of the project area, where they account for about 2% by area and one sample.

Coastal wave-dominated units include beach (B_b) and foredunes (B_d) bordering exposures of the King Leopold and Warton Sandstones. Coastal tide-dominated regolith is represented by tidal flats (T_f; one sample), supratidal flats (T_u), and mangroves (T_m), which are found in estuaries, rias and tidal inlets. These units are characterized by silt and sand, and localized surface salt deposits.

Marine regolith (*M*) refers to offshore marine deposits, and accounts for approximately 1% of the project area. Submerged rock outcrops in coastal areas (M_r) account for <1% by area.

Summary

In the Balanggarra project area, outcrop (*X*) and residual–relict regime regolith (*R*), which is derived by in situ weathering of the underlying bedrock (i.e. is residual), account for over 70% of regolith by area. Colluvium, the dominant type of depositional regolith, is usually found adjacent to areas of outcrop, and accounts for a further 20% by area. The small amount of alluvial/fluvial regolith (7% by area), and lack of sheetwash reflects the rugged topography and short transportation distances of regolith.

Regolith profiles are better developed on the Carson Volcanics, due to its propensity for chemical weathering. Residual ferruginous and aluminous duricrust, found as mesas and capping hills, are interpreted as remnants of a once more extensive land surface. The weathering of this unit has resulted in a broad and subdued land surface that developed by in situ weathering of the underlying bedrock. In contrast, the chemical maturity of quartz-rich siliciclastic rocks makes them less prone to chemical weathering, resulting in rugged plateaus, cliffs and gorges. Regolith on these rocks is typically thin, with few well-developed profiles.

Table 2. Summary of regolith–landform units in the Balanggarra project area in terms of onland area and number of regolith samples

Regolith–landform code	*Area (km²)*	*Area (%)*	*Number of regolith samples*	*Regolith samples (%)*
Residual				
$R_r fs$	171	1.6	2	0.5
$R_r fv_b$	76	0.7	8	2.0
$R_r x_a v_b$	92	0.9	1	0.2
R_s	667	6.3	23	5.7
Relict				
$R_t f$	99	0.9	4	1.0
Total	**1 105**	**10.4**	**38**	**9.4**
Exposed				
$Xx_i s_m$	75	0.7	3	0.7
Xmv_b	1 886	17.9	83	19.7
Xqs_s	4 362	41.5	196	45.8
Total	**6 323**	**60.2**	**282**	**69.3**
Depositional				
	Colluvial			
$Cx_i s$	33	0.3	2	0.5
Cmv_b	493	4.7	18	4.4
Cqs	1 644	15.6	46	11.3
Subtotal	**2 170**	**20.6**	**66**	**16.2**
	Alluvial/fluvial			
A	730	6.9	20	4.9
$A_a c_b$	4	<0.1	0	0.0
Subtotal	**734**	**7.0**	**20**	**4.9**
	Coastal – wave dominated			
B_b	13	0.1	0	0.0
B_d	2	<0.1	0	0.0
Subtotal	**15**	**0.1**	**0**	**0.0**
	Coastal – tide dominated			
T_f	2	<0.1	1	0.3
T_m	71	0.7	0	0.0
T_u	12	0.1	0	0.0
Subtotal	**85**	**0.8**	**1**	**0.3**
	Marine			
M_r	79	0.8	0	0.0
Total	**3 083**	**29.3**	**87**	**21.4**
Overall total	**10 511**		**407**	

Ferruginous duricrust (R_1f) developed over the King Leopold Sandstone northwest of Kalumburu is more heterogeneous than iron-rich, in situ duricrust units developed over the Carson Volcanics. It consists of variably ferruginized siliciclastic sedimentary rock fragments, pisoliths, and ferruginous duricrust fragments, mostly in an iron-rich cement, indicating input from both the Carson Volcanics and King Leopold Sandstone. This unit is interpreted as weathered and transported Carson Volcanics material deposited on the adjacent sandstone. Other pockets of compositionally similar material elsewhere on the King Leopold Sandstone could mean that this unit once extended over several hundred square kilometres.

Regolith sampling

Assessment of heritage

During the planning of GSWA's sampling programs in the Kimberley area, meetings were held with a number of indigenous groups, either directly, or through the Kimberley Land Council (KLC). These meetings provided the opportunity for GSWA to explain the scope and outcomes of its program, and to ensure that regolith sampling would not adversely affect heritage. In December 2012, GSWA met with the Balanggarra Aboriginal Corporation in Kununurra to discuss regolith and rock sampling on part of Balanggarra country. Agreement was reached at this meeting that GSWA's program could proceed in the 2013 dry season, following satisfactory heritage assessment. An early part of this assessment involved examining the location of aboriginal heritage sites registered with the Department of Aboriginal Affairs, and relocating or excising proposed regolith sample sites. These revised sampling maps were then provided to the KLC and Balanggarra Aboriginal Corporation, and used as the basis for an on-country heritage assessment program immediately prior to regolith sampling. This helicopter-supported survey was carried out on Tuesday 20 and Wednesday 21 August 2013, involving four traditional owners and a KLC anthropologist. Following the survey, two sample sites to the north of the area were moved approximately one kilometre to the east, and one site in the northeast of the program area was excised.

Sample collection

Regolith sampling was carried out from Thursday 22 August to Wednesday 4 September 2013 using a Bell Jetranger helicopter based at Kalumburu (Fig. 2). Each sampling team consisted of a geologist, who recorded site information, and a field assistant, who collected the regolith sample.

Regolith was collected from 407 sites. At approximately every tenth site, a second sample of regolith (site duplicate) was collected from a location approximately one metre from the primary sample location (Fig. 6). At each site, a form was completed (Fig. 7, Table 3) recording the sample location, site characteristics (e.g. landform position, vegetation, sample depth), composition of the surface and downhole regolith, and composition of any nearby bedrock. Representative site photographs were also taken (Fig. 8a–d). To avoid surface contamination by animal droppings, organic material, etc., the surface cover was scraped off and, where possible, a hole was excavated to between 20 and 30 cm depth, from which the sample of regolith was collected using a small shovel. The majority of regolith samples were dry and unconsolidated, apart from a few clay-rich samples which were weakly aggregated. Individual samples weighed about 5 kg.

Figure 6. Example of a site duplicate. Site M3521, regolith in an area of outcrop, Warton Sandstone. (MGA 03451E 8451056N): a) sample site showing depth of excavation achieved; b) overview of the sample site landscape. Sample bag is 40 cm x 30 cm

BALANGGARRA SAMPLING PROGRAM

GSWA No		***Site No***	M
EASTING		***NORTHING***	

Sampler		Date		Time	

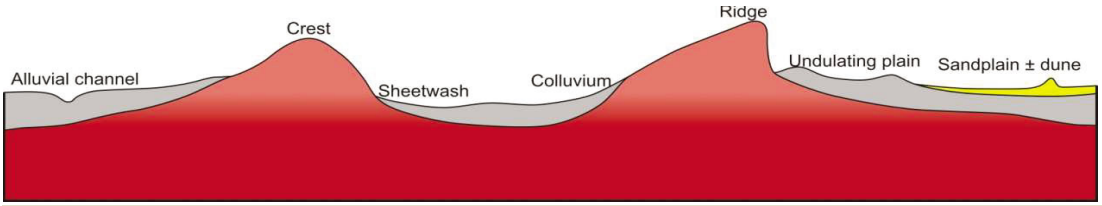

REGOLITH-LANDFORM					***R-L other***
Residual/relict	Outcrop	Colluvium	Sheetwash	Sandplain	
REGOLITH-COLOUR					***Colour-other***
Red	**Brown**	**Yellow**	**Orange**	**Grey**	
VEGETATION					
Spinifex	Eucalypt	Grass	Shrubs		

SURFACE REGOLITH					
%	Fe-rich	Al-rich	Lithic	Quartz	Other
Nodules/granules					
Sand					
Silt/clay			**N/A**	**N/A**	

DOWNHOLE REGOLITH					
%	Fe-rich	Al-rich	Lithic	Quartz	Depth-cm
Nod/grans					
Sand					
Silt/clay			**N/A**	**N/A**	

LITHIC MATERIAL					
%	Surface	Downhole	Outcrop	Dist (m)	Dirn (bearing)
Mafic					
Fg felsic					
Granitic					
Sedimentary					
Schistose					
Gneissose					
Vein quartz					
Other					

Secondary coating	Fe	Mn	Si	CO3	Other

Units nearby	Channel	Lake	Saprock	Saprolite	Other
Sample features	HCl reaction		Dry?	Damp?	
Photo taken?					

Comments

Figure 7. Sample form used for recording site information during the Balanggarra regolith sampling program. Terminology is summarized in Table 3.

Table 3. Description of fields in sample site form (Fig. 7) used for the Balanggarra regolith sampling program

Field	*Type*	*Description*	*Example*
GSWA No	Numeric	A unique number for samples held in the GSWA collection	213127
Site No	Text	Unique site identifier for collection of regolith sample	M3454
Easting	Numeric	GDA east coordinate for sample site	504438
Northing	Numeric	GDA north coordinate for sample site	6683431
Sampler	Text	Initials of the geologist who made the site observations	AS (Andreas Scheib)
Date	Text	Date on which the sample was collected	
Time	Numeric	Time at which the sample was taken (24-hour format)	
REGOLITH–LANDFORM	Text	Primary regolith–landform code (GSWA regolith classification scheme); the regolith within a 50 m radius of the sample site	
REGOLITH COLOUR	Numeric (text)	Colour of the regolith within a 50 m radius of the site. Predominant colour designated 1, with subordinate or modifying colours designated 2, 3, 4 etc. 'Colour-other' category allows text entry of other colours	Brown-red is designated red (1), brown (2), whereas red-brown is designated red (2) brown (1).
VEGETATION	Numeric (text)	Vegetation types shown in decreasing order of abundance from 1 (most abundant) to 4, 5 etc. (least abundant). Broad groupings only shown. 'Eucalypt' used for all trees. Grass and shrub types undivided	
SURFACE REGOLITH	Numeric/text	Percentage values of components seen within a 50 m radius of the designated sample site. Clay is designated as Lithic – Silt/clay unless otherwise shown. 'Other' allows text entry of unlisted components. Estimates probably accurate to within 10%. Trace amounts shown as 2%. If any Lithic component is listed for Nodules/ granules, then rock type(s) must be entered in LITHIC MATERIAL part of form	
DOWNHOLE REGOLITH	Numeric/text	As for SURFACE REGOLITH. Depth-cm is maximum of depth of sampling hole (which may be depth to bedrock). Estimates probably accurate to within 10%. Trace amounts shown as 2%. If any Lithic component is listed for Nodules/granules, then identification must be entered in LITHIC MATERIAL part of form	
LITHIC MATERIAL	Numeric/text	Percentage of Lithic material identified in either surface or downhole. Facility also for entry of outcrop, and its distance and bearing from the sample site. 'Other' allows for entry of lithic type not listed. Estimates probably accurate to within 10%. Trace amounts shown as 2%. When Outcrop is at site, distance is entered as 0	
Secondary coating	Numeric/text	Coating observed on regolith material (e.g. iron staining, clay). 'Other' allows for entry of coatings not listed	
Units nearby	Numeric/text	Allows designation of any secondary units seen close to the site. Estimated distance can be entered in Comments. 'Other ' allows listing of units not listed	
Sample features	Text	Due to restrictions on carrying corrosive material in the helicopter, testing for carbonate in the field using HCl was not carried out. Dry and damp allow recording of the state of the sample	
Photo taken?	Numeric	Whether a series of two digital photographs (one of the sample site and bag, and one of the sample in the foreground with the bag for scale) have been taken	
Comments	Text	Information unique to the site	Particular site characteristics (e.g. resistant layers in hole, such as carbonate, Fe nodules etc), distance to secondary features (e.g. channels), presence of animal droppings, unusually extensive consolidated colluvial layers, weather conditions

Figure 8. Examples of sample sites and regolith materials on contrasting bedrock lithologies: a), b) quartz-rich regolith typical of that found on or close to outcrops of siliciclastic sedimentary rocks. Site M3531, Warton Sandstone (MGA 288377E 8456204N); c), d) typical grass-covered area found on regolith of the Carson Volcanics Site M3324 (MGA 279841E 8411179N). In (d), note clast-rich regolith in clay-rich matrix

Most regolith samples are from the Pentecost Sandstone (141 samples or 34.6% of all samples), with 116 samples (28.5%) from the Carson Volcanics, and a similar number of samples from the Warton (73, 17.9%) and King Leopold Sandstones (66, 16.2%; Table 1). The limited extent of the Elgee Siltstone (Fig. 2; Table 1) has resulted in only 10 samples (2.5%), and there is only one sample collected from regolith over the Bastion Group.

In terms of regolith–landform unit (GSWA, 2014; Fig. 5, Table 2), the highest proportion of samples (282 or 69%) have been collected from areas of outcrop, with 38 samples from areas of residual or relict regolith (>10%). Colluvium accounts for 66 samples (21%), with 20 samples from areas of alluvium (5% of all samples) and one sample from a tidal area (Table 2). The high proportion of samples collected on or near to areas of outcrop reflects both the purpose of GSWA's Kimberley Science and Conservation Strategy program (i.e. to examine how regolith is related to bedrock) and the high proportion of exposed bedrock on the Kimberley Plateau.

Relationship of regolith and vegetation

At 387 sample sites, the relative abundance of grass, spinifex, trees, and shrubs was recorded (Fig. 7; Table 3). Data for the four most extensive lithological units (Table 4) show that approximately two-thirds of sites on both the King Leopold and Pentecost Sandstones have spinifex as the most common vegetation type, with grass as the second most common type. The proportions of spinifex and grass are broadly equal for sites on the Warton Sandstone, whereas grass is the most common vegetation type at 75% of sites on the Carson Volcanics. Trees and shrubs are only minor components of all vegetation regardless of lithology. These data show the strong relationship between bedrock, regolith and vegetation.

Sample hole depth and thickness of regolith

The heterogeneous nature of regolith and the often thin regolith cover in areas of outcrop meant that in some cases, the sample depth of 20–30 cm could not be reached. Thus, in some cases, the recorded hole depth could reflect the total thickness of regolith. Hole depth data for 368 sites (Fig. 9a, Table 5) show similar mean values of about 20 cm for holes on siliciclastic sedimentary units, with a lower mean value of 17 cm for holes on the Carson Volcanics. For the three most common regolith–landform types (regolith from areas of outcrop, colluvium, and residual–relict regolith) there is an overall similarity in sample hole depth (Fig. 9b, Table 5) and no consistent difference in terms of mean depth according to regolith type.

Chemical analysis of regolith

Introduction

Seventy components were analysed for each sample, comprising 13 analytes as oxides, 54 analytes as trace elements or rare earth elements (REE; La–Lu), loss-on-ignition (LOI), pH, and total dissolved solids (TDS). Of the trace elements, Ba and Cr were determined as oxides (BaO and Cr_2O_3) and as trace elements (Table 6). The analytical approach was based on X-ray fluorescence (XRF), and inductively coupled plasma (ICP) spectrometry.

The preparation and analysis of regolith samples was carried out by Intertek Genalysis Laboratory Services (Intertek Genalysis, Maddington, Perth). Approximately 2 kg of each sample was supplied to the laboratory in cable-tied plastic bags, labelled with the sample site number. Each sample was dry screened to <10 mm, and (if necessary) 1 kg of the screened material was crushed to <2 mm in a Boyd crusher. Two hundred grams of the <2 mm material was set aside for the determination of TDS and pH. The remainder of the <2 mm material was pulverized in a low-Cr steel ring mill to a nominal 85% passing 75 µm. Of this, about 150 g was retained for geochemical analysis, and the remainder placed in a sealed plastic bag. Both bags of pulverized material were returned to GSWA, along with any residual material.

Samples were analysed in two batches of about 200 samples each. The 150 g pulp aliquot for geochemistry was relabelled with a GSWA number and resubmitted with a series of 'blind' samples, also labelled with GSWA numbers, to assess quality of analysis.

Table 4. Summary of primary vegetation type recorded at each of 387 regolith sampling sites according to major lithological unit

	Grass	*Spinifex*	*Trees*	*Shrubs*	*Total*
KLS	20	43	2	0	65
Percent	*31*	*66*	*3*	*0*	
Carson	83	18	4	5	110
Percent	*75*	*16*	*4*	*5*	
Warton	31	34	3	3	71
Percent	*44*	*48*	*4*	*4*	
Pentecost	36	100	2	3	141
Percent	*26*	*71*	*1*	*2*	
					387

Table 5. Summary of maximum sample hole depth in centimetres for 368 sample sites according to lithological unit and regolith type. Hole depth could be either thickness of regolith or depth at which regolith was sampled

	N	*Mean*	*Median*	*Min.*	*Max.*	*Std Dev.*
All data	368	19	20	5	35	6.6
Carson Volcanics	98	17	20	5	30	6.0
King Leopold Sandstone	61	21	25	5	30	7.1
Warton Sandstone	67	20	20	5	30	6.8
Elgee Sandstone	10	22	20	10	30	5.9
Pentecost Sandstone	132	20	20	5	35	6.3
Total	**368**					
According to regolith type (map)						
Outcrop	257	19	20	5	35	6.7
Colluvium	62	22	20	10	30	5.2
Alluvium	19	18	20	5	30	6.5
Residual–relict	30	21	20	5	35	6.8

These consisted of a second pulp aliquot of 71 samples (i.e. sample duplicate; 17% of all samples) and multiple aliquots of five GSWA reference materials (basalt BB1, granite RH1, gossan IQC45, laterite IQC47, and copper ore IQC46; Morris, 2000, 2007). Additional sample duplicates, reference materials (some of which have certified values for all or some analytes), and blanks were inserted by Intertek Genalysis in both batches.

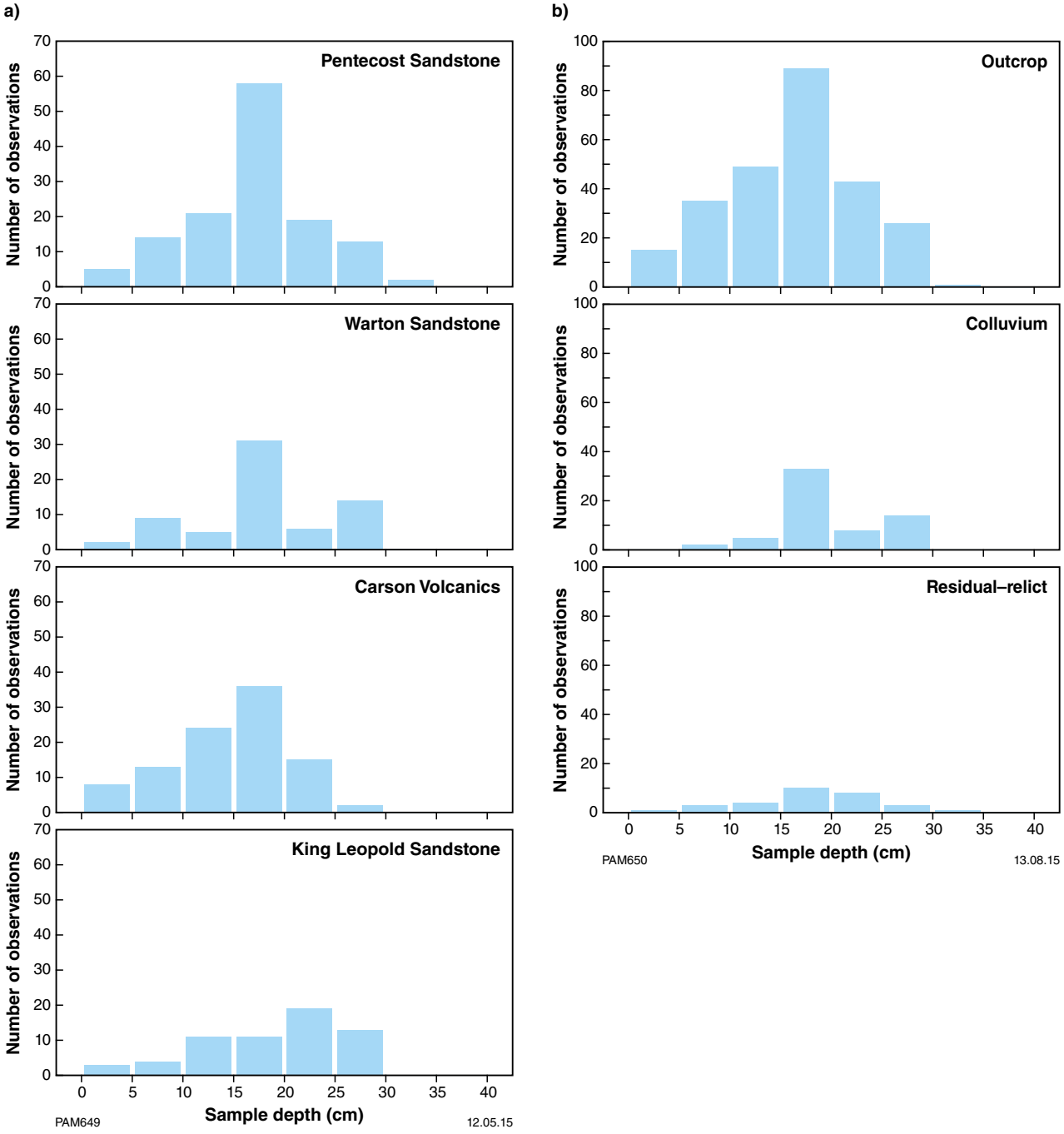

Figure 9. Histograms of sample hole depth for 368 sites: a) according to major lithological units; b) according to regolith type

Table 6. Statistical data for regolith samples collected in the Balanggarra project. Shaded analytes have not been statistically analysed due to high proportion of censored data

	Method	*Unit*	*LLD*	*No. < LLD (n = 407)*	*% < LLD*	*Lower outlier/ extreme*	*Minimum*	*10th pctl*	*Lower qtl*	*Median*	*Upper qtl*	*Outlier*	*Extreme*	*Maximum*	*Skewness*
Au	FA25/MS	ppb	1	388	95.3		<1							12	
Ag	4A/MS	ppm	0.05	368	90.4		<0.05							0.13	
Al_2O_3	FB1/XRF	%	0.01	0	0.0		0.77	2.23	3.29	4.76	10.46	21.215	31.97	22.44	0.96
As	4A/MS	ppm	0.5	3	0.7		<0.5	1.5	2.9	7.1	14.1	30.9	47.7	48.4	1.5
Ba	CD/MS	ppm	0.2	0	0.0		9.4	23.4	33.8	50.4	130.1	274.55	419	923.6	2.4
Be	4A/MS	ppm	0.05	13	3.2		<0.05	0.13	0.18	0.32	0.75	1.605	2.46	5.11	2.7
Bi	4A/MS	ppm	0.01	0	0.0		0.02	0.05	0.07	0.10	0.16	0.295	0.43	0.59	1.9
C	/CSA	%	0.01	0	0.0		0.13	0.28	0.36	0.48	0.62	1.01	1.4	8.88	9.6
CaO	FB1/XRF	%	0.01	162	39.8		<0.01							39.53	
Cd	4A/MS	ppm	0.02	343	84.3		<0.02							0.29	
Ce	CD/MS	ppm	0.02	0	0.0		6.79	16.19	19.88	24.76	38.35	66.055	93.76	263.52	3.9
Co	4A/MS	ppm	0.1	0	0.0		0.6	1.1	1.7	2.7	14.3	33.2	52.1	122.7	1.9
Cr	4A/OES	ppm	5	0	0.0		7	15	26	58	95	198.5	302	376	2
Cs	CD/MS	ppm	0.1	0	0.0		0.1	0.4	0.5	0.8	1.1	2	2.9	12.8	8.0
Cu	4A/OES	ppm	1	3	0.7		<1	2	3	4	20	45.5	71	265	2
Dy	CD/MS	ppm	0.02	0	0.0		0.42	1.09	1.31	1.66	2.81	5.06	7.31	30.66	6.9
Er	CD/MS	ppm	0.02	0	0.0		0.26	0.68	0.82	1.01	1.77	3.195	4.62	16.26	6.1
Eu	CD/MS	ppm	0.02	0	0.0		0.09	0.26	0.32	0.42	0.72	1.32	1.92	9.37	8.1
Fe_2O_3	FB1/XRF	%	0.02	0	0.0		0.97	1.66	2.57	6.36	13.85	30.77	47.69	50.00	1.6
Ga	CD/MS	ppm	0.1	0	0.0		1.4	3.2	4.7	7.7	17.1	35.7	54.3	49.4	1.1
Gd	CD/MS	ppm	0.02	0	0.0		0.39	1.12	1.34	1.75	2.73	4.815	6.9	33.18	7.7
Ge	4A/MS	ppm	0.05	0	0.0		0.05	0.67	0.78	0.87	1.00	1.33	1.66	3.10	1.6
Hf	CD/MS	ppm	0.1	0	0.0	1	1.0	5.2	6.7	8.4	10.5	16.2	21.9	25.0	1.5
Ho	CD/MS	ppm	0.02	0	0.0		0.09	0.22	0.27	0.35	0.59	1.07	1.55	6.08	6.6
In	4A/MS	ppm	0.005	34	8.4		<0.005	0.006	0.014	0.030	0.070	0.154	0.238	0.240	1.3
K_2O	FB1/XRF	%	0.01	0	0.0		0.01	0.06	0.11	0.22	0.36	0.735	1.11	4.41	4.4
LOI	/TGA	%	0.01	0	0.0		0.39	1.30	1.86	2.62	5.08	9.91	14.74	33.39	3.2
La	CD/MS	ppm	0.02	0	0.0	0.64	3.40	8.05	10.04	12.65	16.31	25.715	35.12	183.65	10.9
Li	4A/MS	ppm	0.1	0	0.0		1.6	3.5	4.7	6.3	11.8	22.45	33.1	41.3	1.7
Lu	CD/MS	ppm	0.01	0	0.0		0.04	0.12	0.15	0.18	0.30	0.525	0.75	2.14	5.3
MgO	FB1/XRF	%	0.01	1	0.2		<0.01	0.03	0.05	0.08	0.17	0.35	0.53	3.40	3.7
MnO	FB1/XRF	ppm	0.01	234	57.5		<0.01							0.57	
Mo	4A/MS	ppm	0.1	0	0.0		0.2	0.4	0.6	0.9	1.7	3.35	5	7.1	1.9
Na_2O	FB1/XRF	%	0.01	1	0.2		<0.01	0.02	0.02	0.03	0.05	0.095	0.14	3.67	4.7
Nb	CD/MS	ppm	0.1	0	0.0		0.7	3.1	3.8	5.0	7.5	13.05	18.6	18.9	1.0

Table 6. continued

	Method	*Unit*	*LLD*	*No. < LLD (n = 407)*	*% < LLD*	*Lower outlier/ extreme*	*Minimum*	*10th pctl*	*Lower qtl*	*Median*	*Upper qtl*	*Outlier*	*Extreme*	*Maximum*	*Skewness*
Nd	CD/MS	ppm	0.02	0	0.0		2.75	6.44	7.80	9.89	14.76	25.2	35.64	177.34	10.2
Ni	4A/OES	ppm	1	4	1.0		<1	3	4	6	20	44	68	94	1.6
P_2O_5	FB1/XRF	%	0.002	0	0.0		0.010	0.019	0.027	0.048	0.074	0.1445	0.215	0.246	1.5
Pb	4A/MS	ppm	0.5	0	0.0		1.8	3.5	4.4	6.5	11.6	22.4	33.2	69.9	3.0
Pd	FA25/MS	ppb	1	401	98.5		<1							7	
Pr	CD/MS	ppm	0.01	0	0.0		0.75	1.79	2.21	2.75	3.96	6.585	9.21	45.02	10.3
Pt	FA25/MS	ppb	1	395	97.1		<1							11	
Rb	CD/MS	ppm	0.1	0	0.0		1.0	4.3	8.3	14.3	22.5	43.8	65.1	205.4	4.3
S	/CSA	ppm	0.005	4	1.0		<0.005	0.010	0.011	0.016	0.020	0.0335	0.047	0.110	5.4
SO_3	FB1/XRF	%	0.01	86	21.1		<0.01	0.01	0.01	0.01	0.02	0.035	0.05	0.26	9.4
Sb	4A/MS	ppm	0.05	0	0.0		0.07	0.14	0.22	0.36	0.60	1.17	1.74	2.98	2.0
Sc	CD/OES	ppm	2	31	7.6		<2	2	3	5	16	35.5	55	60	1.5
Se	4A/MS	ppm	0.5	174	42.8		<0.25							4.2	
SiO_2	FB1/XRF	%	0.01	0	0.0	31.07	23.09	50.47	66.78	85.44	90.59	126.305	162.02	97.23	-1.1
Sm	CD/MS	ppm	0.02	0	0.0		0.51	1.25	1.49	1.89	2.93	5.09	7.25	35.67	9.5
Sn	CD/MS	ppm	0.2	0	0.0		0.3	0.6	0.8	1.0	1.5	2.55	3.6	3.9	1.4
Sr	CD/MS	ppm	0.1	0	0.0		2.5	5.7	7.0	9.1	16.7	31.25	45.8	3603.1	19.3
Ta	CD/MS	ppm	0.02	0	0.0		0.05	0.26	0.31	0.41	0.61	1.06	1.51	1.48	1.0
Tb	CD/MS	ppm	0.01	0	0.0		0.08	0.18	0.21	0.28	0.45	0.81	1.17	5.16	7.4
Te	4A/MS	ppm	0.05	179	44.0		<0.05							0.50	
Th	CD/MS	ppm	0.02	0	0.0		1.47	4.03	4.99	6.37	8.40	13.515	18.63	24.66	1.8
TiO_2	FB1/XRF	%	0.01	0	0.0		0.05	0.18	0.21	0.29	0.68	1.385	2.09	1.94	1.4
Tl	4A/MS	ppm	0.02	7	1.7		<0.02	0.04	0.06	0.09	0.13	0.235	0.34	0.87	2.9
Tm	CD/MS	ppm	0.02	0	0.0		0.04	0.11	0.13	0.16	0.27	0.48	0.69	2.34	5.9
U	CD/MS	ppm	0.02	0	0.0	0.19	0.43	1.01	1.19	1.45	1.86	2.865	3.87	4.44	1.7
V	CD/OES	ppm	2	0	0.0		4	20	38	109	258	588	918	932	1.6
W	CD/MS	ppm	0.2	8	2.0		<0.2	0.5	0.6	0.9	1.2	2.1	3	9.0	4.5
Y	CD/MS	ppm	0.1	0	0.0		2.5	6.3	7.6	9.5	15.4	27.1	38.8	166.2	6.9
Yb	CD/MS	ppm	0.02	0	0.0		0.26	0.77	0.90	1.14	1.90	3.4	4.9	14.76	5.6
Zn	4A/OES	ppm	1	0	0.0		2	3	4	6	12	24	36	155	2.9
Zr	CD/MS	ppm	1	0	0.0	22	34	204	259	324	417	654	891	1046	1.7
pH	ws/MTR		0.1	0	0.0	4.3	4.3	4.9	5.2	5.5	5.8	6.7	7.6	7.3	0.3
TDS	CALC	mg/Kg	20	0	0.0		30	42	51	81	138	268.5	399	1341	3.8

Quality control

Sample duplicates

The level of agreement between a parent sample and its duplicate depends on several factors including the homogeneity of the pulp (a function of the crushing and milling process), the preparation of the pulp for analysis (e.g. digestion, fusion), and the chemical analysis (analytical finish). This has been assessed using the Half Relative Deviation (HRD):

$$HRD = |100 \times [(analysis1 - analysis2)/(analysis1 + analysis2)]|$$

At what level HRD is acceptable is debatable, but in the GSWA regolith program HRD <10% is adopted, as long as the analyte concentration is at least ten times the lower level of detection (LLD; Morris and Verren, 2001). This takes into account the decrease in precision at lower concentration levels.

There is generally good agreement between parent and duplicate samples for all elements in batch 1 (Appendix 1), with only a few samples having HRD values >10 for more than two elements. The sample with the highest number of elements with HRD >10 is GSWA 213683, which is a duplicate analysis of the GSWA reference material IQC47 (laterite; Morris, 2000). For this analysis, Sb, Tb, Y and Yb have HRD >10, although the concentrations of these elements are close to the threshold of 10 times the LLD. Elements showing the poorest agreement include Be and Ge (seven samples; both are usually at low concentrations) and Zr (four samples). The latter may reflect the difficulty of getting resistate minerals such as zircon into solution prior to analysis.

Similar to batch 1, there is a high level of agreement between parent and duplicate samples for batch 2 (Appendix 1), with few exceptions. For colluvium, sample 213158 from the King Leopold Sandstone has HRD >10 for Cu, Hf, Pb, Rb and W, although concentrations of some elements (e.g. W) are low, and there are only small differences in the concentration of other elements (e.g. Rb = 5.2 and 6.6 ppm). One parent–duplicate pair (213442, residual regolith from the Warton Sandstone) shows poor agreement for a number of elements including Ba, Ga, Hf, Nb, Rb, Sr, Ta, Th, U, Zn, Zr and REE. The concentrations of some elements for which HRD >10 are low (e.g. Sr = 5.9 and 3.5 ppm; Y = 5.9 and 3.7 ppm), whereas the behaviour of other elements (e.g. Zr = 209 and 123 ppm) can be accounted for by small differences in the concentration of minerals such as zircon, which are resistant to acid digestion. This is likely to be more of an issue for samples from areas of relict or residual regolith, where resistate mineral phases are more common.

Site duplicates

The chemistry of site duplicates (Appendix 2) shows good agreement for most sample pairs, with HRD <10 for most elements if the concentration is at least 10 times the LLD. However, six samples have HRD >10 for more than 10 elements, and at one site (213232, colluvium from the King Leopold Sandstone), HRD >10 for 35 elements. Elevated HRD values for REE (e.g. 213279, 213265, 213232) can be accounted for by the inhomogeneous distribution of even small amounts of minerals such as allanite and monazite. Similarly, variations in even accessory amounts of minerals such as rutile, sphene and zircon could account for high HRD values for the high field strength elements (HFSE) Nb, Ta, Hf, Zr and Ti (e.g. 213265, 213232). The effect of these accessory minerals is exacerbated by their resistance to acid digestion. Poor agreement for elements such as As, Cr, Pb, Zn, Sb, Mo, V and Fe could reflect small variations in the content of sulfides or oxides, whereas variations in Al_2O_3, Li, LOI and Ga could be related to variable clay contents. The lack of agreement for P_2O_5 could be related to the distribution of monazite or secondary phosphate minerals such as florencite or rhabdophane. Variations in carbon content are difficult to explain in terms of mineralogy, and most likely reflect the presence of carbonaceous material resulting from bushfires. In terms of regolith–landform unit and lithology, there is no clear pattern to explain site inhomogeneity. For example, sample 213229 (regolith in an area of outcrop from the King Leopold Sandstone) has HRD <10 for all elements, yet HRD >10 for 20 analytes in 213279 and 7 elements in 213530, both of which are regolith samples from areas of outcrop in the Warton Sandstone.

Reference materials

The analysis of material of a known composition (reference materials or standards; Kane, 1990) is an important part of assessing the quality of geochemical data. If the reference material is well characterized in that element concentrations are certified, it can be used to assess accuracy. As reference materials are prepared under rigorous conditions, they have a high level of homogeneity and multiple analyses of reference materials, regardless of whether they are certified or not, can provide information on precision.

Forty-nine different reference materials have been analysed in the two batches, some of them more than once. Of these, five are in-house (GSWA) reference materials, which do not have certified values (Morris, 2000, 2007), but one (BB1) is well characterized. The remaining 44 reference materials, inserted by Intertek Genalysis, cover a wide range in terms of type (soil, rock), matrix (oxides, silicates), and element concentration (from barren to mineralized). Of these, values are certified for some or all elements in 36, and recommended in the remaining eight.

For the GSWA reference material BB1, HRD <10 for all elements — apart from Au and Ge in batch 1, and Au, As, Cr, Ge, Ta and U in batch 2 (Appendix 3) — when the average of four analyses and values listed in Morris (2007) are compared. For elements where the concentration is greater than 10 times the LLD, precision can be examined using the percent relative standard deviation (RSD%, also known as the covariance), which is the percent standard deviation divided by the average. An arbitrary value of <20 is taken as showing an acceptable level of precision. For BB1, RSD% is <20 for all elements apart from Au and Ge. For gossan IQC45 (Morris, 2000), RSD% is <20 for elements with concentrations greater than 10 times

the LLD. For laterite IQC47, RSD% >20 for Bi, Cu, Ge, Pb and Y in batch 1, with Bi, Cu and most REE having RSD% >20 in batch 2, although concentrations are generally low. For copper ore IQC46, RSD% >20 for Bi in batch 1 and Nb in batch 2.

There are no well-characterized values for granite RH1, and only precision has been assessed, with RSD% <20 for all elements apart from Bi, Ge and Mo in batch 1 and Cu in batch 2. As there is only a single analysis of copper ore IQC46 in Morris (2000), accuracy has not been assessed. Bismuth has RSD% >20, but the concentration is close to 1 ppm.

Of the certified reference materials inserted by Intertek Genalysis, there is generally good agreement between observed and certified values, with no consistent discrepancies in terms of elements or reference materials. The few discrepancies include: Pb and Zn in peridotite WPR-1a (17.5 and 7.92 ppm, and 201 and 160 ppm respectively); Sc in anomalous ferruginous soil OREAS 45d (61 and 49 ppm); Hf (6.2 and 3.11 ppm) and Zr (245 and 100 ppm) in lateritic soil OREAS 45e; and Cu (80 and 38 ppm) in granodiorite OREAS 24b.

Blanks

Four sample blanks and one acid blank were measured in each batch (Appendix 4). In both batches all blanks were acceptably low (i.e. less than three times the LLD), apart from a measurement of 9 ppm for Zr in batch 1, and 0.6 ppm Hf, and 4 ppm and 20 ppm Zr in batch 2 (Appendix 4).

Statistical treatment of geochemical data

To determine whether elements are at anomalously high or low concentrations, the data must be examined statistically (cf. Davis, 1973; Reimann et al., 2008; Grunsky, 2010). Statistical treatment of geochemical data requires that concentrations less than the LLD (i.e. censored data; Reimann et al., 2008) are accounted for. Here, censored data are replaced by a value equal to half of the LLD. Although this will have minimal effect on statistics where only a few data are censored, with increasing proportions of censored data, the reliability of statistical analysis decreases. For the Balanggarra regolith geochemical data, Au, Ag, CaO, Cd, MnO, Pd, Pt, Se and Te are censored for >30% of samples, with >80% of data censored for Au, Ag, Cd, Pd and Pt (Table 6). Accordingly, these nine elements have not been statistically treated.

Box and whisker plots using ranked data (Reimann et al., 2008) have been used to identify anomalous analyte concentrations, and set breaks in data for bubble plots, which show the range in analyte concentrations. In these plots (Figs B10–B17*), the diameter of the bubble is proportional to a range in element concentration, unless an element is at anomalously high levels, where it is shown as a star (purple – outlier value; red – extreme value). For the nine elements with a high proportion of censored data, natural breaks have been used for bubble sizes. For plotting of bubble maps, class boundaries are taken at the 10th, 25th (lower quartile), 50th (median), and 75th (upper quartile) percentiles, and the outlier–extreme boundary (Table 6).

* Bubble plots B10–B17 are assembled in a separate section at the end of this Record. Hyperlinks inserted at figure numbers provide access to the figures. The back arrow in Adobe Reader or Adobe Acrobat will return the document to the in-text figure reference.

Grouping of elements

In this Record, analytes are discussed in eight categories: oxides (including LOI, pH, and TDS), precious metals, lithophile elements, REE (La–Lu plus Y), chalcophile elements, transition elements, HFSE, and base metals (Table 7). The categories used here are somewhat arbitrary, in that elements can be grouped using different criteria. These include the element's position in the periodic table (Krauskopf, 1967), charge/ionic radius (e.g. Rollinson, 1993), or association with mineral groups (e.g. chalcophile elements). Because of this, some elements may belong to more than one group. For example, Fe is a transition element, and is common in both sulfide deposits and igneous rocks, and could therefore be grouped with other transition elements; alternatively, it could be grouped as a chalcophile or siderophile element (Krauskopf, 1967). Similarly, Ti is often grouped with other oxides (as TiO_2), but its charge/ionic radius means it is also a HFSE, and could be grouped with Nb, Hf, Ta and Zr.

Oxides, pH, and total dissolved solids

There are no regolith samples with anomalously high SiO_2 concentrations (Fig. B10a), and SiO_2 is the only analyte which is negatively skewed (Table 6), reflecting the high proportion of regolith samples from quartz-rich siliciclastic units. Regolith from the Carson Volcanics has higher median values for TiO_2 (Fig. B10b), Al_2O_3 (Fig. B10c), Fe_2O_3 (Fig. B10d), MgO (Fig. B10f), Na_2O (Fig. B10h), P_2O_5 (Fig. B10j), LOI (Fig. B10l), and pH (Fig. B10m), and only regolith from the Carson Volcanics has samples with anomalous concentrations of Fe_2O_3 (several samples) and Al_2O_3 (one sample). For oxides at low concentrations where class boundaries use natural breaks (MnO and CaO; Fig. B10e,g), concentrations appear higher in regolith from the Carson Volcanics.

Although most regolith samples with anomalous oxide, pH and LOI levels are from the Carson Volcanics, one sample (213314) from the Warton Sandstone and the one sample from the Bastion Group (213351) have anomalous concentrations of MgO, Na_2O and K_2O (Fig. B10f,h,i). The most samples with anomalous K_2O are found in the Pentecost Sandstone. High CaO (Fig. B10g), anomalous TDS (Fig. B10n) and SO_3 (Fig. B10k), and anomalously low SiO_2 are found in 213358 on the coast over the King Leopold Sandstone. This is the only sample from the project area with pH >7 (Fig. B10m). Other samples with anomalously high TDS over this unit are also found near the coast.

Table 7. Grouping of elements, unit of measurement, lower level of detection (LLD), analytical code (acronym), explanation of acronym

Analyte	*Group*	*Unit*	*LLD*	*Method acronym*	*Method description*
SiO_2	Oxide	wt%	0.01	FB1/XRF	Lithium metaborate fusion (glass disc) and XRF analysis
TiO_2	Oxide	wt%	0.01	FB1/XRF	Lithium metaborate fusion (glass disc) and XRF analysis
Al_2O_3	Oxide	wt%	0.01	FB1/XRF	Lithium metaborate fusion (glass disc) and XRF analysis
Fe_2O_3	Oxide	wt%	0.02	FB1/XRF	Lithium metaborate fusion (glass disc) and XRF analysis
MnO	Oxide	wt%	0.01	FB1/XRF	Lithium metaborate fusion (glass disc) and XRF analysis
MgO	Oxide	wt%	0.01	FB1/XRF	Lithium metaborate fusion (glass disc) and XRF analysis
CaO	Oxide	wt%	0.01	FB1/XRF	Lithium metaborate fusion (glass disc) and XRF analysis
Na_2O	Oxide	wt%	0.01	FB1/XRF	Lithium metaborate fusion (glass disc) and XRF analysis
K_2O	Oxide	wt%	0.01	FB1/XRF	Lithium metaborate fusion (glass disc) and XRF analysis
P_2O_5	Oxide	wt%	0.002	FB1/XRF	Lithium metaborate fusion (glass disc) and XRF analysis
SO_3	Oxide	wt%	0.01	FB1/XRF	Lithium metaborate fusion (glass disc) and XRF analysis
LOI	Oxide	wt%	0.01	/TGA	Weight loss at 1000ºC
pH		µs/cm	0.1	ws/MTR	1:5 sample:water solution and pH meter
TDS		mg/kg	20	ws/MTR	1:5 sample:water solution and eC meter
Ag	Precious metal	ppm	0.05	4A/MS	Four-acid digestion and ICP-MS finish
Au	Precious metal	ppb	1	FA25/MS	Fire assay preconcentration and ICP-MS finish
Pd	Precious metal	ppb	1	FA25/MS	Fire assay preconcentration and ICP-MS finish
Pt	Precious metal	ppb	1	FA25/MS	Fire assay preconcentration and ICP-MS finish
Ba	Lithophile	ppm	0.2	CD/MS	Acid and fusion digestion and ICP-MS finish
Be	Lithophile	ppm	0.05	4A/MS	Four-acid digestion and ICP-MS finish
C	Lithophile	wt%	0.01	/CSA	Acid digestion, CS analyser
Cs	Lithophile	ppm	0.1	CD/MS	Acid and fusion digestion and ICP-MS finish
Ga	Lithophile	ppm	0.1	CD/MS	Acid and fusion digestion and ICP-MS finish
Ge	Lithophile	ppm	0.05	4A/MS	Four-acid digestion and ICP-MS finish
In	Lithophile	ppm	0.005	4A/MS	Four-acid digestion and ICP-MS finish
Li	Lithophile	ppm	0.1	4A/MS	Four-acid digestion and ICP-MS finish
Rb	Lithophile	ppm	0.1	CD/MS	Acid and fusion digestion and ICP-MS finish
Sn	Lithophile	ppm	0.2	CD/MS	Acid and fusion digestion and ICP-MS finish
Sr	Lithophile	ppm	0.1	CD/MS	Acid and fusion digestion and ICP-MS finish
Th	Lithophile	ppm	0.02	CD/MS	Acid and fusion digestion and ICP-MS finish
Tl	Lithophile	ppm	0.02	4A/MS	Four-acid digestion and ICP-MS finish
U	Lithophile	ppm	0.02	CD/MS	Acid and fusion digestion and ICP-MS finish
La	REE	ppm	0.02	CD/MS	Acid and fusion digestion and ICP-MS finish
Ce	REE	ppm	0.02	CD/MS	Acid and fusion digestion and ICP-MS finish
Pr	REE	ppm	0.01	CD/MS	Acid and fusion digestion and ICP-MS finish
Nd	REE	ppm	0.02	CD/MS	Acid and fusion digestion and ICP-MS finish
Sm	REE	ppm	0.02	CD/MS	Acid and fusion digestion and ICP-MS finish
Eu	REE	ppm	0.02	CD/MS	Acid and fusion digestion and ICP-MS finish
Gd	REE	ppm	0.02	CD/MS	Acid and fusion digestion and ICP-MS finish
Tb	REE	ppm	0.01	CD/MS	Acid and fusion digestion and ICP-MS finish
Dy	REE	ppm	0.02	CD/MS	Acid and fusion digestion and ICP-MS finish
Ho	REE	ppm	0.02	CD/MS	Acid and fusion digestion and ICP-MS finish
Er	REE	ppm	0.02	CD/MS	Acid and fusion digestion and ICP-MS finish
Tm	REE	ppm	0.02	CD/MS	Acid and fusion digestion and ICP-MS finish
Yb	REE	ppm	0.02	CD/MS	Acid and fusion digestion and ICP-MS finish
Lu	REE	ppm	0.01	CD/MS	Acid and fusion digestion and ICP-MS finish
Y	REE	ppm	0.1	CD/MS	Acid and fusion digestion and ICP-MS finish

Table 7. continued

Analyte	Group	Unit	LLD	Method acronym	Method description
As	Chalcophile	ppm	0.5	4A/MS	Four-acid digestion and ICP-MS finish
Bi	Chalcophile	ppm	0.01	4A/MS	Four-acid digestion and ICP-MS finish
Cd	Chalcophile	ppm	0.02	4A/MS	Four-acid digestion and ICP-MS finish
Mo	Chalcophile	ppm	0.1	4A/MS	Four-acid digestion and ICP-MS finish
S	Chalcophile	wt%	0.005	/CSA	Acid digestion, CS analyser
Sb	Chalcophile	ppm	0.05	4A/MS	Four-acid digestion and ICP-MS finish
Se	Chalcophile	ppm	0.5	4A/MS	Four-acid digestion and ICP-MS finish
Te	Chalcophile	ppm	0.05	4A/MS	Four-acid digestion and ICP-MS finish
W	Chalcophile	ppm	0.2	CD/MS	Acid and fusion digestion and ICP-MS finish
Co	Transition	ppm	0.1	4A/MS	Four-acid digestion and ICP-MS finish
Cr	Transition	ppm	5	4A/OES	Four-acid digestion and ICP-OES finish
Ni	Transition	ppm	1	4A/OES	Four-acid digestion and ICP-OES finish
Sc	Transition	ppm	2	CD/OES	Acid and fusion digestion and ICP-OES finish
V	Transition	ppm	2	CD/OES	Acid and fusion digestion and ICP-OES finish
Hf	High field strength	ppm	0.1	CD/MS	Acid and fusion digestion and ICP-MS finish
Nb	High field strength	ppm	0.1	CD/MS	Acid and fusion digestion and ICP-MS finish
Ta	High field strength	ppm	0.02	CD/MS	Acid and fusion digestion and ICP-MS finish
Zr	High field strength	ppm	1	CD/MS	Acid and fusion digestion and ICP-MS finish
Cu	Base metal	ppm	1	4A/OES	Four-acid digestion and ICP-OES finish
Pb	Base metal	ppm	0.5	4A/MS	Four-acid digestion and ICP-MS finish
Zn	Base metal	ppm	1	4A/OES	Four-acid digestion and ICP-OES finish

Precious metals

The concentrations of Ag, Au, Pd and Pt in regolith are generally low with more than 95% of samples returning censored data for these elements (Table 6). There are few samples with detectable Ag (Table 6; Fig. B11a), and the samples with the highest concentration of this element (0.13 ppm) are from regolith in an area of outcrop in the King Leopold Sandstone (213217), and from residual–relict regolith on the Carson Volcanics (213440).

Of the 19 samples with detectable Au (>1 ppb), nine are from regolith derived from the Carson Volcanics (Fig. B11b), but the sample with highest Au concentration of 12 ppb is from an area of outcrop in the King Leopold Sandstone (213294). A sample of regolith from an area of outcrop in the same vicinity (213535) has the highest concentration of Pd (7 ppb) and Pt (11 ppb; Fig. B11c,d).

Lithophile elements

Several lithophile elements, such as Be, C, Cs, Ge, In and Tl, are at low concentrations in most regolith samples, with median values <1 ppm (Table 6). Most samples with anomalous concentrations of lithophile elements are found in regolith from the Carson Volcanics; these elements include Ba (Fig. B12a), Be (Fig. B12b), C (Fig. B12c), Ga (Fig. B12e), Ge (Fig. B12f), In (Fig. B12g), Li (Fig. B12h), Sr (Fig. B12k), and Tl (Fig. B12m). Compared to the Warton and Pentecost Sandstones, regolith from the King Leopold Sandstone appears to have lower concentrations of lithophile elements, although 213258 has the highest Sr content of regolith sampled (3603 ppm). Most samples with anomalous Rb contents are found in the Pentecost Sandstone (Fig. B12i), especially in the southeast part. In this area, there are also samples with anomalous concentrations of Ba (Fig. B12a), Cs (Fig. B12d), Ge (Fig. B12f), Sn (Fig. B12j), Th (Fig. B12l), and U (Fig. B12n), and the one sample from the Bastion Group (213351) also has anomalous concentrations of these elements. Several samples with anomalous concentrations of Cs are found in regolith from the Elgee Siltstone (Fig. B12d).

Rare earth elements and Y

Elevated and anomalous concentrations of REE and Y are commonly found in regolith samples from the Carson Volcanics (Fig. B13a–o), and regolith from the King Leopold Sandstone has some of the lowest REE and Y contents. The median La content of regolith is 12.65 ppm, whereas for the heavy REE (HREE), the median Yb content is 1.14 ppm. Of the samples with anomalous REE contents in the Warton Sandstone, 213314 has elevated concentrations of La–Er (e.g. Fig. B13a). The one sample from the Bastion Group (213351) has anomalous La–Sm, whereas sample 213458 in the Pentecost Sandstone has anomalous concentrations of the middle and heavy REE Eu–Lu, as well as Y (e.g. Fig. B13j).

Chalcophile elements

As a group, chalcophile elements show no clear relationship with any particular lithological unit, although most samples with high As concentrations (median = 7.1 ppm) and samples with detectable Cd (maximum concentration = 0.29 ppm) are found over the Carson Volcanics (Fig. B14a,d). Bismuth concentrations are generally low, with a median value of 0.1 ppm and a maximum of 0.59 ppm (Table 6). A group of samples with anomalous Bi concentrations is found in the northern part of the Warton Sandstone (Fig. B14b), and a few anomalous samples are found in the southeast part of the project area over part of the Pentecost Sandstone and the Bastion Group, as well as on parts of the King Leopold Sandstone. Median values for Mo are similar for different lithological units (Fig. B14e), with a few anomalous samples on parts of the King Leopold Sandstone and the northern part of the Warton Sandstone. Sulfur contents are generally low (median = 0.016 wt%; Fig. 14f), although sample 213358 has an anomalously high S content of 0.11 wt%.

Similar to Bi, samples with anomalous concentrations of Sb (Fig. B14c) are found in the northern part of the Warton and King Leopold Sandstones respectively, and in the southeastern part of the Pentecost Sandstone. Both Se and Te (Fig. B14g,h) have about 40% censored data and low concentrations (maximum = 4.2 and 0.5 ppm respectively), with detectable concentrations not tied to any particular lithological unit. Tungsten (Fig. B14i) shows a similar distribution to Sb and As, with anomalous concentrations found in the northern part of the Warton Sandstone and the southeastern part of the Pentecost Sandstone.

Transition elements

The mafic lithology of the Carson Volcanics is reflected in the high concentrations of transition elements in regolith, and the high proportion of regolith samples with anomalous transition element concentrations (Fig. B15a–e). The median values of all transition elements apart from Cr and V are <10 ppm, reflecting the dominance of samples from quartz-rich siliciclastic units. Samples with anomalous Cr concentrations are found in regolith from the northern part of the King Leopold Sandstone, as well as at or near the base of the Carson Volcanics (Fig. B15b).

High field strength elements

Median values for Nb and Ta are higher for regolith from the Carson Volcanics than for the Pentecost and Warton Sandstones (Fig. B16b,c). There are a few samples with anomalous Hf in the King Leopold Sandstone, Carson Volcanics, and Elgee Siltstone (Fig. B16a), but the majority of samples with anomalous Zr (Fig. B16d) and Hf are found in nine samples from the southeast part of the Pentecost Sandstone which lie on a NE–SW trend. Other HFSE, such as Nb and Ta, are not at anomalous concentrations in these samples, although HFSE are generally higher in the southeast part of the Pentecost Sandstone compared to lower parts of the unit.

Base metals

The median base metal concentrations of regolith from the project area (Table 6) reflect the low concentrations of these elements in siliciclastic sedimentary rocks. Higher values (up to 265 ppm Cu and 155 ppm Zn) are found in regolith from the Carson Volcanics (Fig. B17a,c), although the highest Pb content of 69.9 ppm is found in a sample of colluvium (213451) from the King Leopold Sandstone (Fig. B17b). Several samples with anomalous concentrations of base metals are found in siliciclastic sedimentary units, but samples with anomalous base metal concentrations are largely confined to the Carson Volcanics.

Discussion

Bubble plots and box and whisker plots of analytes such as SiO_2 (Fig. B10a), TiO_2 (Fig. B10b), Ni (Fig. B15c) and Cu (Fig. B17a) show the strong lithological contrast between regolith from the mafic volcanic-dominated Carson Volcanics and quartz-rich siliciclastic sedimentary rocks of the King Leopold, Warton, and Pentecost Sandstones, and the Elgee Siltstone. As would be expected, the median SiO_2 values for the regolith from the King Leopold, Warton and Pentecost Sandstones spans a narrow range from about 88 to 90 wt%, compared to 54 wt% for the Carson Volcanics (Tables 8–12). However, the SiO_2 content of regolith from both the Carson Volcanics and King Leopold Sandstone shows a wide range from about 25 wt% to 95 wt%, which is inconsistent with the dominant bedrock lithologies of each unit (Table 1). Other elements show similar behaviour; for example, Cr in regolith from the King Leopold Sandstone ranges in concentration from 12 to 273 ppm (Table 8). These wide variations could reflect the effects of chemical weathering, lithological diversity within individual units, and/or the assigning of regolith samples to the incorrect lithological unit.

Assessment of chemical weathering

Before using regolith composition as a proxy for that of bedrock, chemical weathering must be taken into account. This is illustrated using multi-element variation diagrams (spider plots) for regolith from the Carson Volcanics and the King Leopold Sandstone, the latter taken as a representative of regolith from siliciclastic sedimentary rocks.

Carson Volcanics

The composition of representative regolith samples from areas of outcrop, colluvium, and residual regolith from the Carson Volcanics is shown in relation to the average of 37 analyses of fresh Carson Volcanics from the Balanggarra area (Table 13, Fig. 18a–d). Two examples of regolith from areas of outcrop (213227 and 213228; Fig. 18a) have broadly similar concentrations of SiO_2, Al_2O_3, REE and

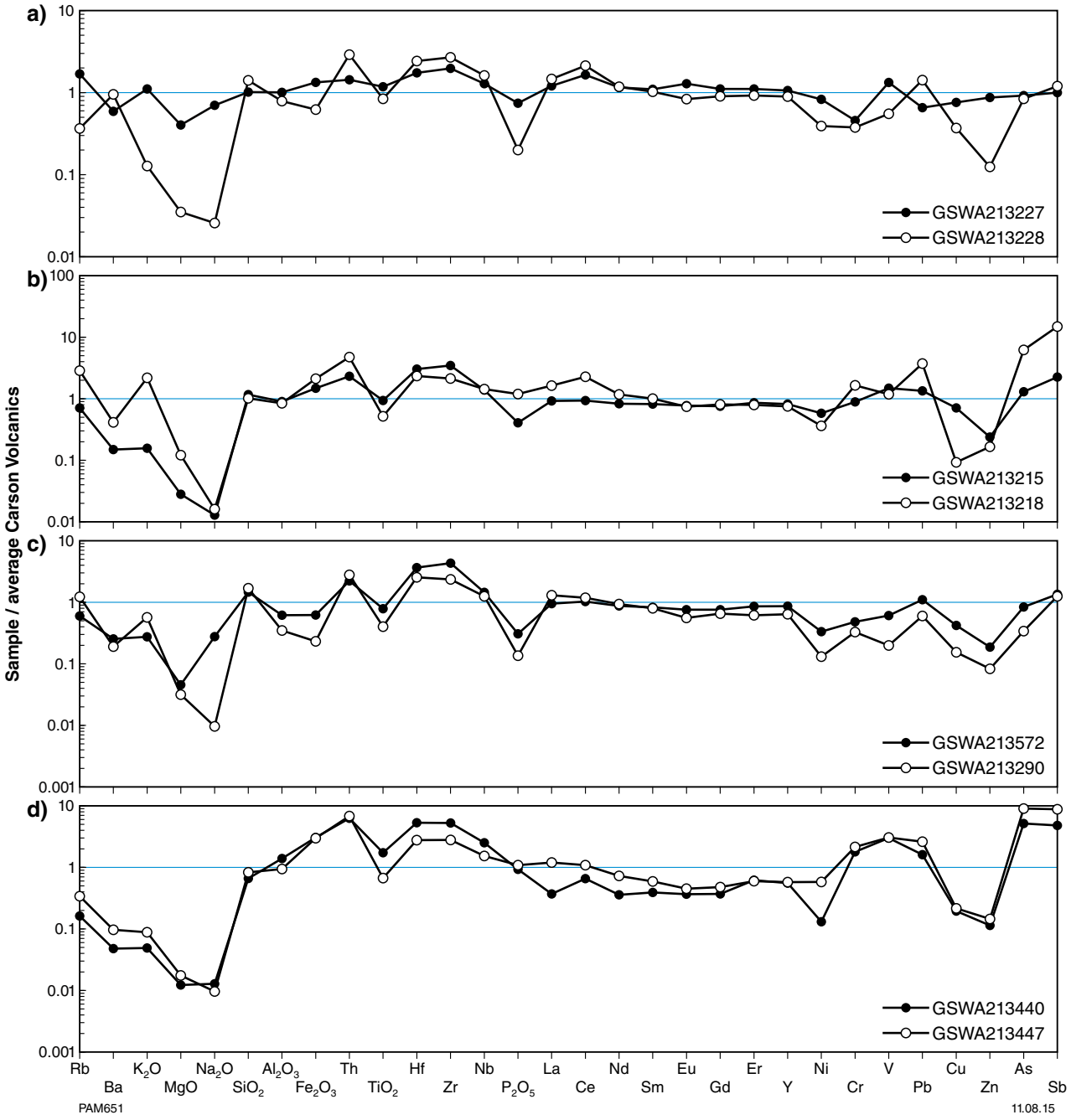

Figure 18. Multi-element spider diagrams summarizing the chemistry of regolith from the Carson Volcanics in relation to fresh bedrock. Normalizing composition is the average of 37 analyses of the Carson Volcanics from the Balanggarra area (K Orth, written comm., 2014; Table 13): a) regolith from areas of outcrop; b) colluvium; c) alluvium; d) residual

chalcophile elements (As and Sb) to bedrock, but Th, Hf, Nb and Zr are weakly enriched in regolith, and Rb, Ba, MgO, K_2O, and Na_2O are generally depleted. Two samples of colluvium (213215 and 213218; Fig. 18b) show similar patterns to regolith from areas of outcrop, but Na_2O, MgO, Cu and Zn are more depleted in the colluvial samples, and the HFSE, Cr and Pb are more enriched. Samples of alluvium (e.g. 213572 and 213290; Fig. 18c) show similar patterns to colluvium for the interval Rb–Y, but base metals and chalcophile elements are depleted in alluvium, with the latter at similar concentrations to fresh bedrock. Two samples of residual regolith show uniform depletion relative to bedrock for the interval Rb–Na_2O, similar SiO_2 and Al_2O_3, and elevated Fe_2O_3 (Fig. 18d). Unlike regolith from areas of outcrop, colluvium and alluvium, the REE are depleted (HREE more so than LREE), as are some base metals (Cu and Zn) and Ni, but Th, HFSE, Pb, V, Cr and the chalcophile elements are enriched.

Table 8. Statistical data for regolith samples from the King Leopold Sandstone (n = 66). Boxed values show analytes with the highest or lowest concentrations for all regolith data

	Unit	*LLD*	*No. < LLD*	*% < LLD*	*Minimum*	*Maximum*	*Range*	*Mean*	*SD*	*25 pctl*	*Median*	*75 pctl*	*Skewness*
Au	ppb	1	60	91	<0.5	12	12						
Ag	ppm	0.05	66	100	<0.05	0.13	0.13						
Al_2O_3	%	0.01	0	0	0.77	19.05	18.28	4.84	4.06	2.20	3.54	5.10	1.7
As	ppm	0.5	0	0	0.9	26.4	25.5	8.0	7.7	2.3	4.4	13.7	1.1
Ba	ppm	0.2	0	0	9.4	283.7	274.3	31.3	38.1	17.0	23.2	30.5	5.3
Be	ppm	0.05	0	0	0.08	1.46	1.38	0.32	0.28	0.15	0.22	0.36	2.2
Bi	ppm	0.01	0	0	0.02	0.47	0.45	0.15	0.12	0.07	0.11	0.18	1.5
C	ppm	0.01	0	0	0.16	8.88	8.72	0.56	1.07	0.27	0.38	0.54	7.5
CaO	%	0.01	45	68	<0.01	39.53	39.53						
Cd	ppm	0.02	63	95	<0.01	0.07	0.07						
Ce	ppm	0.02	0	0	6.79	62.46	55.67	21.31	10.82	14.64	18.21	22.65	1.8
Co	ppm	0.1	0	0	0.6	56.4	55.8	4.9	8.8	1.2	2.0	3.9	4.0
Cr	ppm	5	0	0	12	273	261	65	64	20	35	96	1.6
Cs	ppm	0.1	0	0	0.1	3.2	3.1	0.7	0.5	0.3	0.5	0.8	2.5
Cu	ppm	1	0	0	1	97	96	8	14	3	4	7	5.0
Dy	ppm	0.02	0	0	0.42	5.33	4.91	1.65	0.97	1.04	1.33	1.81	2.1
Er	ppm	0.02	0	0	0.26	3.07	2.81	1.01	0.58	0.69	0.84	1.12	1.8
Eu	ppm	0.02	0	0	0.09	1.94	1.85	0.36	0.28	0.22	0.29	0.40	3.6
Fe_2O_3	%	0.01	0	0	1.08	28.53	27.45	5.74	5.51	1.83	2.97	8.59	1.7
Ga	ppm	0.1	0	0	1.4	22.3	20.9	7.1	5.8	3.2	5.1	9.0	1.4
Gd	ppm	0.02	0	0	0.49	5.85	5.36	1.59	0.95	1.03	1.33	1.74	2.5
Ge	ppm	0.05	0	0	0.14	3.10	2.96	0.87	0.35	0.75	0.82	0.90	4.1
Hf	ppm	0.1	0	0	1.0	18.6	17.6	8.3	3.9	5.3	7.2	11.0	0.6
Ho	ppm	0.02	0	0	0.09	1.03	0.94	0.34	0.20	0.21	0.28	0.38	1.9
In	ppm	0.005	15	23	<0.005	0.120	0.120	0.029	0.028	0.010	0.020	0.040	1.2
K_2O	%	0.01	0	0	0.01	0.39	0.38	0.09	0.08	0.04	0.07	0.09	2.4
LOI	%	0.01	0	0	0.67	33.39	32.72	3.04	4.13	1.39	1.96	3.73	6.3
La	ppm	0.02	0	0	3.43	27.56	24.13	10.67	5.28	7.60	9.10	11.32	1.5
Li	ppm	0.1	0	0	1.6	41.3	39.7	6.2	5.8	3.0	4.3	7.1	3.8
Lu	ppm	0.01	0	0	0.04	0.51	0.47	0.18	0.09	0.13	0.15	0.22	1.6
MgO	%	0.01	1	2	<0.01	1.54	1.54	0.09	0.23	0.02	0.03	0.06	5.6
MnO	ppm	0.01	54	82	<0.01	0.20	0.20						
Mo	ppm	0.1	0	0	0.2	4.7	4.5	1.4	1.2	0.6	0.9	2.4	1.2
Na_2O	%	0.01	1	2	0.01	3.55	3.55	0.10	0.44	0.02	0.03	0.03	7.7
Nb	ppm	0.1	0	0	0.7	18.9	18.2	5.0	3.2	3.2	3.9	5.9	2.1
Nd	ppm	0.02	0	0	2.75	27.02	24.27	8.63	4.68	5.97	7.22	9.15	1.9
Ni	ppm	1	0	0	1	73	72	9	13	3	5	8	3.8
P_2O_5	%	0.002	0	0	0.014	0.140	0.126	0.047	0.033	0.020	0.031	0.065	1.1

Table 8. continued

	Unit	*LLD*	*No. < LLD*	*% < LLD*	*Minimum*	*Maximum*	*Range*	*Mean*	*SD*	*25 pctl*	*Median*	*75 pctl*	*Skewness*
Pb	ppm	0.5	0	0	2.0	69.9	67.9	7.8	9.2	3.7	4.8	8.2	5.0
Pd	ppb	1	64	97	<1	7	7						
Pr	ppm	0.01	0	0	0.75	6.74	5.99	2.36	1.22	1.63	1.98	2.54	1.7
Pt	ppb	1	64	97	<1	11	11						
Rb	ppm	0.1	0	0	1.0	18.5	17.5	5.4	3.1	3.4	4.6	6.1	1.8
S	ppm	0.005	1	2	<0.005	0.110	0.110	0.020	0.013	0.010	0.020	0.020	4.8
SO_3	%	0.01	11	17	<0.01	0.26	0.26	0.02	0.03	0.01	0.01	0.02	6.9
Sb	ppm	0.05	0	0	0.08	1.49	1.41	0.48	0.39	0.20	0.30	0.64	1.2
Sc	ppm	2	0	0	2	25	23	7	5	3	5	9	1.7
Se	ppm	0.5	37	56	<0.5	2.1							
SiO_2	%	0.01	0	0	23.09	96.71	73.62	84.83	13.02	79.27	90.02	93.56	-2.2
Sm	ppm	0.02	0	0	0.51	5.47	4.96	1.71	0.94	1.15	1.43	1.91	2.1
Sn	ppm	0.2	0	0	0.3	3.9	3.6	1.1	0.7	0.7	0.9	1.3	2.0
Sr	ppm	0.1	0	0	3.3	3603.1	3599.8	75.7	443.6	7.7	9.9	16.5	8.0
Ta	ppm	0.02	0	0	0.05	1.48	1.43	0.42	0.26	0.27	0.33	0.54	1.9
Tb	ppm	0.01	0	0	0.08	0.89	0.81	0.26	0.15	0.17	0.22	0.29	2.2
Te	ppm	0.05	33	50	<0.05	0.44							
Th	ppm	0.02	0	0	1.47	19.16	17.69	6.91	4.35	4.03	5.12	8.33	1.4
TiO_2	%	0.01	0	0	0.05	1.39	1.34	0.33	0.24	0.18	0.25	0.45	2.0
Tl	ppm	0.02	6	9	0.01	0.15	0.14	0.04	0.03	0.03	0.04	0.06	1.6
Tm	ppm	0.02	0	0	0.04	0.50	0.46	0.16	0.09	0.11	0.14	0.19	1.7
U	ppm	0.02	0	0	0.43	3.68	3.25	1.71	0.71	1.17	1.65	2.10	0.7
V	ppm	2	0	0	11	759	748	115	124	31	59	163	2.5
W	ppm	0.2	2	3	0.1	9.0	8.9	1.6	1.3	0.8	1.2	2.0	3.3
Y	ppm	0.1	0	0	2.5	31.1	28.6	9.6	5.9	6.2	7.6	10.5	2.1
Yb	ppm	0.02	0	0	0.26	3.27	3.01	1.12	0.59	0.78	0.94	1.35	1.6
Zn	ppm	1	0	0	2	49	47	6	6	4	4	6	5.5
Zr	ppm	1	0	0	34	648	614	306	143	198	266	406	0.6
pH		0.1	0	0	4.4	7.3	2.9	5.4	0.5	5.1	5.4	5.7	0.6
TDS	mg/Kg	20	0	0	30	1341	1311	140	173	69	95	153	5.5

Table 9. Statistical data for regolith samples from the Carson Volcanics (n = 116). Boxed values show analytes with the highest or lowest concentrations for all regolith data

	Unit	*LLD*	*No. < LLD*	*% < LLD*	*Minimum*	*Maximum*	*Range*	*Mean*	*SD*	*25 pctl*	*Median*	*75 pctl*	*Skewness*
Au	ppb	1	107	92	<0.5	3	3						
Ag	ppm	0.05	89	77	<0.05	0.13	0.13						
Al_2O_3	%	0.01	0	0	1.19	22.44	21.25	11.81	4.36	9.96	12.51	14.59	-0.7
As	ppm	0.5	1	1	<0.5	48.4	48.4	12.8	10.1	5.3	10.1	17.0	1.4
Ba	ppm	0.2	0	0	12.0	923.6	911.6	248.0	181.0	111.1	222.7	344.3	1.2
Be	ppm	0.05	0	0	0.06	5.11	5.05	1.09	0.60	0.80	1.08	1.34	2.7
Bi	ppm	0.01	0	0	0.02	0.59	0.57	0.10	0.09	0.05	0.08	0.11	3.5
C	ppm	0.01	0	0	0.13	3.27	3.14	0.69	0.54	0.37	0.54	0.78	2.56
CaO	%	0.01	5	4	<0.005	4.11	4.11	0.67	0.91	0.09	0.27	0.88	2.1
Cd	ppm	0.02	73	63	<0.02	0.21	0.20	0.02	0.03	0.01	0.01	0.03	
Ce	ppm	0.02	0	0	7.34	263.52	256.18	52.11	30.07	34.51	49.37	63.86	3.2
Co	ppm	0.1	0	0	0.8	122.7	121.9	45.4	28.1	24.9	47.3	67.0	0.2
Cr	ppm	5	0	0	9	376	367	102	66	61	91	121	1.7
Cs	ppm	0.1	0	0	0.2	12.8	12.6	1.0	1.2	0.6	0.8	1.2	7.7
Cu	ppm	1	0	0	2	265	263	75	46	36	84	106	0.4
Dy	ppm	0.02	0	0	0.68	30.66	29.98	4.03	3.06	2.72	3.64	4.68	6.1
Er	ppm	0.02	0	0	0.47	16.26	15.79	2.42	1.63	1.71	2.22	2.80	5.7
Eu	ppm	0.02	0	0	0.17	9.37	9.20	1.06	0.92	0.62	0.93	1.34	6.6
Fe_2O_3	%	0.02	0	0	1.58	50.00	48.42	20.16	11.10	12.77	19.19	27.90	0.3
Ga	ppm	0.1	0	0	1.7	49.4	47.7	19.5	7.9	16.1	20.5	24.6	-0.2
Gd	ppm	0.02	0	0	0.63	33.18	32.55	3.97	3.28	2.39	3.53	4.66	6.4
Ge	ppm	0.05	0	0	0.09	1.78	1.69	1.02	0.28	0.88	1.04	1.19	-0.2
Hf	ppm	0.1	0	0	4.1	18.6	14.5	8.1	2.6	6.3	7.8	9.0	1.6
Ho	ppm	0.02	0	0	0.14	6.08	5.94	0.83	0.61	0.58	0.76	0.96	6.0
In	ppm	0.005	2	2	<0.005	0.240	0.240	0.080	0.038	0.060	0.081	0.100	0.4
K_2O	%	0.01	0	0	0.01	3.59	3.59	0.41	0.52	0.09	0.24	0.53	3.1
LOI	%	0.01	0	0	0.63	13.07	12.44	6.64	2.70	5.28	6.77	8.39	-0.2
La	ppm	0.02	0	0	3.40	183.65	180.25	18.92	17.18	12.48	16.50	21.08	7.8
Li	ppm	0.1	0	0	2.9	31.4	28.5	15.2	6.4	11.3	15.3	19.0	0.1
Lu	ppm	0.01	0	0	0.09	2.14	2.05	0.37	0.21	0.29	0.35	0.42	5.3
MgO	%	0.01	0	0	0.02	3.40	3.38	0.63	0.71	0.16	0.36	0.70	1.9
MnO	ppm	0.01	9	8	<0.01	0.57	0.57	0.17	0.13	0.07	0.17	0.24	0.7
Mo	ppm	0.1	0	0	0.3	7.1	6.8	1.3	1.1	0.6	1.0	1.9	2.3
Na_2O	%	0.01	0	0	0.01	3.67	3.66	0.49	0.79	0.05	0.15	0.58	2.4
Nb	ppm	0.1	0	0	2.4	15.1	12.7	7.8	2.1	6.7	8.0	9.2	-0.1
Nd	ppm	0.02	0	0	3.16	177.34	174.18	18.76	16.75	12.27	16.91	21.72	7.6
Ni	ppm	1	0	0	2	94	92	40	20	28	42	52	-0.1
P_2O_5	%	0.002	0	0	0.011	0.246	0.235	0.093	0.052	0.056	0.088	0.127	0.6

Table 9. continued

	Unit	*LLD*	*No. < LLD*	*% < LLD*	*Minimum*	*Maximum*	*Range*	*Mean*	*SD*	*25 pctl*	*Median*	*75 pctl*	*Skewness*
Pb	ppm	0.5	0	0	1.8	43.5	41.7	14.3	8.3	8.9	12.5	18.3	1.2
Pd	ppb	1	114	98	<1	2	2						
Pr	ppm	0.01	0	0	0.85	45.02	44.17	4.80	4.24	3.16	4.32	5.47	7.6
Pt	ppb	1	109	94	<1	4							
Rb	ppm	0.1	0	0	1.5	194.9	193.4	26.2	27.5	7.9	17.6	35.0	2.8
S	ppm	0.005	2	2	<0.005	0.030	0.028	0.016	0.007	0.010	0.017	0.020	0.4
SO_3	%	0.01	16	14	<0.01	0.07	0.07	0.02	0.01	0.01	0.02	0.02	1.3
Sb	ppm	0.05	0	0	0.08	2.98	2.90	0.54	0.50	0.26	0.36	0.56	2.3
Sc	ppm	2	2	2	<2	60	59	27	13	20	29	36	-0.2
Se	ppm	0.5	31	27	<0.5	3.6	3.6	1.0	0.7	0.3	0.9	1.4	1.4
SiO_2	%	0.01	0	0	24.61	95.68	71.07	57.73	16.51	46.27	53.59	66.77	0.7
Sm	ppm	0.02	0	0	0.70	35.67	34.97	3.99	3.41	2.52	3.66	4.59	7.2
Sn	ppm	0.2	0	0	0.4	3.5	3.1	1.5	0.5	1.2	1.5	1.7	0.6
Sr	ppm	0.1	0	0	2.5	160.4	157.9	37.2	35.8	10.5	22.5	51.9	1.5
Ta	ppm	0.02	0	0	0.19	1.11	0.92	0.64	0.17	0.55	0.64	0.74	-0.1
Tb	ppm	0.01	0	0	0.11	5.16	5.05	0.64	0.51	0.42	0.58	0.76	6.4
Te	ppm	0.05	61	53	<0.05	0.35	0.35						
Th	ppm	0.02	0	0	2.53	23.57	21.04	6.82	3.49	4.96	6.06	7.25	2.7
TiO_2	%	0.01	0	0	0.15	1.94	1.79	1.03	0.40	0.76	1.10	1.29	-0.3
Tl	ppm	0.02	1	1	<0.01	0.80	0.79	0.20	0.13	0.09	0.18	0.27	1.4
Tm	ppm	0.02	0	0	0.08	2.34	2.26	0.36	0.23	0.27	0.34	0.42	5.7
U	ppm	0.02	0	0	0.65	4.44	3.79	1.61	0.68	1.19	1.46	1.78	2.3
V	ppm	2	0	0	10	932	922	385	222	243	359	541	0.3
W	ppm	0.2	1	1	<0.2	3.2	3.1	1.0	0.5	0.7	0.9	1.1	2.2
Y	ppm	0.1	0	0	4.2	166.2	162.0	21.9	16.4	14.5	19.9	25.8	6.2
Yb	ppm	0.02	0	0	0.56	14.76	14.20	2.44	1.48	1.86	2.21	2.75	5.4
Zn	ppm	1	0	0	3	155	152	35	27	15	30	48	1.5
Zr	ppm	1	0	0	154	729	575	306	102	239	285	341	1.7
pH		0.1	0	0	4.4	6.8	2.4	6.0	0.5	5.6	6.2	6.4	-0.8
TDS	mg/Kg	20	0	0	48	744	696	220	172	107	156	236	0.2

Table 10. Statistical data for regolith samples from the Warton Sandstone (n = 73)

	Unit	*LLD*	*No. < LLD*	*% < LLD*	*Minimum*	*Maximum*	*Range*	*Mean*	*SD*	*25 pctl*	*Median*	*75 pctl*	*Skewness*
Au	ppb	1	72	99	<1	3	3						
Ag	ppm	0.05	72	99	<0.05	0.05	0.05						
Al_2O_3	%	0.01	0	0	1.51	14.80	13.29	5.18	2.97	3.06	4.15	6.20	1.4
As	ppm	0.5	0	0	0.8	48.1	47.3	9.7	8.8	2.6	8.0	15.0	1.6
Ba	ppm	0.2	0	0	20.8	334.7	313.9	49.0	40.1	31.8	38.2	49.4	5.4
Be	ppm	0.05	2	3	<0.05	1.80	1.80	0.33	0.24	0.19	0.28	0.39	3.5
Bi	ppm	0.01	0	0	0.03	0.43	0.40	0.14	0.09	0.08	0.12	0.17	1.4
C	ppm	0.01	0	0	0.22	1.29	1.07	0.52	0.22	0.36	0.48	0.61	1.4
CaO	%	0.01	35	48	<0.01	1.41	1.41						
Cd	ppm	0.02	64	88	<0.02	0.29	0.29						
Ce	ppm	0.02	0	0	13.46	90.70	77.24	25.02	11.10	19.41	22.57	27.46	3.7
Co	ppm	0.1	0	0	0.9	51.0	50.1	4.0	6.6	2.0	2.7	4.2	6.1
Cr	ppm	5	0	0	8	181	173	58	47	21	41	78	1.1
Cs	ppm	0.1	0	0	0.2	2.6	2.4	0.9	0.4	0.6	0.8	1.1	1.3
Cu	ppm	1	0	0	2	71	69	6	8	3	4	6	7.8
Dy	ppm	0.02	0	0	0.74	6.15	5.41	1.72	0.90	1.22	1.58	1.80	3.2
Er	ppm	0.02	0	0	0.48	3.35	2.87	1.04	0.50	0.75	0.94	1.13	2.8
Eu	ppm	0.02	0	0	0.20	2.21	2.01	0.42	0.24	0.31	0.37	0.45	5.8
Fe_2O_3	%	0.01	0	0	0.97	23.40	22.43	6.50	5.20	2.28	5.67	8.65	1.3
Ga	ppm	0.1	0	0	2.1	21.3	19.2	7.9	5.1	4.2	5.9	9.6	1.2
Gd	ppm	0.02	0	0	0.83	7.51	6.68	1.74	0.88	1.29	1.60	1.84	4.4
Ge	ppm	0.05	0	0	0.24	1.60	1.36	0.81	0.20	0.72	0.82	0.87	0.4
Hf	ppm	0.1	0	0	4.6	14.4	9.8	8.5	2.2	6.8	8.4	9.7	0.6
Ho	ppm	0.02	0	0	0.15	1.26	1.11	0.35	0.19	0.25	0.31	0.38	3.1
In	ppm	0.005	5	7	<0.005	0.094	0.094	0.031	0.024	0.013	0.020	0.040	1.1
K_2O	%	0.01	0	0	0.06	1.09	1.03	0.25	0.17	0.13	0.20	0.30	2.3
LOI	%	0.01	0	0	0.97	7.83	6.86	2.76	1.25	1.90	2.51	3.51	1.3
La	ppm	0.02	0	0	7.13	37.82	30.69	12.75	4.61	10.11	11.53	14.49	2.9
Li	ppm	0.1	0	0	2.5	26.6	24.1	6.1	3.5	4.1	5.5	6.7	3.4
Lu	ppm	0.01	0	0	0.09	0.42	0.33	0.18	0.07	0.13	0.17	0.21	1.7
MgO	%	0.01	0	0	0.02	0.95	0.93	0.08	0.11	0.05	0.06	0.07	7.7
MnO	ppm	0.01	50	68	<0.01	0.26	0.26						
Mo	ppm	0.1	0	0	0.2	4.3	4.1	1.4	1.0	0.6	1.2	2.0	0.9
Na_2O	%	0.01	0	0	0.01	3.00	2.99	0.07	0.35	0.02	0.02	0.03	8.5
Nb	ppm	0.1	0	0	2.3	12.2	9.9	5.1	1.9	3.5	4.9	6.0	1.0
Nd	ppm	0.02	0	0	5.40	38.62	33.22	9.92	4.45	7.85	9.28	10.96	4.3
Ni	ppm	1	0	0	2	37	35	7	5	4	6	9	3.4
P_2O_5	%	0.002	0	0	0.011	0.146	0.135	0.052	0.029	0.025	0.049	0.070	0.7

Table 10. continued

	Unit	*LLD*	*No. < LLD*	*% < LLD*	*Minimum*	*Maximum*	*Range*	*Mean*	*SD*	*25 pctl*	*Median*	*75 pctl*	*Skewness*
Pb	ppm	0.5	0	0	2.6	19.9	17.3	6.9	3.9	4.2	5.2	8.2	1.3
Pd	ppb	1	72	99	<1	3	3						
Pr	ppm	0.01	0	0	1.49	9.59	8.10	2.78	1.14	2.20	2.56	3.04	3.7
Pt	ppb	1	72	99	<1	3	3						
Rb	ppm	0.1	0	0	3.7	38.8	35.1	12.9	6.0	9.2	11.5	14.6	1.7
S	ppm	0.005	1	1	<0.005	0.0300	0.0300	0.0175	0.0053	0.0140	0.0200	0.0200	-0.3
SO_3	%	0.01	10	14	<0.01	0.04	0.04	0.02	0.01	0.01	0.02	0.02	0.9
Sb	ppm	0.05	0	0	0.09	1.80	1.71	0.48	0.37	0.18	0.37	0.64	1.3
Sc	ppm	2	3	4	<2	31	31	6	4	3	4	7	3.5
Se	ppm	0.5	34	47	<0.5	2.9	2.9	0.7	0.6	0.3	0.6	1.0	1.4
SiO_2	%	0.01	0	0	58.14	95.43	37.29	84.64	8.89	81.87	87.48	90.90	-1.3
Sm	ppm	0.02	0	0	0.97	7.65	6.68	1.89	0.87	1.46	1.72	2.04	4.6
Sn	ppm	0.2	0	0	0.5	2.8	2.3	1.1	0.5	0.7	0.9	1.3	1.4
Sr	ppm	0.1	0	0	3.4	158.2	154.8	13.1	19.4	6.7	8.5	12.0	6.2
Ta	ppm	0.02	0	0	0.20	0.97	0.77	0.43	0.17	0.29	0.40	0.51	0.9
Tb	ppm	0.01	0	0	0.13	1.07	0.94	0.28	0.14	0.20	0.25	0.29	3.5
Te	ppm	0.05	28	38	<0.05	0.40	0.40						
Th	ppm	0.02	0	0	2.95	17.64	14.69	7.74	3.65	5.17	6.56	8.89	1.1
TiO_2	%	0.01	0	0	0.12	1.12	1.00	0.30	0.16	0.20	0.27	0.36	2.5
Tl	ppm	0.02	0	0	0.03	0.24	0.21	0.08	0.03	0.06	0.07	0.09	2.1
Tm	ppm	0.02	0	0	0.08	0.43	0.35	0.16	0.07	0.12	0.15	0.18	2.3
U	ppm	0.02	0	0	0.75	3.57	2.82	1.49	0.48	1.17	1.40	1.69	1.6
V	ppm	2	0	0	15	476	461	119	103	37	87	165	1.2
W	ppm	0.2	1	1	<0.2	5.8	5.8	1.1	0.9	0.6	0.9	1.2	3.0
Y	ppm	0.1	0	0	4.3	33.5	29.2	9.9	5.3	6.7	8.7	10.5	2.9
Yb	ppm	0.02	0	0	0.60	3.00	2.40	1.13	0.44	0.82	1.05	1.27	2.2
Zn	ppm	1	0	0	3	65	62	7	9	4	5	6	5.7
Zr	ppm	1	0	0	170	535	365	327	82	270	318	378	0.4
pH		0.1	0	0	4.3	6.2	1.9	5.3	0.5	5.0	5.4	5.7	-0.5
TDS	mg/Kg	20	0	0	30	225	195	91	46	54	84	117	0.9

Table 11. Statistical data for regolith samples from the Elgee Siltstone (n = 10)

	Unit	*LLD*	*No. < LLD*	*% < LLD*	*Minimum*	*Maximum*	*Range*	*Mean*	*SD*	*25 pctl*	*Median*	*75 pctl*	*Skewness*
Au	ppb	1	10	100	<1	<1	0						
Ag	ppm	0.05	10	100	<0.05	<0.05	0						
Al_2O_3	%	0.01	0	0	1.42	8.74	7.32	4.72	2.63	2.29	4.47	7.28	0.3
As	ppm	0.5	0	0	1.0	18.8	17.8	4.1	5.4	1.5	2.2	4.5	2.8
Ba	ppm	0.2	0	0	29.2	288.7	259.5	128.6	103.0	43.4	75.3	255.0	0.7
Be	ppm	0.05	0	0	0.06	0.90	0.84	0.42	0.29	0.22	0.31	0.67	0.7
Bi	ppm	0.01	0	0	0.05	0.32	0.27	0.14	0.09	0.06	0.11	0.23	0.9
C	ppm	0.01	0	0	0.19	0.86	0.67	0.53	0.23	0.38	0.48	0.72	0.2
CaO	%	0.01	5	50	<0.01	0.02	0.02						
Cd	ppm	0.02	10	100	<0.01	<0.01	0						
Ce	ppm	0.02	0	0	11.61	65.19	53.58	30.86	17.30	19.38	22.26	40.75	1.0
Co	ppm	0.1	0	0	1.1	6.1	5.0	3.2	1.9	1.1	2.9	4.8	0.2
Cr	ppm	5	0	0	11	108	97	32	29	14	21	39	2.3
Cs	ppm	0.1	0	0	0.5	3.5	3.0	1.7	1.1	0.6	1.4	2.3	0.7
Cu	ppm	1	0	0	3	18	15	6	5	3	4	4	2.5
Dy	ppm	0.02	0	0	0.73	3.15	2.42	1.92	0.75	1.32	1.96	2.33	0.1
Er	ppm	0.02	0	0	0.43	1.92	1.49	1.18	0.44	0.85	1.20	1.45	0.0
Eu	ppm	0.02	0	0	0.15	0.79	0.64	0.46	0.21	0.30	0.43	0.66	0.2
Fe_2O_3	%	0.02	0	0	1.41	12.11	10.70	3.29	3.22	1.60	2.07	3.24	2.8
Ga	ppm	0.1	0	0	2.4	17.5	15.1	6.7	4.7	3.1	5.6	9.5	1.5
Gd	ppm	0.02	0	0	0.72	3.59	2.87	2.00	0.90	1.33	1.77	2.68	0.5
Ge	ppm	0.05	0	0	0.05	1.19	1.14	0.86	0.32	0.81	0.95	1.02	-2.0
Hf	ppm	0.1	0	0	3.4	19.8	16.4	11.1	5.0	7.0	11.4	14.6	0.2
Ho	ppm	0.02	0	0	0.15	0.65	0.50	0.40	0.15	0.28	0.42	0.46	0.1
In	ppm	0.005	2	20	<0.005	0.080	0.080	0.019	0.023	0.007	0.013	0.020	2.5
K_2O	%	0.01	0	0	0.14	2.28	2.14	0.84	0.84	0.20	0.50	1.59	1.0
LOI	%	0.01	0	0	0.69	4.58	3.89	2.24	1.13	1.36	2.29	2.90	0.8
La	ppm	0.02	0	0	6.55	33.64	27.09	15.77	8.58	9.73	12.44	19.15	1.2
Li	ppm	0.1	0	0	3.0	9.0	6.0	6.2	2.0	4.6	6.4	7.7	-0.2
Lu	ppm	0.01	0	0	0.07	0.34	0.27	0.20	0.08	0.15	0.19	0.27	0.1
MgO	%	0.01	0	0	0.02	0.62	0.60	0.22	0.22	0.07	0.16	0.22	1.4
MnO	ppm	0.01	5	50	<0.01	0.010	0.010						
Mo	ppm	0.1	0	0	0.3	2.1	1.8	0.6	0.5	0.3	0.5	0.6	2.9
Na_2O	%	0.01	0	0	0.01	0.08	0.07	0.03	0.02	0.02	0.03	0.05	1.0
Nb	ppm	0.1	0	0	2.3	8.7	6.4	5.4	2.1	3.7	5.0	7.4	0.3
Nd	ppm	0.02	0	0	4.39	25.57	21.18	12.51	7.03	7.86	8.86	16.65	0.8
Ni	ppm	1	1	10	<1	12	12	6	4	3	6	10	0.1
P_2O_5	%	0.002	0	0	0.014	0.064	0.050	0.029	0.015	0.021	0.024	0.033	1.8

Table 11. continued

	Unit	*LLD*	*No. < LLD*	*% < LLD*	*Minimum*	*Maximum*	*Range*	*Mean*	*SD*	*25 pctl*	*Median*	*75 pctl*	*Skewness*
Pb	ppm	0.5	0	0	2.7	13.6	10.9	6.6	3.8	3.4	6.2	9.2	0.8
Pd	ppb	1	9	90	<1	1	1						
Pr	ppm	0.01	0	0	1.28	7.20	5.92	3.48	1.93	2.17	2.56	4.58	0.9
Pt	ppb	1	9	90	<1	1.0	1.0						
Rb	ppm	0.1	0	0	10.1	97.7	87.6	41.2	32.3	15.3	31.7	60.4	0.9
S	ppm	0.005	0	0	0.011	0.022	0.011	0.016	0.004	0.014	0.015	0.020	0.1
SO_3	%	0.01	5	50	<0.01	0.02	0.02	0.01	0.01	0.01	0.01	0.02	0.8
Sb	ppm	0.05	0	0	0.10	0.97	0.87	0.36	0.28	0.18	0.26	0.58	1.4
Sc	ppm	2	2	20	<2	10	10	4	3	2	4	6	1.0
Se	ppm	0.5	7	70	<0.5	1.7	1.7						
SiO_2	%	0.01	0	0	73.43	96.01	22.58	88.07	7.00	82.25	89.47	93.76	-1.0
Sm	ppm	0.02	0	0	0.83	4.41	3.58	2.32	1.18	1.49	1.78	3.10	0.7
Sn	ppm	0.2	0	0	0.6	1.7	1.1	1.1	0.4	0.7	1.1	1.5	0.3
Sr	ppm	0.1	0	0	3.7	23.7	20.0	10.7	6.8	5.9	8.3	17.2	1.0
Ta	ppm	0.02	0	0	0.17	0.76	0.59	0.47	0.20	0.32	0.44	0.70	0.2
Tb	ppm	0.01	0	0	0.13	0.54	0.41	0.32	0.13	0.22	0.31	0.41	0.4
Te	ppm	0.05	7	70	<0.05	0.20	0.20						
Th	ppm	0.02	0	0	2.83	13.74	10.91	7.39	3.71	4.41	6.39	11.30	0.6
TiO_2	%	0.01	0	0	0.12	0.43	0.31	0.26	0.10	0.17	0.26	0.34	0.4
Tl	ppm	0.02	0	0	0.04	0.43	0.39	0.19	0.14	0.06	0.17	0.26	0.7
Tm	ppm	0.02	0	0	0.06	0.30	0.24	0.19	0.07	0.14	0.18	0.24	-0.2
U	ppm	0.02	0	0	0.65	3.18	2.53	1.70	0.79	1.21	1.46	2.27	0.7
V	ppm	2	0	0	17	217	200	44	61	17	25	33	3.1
W	ppm	0.2	0	0	0.4	1.7	1.3	0.9	0.4	0.6	0.9	1.2	0.6
Y	ppm	0.1	0	0	3.9	17.9	14.0	11.1	4.2	8.0	11.5	13.7	-0.1
Yb	ppm	0.02	0	0	0.53	2.16	1.63	1.32	0.47	1.00	1.24	1.66	0.2
Zn	ppm	1	0	0	4	11	7	7	2	5	7	8	0.5
Zr	ppm	1	0	0	141	827	686	444	204	288	427	567	0.4
pH		0.1	0	0	4.3	5.5	1.2	5.1	0.5	4.8	5.3	5.5	-1.1
TDS	mg/Kg	20	0	0	42	249	207	94	65	51	66	111	1.8

Table 12. Statistical data for regolith samples from the Pentecost Sandstone (n = 141). Boxed values show analytes with the highest or lowest concentrations for all regolith data

	Unit	*LLD*	*No. < LLD*	*% < LLD*	*Minimum*	*Maximum*	*Range*	*Mean*	*SD*	*25 pctl*	*Median*	*75 pctl*	*Skewness*
Au	ppb	1	139	99	<1	2	2						
Ag	ppm	0.05	132	94	<0.05	0.10	0.10						
Al_2O_3	%	0.01	0	0	0.94	13.00	12.06	4.40	1.90	3.23	4.09	5.06	1.9
As	ppm	0.5	2	1	<0.5	25.9	25.9	8.0	6.4	2.4	6.4	11.7	0.9
Ba	ppm	0.2	0	0	28.3	407.2	378.9	70.1	57.3	42.3	50.4	71.5	3.4
Be	ppm	0.05	11	8	<0.05	0.87	0.87	0.26	0.17	0.15	0.24	0.35	1.1
Bi	ppm	0.01	0	0	0.03	0.46	0.43	0.13	0.08	0.08	0.11	0.17	1.6
C	ppm	0.01	0	0	0.18	1.68	1.50	0.54	0.23	0.40	0.50	0.59	2.4
CaO	%	0.01	72	51	<0.01	0.04	0.04						
Cd	ppm	0.02	132	94	<0.01	0.10	0.10						
Ce	ppm	0.02	0	0	14.88	49.01	34.13	25.14	6.90	20.64	23.74	28.24	1.3
Co	ppm	0.1	0	0	0.7	7.3	6.6	2.2	1.2	1.4	2.0	2.5	1.9
Cr	ppm	5	0	0	7	191	184	56	41	23	46	77	1.3
Cs	ppm	0.1	0	0	0.3	2.6	2.3	1.0	0.5	0.6	0.9	1.1	1.5
Cu	ppm	1	3	2	<1	26	26	4	3	3	3	4	4.0
Dy	ppm	0.02	0	0	0.89	16.38	15.49	1.69	1.33	1.30	1.46	1.73	9.8
Er	ppm	0.02	0	0	0.48	8.23	7.75	1.04	0.67	0.81	0.92	1.06	9.0
Eu	ppm	0.02	0	0	0.23	3.20	2.97	0.44	0.28	0.32	0.38	0.49	7.2
Fe_2O_3	%	0.02	0	0	1.07	21.44	20.37	5.48	3.70	2.47	4.87	7.37	1.3
Ga	ppm	0.1	0	0	1.5	27.3	25.8	7.2	3.8	4.7	6.3	8.8	2.2
Gd	ppm	0.02	0	0	0.39	15.53	15.14	1.79	1.29	1.34	1.53	1.88	8.8
Ge	ppm	0.05	0	0	0.17	1.35	1.18	0.85	0.17	0.79	0.86	0.94	-0.9
Hf	ppm	0.1	0	0	3.9	25.0	21.1	10.2	3.9	7.8	9.3	11.5	1.8
Ho	ppm	0.02	0	0	0.17	3.13	2.96	0.35	0.25	0.27	0.31	0.36	9.5
In	ppm	0.005	10	7	<0.005	0.102	0.102	0.024	0.017	0.013	0.020	0.030	1.7
K_2O	%	0.01	0	0	0.11	2.32	2.21	0.38	0.34	0.20	0.26	0.40	3.3
LOI	%	0.01	0	0	0.39	6.60	6.21	2.34	0.95	1.72	2.27	2.70	1.2
La	ppm	0.02	0	0	7.68	24.48	16.80	12.88	3.33	10.80	12.33	14.16	1.3
Li	ppm	0.1	0	0	2.9	29.5	26.6	6.2	2.8	4.7	5.7	6.7	4.7
Lu	ppm	0.01	0	0	0.07	0.90	0.83	0.18	0.08	0.14	0.16	0.19	5.8
MgO	%	0.01	0	0	0.03	0.45	0.42	0.09	0.05	0.06	0.08	0.10	4.1
MnO	ppm	0.01	116	82	<0.01	0.04	0.04						
Mo	ppm	0.1	0	0	0.2	2.7	2.5	1.1	0.6	0.6	0.9	1.4	0.9
Na_2O	%	0.01	0	0	0.01	0.13	0.12	0.02	0.02	0.02	0.02	0.03	4.2
Nb	ppm	0.1	0	0	1.8	9.8	8.0	4.6	1.5	3.7	4.3	5.0	1.3
Nd	ppm	0.02	0	0	5.79	20.63	14.84	10.11	3.08	7.88	9.14	11.42	1.3
Ni	ppm	1	3	2	<1	18	18	5	3	3	5	7	1.3
P_2O_5	%	0.002	0	0	0.010	0.113	0.103	0.042	0.020	0.026	0.039	0.054	0.9

Table 12. continued

	Unit	*LLD*	*No. < LLD*	*% < LLD*	*Minimum*	*Maximum*	*Range*	*Mean*	*SD*	*25 pctl*	*Median*	*75 pctl*	*Skewness*
Pb	ppm	0.5	0	0	2.1	21.5	19.4	6.4	3.2	4.5	5.5	7.2	2.0
Pd	ppb	1	141	100	<1	<1	0						
Pr	ppm	0.01	0	0	1.65	5.73	4.08	2.83	0.82	2.25	2.62	3.20	1.4
Pt	ppb	1	140	99	<1	2	2						
Rb	ppm	0.1	0	0	7.8	87.4	79.6	20.5	11.4	14.3	17.2	23.2	2.9
S	ppm	0.005	0	0	0.006	0.025	0.019	0.015	0.003	0.013	0.014	0.017	-0.1
SO_3	%	0.01	44	31	<0.01	0.05	0.05	0.01	0.01	0.01	0.01	0.02	1.7
Sb	ppm	0.05	0	0	0.07	1.51	1.44	0.47	0.33	0.22	0.38	0.57	1.4
Sc	ppm	2	24	17	<2	14	14	4	2	2	3	4	1.7
Se	ppm	0.5	64	45	<0.5	4.2	4.2						
SiO_2	%	0.01	0	0	60.16	97.23	37.07	86.86	5.82	84.64	87.75	90.61	-1.5
Sm	ppm	0.02	0	0	1.03	4.32	3.29	1.90	0.60	1.49	1.70	2.13	1.4
Sn	ppm	0.2	0	0	0.4	2.4	2.0	0.9	0.4	0.7	0.8	1.0	2.0
Sr	ppm	0.1	0	0	2.7	39.8	37.1	8.7	4.8	6.4	7.6	9.2	3.8
Ta	ppm	0.02	0	0	0.16	0.84	0.68	0.37	0.11	0.30	0.35	0.41	1.5
Tb	ppm	0.01	0	0	0.16	2.77	2.61	0.28	0.23	0.21	0.24	0.29	9.7
Te	ppm	0.05	49	35	<0.05	0.50	0.50						
Th	ppm	0.02	0	0	2.54	24.66	22.12	7.60	3.16	5.63	7.19	8.77	2.3
TiO_2	%	0.01	0	0	0.10	0.58	0.48	0.26	0.09	0.21	0.24	0.28	1.5
Tl	ppm	0.02	0	0	0.04	0.33	0.29	0.10	0.04	0.07	0.09	0.11	2.4
Tm	ppm	0.02	0	0	0.06	1.05	0.99	0.16	0.09	0.13	0.14	0.17	7.9
U	ppm	0.02	0	0	0.60	3.28	2.68	1.54	0.49	1.22	1.46	1.73	1.1
V	ppm	2	0	0	4	292	288	84	66	29	66	121	1.0
W	ppm	0.2	4	3	<0.2	8.8	8.8	1.0	0.8	0.6	0.8	1.1	6.3
Y	ppm	0.1	0	0	4.3	93.1	88.8	9.7	7.6	7.5	8.4	9.9	9.6
Yb	ppm	0.02	0	0	0.54	6.45	5.91	1.13	0.54	0.89	1.02	1.20	7.0
Zn	ppm	1	0	0	2	29	27	5	3	4	5	7	3.8
Zr	ppm	1	0	0	146	1046	900	414	168	317	377	470	1.8
pH		0.1	0	0	4.6	5.9	1.3	5.3	0.3	5.2	5.3	5.5	-0.4
TDS	mg/kg	20	0	0	30	204	174	59	27	42	51	66	2.4

Table 13. Lithogeochemical data for bedrock lithologies from the Balanggarra area. NA – not analysed

	Carson Volcanics (n = 37)[a]		*Carson Volcanics, Roadside Hill (213111)[b]*	*King Leopold Sandstone, King Edward River (213117)[c]*	*Bastion Group regolith (213351)[d]*
	Average wt%	**SD**			
SiO_2	52.13	1.40	51.12	96.91	64.29
TiO_2	1.12	0.28	1.33	0.08	0.68
Al_2O_3	14.15	0.72	14.22	0.87	18.15
Fe_2O_3	12.10	1.83	14.12	1.24	5.22
MnO	0.18	0.03	0.19	0.02	0.03
MgO	5.70	1.63	5.14	0.12	1.8
CaO	8.06	2.72	7.71	0.15	0.18
Na_2O	3.11	1.31	3.04	0.07	0.35
K_2O	1.02	0.57	1.27	0.16	4.41
P_2O_5	0.14	0.04	0.178	0.017	0.037
SO_3	NA	NA	0.07	0.003	0.01
LOI	2.30	1.10	1.96	0.16	5.15
	ppm unless otherwise shown				
Ag	0.08	0.06	<0.05	<0.05	<0.05
As	5.0	7.8	4	1.2	3.9
Au (ppb)	NA	NA	<1	<1	2
Ba	533.0	324.0	670.3	33.3	541.5
Be	0.8	0.2	0.74	<0.05	2.22
Bi	NA	NA	0.02	<0.01	0.31
C	NA	NA	<0.01	0.11	0.39
Cd	NA	NA	0.08	<0.02	<0.02
Ce	36.6	9.1	42.4	19	0.31
Co	52.0	6.0	47.8	1.6	14.9
Cr	124.8	116.4	58	10	69
Cs	0.5	0.4	0.37	0.14	10.6
Cu	97.3	97.4	96.6	4.9	4
Dy	4.6	1.2	5.47	0.75	3.73
Er	2.7	0.7	3.19	0.42	2.21
Eu	1.2	0.3	1.47	0.2	0.91
Ga	19.1	2.7	20.2	0.8	3.73
Gd	4.7	1.2	5.46	1.16	4.28
Ge	1.0	0.5	1.17	0.72	1.69
Hf	3.5	0.8	4	2.9	6.6
Ho	0.9	0.2	1.06	0.13	0.8
In	0.1	0.0	0.079	<0.005	0.043
La	17.3	4.3	19.4	9.1	46.49
Li	21.8	10.7	23.8	2.1	31.4
Lu	0.4	0.1	0.46	0.06	0.35
Mo	0.7	0.7	0.5	0.3	0.7
Nb	6.0	1.6	7.1	1.4	12.7
Nd	19.7	5.0	23.7	7.5	34.45
Ni	68.9	47.5	49.9	3.3	31
Pb	9.0	13.6	9.2	1.6	10.4
Pd (ppb)	NA	NA	<1	<1	<1

Table 13. continued

	Carson Volcanics (n = 37)[a]		*Carson Volcanics, Roadside Hill (213111)[b]*	*King Leopold Sandstone, King Edward River (213117)[c]*	*Bastion Group regolith (213351)[d]*
Pr	4.8	1.1	5.43	2.05	10.15
Pt (ppb)	NA	NA	<1	<1	<1
Rb	32.0	18.2	44.1	5	205.4
S	0.03	0.01	0.02	0.03	0.012
Sb	0.2	0.3	0.06	0.07	0.48
Sc	32.1	3.1	35	<10	17
Se	NA	NA	0.6	<0.5	<0.5
Sm	4.4	1.1	4.85	1.16	5.67
Sn	1.0	0.0	1	<1	3.3
Sr	197.9	134.8	207.8	9.2	44.3
Ta	0.4	0.1	0.4	0.1	1.05
Tb	0.7	0.2	0.87	0.13	0.6
Te	NA	NA	<0.05	<0.05	<0.05
Th	3.1	0.8	3.51	4.7	18.13
Tl	0.2	0.1	0.24	<0.02	0.87
Tm	0.4	0.1	0.54	0.09	0.31
U	0.7	0.2	0.87	0.81	3.43
V	246.6	42.0	299	12	96
W	NA	NA	<1	<1	1.6
Y	25.0	6.1	29.4	4	20.9
Yb	2.6	0.6	3.28	0.37	2.19
Zn	96.4	28.0	105	4	42
Zr	125.2	29.1	146	116	258

NOTES: a) Average and standard deviation of 37 analyses (K Orth, written comm., 2014)
b) See Table 21
c) See Table 21
d) MGA 3₀08216E 8₃11516N

The breakdown of phenocryst phases such as olivine, clinopyroxene and feldspar in the early stages of weathering to form regolith in areas of outcrop can account for the depletion in Rb–Na_2O, and Ni. At the same time, an increase in the concentration of resistate phases such as monazite, rutile, and zircon can explain the increase in Th and HFSE. There is little change in the concentration of SiO_2, Al_2O_3 or Fe_2O_3, probably due to the development of clay minerals such as kaolinite ($Al_2Si_2O_5(OH)_4$) after feldspar, and some ferruginization. The enrichment in chalcophile elements during chemical weathering (Smith et al. 1989; Smith and Singh, 2007) could be due to the development of secondary iron oxide minerals after base metal sulfides, as reported by Smith et al. (1987).

Colluvium shows similar multi-element patterns to regolith from areas of outcrop, which is consistent with colluvium being found immediately downslope from areas of outcrop. However, the Rb–Na_2O interval is more markedly depleted relative to fresh bedrock, and Th, HFSE and Cr are at correspondingly higher concentrations. Elevated Fe_2O_3 indicates more extensive ferruginization has taken place. The pattern for alluvium is broadly similar to that of colluvium, but the decrease in chalcophile elements could mean that secondary chalcophile-rich minerals have broken down. Residual regolith represents the most intense phase of chemical weathering, with slight variations in Al_2O_3 possibly indicating some formation of Al-rich oxides such as gibbsite ($Al(OH)_3$) or boehmite (AlO(OH)). This level of chemical weathering may also involve crystallization of secondary base metal iron-rich oxides (Smith et al., 1987). There is also a pronounced depletion in REE, especially the HREE. The low mineral/melt partition coefficients for olivine, pyroxene and feldspar in terms of REE (Rollinson, 1993, table 4.1), means that REE are preferentially partitioned into the glass or mesostasis of fine-grained volcanic rocks. Thus, chemical weathering should mobilize REE early in the weathering cycle due to the metastable nature of the groundmass. However, as this is not what was observed from areas of Carson Volcanics (Fig. 18a,b), intense weathering associated with the development of residual regolith must involve the breakdown of secondary REE-bearing minerals that formed earlier in the weathering cycle.

King Leopold Sandstone

A similar approach has been used to assess regolith from the King Leopold Sandstone, by comparing the chemistry of regolith to an analysis of fresh sandstone from north of Kalumburu (213117; Table 13). For regolith in areas of outcrop, only MgO, Na_2O and Cu are depleted relative to bedrock (Fig. 19a). Aluminium, HFSE, V, Cr, Pb, Zn and the chalcophile elements are all relatively enriched, but as concentrations are low in fresh rock, any enrichments or depletions must be viewed with caution (Table 8). For colluvium (Fig. 19b), Rb, Ba, K_2O, MgO, Na_2O, and some base metals (e.g. Cu) are depleted. Vanadium, Cr, Pb, Ni, chalcophile elements and the REE (HREE > LREE) are enriched. Alluvium is broadly similar to colluvium (Fig. 19c), but the LREE and some HREE (Gd) are, in this case, depleted relative to bedrock. Both Al_2O_3 and Fe_2O_3 are less enriched relative to colluvium.

The chemical maturity (i.e. SiO_2-rich nature) of the King Leopold Sandstone means that it is less susceptible to chemical weathering. Even though feldspar is in low modal proportions, the depletion in the interval Rb–Na_2O relative to fresh bedrock is consistent with the breakdown of this phase, with the negligible change in Al_2O_3 attributed to the presence of clay, which may also account for the variable behaviour of K_2O (e.g. illite, $KAl_3Si_3O_{10}(OH)_2$). The chemistry of colluvium shows the effects of more intensive weathering, in that higher concentrations of resistate phases such as chromite, rutile, zircon and monazite affect the concentrations of Cr, HFSE and Th. The REE are also affected, the LREE more so than the HREE (cf. Carson Volcanics), but concentrations are similar to bedrock.

For mafic volcanic rocks and quartz-rich siliciclastic sedimentary rocks, there are similarities in the behaviour of element groups in response to chemical weathering. Some of these can be explained by the breakdown of rock-forming minerals (affecting lithophile elements), and the increase in resistate minerals, which results in higher concentrations of elements such as Th, HFSE and Cr. In some cases, such as the development of clay minerals after feldspar and secondary iron-rich minerals after sulfides, the breakdown products of some minerals are conserved in secondary phases. For example, Al_2O_3 from the breakdown of feldspars is preserved in clay minerals, base metals and chalcophile elements are sequestered in secondary Fe-oxides, and V and Ti from the breakdown of magnetite and ilmenite are found in rutile.

Weathering effects on REE is not seen in regolith from areas of outcrop of Carson Volcanics, and are only apparent as weak LREE enrichment in colluvium and alluvium. The depletion of REE in residual regolith from this unit indicates loss of REE during intense weathering, especially LREE (Fig. 18d). Rare earth elements behave differently in regolith from the King Leopold Sandstone, which suggests that bedrock composition has a strong influence on REE behaviour during regolith formation, whereby the LREE enrichment typical of sedimentary rocks (Rudnick and Gao, 2003) is preserved in regolith chemistry.

Regolith chemistry of individual units

The marked difference in composition of the Carson Volcanics compared to siliciclastic sedimentary rocks means that statistical analysis of regolith data as one population can obscure subtle variations in the regolith chemistry of individual units. This section discusses the statistical analysis of regolith chemistry according to lithological unit, focusing on samples with anomalous concentrations of two or more analytes. For these samples, the presence of detectable Au, Pd or Pt is also recorded (Tables 14–18).

King Leopold Sandstone

Twenty-four regolith samples from the King Leopold Sandstone have anomalous concentrations of two or more analytes (Table 14). Sample 213358, from the King Leopold Sandstone on the coast north of Kalumburu, has anomalously high MgO, Na_2O, LOI, pH (the only regolith sample with pH >7 from the project area), TDS, S and C, and low SiO_2. The chemistry of this sample, its coastal location, and the presence of shell fragments in regolith indicate it is a recent carbonate deposit. The coastal location of 213285 could also account for its high TDS and SO_3 content.

A number of regolith samples from the King Leopold Sandstone have anomalous concentrations of REE, lithophile elements, and some oxides (Table 14) and are found close to the upper contact of the sandstone with the Carson Volcanics (213244, 213246 – with detectable Au, Pd and Pt, 213557, 213270, 213332, 213466, 213473, and 213609). Two of these samples (213246 and 213473) are from an area of relict regolith (R_tf) derived from the Carson Volcanics, but apart from 213557, the remaining samples are all regolith from areas of outcrop. It is possible that some of these samples may be sourced from the Carson Volcanics, although the high SiO_2 content of some samples (e.g. 89 wt % in 213270) is more consistent with a dominant input from the King Leopold Sandstone and minor mafic volcanic input.

A second group of samples has anomalous concentrations of $Al_2O_3 \pm Fe_2O_3 \pm TiO_2$, transition elements, some base metals and REE (e.g. 213235, 213236, 213272, 213313, 213326, 213438, 213451, and 213606). Site observations indicate a high proportion of ferruginous lag, Fe-rich granules and nodules, ferruginous duricrust, or ferruginized lithic fragments, and as some of these samples are from the area of ferricrete (R_tf) in the northern part of the King Leopold Sandstone, they could represent eroded and transported Carson Volcanics mixed with King Leopold Sandstone. A smaller number of samples from areas of outcrop have anomalous concentrations of analytes such as K_2O, Rb, Th, and some REE (213226, 213294, 213373, 213616). Site observations include the presence of more silt-rich material and only weak ferruginization, and these regolith samples may represent more feldspathic parts of the King Leopold Sandstone.

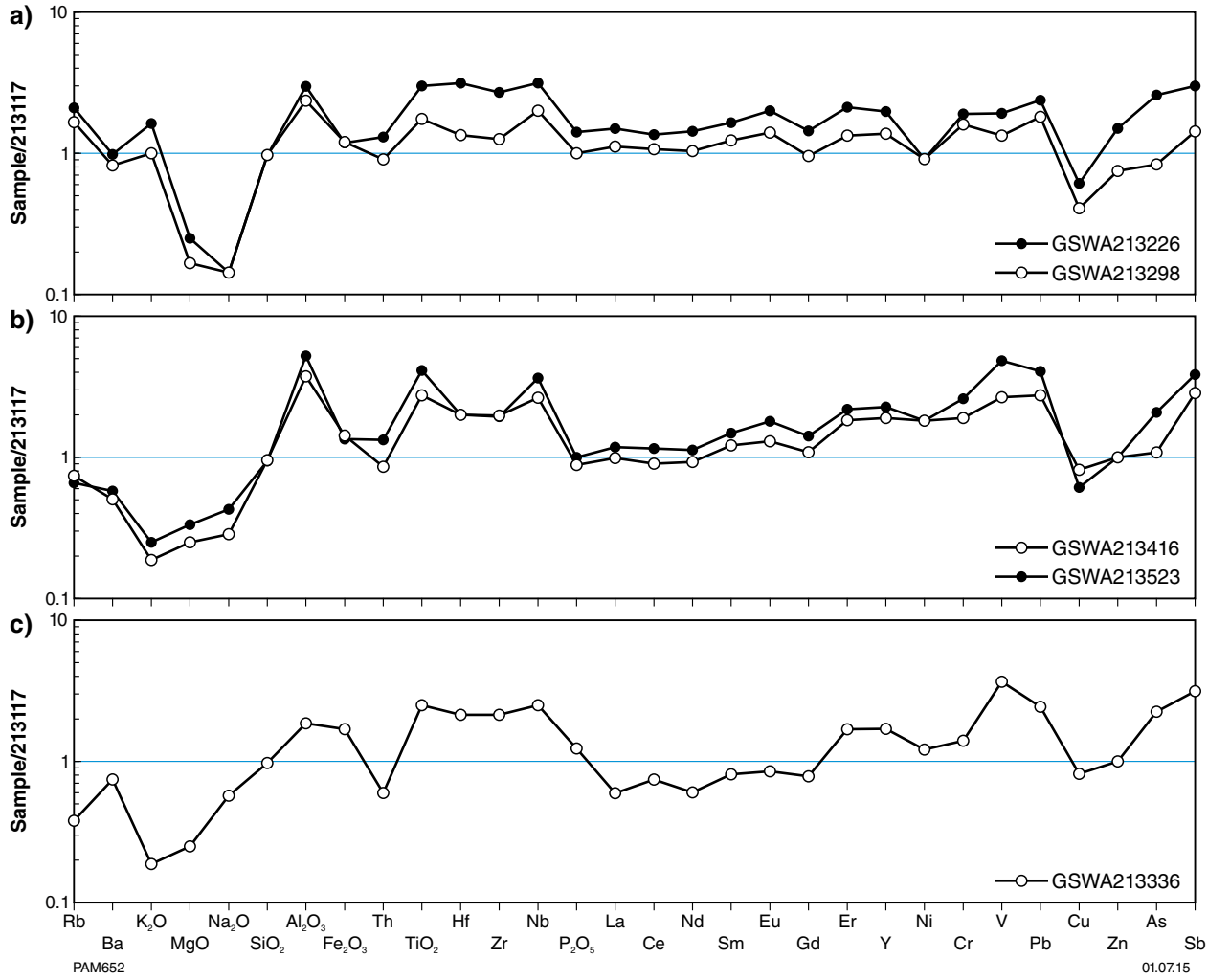

Figure 19. Multi-element spider diagrams summarizing the chemistry of regolith from the King Leopold Sandstone relative to fresh bedrock. Normalizing composition is King Leopold Sandstone from north of Kalumburu (GSWA213117; Table 13): a) regolith from areas of outcrop; b) colluvium; c) alluvium

Carson Volcanics

Regolith from the Carson Volcanics has the highest concentrations in the project area of a number of major element oxides (Al_2O_3, Fe_2O_3, MgO, Na_2O, P_2O_5, and TiO_2), chalcophile elements, transition elements, base metals, and REE (Table 9), including sample 213316, which has the highest concentration of Cu (265 ppm), Zn (155 ppm), and REE (e.g. La = 183.65 ppm, Yb = 14.76 ppm). Fourteen samples with anomalous concentrations of lithophile elements such as K_2O, Cs, Rb, Th, U, and some HFSE (e.g. Zr; Table 15) are found close to either the upper or lower contacts of this unit, and it is likely that these sites are either in the adjacent sedimentary units, or have received detritus eroded from them. Samples 213218 and 213245 are distant from the contact, and as sedimentary material is recorded at both sites, it is likely that regolith has been derived from intercalated siliciclastic rocks. Several of these samples have unusually low concentrations of Al_2O_3, Nb and Ta, typical of regolith derived from siliciclastic sedimentary rocks.

Twelve samples have anomalous concentrations of labile components such as MgO, Na_2O, Sr and Rb. Apart from colluvial samples 213500 and 213547, these samples are all from regolith in areas of outcrop. As these components are susceptible to chemical weathering (Fig. 18a,b), the preservation of labile components indicates that they represent regolith that has undergone relatively little chemical weathering. Seven samples, most of which are from areas of outcrop, have anomalous concentrations of Al_2O_3, Cr, Th, HFSE (Zr, Nb, Ta), chalcophile elements (As, Bi), or some REE. Ferruginized lithic fragments, lag, duricrust, and nodules are common at sample sites, and it is likely these are examples of residual regolith derived by in situ weathering of the Carson Volcanics.

Table 14. Samples with anomalous concentrations of two or more analytes for regolith from the King Leopold Sandstone in the Balanggarra project area. Anomalous samples are those that have outlier or extreme concentrations for box and whisker plots using all regolith geochemical data for this unit. Occurrence of Au, Pd or Pt also tabulated, but other censored data not considered. REE represented by La, Ce, Nd, Sm, Eu, Tb, Er, Yb and Y

GSWA	*Site*	*Easting*	*Northing*	*Regolith*	*Anomalously high*	*Anomalously low*	*Site notes*	*Interpretation*
213226	M3410	259888	8425644	Outcrop	K_2O, Ni, Rb		Well-sorted quartz-rich lithic sand. Some silty clay	More clay-rich version of sandstone
213235	M3436	274595	8431536	Outcrop	S, Bi, In, Sr		Ferricrete; pisolite lag; ferruginous granules and sandstone fragments	Close to residual–relict unit
213236	M3494	268919	8445949	Residual–relict	Al_2O_3, Be, Co, In, Ni, Pb, Sb		Well-developed pisolite-rich lag at surface	Close to residual–relict unit
213244	M3430	244419	8429458	Outcrop	Ce, La		Ferruginized metasedimentary fragments downhole	Close to contact with Carson Volcanics
213246	M3558	277554	8475906	Residual–relict	TiO_2, Al_2O_3, MgO, Co, Ni, Be, Ce, Eu, Ga, Ge, In, La, Li, Nd, Rb, Sm, Tb, Er, Yb, Y, Sr, Nb, Ta, Th, Bi, Cs, Sn, Pb		Nodular ferricrete and abundant ferruginous nodules and some ferruginized lithic fragments	Close to contact with Carson Volcanics
213252	M3512	258884	8450028	Colluvium	Be, Co		Weak ferruginization of lithics	Transported regolith close to contact with Carson Volcanics
213270	M3317	245246	8410820	Outcrop	Ba, Co, Cu, MgO, Na_2O, Rb, Sr, Zn			Upper contact of Carson Volcanics
213272	M3543	268294	8465801	Outcrop	Al_2O_3, Ga		Ferricrete and less common ferruginized siliciclastic rock fragments	Close to residual–relict unit
213285	M3555	264170	8475041	Residual–relict	SO_3, TDS			Close to coast
213294	M3515	273088	8450502	Outcrop	Ba, Ce, K_2O, La, Nd, SO_3, Sr, Th, U		Quartzite outcrop. No ferruginization	Possibly more feldspathic?
213313	M3474	259758	8440907	Residual–relict	Al_2O_3, Fe_2O_3, Be, Co, Cu, Pb, Zn, Ga, In, Ni, Sc, V	SiO_2	Nodular ferricrete fragments in hole	Close to residual–relict unit
213326	M3550	268984	8470749		Al_2O_3, Cr, Sb, Bi, Ga, In, Pb, Sn, Th		Pisolites and ferruginized nodules. Some ferricrete	R_tf unit
213332	M3288	245970	8405448	Outcrop	Ba, Ce, Co, Cu, Er, Eu, K_2O, Li, MgO, Na_2O, Nd, Ni, Rb, Sm, Tb, Tl, Y, Yb, Zn			Upper contact of Carson Volcanics
213358	M3556	268409	8475345	Outcrop	LOI, MgO, Na_2O, SO_3, pH, TDS, S, C (8.8)	Ge, SiO_2		Carbonate
213373	M3478	279284	8439968	Outcrop	K_2O, Rb, Sr		Weakly ferruginized lithic fragments on surface	Possibly more feldspathic?
213438		272760	8465738		TiO_2, Al_2O_3, Be, Co, Ga, Li, Ni, Pb, Er, Yb, Y, Nb, Ta, Sb, Bi, Cs, Sn, Th		Pisolite-rich lag and ferruginized lithic fragments	R_tf unit
213451	M3537	273540	8461422	Colluvium	Be, Co, Li, Nb, Pb, Er, Sn		Ferruginized lithic fragments. Possible mafic fragments	R_tf unit

Table 14. continued

GSWA	Site	Easting	Northing	Regolith	Anomalously high	Anomalously low	Site notes	Interpretation
213466	M3377	240389	8419627	Outcrop	K_2O, La, Rb			Upper contact of Carson Volcanics
213473	M3545	278129	8465724	Residual–relict	TiO_2, Al_2O_3, MgO, LOI, Ba, Be, Ce, Co, Cu, Pb, Sc, Cs, Eu, Ga, Ge, La, Li, Nd, Ni, Rb, Sm, Tb, Er, Yb, Y, Th, Tl, Nb, Ta, Bi, Sn		Fe-rich and abundant clay	Close to contact with Carson Volcanics
213483	M3492	259438	8445765	Outcrop	P_2O_5, Sb		Minor Fe granules	Close to coast
213557	M3516	279755	8451757	Colluvium	Au, Pd, Pt, Al_2O_3, Ba, Ce, Co, Cr, Cu, Er, Eu, Ga, Ge, La, Li, MgO, Na_2O, Nd, Ni, Sc, Sm, Sr, Tb, Y, Zn, TDS	SiO_2		Upper contact of Carson Volcanics
213606	M3435	269379	8430277	Colluvium	Al_2O_3, Ce, Cs, Er, Ge, La, Li, Nb, Nd, Ni, Sm, Sn, Tb, Co, Y		Clay veneer in places with rare ferricrete blocks	Transported mafic regolith?
213609	M3472	249314	8440104	Outcrop	Cu, La,Er, Eu, Nd, SO_3, Sm, Tb, Y, Zn, TDS, C			Upper contact of Carson Volcanics
213616	M3459	279770	8435877	Outcrop	Ce, La, Nd, Sr			Possibly more feldspathic?

Table 15. Samples with anomalous concentrations of two or more analytes for regolith from the Carson Volcanics in the Balanggarra project area. Anomalous samples are those that have outlier or extreme concentrations for box and whisker plots using all regolith geochemical data for this unit. Occurrence of Au, Pd or Pt also tabulated, but other censored data not considered. REE represented by La, Ce, Nd, Sm, Eu, Tb, Er, Yb and Y

GSWA	Site	Easting	Northing	Regolith	Anomalously high	Anomalously low	Site notes	Interpretation
213218	M3445	318957	8431362	Colluvium	Au, Pt, Be, Bi, Cs, K_2O, Pb, Rb, Sb, Th, U, W		Fe granules and nodules (lag). Ferruginized fine-grained sedimentary rock fragments	
213227	M3157	255607	8385081	Outcrop	MgO, Na_2O, Sr		Outcrop and thin regolith	
213245	M3383	269289	8420449	Outcrop		Al_2O_3, Nb, Ta, Ga		Sedimentary unit?
213257	M3465	309363	8436887	Alluvium	As, Pb		Ferricrete fragments	
213266	M3195	255097	8390132	Outcrop	MgO, Na_2O, Sr		Proximal colluvium on plateau. Hill location	
213268	M3381	259999	8419829	Outcrop	Al_2O_3, Er, Eu, La, Nd, SO_3, Sm, Tb, Y, Yb, TDS		In situ duricrust. Ferruginized lithics and some ferricrete	
213274	M3385	279609	8421273	Outcrop	P_2O_5, Sb		Fine deflation lag of pisoliths and mafic lithic fragments	
213276	M3318	249802	8410386	Outcrop	C, TDS		Small ridge. Outcrop. Abundant lithics	

Table 15. continued

GSWA	Site	Easting	Northing	Regolith	Anomalously high	Anomalously low	Site notes	Interpretation
213278	M3292	264513	8405653	Colluvium	Pb, Sb		Fe-pisolites at surface and a few downhole	
213281	M3480	289288	8440317	Outcrop	C, TDS		Scattered boulders of mafic volcanics. Minor quartz vein material	
213286	M3114	240695	8380352	Outcrop	MgO, Na_2O		Thin stony regolith on Carson Volcanics	
213302	M3192	240449	8389457	Outcrop	MgO, Na_2O, Zn		Occasional vein quartz	
213308	M2693	262707	8330501	Outcrop	K_2O, Cs, Rb, Th, U			Possibly from the Warton Sandstone
213310	M3415	284995	8426370	Colluvium	Pb, Sb		Lithics and Fe-nodules. Proximal colluvium within basalt outcrop	
213312	M3295	280602	8406445	Alluvium		Al_2O_3, Ga		
213316	M3352	265331	8416101	Outcrop	Ba, Be, Ce, Cu, Er, Eu, La, MgO, Na_2O, Nd, Ni, Sm, Tb, Y, Yb, Zn		Flat-lying hill top. Some ferricrete	
213320	M3038	261328	8370792	Outcrop	Hf, Zr	Al_2O_3, Ga	Base of sandstone hill	Part of the Warton Sandstone?
213343	M3316	239975	8410730	Outcrop	C, K_2O, TDS			
213346	M3460	285146	8435479	Outcrop	Au, Pd, Pt, C, Cr, Ni, Sr, TDS		Burnt out. Slight cracking of soil here. Quartzite fragments on surface	
213354	M3315	234352	8409955	Outcrop	C, TDS			
213368	M3290	255053	8406027	Outcrop	Au, MgO, Na_2O		Hilltop plateau. Abundant mafics at surface and downhole	
213372	M2945	265221	8359470	Outcrop		Al_2O_3, Ga, Ge		Possibly from the Warton Sandstone
213388	M3319	255391	8411049	Outcrop	C, TDS, Y		Plateau. Outcrop and abundant lithics. Proximal colluvium	
213390	M3120	270897	8380483	Outcrop	Bi, Cs, K_2O, La, MgO, Nd, Rb, Sn, Ta, Th, Tl, U, W		Slate outcrop	Part of Warton Sandstone
213396	M3194	250839	8389466	Outcrop	C, LOI, Ta			
213400	M3518	289034	8451745	Outcrop	Cr, Pb, Sb	Ge	Lithic granules and some Fe-rich nodules	
213405	M3155	245786	8385351	Outcrop	Na_2O, Rb		Thin veneer of colluvium on plateau	
213409	M3552	279251	8470931	Outcrop	Pt, Bi, Th, U, Cr		Nodular ferricrete at surface, possibly residual over flat outcrop	
213417	M3161	276330	8386721	Alluvium	K_2O, Cs, Rb, Th		Sandy and silty regolith on flat plain	
213424	M3538	279286	8460937	Alluvium	W, TDS		Clay matrix. Some Fe-coated granules at surface	
213440	M3321	264345	8410928	Outcrop	Bi, Cr, Ga, Hf, In, Nb, Sn, Ta, Th, U, Zr	Ge	Heavy cover of ferricrete nodules. Fragments up to 10 cm	

Table 15. continued

GSWA	*Site*	*Easting*	*Northing*	*Regolith*	*Anomalously high*	*Anomalously low*	*Site notes*	*Interpretation*
213447	M3547	287774	8466161	Residual–relict	As, Bi, Cr, Mo, Sb, U		Deflation lag. Fe-coated mafic clasts	
213452	M3517	283400	8451343	Outcrop	Ba, Rb, Tl		Carson Volcanics outcrop. Occasional vein quartz	
213454	M3529	278794	8456223	Colluvium		Al_2O_3, Nb, Ta		Possibly from the Warton Sandstone
213459	M3154	241276	8384982	Outcrop	MgO, Na_2O, Sr		Aggregated clay (Carson Volcanics)	
213460	M3444	315595	8432060	Colluvium		Ta		
213464	M2598	253726	8321294	Alluvium	Cs, Ge, K_2O, MgO, Rb, Th		Slaty arkosic sandstone	Part of Warton Sandstone
213471	M3479	284598	8441864	Outcrop	Au, As, Cr		Top of rise of mafic volcanics. Abundant lithic and Fe-rich clasts	
213472	M3411	264648	8425455	Alluvium	Pt, As, Cr, Sb, U, W, C		Very thin regolith	
213494	M3258	245392	8399578	Outcrop		Al_2O_3, Nb, Ta, Ga, Sn		Possibly from the Warton Sandstone
213500	M3227	249888	8395453	Colluvium	MgO, Na_2O, TDS		Shallow regolith. Outcrop	
213505	M3380	254633	8419965	Outcrop	As, Pb, SO_3, Sb		Proximal colluvium. Lithic and ferricrete clasts	
213529	M3121	275417	8381334	Colluvium		Al_2O_3, Ta, Ga, Sn		Possibly from the Warton Sandstone
213538	M3116	250591	8380254	Outcrop	Be, Ce, Er, Nd, Sm, Tb, Yb, Y		Lithics and ferricrete on surface and downhole	
213544	M3115	246132	8379899	Outcrop	MgO, Li, Zn			
213547	M3422	319735	8426896	Colluvium	Hf, Zr, W, Th	Al_2O_3, Ga	Very fine sand	?Sedimentary unit
213552	M3073	240492	8374944	Outcrop	Na_2O, Sb		Volcanics outcrop	
213569	M3553	282965	8471479	Outcrop	As, Bi, Cr, Hf, Mo,Sb, Sn, Th, U, Zr		Conspicuous surface lag of polished granules and nodules	
213573	M3485	313865	8442579	Outcrop	Bi, Mo, Sb		Residual sand on outcrop plateau	
213587	M3497	285021	8446210	Outcrop	K_2O, Zr			Possibly from King Leopold Sandstone
213613	M3439	289412	8432082	Outcrop	C, TDS			
213619	M3353	269436	8415609	Outcrop	MgO, Na_2O		Scree slope. Abundant lithics	

Table 16. Samples with anomalous concentrations of two or more analytes for regolith from the Warton Sandstone in the Balanggarra project area. Anomalous samples are those that have outlier or extreme concentrations for box and whisker plots using all regolith geochemical data for this unit. Occurrence of Au, Pd or Pt also tabulated, but other censored data not considered. REE represented by La, Ce, Nd, Sm, Eu, Tb, Er, Yb and Y

GSWA	*Site*	*Easting*	*Northing*	*Regolith*	*Anomalously high*	*Anomalously low*	*Site notes*	*Interpretation*
213243	M3388	294325	8421117	Outcrop	Ba, Ce, Nd, Sm, Tb, Tl, TDS		Variably ferruginized lithics in depression in sandstone outcrop	Lithological variant
213271	M3502	309507	8446580	Outcrop	Be, Bi, Cr, Fe_2O_3, Ga, MgO, K_2O, Rb, Th	SiO_2	Abundant Fe-rich nodules at surface and at depth	More-mafic lithology
213279	M3123	280946	8381925	Outcrop	Er, Eu, Tb, Y, Yb, Zn		Flat lying sedimentary rocks (some Fe-rich material)	Lithological variant
213293	M3386	284273	8420955	Outcrop	Ba, K_2O		Colluvium derived from sedimentary rocks. Some ferruginization	Close to lower contact with Carson Volcanics
213306	M2989	266147	8365759	Outcrop	As, Cr, Fe_2O_3, In, P_2O_5, SO_3, Th, U, V, Sb	Ge, SiO_2	Ferruginized sandstone and ferricrete at surface and downhole	Residual or relict regolith. Towards lower contact with Carson Volcanics
213314	M3033	266321	8370008	Residual–relict	Al_2O_3, Na_2O, Ba, Be, Ce, Co, Cu, Pb, Er, Eu, Ga, Ge, In, K_2O, La, Li, MgO, Nd, Ni, Rb, Sc, Sm, Sr, Tb, TiO_2, Tl, Y, Yb, Zn	SiO_2	Base of slope. Outcropping mafic volcanics	Carson Volcanics
213335	M3521	303451	8451056	Outcrop	Ba, Bi, Ga, Hf, MgO, Tb, Th, Y	SiO_2	Flat plain (some Fe-rich material)	More-mafic lithology
213450	M3523	313330	8451482	Outcrop	Al_2O_3, Ge		Some ferruginized lithic fragments	Residual or relict regolith
213501	M3417	294951	8426552	Outcrop	C, W			
213550	M3418	299301	8426558	Outcrop	S, Sr, W			
213555	M3519	294096	8451309	Colluvium	Al_2O_3, Cr, W, S, Bi, Ga, Th		Sedimentary lithology	Residual or relict regolith
213560	M3420	309286	8426571	Residual–relict	Mo, Fe_2O_3, V, S, Sb, Bi, Th, Pb	SiO_2	Abunadnt lag of Fe-rich material, ferruginized lithic fragments close to sandstone outcrop	Residual or relict regolith
213571	M3520	298644	8451421	Colluvium	Er, Tb, Y, Yb, Bi, Ga		Thin regolith on sedimentary rock outcrop	Residual or relict regolith
213586	M3416	289446	8426080	Outcrop	Ba, Ce, Eu, K_2O, La, MgO, Nd, Rb, Sm, Tb, Tl, W		Feruginized sandstone clasts and some lag at edge of sandstone cliff	Near base of Warton Sandstone close to contact with Carson Volcanics
213614	M2550	257025	8314860	Outcrop	Ba, Rb		Weakly ferruginized lithic fragments and some vein quartz	Close to top of Warton Sandstone
213627	M3503	314186	8447222	Colluvium	Al_2O_3, Be, Ce, Co, Cs, Cu, Pb, Er, Eu, Ga, LOI, La, Li, Nb, Nd, Ni, SO_3, Sm, Sn, Ta, Tb, TiO_2, U, V, Y, Yb, Bi, C	SiO_2	Abundant ferricrete, at surface and downhole, increasing downhole	More-mafic lithology
213569	M3553	282965	8471479	Outcrop	As, Bi, Cr, Hf, Mo,Sb, Sn, Th, U, Zr		Conspicuous surface lag of polished granules and nodules	
213573	M3485	313865	8442579	Outcrop	Bi, Mo, Sb		Residual sand on outcrop plateau	
213587	M3497	285021	8446210	Outcrop	K_2O, Zr			Possibly from King Leopold Sandstone
213613	M3439	289412	8432082	Outcrop	C, TDS			
213619	M3353	269436	8415609	Outcrop	MgO, Na_2O		Scree slope. Abundant lithics	

Table 17. Samples with anomalous concentrations of two or more analytes for regolith from the Elgee Siltstone in the Balanggarra project area. Anomalous samples are those that have outlier or extreme concentrations for box and whisker plots using all regolith geochemical data for this unit. Occurrence of Au, Pd or Pt also tabulated, but other censored data not considered. REE represented by La, Ce, Nd, Sm, Eu, Tb, Er, Yb and Y

GSWA	*Site No*	*Easting*	*Northing*	*Regolith*	*Elements high*	*Site notes*	*Interpretation*
213209	M2992	279009	8365139	Outcrop	Pd, Pt, MgO, Cu	Base of sandstone outcrop. Clay–silt grade with a few variably ferruginized lithic fragments	Weakly mineralized
213234	M3360	295752	8401333	Residual–relict	As, Cu, Mo, Fe_2O_3, In, P_2O_5, Cr, V	Some Fe-rich lag, granules and nodules	In situ weathered
213259	M2903	275896	8356248	Colluvium	La, MgO	Sedimentary rocks. Regolith is at foot of steep slope. Bordering on sheetwash	Lithological variant

Table 18. Samples with anomalous concentrations of two or more analytes for regolith from the Pentecost Sandstone in the Balanggarra project area. Anomalous samples are those that have outlier or extreme concentrations for box and whisker plots using all regolith geochemical data for this unit. Occurrence of Au, Pd or Pt also tabulated, but other censored data not considered. REE represented by La, Ce, Nd, Sm, Eu, Tb, Er, Yb and Y. Only samples with extreme Co concentrations are tabulated.

GSWA	*Site*	*Easting*	*Northing*	*Regolith*	*Anomalously high*	*Anomalously low*	*Site notes*	*Interpretation*
213204	M2558	296938	8317006	Alluvium	TiO_2, Ge, W, Cs		Homogeneous silty sand derived from sedimentary rocks	
213212	M2784	306986	8341563	Outcrop	Hf, Nb		Abundant lithic fragments at surface, some ferruginized	
213216	M2864	286662	8351307	Outcrop	Cu, W		Fine sand at outcrop of quartz-rich sedimentary rock	
213221	M2862	275461	8350575	Outcrop	K_2O, W, Ba		Weathered sandstone outcrop	
213237	M3273	319553	8402117	Outcrop	C, TDS	pH		
213239	M3331	315418	8412024	Outcrop	TDS	pH		
213253	M3330	309352	8411913	Outcrop	TDS, Mo, Sb, Pb	pH	Sandy regolith near outcrop	
213258	M2656	302149	8326723	Alluvium	Al_2O_3, LOI, As, Cu, Pb, Sb, Bi, Cr, Sc, Ga, Ge, In, Th, V, Ta, C, Sn	SiO_2	Minor Fe-rich material at sandstone outcrop.	More weathered
213260	M2606	293379	8322119	Outcrop	MgO, Na_2O, K_2O, Hf, Nb, Zr, Ba, Rb, Sr, Tl, U, La, Nd, Sm, Eu, Er, Yb	Cu	Sandy material on outcrop	
213263	M3239	309734	8396814	Outcrop	Sb, In, Th		Minor Fe-rich material at quartzite outcrop	
213265	M3081	296060	8376956	Residual–relict	P_2O_5			
213275	M2951	296096	8361075	Outcrop	Cu, Pb, Ni, Zn, S		Weak ferruginization of sedimentary rock fragments	
213282	M2454	297884	8307104	Outcrop	Pb, Zn		Fe-coated and ferruginized sandstone clasts	
213284	M2608	302217	8321788	Alluvium	Al_2O_3, TiO_2, LOI, Cu, Pb, Sc, Tb, Er, Yb, Y, Nb, Ta, W, Cs, Ge, Li, Sn		Clay veneer on surface of outcrop	More weathered
213291	M2783	301780	8341888	Outcrop	Na_2O, K_2O, Hf, Ba, Sr, La, Zr		Proximal colluvial material. Fine quartz-rich sand	

Table 18. continued

GSWA	Site	Easting	Northing	Regolith	Anomalously high	Anomalously low	Site notes	Interpretation
213295	M2607	297144	8321638	Alluvium	Al_2O_3, TiO_2, LOI, Cu, Ge, Co, Ni, Sc, Tb, Er, Yb, Y, Nb, Ta, Th, U, Cs, Ga, Li, Sn		Ferruginous lag cover with granules and less common lithic fragments	More weathered
213296	M3270	304896	8401413	Colluvium	TDS	pH		
213304	M2904	282320	8355830	Outcrop	MgO, K_2O, Cu, Ba, Rb, U, Nd, Sm, Tb, Er, Yb, Y		Bouldery outcrop with abundant lithics at surface	
213363	M3236	296816	8395986	Outcrop	Ba, Sr	Ge	Lithic fragments at surface. Some ferricrete capping	
213370	M2868	306425	8352575	Outcrop	Hf, Zr	Ge	Bottom of footslope. Sheetwash	
213410	M2651	277588	8325999	Outcrop	As, Sb, U, Cr		Stony regolith. Weakly ferruginized lithic fragments	
213428	M2555	281964	8316519	Outcrop	K_2O, Hf, Zr, W, Tl, Eu		Weakly ferruginized angular lithic fragments, in sandy matrix	
213430	M2455	302949	8306515	Alluvium	TiO_2, Cu, Er, Y, Nb, Ta, W, Cs, Li, Sn, Tl	S	Small scattered sandstone outcrops. Variably ferruginized lithic clasts	
213435	M2778	277853	8341434	Colluvium	MgO, K_2O, Ba, Rb, Tl		Thin regolith, with variably ferruginized lithic fragments	
213436	M2825	301375	8346927	Outcrop	Na_2O, K_2O, Hf, Zr, Ba, Sr, La		Sandy regolith	
213458	M2700	298238	8332258	Outcrop	Pt, Sm, Eu, Tb, Er, Yb, Y		Outcropping sedimentary rock	
213462	M2863	281749	8350620	Outcrop	Al_2O_3, MgO, K_2O, SO_3, Sb, Cu, Pb, Ba, Be, Cs, Rb, Tl, U, Co, Cr, Ni, Ce, Er, Yb, Y	SiO_2	Residual sand within area of outcrop. Fine grained sedimentary rocks	Lithologically different parent rock
213463	M3042	306235	8372032	Outcrop	K_2O, Ba		Homogeneous quartz-rich sand adjacent to outcrop	
213467	M2557	292726	8315894	Outcrop	MgO, Na_2O, K_2O, Nb, Ba, Be, Cs, Rb, Sr, Tl, Ce, Nd, Sm	Cu	Residual sandy material on small plateau	
213474	M2657	307651	8326634	Outcrop	Al_2O_3, TiO_2, Sc, Cu, Pb, Ta, Cs, Li, Sn		Ferruginized lithic fragments	
213476	M2743	301747	8337032	Outcrop	Hf, Nb, Zr, Er, Yb		Variably ferruginized lithic fragments. Outcrop nearby	In situ weathering?
213482	M2559	301367	8316045	Colluvium	TiO_2, Nb, Ta, Cu, Be, Sc, Cs, Sn		Thin, clast-rich regolith at area of outcrop	
213484	M2741	292315	8336590	Outcrop	Eu, Tb, Er, Yb, Y		Sandy and gravel-rich regolith with variably ferruginized lithic fragments	
213492	M2600	263983	8319740	Outcrop	LOI, C, Pb		Weakly ferruginized sedimentary rock fragments	
213509	M3207	316271	8390903	Outcrop	Cu, Mo, Sb, Sc		Surface lag of Fe-rich granules developed on sedimentary rocks	

Table 18. continued

GSWA	*Site*	*Easting*	*Northing*	*Regolith*	*Anomalously high*	*Anomalously low*	*Site notes*	*Interpretation*
213515	M2609	307090	8321896	Alluvium	TiO_2, Sc, Ba, Be, Cu, Pb, Er, Y, Nb, Ta, Sn		Outcrop of sedimentary rock	
213518	M2508	297038	8311393	Residual–relict	Al_2O_3, TiO_2, Fe_2O_3, LOI, Ta, Pb, Be, Cs, Cu, Ga, Ge, In, Li, Sn, Th, Co, Cr, Ni, V, Er, Sc, Nb, Mo, Sb, Bi	SiO_2	Ferruginized lithic clasts in sand-dominated matrix	More weathered
213520	M2652	282233	8325285	Outcrop	Sb, Bi		Well-developed fine, dark-brown to black Fe-rich lag. Sandy regolith	
213522	M3300	303865	8405934	Outcrop	TDS	pH		
213551	M2509	302326	8311516	Residual–relict	Al_2O_3, TiO_2, Fe_2O_3, LOI, Cu, Pb, Nb, Ta, Ga, Ge, In, Li, Sn, Th, U, Co, Cr, Ni, Sc, V, Sb, Bi	SiO_2	Ferruginized lithic clasts. Flat lying area, with occasional ferricrete blocks	More weathered
213564	M2699	292014	8331972	Outcrop	Na_2O, Ba, Rb, Sr, Tl, Eu		Sandy regolith developed on thinly bedded sandstone	
213575	M3203	296943	8391449	Outcrop	MgO, P_2O_5, Sb, Ba, Be, Y		Weakly ferruginized lithic fragments. Quartz-rich sandstone	
213580	M2742	298356	8336021	Outcrop	TiO_2, Na_2O, K_2O, Nb, Zr, Ba, Rb, Sr, Tl, La, Ce, Nd, Sm, Eu, U, Yb, Y	Cu	Sandy regolith adjacent to sedimentary rocks on small plateau	
213585	M2782	296536	8341628	Outcrop	TiO_2, Nb, La, Ce, Er, Yb, Y		Sandy matrix. Localised colluvium–sheetwash	
213588	M2906	292279	8356051	Outcrop	Eu, Tb, Er, Y		Some lag of ferruginized lithic fragments. Sandy regolith (thin) over outcrop	
213589	M2696	277751	8329703	Outcrop	Ba, Sm, Eu, Tb, Y		Outcrop with clast-rich regolith. Variably ferruginized fragments	
213601	M2456	307829	8306745	Colluvium	Cs, Li		Fine sand with some sandstone clasts	
213607	M2654	292341	8326028	Outcrop	Na_2O, K_2O, Hf, Nb, Zr, Ba, Rb, Sn, Sr, U, La, Ce, Nd, Sm, Eu, Yb	Cu	Well-sorted silty sand adjacent to outcrop. No ferruginization	
213622	M2560	307223	8317527	Colluvium	Cu, Pb, Er, TiO_2, Cs, Li, Sn, Tl		Variably ferruginized angular sedimentary clasts	

Warton Sandstone

Similar to regolith derived from other quartz-rich siliciclastic sedimentary rock units, regolith from the Warton Sandstone has high SiO_2 (median value of 87.5 wt%; n = 73) and low median values for lithophile elements (Table 10). However, regolith from this unit northeast of Kalumburu has high and locally anomalous concentrations of several oxides, chalcophile elements and some lithophile elements. Three samples (213271, 213335, 213627) have anomalous lithophile element and REE contents, and two have anomalous MgO concentrations (Table 16). This chemistry indicates some mafic rock influence on regolith, yet none of the three samples is close to the lower contact with the Carson Volcanics.

Four samples (213293, 213306, 213314, and 213586) were found close to the lower contact with the Carson Volcanics. They have elevated contents of Na_2O, K_2O, lithophile elements, REE, and transition elements. The proximity to the lower contact could mean direct input from mafic volcanic rocks, or the presence of material transported from the Carson Volcanics.

Two samples (213243 and 213279) have higher concentrations of REE and some lithophile element contents, which may reflect bedrock heterogeneity. Samples 213450, 213555, 213560, and 213571 have higher chalcophile elements, Fe_2O_3, Al_2O_3 or REE. These come from sites with duricrust, and are interpreted as remnants of a ferricrete sheet, similar to that found in the northern part of the King Leopold Sandstone (*R_tf*). Three of these four samples are from the northern part of the unit, and comprise a range of regolith types, including regolith from areas of outcrop, residual–relict regolith, and colluvium.

Elgee Siltstone

Only 10 regolith samples have been collected from the Elgee Siltstone, but three of these have anomalous concentrations of two or more analytes (Table 17). The enrichment of Fe_2O_3, transition elements, and chalcophile elements in 213234 is consistent with chemical weathering, whereas higher MgO in 213209 and 213259 could indicate some local variations in bedrock chemistry. Sample 213209 contains detectable Pt and Pd, and could be weakly mineralized, consistent with anomalous Cu concentrations.

Pentecost Sandstone

There are 51 samples with anomalous concentrations of two or more analytes in the Pentecost Sandstone (Table 18), the highest proportion (41%) of samples of regolith from the major siliciclastic sedimentary units. Of these, the significance of nine samples with anomalous Zr and Hf concentrations are discussed below. However, statistical treatment of the Pentecost Sandstone data alone (i.e. Table 18) shows that these samples also have anomalous concentrations of a range of oxides, lithophile elements and REE, which is taken as evidence of regolith derived from compositionally different bedrock within the Pentecost Sandstone.

Some samples with anomalous concentrations of analytes such as Al_2O_3, LOI, chalcophile elements, transition elements, and REE have anomalously low SiO_2 contents (e.g. 213258, 213462, 213518, 213551). Ferruginous material is common at some sites, and these samples show the influence of chemical weathering. In other cases, samples with anomalous REE, HFSE, some oxides and lithophile elements (e.g. 213304, 213435, 213458 – with detectable Pt, 213515) lack elevated concentrations of either Al_2O_3 or Fe_2O_3, and ferruginized material is uncommon. These samples are from areas of outcrop, colluvium and alluvium, so regolith composition cannot be solely attributed to the effects of chemical weathering. Instead, it is more likely that regolith composition reflects the combined effects of bedrock compositional variability and chemical weathering. Four samples with anomalously low SiO_2 include 213462, which, judging by its chemistry, appears to represent a lithologically unusual part of the Pentecost Sandstone. The three other samples (213518, 213258 and 213551) have a high content of ferruginized material.

Discussion

The strong contrast in lithology between mafic volcanic rocks of the Carson Volcanics and quartz-rich siliciclastic rocks typical of the King Leopold, Warton and Pentecost Sandstones is reflected in the chemistry of regolith. Where labile components such as MgO, K_2O, Na_2O, Rb, Sr and Ni are found in elevated or anomalous concentrations in regolith from the Carson Volcanics, this indicates relatively little chemical weathering. Alternatively, where regolith sites are found near contacts with the Carson Volcanics, incorrect assigning in terms of lithological unit or input of eroded Carson Volcanics are indicated. However, where the sample site is distant from the contact, anomalous concentrations of labile elements indicate that regolith has been sourced from a different bedrock parent. For example, regolith with elevated SiO_2 but low Fe_2O_3, V and Cr found in the Carson Volcanics would be indicative of interflow sedimentary rock.

The association of Al_2O_3, TiO_2, Fe_2O_3, HFSE, chalcophile elements and some transition elements such as Cr and V in anomalous concentrations is consistent with the effects of chemical weathering. For regolith from both sedimentary and mafic igneous rocks, REE are typically depleted during weathering, but with advanced weathering to produce colluvium and alluvium, HREE can become more concentrated. A key factor in making these interpretations is integrating them with site observations. For example, in quartz-dominated sedimentary rock successions, regolith with elevated K_2O and Rb indicate more silt-rich bedrock, generally confirmed by the presence of finer grained rocks at the site. Similarly, regolith with anomalous Al_2O_3, Fe_2O_3, HFSE and chalcophile elements (generally with lower SiO_2) commonly comes from a site where there are ferruginized rock fragments, ferricrete fragments and pisolites.

The high proportion of regolith samples from the Pentecost Sandstone with two or more elements at anomalous concentrations points to the more extreme lithological diversity of this unit compared to other units of siliciclastic sedimentary rocks.

Statistical examination of regolith chemistry according to regolith type

Bedrock lithology has a strong influence on regolith chemistry, but multi-element spider plots (e.g. Figs 18 and 19) illustrate the importance of chemical weathering. Statistical analysis allows the quantitative comparison of chemistry according to regolith type (residual–relict, exposed, colluvium, alluvium), also taking into account bedrock lithology. As geochemical datasets are usually positively skewed, parametric statistical tests for comparison of populations (e.g. Student's t-test) are inappropriate, and a non-parametric approach, the Mann–Whitney U test, has been used to compare population medians (cf. Reimann et al., 2008; Morris and Verren, 2001). As this approach uses ranked data, it is less susceptible to the effects of outliers. The results of significance testing of medians at the 95% level (i.e. p = 0.05) are shown in Tables 19 and 20.

Regolith from siliciclastic sedimentary rocks

The three sandstone units in the project area (King Leopold, Warton and Pentecost Sandstones) are lithologically similar, and regolith samples from these three units have been grouped together for statistical comparison of chemistry according to regolith type (Table 19). Three samples have been excluded from the comparison, comprising the one sample from the Bastion Group (213351), a sample of tidal regolith (213495), and carbonate sample 213358 from the King Leopold Sandstone.

For regolith from siliciclastic units, some median values are low, and approach the LLD, meaning caution should be exercised in interpreting these data. Residual–relict regolith has statistically lower median values than regolith from areas of outcrop for SiO_2, K_2O, Ba and Rb, but higher median values for TiO_2, Al_2O_3, Fe_2O_3, P_2O_5, LOI, pH, all chalcophile elements, a range of lithophile elements (Be, Cs, Ga, In, Li, Sn, Th, U), the HREE, all transition and base metals, and some HFSE (Nb and Ta). The small number of samples collected from areas of residual–relict regolith compared with siliciclastic sedimentary rocks (particularly that over the King Leopold Sandstone) derived by erosion of the adjacent Carson Volcanics could have some influence on these results.

A comparison of median values for regolith from areas of outcrop and colluvium (Table 19) shows that colluvium has statistically higher median values for W, the lithophile elements Be, Li and Sn, and the transition elements Co and Ni, and lower median values for K_2O, P_2O_5, Rb, LREE, Hf and Zr. Lower K and Rb could reflect loss of these elements due to chemical weathering, consistent with higher values for Be, Sn and the transition elements. However, this is inconsistent with the lower median values for Hf and Zr, and some element variations may result from sorting of heavier minerals during transportation. Only Rb shows any statistical difference in median values for a comparison of colluvium and alluvium (possibly due to different clay contents), indicating that both these types of depositional regolith have undergone a similar degree of chemical weathering.

Regolith from the Carson Volcanics

The same statistical approach has been taken for regolith from the Carson Volcanics (Table 19), although there are only three samples of residual regolith. Despite this, the results of the Mann–Whitney U test are logical in that residual–relict regolith has statistically lower median values than regolith from areas of outcrop for MgO, Na_2O, Ba, Tl, Eu, Co, Cu, and Zn, and higher median values for Fe_2O_3, the chalcophile elements, Sn, Th, U, Cr, V, and all the HFSE. The loss of MgO and Co is consistent with weathering of minerals such as olivine and pyroxene, whereas lower Na_2O, Ba and Eu are consistent with the weathering of feldspar. Higher median values for Fe_2O_3 indicate some ferruginization, and elevated Sn, Th, U, Cr, V and HFSE can be explained by concentration of resistate metals and minerals (e.g. tin, rutile, chromite) due to chemical weathering. For both siliciclastic sedimentary rocks and the Carson Volcanics, chalcophile elements are enriched in residual–relict regolith (cf. Smith et al., 1989), but base metals and REE are unaffected.

Compared to regolith from areas of outcrop, median values for colluvium from the Carson Volcanics are higher for SiO_2 and Th, and lower for TiO_2, Al_2O_3, MgO, Na_2O, Ga, Rb, Sr, Tl, Co, Ni, Sc, V, Cu and Zn (Table 19). The increase in SiO_2 at the expense of TiO_2, Al_2O_3, MgO, and Na_2O reflects chemical weathering (the breakdown of ferromagnesian silicate phases and feldspar), which can also account for the lower median values for lithophile elements, transition elements and base metals, and the increase in Th in colluvium. However, unlike the comparison of regolith from areas of outcrop and residual–relict regolith (Table 19), there is no statistical difference in the median values for REE and HFSE. Median values for alluvium and colluvium are similar, indicating that both have undergone similar degrees of chemical weathering (cf. regolith from siliciclastic sedimentary rocks).

For both siliciclastic sedimentary rocks and mafic volcanic rocks, compositional differences between regolith from areas of outcrop relative to colluvium and residual regolith reflect chemical weathering, involving the breakdown of labile mineral phases such as ferromagnesian silicates and feldspars in mafic volcanic rocks, and feldspars in sedimentary rocks. This is accompanied by the concentration of more resistant mineral phases, causing higher concentrations of HFSE, Cr, Al_2O_3 and Fe_2O_3. The REE are relatively unaffected, possibly reflecting their low concentrations, both in terms of bedrock and rock-forming minerals.

Table 19. Results of Mann–Whitney U test for statistical comparison of median values according to regolith type, at the 95% confidence level (i.e. p <0.05). For assessing regolith over siliciclastic rocks, data for the King Leopold, Warton Sandstone, and Pentecost Sandstones have been combined. Where median values approach the LLD, results should be viewed with caution. Analytes with high proportions of censored data have been excluded. Grey cells have median values that are statistically significant at the 95% level. Boxed values are less than three times the level of detection and have not been assessed statistically. R–R is residual–relict; Coll is colluvium; All is alluvium

				Siliciclastic rocks						*Carson Volcanics*					
N				*29*	*192*	*192*	*47*	*47*	*10*	*3*	*86*	*86*	*17*	*17*	*10*
Regolith	*Unit*	*LLD*	*LLD*3*	*R–R*	*Outcrop*	*Outcrop*	*Coll*	*Coll*	*All*	*R–R*	*Outcrop*	*Outcrop*	*Coll*	*Coll*	*All*
SiO_2	%	0.01	0.03	78.05	88.5	88.5	89.98	89.98	84.94	43.7	52.66	52.66	63.47	63.47	71.71
TiO_2	%	0.01	0.03	0.38	0.24	0.24	0.24	0.24	0.39	0.99	1.55	1.55	0.98	0.98	0.69
Al_2O_3	%	0.01	0.03	6.89	3.95	3.95	4.07	4.07	6.07	13.3	12.95	12.95	11.95	11.95	9.1
Fe_2O_3	%	0.01	0.03	9.35	4.26	4.26	2.78	2.78	4.36	36.06	19.78	19.78	13.88	13.88	8.1
MgO	%	0.01	0.03	0.06	0.07	0.07	0.06	0.06	0.06	0.1	0.42	0.42	0.18	0.18	0.37
Na_2O	%	0.01	0.03	0.03	0.02	0.02	0.02	0.02	0.02	0.03	0.21	0.21	0.08	0.08	0.19
K_2O	%	0.01	0.03	0.17	0.25	0.25	0.13	0.13	0.18	0.08	0.26	0.26	0.1	0.1	0.31
P_2O_5	%	0.002	0.006	0.06	0.04	0.04	0.03	0.03	0.03	0.13	0.1	0.1	0.06	0.06	0.06
LOI	%	0.01	0.03	3.49	2.13	2.13	2.24	2.24	3.12	5.9	7.23	7.23	5.94	5.94	5.2
pH		0.1	0.3	5.7	5.3	5.3	5.5	5.5	5.5	6.2	6.2	6.2	5.9	5.9	6.1
TDS	mg/kg	20	60	72	57	57	99	99	78	138	170	170	138	138	189
As	ppm	0.5	1.5	14.3	5.3	5.3	3	3	5.1	25.8	10.4	10.4	9.2	9.2	4.1
Bi	ppm	0.01	0.03	0.20	0.10	0.10	0.10	0.10	0.20	0.30	0.10	0.10	0.10	0.10	0.10
Mo	ppm	0.1	0.3	1.9	0.9	0.9	0.6	0.6	0.8	2.8	1	1	0.8	0.8	0.5
S	%	0.005	0.015	0.020	0.020	0.020	0.020	0.020	0.010	0.030	0.010	0.010	0.020	0.020	0.020
Sb	ppm	0.05	0.15	0.70	0.30	0.30	0.30	0.30	0.40	1.00	0.40	0.40	0.50	0.50	0.30
W	ppm	0.2	0.6	1.1	0.8	0.8	1	1	1.8	1.2	0.8	0.8	0.8	0.8	1
Ba	ppm	0.2	0.6	35.8	44.7	44.7	38.2	38.2	41.4	51.6	233	233	187	187	183
Be	ppm	0.05	0.15	0.40	0.20	0.20	0.29	0.29	0.40	0.80	1.10	1.10	1.00	1.00	1.00
Cs	ppm	0.1	0.3	1.1	0.7	0.7	0.8	0.8	1.4	1.3	0.8	0.8	0.7	0.7	1.0
Ga	ppm	0.1	0.3	10.9	5.8	5.8	5.8	5.8	8.9	27.3	21.6	21.6	18.8	18.8	11.9
Li	ppm	0.1	0.3	7.0	5.0	5.0	6.2	6.2	7.1	8.2	15.9	15.9	14.3	14.3	14.7
Rb	ppm	0.1	0.3	11.1	14.3	14.3	8.7	8.7	16.2	9.1	20.8	20.8	10.1	10.1	24.9
Sn	ppm	0.2	0.6	1.4	0.8	0.8	1	1	1.5	2.3	1.5	1.5	1.5	1.5	1.1
Sr	ppm	0.02	0.06	8.1	8.1	8.1	8.2	8.2	7.2	9.4	26.7	26.7	13.3	13.3	20.9
Th	ppm	0.02	0.06	10.1	6.4	6.4	5.1	5.1	9.3	19.5	5.8	5.8	6.9	6.9	6.2
Tl	ppm	0.02	0.06	0.1	0.1	0.1	0.1	0.1	0.1	0.1	0.2	0.2	0.1	0.1	0.2
U	ppm	0.02	0.06	1.8	1.4	1.4	1.3	1.3	1.8	2.6	1.4	1.4	1.6	1.6	1.7

Table 19. continued

				Siliciclastic rocks						Carson Volcanics					
N				*29*	*192*	*192*	*47*	*47*	*10*	*3*	*86*	*86*	*17*	*17*	*10*
Regolith	*Unit*	*LLD*	*LLD*3*	*R–R*	*Outcrop*	*Outcrop*	*Coll*	*Coll*	*All*	*R–R*	*Outcrop*	*Outcrop*	*Coll*	*Coll*	*All*
La	ppm	0.02	0.06	11.4	11.7	11.7	10.8	10.8	12.5	10.6	16.9	16.9	13.4	13.4	16.5
Ce	ppm	0.02	0.06	21.7	22.7	22.7	20.3	20.3	24.1	24.1	52.1	52.1	49.8	49.8	41.2
Pr	ppm	0.01	0.03	2.5	2.6	2.6	2.3	2.3	2.6	3.2	4.4	4.4	3.6	3.6	4.4
Nd	ppm	0.02	0.06	8.7	9.1	9.1	8.2	8.2	9.1	12.1	17.4	17.4	14.1	14.1	17.4
Sm	ppm	0.02	0.06	1.6	1.7	1.7	1.6	1.6	1.8	2.6	3.8	3.8	2.9	2.9	3.6
Eu	ppm	0.02	0.06	0.3	0.4	0.4	0.3	0.3	0.4	0.5	1	1	0.8	0.8	0.7
Gd	ppm	0.02	0.06	1.5	1.5	1.5	1.4	1.4	1.7	2.3	3.9	3.9	2.9	2.9	3.3
Tb	ppm	0.01	0.03	0.2	0.2	0.2	0.2	0.2	0.3	0.4	0.6	0.6	0.5	0.5	0.5
Dy	ppm	0.02	0.06	1.4	1.5	1.5	1.5	1.5	1.64	2.5	4	4	2.9	2.9	3
Ho	ppm	0.02	0.06	0.3	0.3	0.3	0.3	0.3	0.3	0.5	0.8	0.8	0.6	0.6	0.6
Er	ppm	0.02	0.06	1	0.9	0.9	0.9	0.9	0.99	1.7	2.4	2.4	1.8	1.8	1.7
Tm	ppm	0.02	0.06	0.2	0.1	0.1	0.1	0.1	0.2	0.3	0.4	0.4	0.3	0.3	0.3
Yb	ppm	0.02	0.06	1.10	1.00	1.00	1.00	1.00	1.10	1.90	2.40	2.40	2.00	2.00	1.80
Lu	ppm	0.01	0.03	0.2	0.2	0.2	0.2	0.2	0.2	0.3	0.4	0.4	0.3	0.3	0.3
Y	ppm	0.1	0.3	8.6	8.4	8.4	8.3	8.3	9.1	14.4	21.9	21.9	15.2	15.2	16.9
Co	ppm	0.1	0.3	4.9	2	2	2.5	2.5	3	21.4	51.2	51.2	33.2	33.2	25.3
Cr	ppm	5	15	106	39.5	39.5	30	30	48	223	91	91	80	80	62
Ni	ppm	1	3	10	5	5	6	6	7	30	47	47	31	31	27
Sc	ppm	2	6	8	3	3	4	4	6	26	32	32	22	22	17
V	ppm	2	6	169	60	60	50	50	70	754	370	370	257	257	143
Cu	ppm	1	3	7	3	3	4	4	6	21	93	93	46	46	43
Pb	ppm	0.5	1.5	11.7	5.0	5.0	5.4	5.4	8.4	23.0	12.3	12.3	12.9	12.9	10.6
Zn	ppm	1	3	6	5	5	4	4	4	11	38	38	16	16	17
Hf	ppm	0.1	0.3	8.8	9	9	7.1	7.1	8.4	9.7	7.8	7.8	8.2	8.2	6.8
Nb	ppm	0.1	0.3	5.9	4.2	4.2	4.3	4.3	6.4	10.3	8	8	7.5	7.5	7.1
Ta	ppm	0.02	0.06	0.50	0.30	0.30	0.40	0.40	0.60	0.80	0.60	0.60	0.60	0.60	0.60
Zr	ppm	1	3	333	349	349	286	286	338	384	280	280	322	322	256

Table 20. Results of Mann–Whitney U test for statistical comparison of median values according to lithological unit for the King Leopold (KLS), Warton and Pentecost Sandstones, at the 95% confidence level (i.e. p <0.05). Only regolith from areas of outcrop has been used to reduce the effects of chemical weathering. Analytes with high proportions of censored data have been excluded. Grey cells have median values that are statistically significant at the 95% level. Boxed values are less than three times the level of detection and have not been assessed statistically.

	Unit	*LLD*	*LLD*3*	*KLS*	*Warton*	*Warton*	*Pentecost*	*KLS*	*Pentecost*
SiO_2	%	0.01	0.03	91.55	88.39	88.39	87.94	91.55	87.94
TiO_2	%	0.01	0.03	0.23	0.25	0.25	0.24	0.23	0.24
Al_2O_3	%	0.01	0.03	2.78	4.01	4.01	4.06	2.78	4.06
Fe_2O_3	%	0.01	0.03	2.97	5.45	5.45	4.68	2.97	4.68
MgO	%	0.01	0.03	0.03	0.06	0.06	0.08	0.03	0.08
Na_2O	%	0.01	0.03	0.03	0.02	0.02	0.02	0.03	0.02
K_2O	%	0.01	0.03	0.08	0.29	0.29	0.28	0.08	0.28
P_2O_5	%	0.002	0.006	0.03	0.05	0.05	0.04	0.03	0.04
LOI	%	0.01	0.03	1.71	2.36	2.36	2.19	1.71	2.19
pH		0.1	0.3	5.4	5.3	5.3	5.3	5.4	5.3
TDS	mg/kg	20	60	78	66	66	51	78	51
As	ppm	0.5	1.5	3.6	7.6	7.6	5.8	3.6	5.8
Bi	ppm	0.01	0.03	0.10	0.11	0.11	0.11	0.10	0.11
Mo	ppm	0.1	0.3	0.9	1.0	1.0	0.9	0.9	0.9
S	%	0.005	0.015	0.020	0.019	0.019	0.015	0.020	0.015
Sb	ppm	0.05	0.15	0.27	0.33	0.33	0.37	0.27	0.37
W	ppm	0.2	0.6	1.1	0.9	0.9	0.7	1.1	0.7
Ba	ppm	0.2	0.6	23.2	43.7	43.7	50.1	23.2	50.1
Be	ppm	0.05	0.15	0.20	0.25	0.25	0.23	0.20	0.23
Cs	ppm	0.1	0.3	0.5	0.7	0.7	0.8	0.5	0.8
Ga	ppm	0.1	0.3	4.1	5.5	5.5	6.1	4.1	6.1
Li	ppm	0.1	0.3	3.6	4.8	4.8	5.7	3.6	5.7
Rb	ppm	0.1	0.3	4.7	13.4	13.4	17.4	4.7	17.4
Sr	ppm	0.1	0.3	10.7	8.5	8.5	7.7	10.7	7.7
Sn	ppm	0.2	0.6	0.8	0.8	0.8	0.8	0.8	0.8
Th	ppm	0.02	0.06	4.77	6.46	6.46	6.79	4.77	6.79
U	ppm	0.02	0.06	1.44	1.44	1.44	1.46	1.44	1.46
La	ppm	0.02	0.06	9.45	12.68	12.68	12.56	9.45	12.56
Ce	ppm	0.02	0.06	18.67	25.65	25.65	23.65	18.67	23.65
Nd	ppm	0.02	0.06	7.39	9.66	9.66	9.19	7.39	9.19
Sm	ppm	0.02	0.06	1.43	1.81	1.81	1.75	1.43	1.75
Eu	ppm	0.02	0.06	0.29	0.39	0.39	0.39	0.29	0.39
Gd	ppm	0.02	0.06	1.31	1.67	1.67	1.54	1.31	1.54
Tb	ppm	0.01	0.03	0.21	0.27	0.27	0.24	0.21	0.24
Dy	ppm	0.02	0.06	1.29	1.63	1.63	1.47	1.29	1.47
Ho	ppm	0.02	0.06	0.27	0.32	0.32	0.31	0.27	0.31
Er	ppm	0.02	0.06	0.80	0.97	0.97	0.92	0.80	0.92
Tm	ppm	0.02	0.06	0.13	0.15	0.15	0.14	0.13	0.14
Yb	ppm	0.02	0.06	0.85	1.06	1.06	1.03	0.85	1.03
Lu	ppm	0.01	0.03	0.15	0.17	0.17	0.17	0.15	0.17
Y	ppm	0.1	0.3	7.2	9.2	9.2	8.6	7.2	8.6

Table 20. continued

	Unit	LLD	LLD*3	KLS	Warton	Warton	Pentecost	KLS	Pentecost
Co	ppm	0.1	0.3	1.5	2.3	2.3	1.9	1.5	1.9
Cr	ppm	5	15	30	39	39	43	30	43
Ni	ppm	1	3	4	5	5	5	4	5
V	ppm	2	6	58	84	84	60	58	60
Cu	ppm	1	3	3	4	4	3	3	3
Pb	ppm	0.5	1.5	4.2	4.6	4.6	5.4	4.2	5.4
Zn	ppm	1	3	4	5	5	5	4	5
Hf	ppm	0.1	0.3	7.2	8.4	8.4	9.6	7.2	9.6
Nb	ppm	0.1	0.3	3.8	4.6	4.6	4.3	3.8	4.3
Ta	ppm	0.02	0.06	0.31	0.39	0.39	0.35	0.31	0.35
Zr	ppm	1	3	266	332	332	382	266	382

Statistical comparison of siliciclastic sedimentary rocks using regolith chemistry

Despite similar mineralogy, and the overall silica-rich chemistry of the three main siliciclastic sedimentary units in the project area, bubble plots and statistical analysis of regolith chemistry have highlighted some compositional variations in bedrock. A statistical comparison of medians for regolith from the King Leopold, Warton and Pentecost Sandstones has been carried out using the Mann–Whitney U test (Reimann et al., 2008; Table 20). To minimize the effects of regolith type, only regolith samples from areas of outcrop have been included, and carbonate sample 213358 from the King Leopold Sandstone has been removed. Based on site location, chemistry and site information, six samples have been reassigned to different units.

King Leopold Sandstone compared to the Warton and Pentecost Sandstones

A comparison of medians at the 95% confidence level (Table 20) shows that there is a strong compositional contrast between the King Leopold Sandstone and both the Warton and Pentecost Sandstones. The King Leopold Sandstone has a higher median value for SiO_2 and Sr than the Warton Sandstone, and lower median values for Al_2O_3, MgO, and K_2O, as well as LOI, although some median values (e.g. MgO) are close to the level of detection. Base metal and chalcophile element median values are similar, but the majority of HFSE, lithophile elements and REE are higher in the Warton and Pentecost Sandstones compared to the King Leopold Sandstone. There is no statistical difference in median values between the King Leopold and Pentecost Sandstones for the transition elements, but Co and Ni are higher in the Warton Sandstone.

Warton Sandstone compared to the Pentecost Sandstone

There are relatively few differences in chemistry between the Warton and Pentecost Sandstones, especially in terms of major element oxides, REE and transition elements. Copper, W and Co have higher median values in the Warton Sandstone, and lower median values for HFSE (Hf and Zr) and lithophile elements (Ba, Cs, Li, Rb).

Summary

This statistical analysis highlights the chemical maturity of the King Leopold Sandstone compared to the two other major siliciclastic sedimentary rock units. This points to a fundamental change for sedimentary rocks pre- and post-deposition of the Carson Volcanics. The higher median values for elements such as Li, Cs and Rb indicate more lithic-rich lithologies in units overlying the Carson Volcanics, and higher median values for S, W and Co in the Warton Sandstone point to some chalcophile enrichment (i.e. it is more mineralized). Of the incompatible elements, only Zr and Hf have higher median values in the Pentecost Sandstone as a result of higher zircon contents.

Variations in bedrock composition traced by regolith chemistry

Understanding the extent of chemical weathering (e.g. Figs 18 and 19) means that regolith geochemical data can be used to better understand compositional variations within different lithological units. Three examples are discussed below, two from the Carson Volcanics and one from the Pentecost Sandstone.

Changes in chemistry with stratigraphic height in the Carson Volcanics

Several samples with anomalous concentrations of transition elements such as Cr, and chalcophile elements such as As, are found on or near to the lower contact of the Carson Volcanics with the King Leopold Sandstone (Figs B15b and B14a). There is an overall increase in concentration of both elements towards the bottom of the unit (Fig. 20a,b), which is also shown by MgO and Ni (Fig. 20c,d).

Concentrations of Ag, Au, Pd and Pt in regolith samples from the Carson Volcanics are commonly less than the lower level of detection (Table 9). However, of the seven samples with detectable Pt in regolith from this unit, four are within 1500 m of the lower contact (Fig. 20e), and the sample with the highest Pt concentration of 4 ppb (213346) also has the highest Cr content of 376 ppm. Similar to Pt, few regolith samples have detectable Au (Fig. 20f), yet the sample with the highest Au content in the Carson Volcanics (213471, 3 ppb) also has elevated As (35.7 ppm) and Cr (212 ppm), and regolith samples with detectable Au are found closer to the lower contact. Total dissolved solids also shows a well-developed relationship between concentration and stratigraphic height (Fig. 20g), but other elements, such as Cu (Fig. 20h), show no clear relationship.

Both Cr and As can be enriched during chemical weathering (Fig. 18d), but chemical weathering cannot account for the high MgO and Ni contents of some samples found near the base of this unit. Instead, it is argued that regolith found near the base of the Carson Volcanics is derived from less fractionated (elevated MgO and Cr), chalcophile-rich flow units, with higher precious metal contents than overlying units. Higher TDS values could mean that earlier-erupted parts of the Carson Volcanics have undergone more hydrothermal alteration. Copper mineralization has been reported from the Carson Volcanics (Marston, 1979), and the Londonderry Cu deposit is found near the base of this unit (Fig. 4). However, most regolith samples have between about 75 and 150 ppm Cu, and there is no clear relationship between Cu concentration in regolith and distance from the base of the Carson Volcanics (Fig. 20h).

Anomalous REE chemistry in regolith from the Carson Volcanics

The early stages of chemical weathering of mafic volcanic rocks involves depletion in Rb, Ba, K_2O, MgO, Na_2O and Ni, and enrichment in Al_2O_3, Fe_2O_3, HFSE and Cr. In contrast, the REE and Y are little affected (Fig. 18a,b), although they are depleted at more advanced stages of weathering (Fig. 18d). A REE index has been calculated for samples from the Carson Volcanics by summing the standard scores for all the REE plus Y. The method of calculating standard scores has been discussed by Morris and Verren (2001). By adopting this approach, as opposed to calculating the total REE content of each sample, potentially important differences in the concentrations of REE found at low concentrations (e.g. Tm, Lu) are not lost.

Two regolith samples from areas of outcrop in the middle of the Carson Volcanics (213316 and 213228) have statistically anomalous REE index values. The concentrations of Rb–MgO (but not Ba in 213316), SiO_2, Al_2O_3, Fe_2O_3, HFSE, V, Cr, Pb and chalcophile elements of these two samples are similar to typical samples of regolith found in areas of Carson Volcanics outcrop (Fig. 21), but the REE and Y are enriched in both samples (especially in 213316, the highest concentrations for the project area). Sample 213316 also has elevated Cu, Zn (the highest in the project area, 155 ppm) and Ni.

In a study of the chemistry of Cenozoic mafic volcanic flows from southeastern Victoria, Frey et al. (1978) and McDonough et al. (1985) noted that some basalts had two to three times the total REE contents of other units, yet the concentrations of other elements were similar. Price et al. (1991) also discussed the unusually high concentrations of REE, Ba and Y of basalts from southeastern Victoria area in terms of weathering, and noted that some samples had elevated Ba concentrations. Basaltic rocks with similar REE enrichments have also been reported from Hawaii (Fodor et al., 1987), and ascribed to post-magmatic hydrothermal activity associated with the formation of secondary REE-bearing minerals, such as rhabdophane [$(Ce,La)PO_4 \cdot (H_2O)$]. Scanning electron microscope work by Price et al. (1991) confirmed the presence of secondary REE minerals in high-REE basaltic flows in southeastern Australia. A Ba- and REE-enriched basalt from southeastern Victoria (Price et al., 1991) shows a remarkably similar pattern to 213316 (Fig. 21), including the enrichment relative to fresh rock in Ba and REE. Although more subdued, and the Ba anomaly is absent, the pattern for 213228 is also similar. Labile elements such as Ba are usually depleted during the early stages in regolith formation, so the enrichment in Ba and REE of 213316 is unusual, and could post-date the formation of regolith.

Both 213316 and 213268 plot on or close to northeast-trending magnetic units (Fig. 22), interpreted as mafic dykes. The affinity of these dykes is unknown, although multi-element data (Fig. 23) show the overall similarity of possible candidates such as the Hart Dolerite or the c. 500 Ma Kalkarinji LIP (Glass and Phillips, 2006) to the Carson Volcanics. Thus, none of these magmatic rocks is a likely parent to the two regolith samples. Instead, these linear features may represent conduits for hydrothermal alteration by fluids that modified, in particular, the REE chemistry of regolith after it had formed, and led in some cases to the enrichment of base metals and chalcophile elements.

Zr and Hf enrichment of units within the Pentecost Sandstone

Statistical analysis of all regolith geochemical data from the project area, as well as analysis of data from the Pentecost Sandstone alone, has identified nine regolith samples which have anomalous concentrations of Zr and Hf, including one sample (213580) with the highest concentration of Zr (1046 ppm) and Hf (25 ppm) from the project area. These nine samples form a linear array

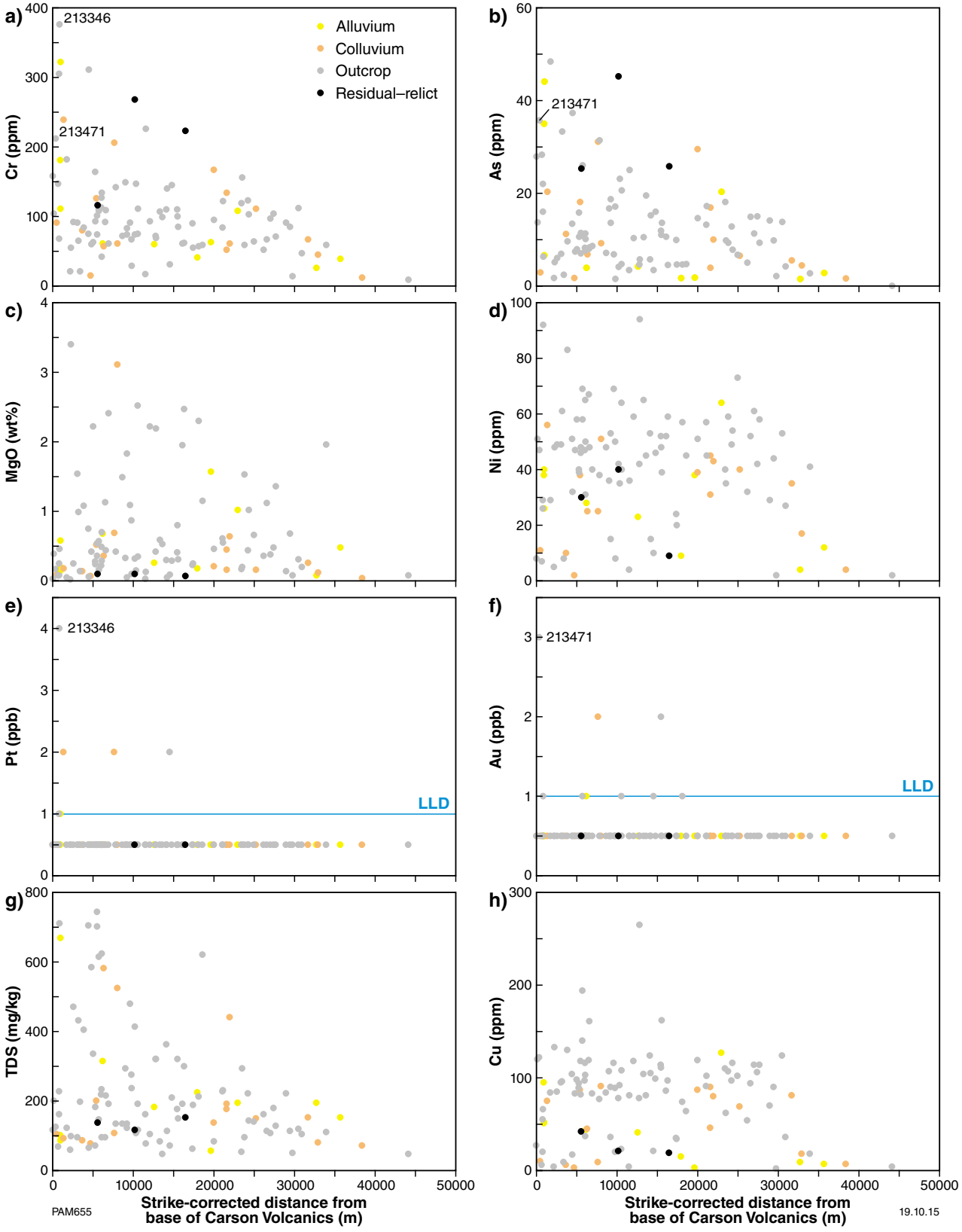

Figure 20. Analyte concentration plotted against distance of sample from the lower contact of the Carson Volcanics with the King Leopold Sandstone, corrected for strike (023°). Symbol colours show different regolith types: a) Cr (ppm); b) As (ppm); c) MgO (wt%); d) Ni (ppm); e) Pt (ppb); f) Au (ppb); g) TDS (mg/kg); h) Cu (ppm). Sample with the highest Pt concentration (GSWA213346) also has the highest Cr concentration of 376 ppm. Sample with the highest Au concentration (GSWA213471) has 35.7 ppm As and 212 ppm Cr.

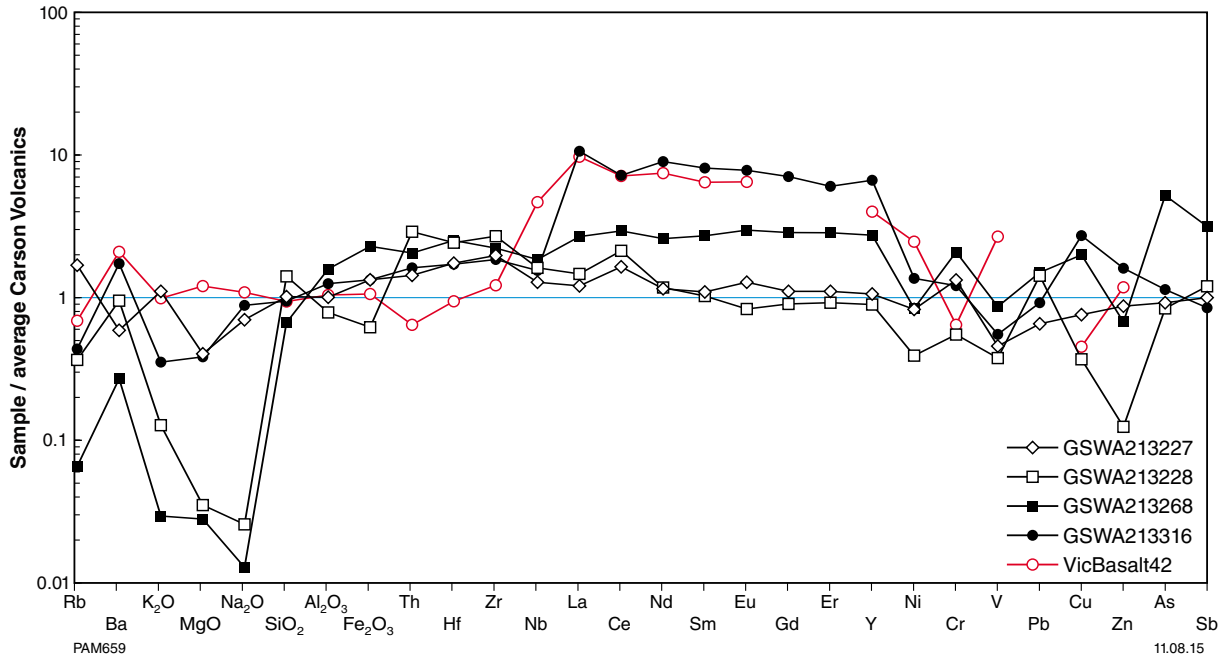

Figure 21. Spider diagram of four samples of regolith from areas of outcrop in the Carson Volcanics, normalized to the average of 37 analyses of the Carson Volcanics (K Orth, written comm., 2014; Table 13). Also shown is a sample of Cenozoic basalt (VicBasalt42) from the southeast part of Victoria (Price et al., 1991).

trending north-northwest roughly parallel to strike (Fig. B16a,d), and correspond to the more feldspathic central part of the Pentecost Sandstone (Gellatly and Sofoulis, 1969). A tenth sample (213484) has anomalous Zr, but not Hf. Of the nine samples with anomalous Zr and Hf, five also have anomalous K_2O, and two of these also have anomalous Rb. Sample 213580 also has anomalous concentrations of Na_2O, Ba and Sr, and 213260 has anomalous Tl and U. If these regolith samples reflect the composition of the bedrock, then they appear to be tracing out a lithological unit that has unusually high Zr and Hf contents, as well as high clay and silt contents (shown by elevated K_2O and Rb).

These samples do not have anomalous concentrations of other HFSE (Nb, Ta), REE or Cr, and as they are from areas of outcrop, the high Zr and Hf cannot be ascribed to the effects of chemical weathering. The association of Zr and Hf most likely represents a zircon-rich heavy-mineral unit within the Pentecost Sandstone. Zircon has a higher density (at 4.68) than many other heavy minerals, such as rutile (4.18 – 4.25), garnet (3.5 – 4.3), allanite (3.5 – 4.2), but not monazite (5.0 – 5.3; Berkman, 1989). Thus, the Zr and Hf enrichment of these nine regolith samples shows the effects of the source region of parts of the Pentecost Sandstone coupled with the effects of mechanical sorting during sediment transport. If high K_2O and Rb result from high clay contents, this is difficult to resolve with mechanical sorting, although this central part of the Pentecost Sandstone has feldspathic interbeds, and is more siltstone-rich towards the base (Gellatly and Sofoulis, 1969).

Chemistry of duricrust in the Balanggarra area

Residual–relict regolith and, in some cases, regolith in areas of outcrop has undergone varying degrees of chemical weathering, which is more obvious in chemically immature rocks such as the Carson Volcanics. The wide spacing of regolith samples collected during the Balanggarra program limits the amount of information available at each site in relation to the extent of weathering, and offers little information on the depth of weathering. More detailed examination of duricrust can provide information on the nature of chemical weathering, and the characteristics of in situ versus transported material. Furthermore, where duricrust profiles are preserved, the development of duricrust over time can be evaluated.

Duricrust is cemented regolith, or the cement only, usually found in the upper part of an in situ or transported regolith profile (Eggleton, 2001). Duricrust types can be separated based on their composition, such as ferruginous (ferricrete, lateritic duricrust), aluminous (alcrete), or calcareous (calcrete; Eggleton, 2001). Both ferruginous and aluminous duricrust are found in the Balanggarra project area, mainly over the Carson Volcanics, but also over areas of siliciclastic sedimentary rocks (Plate 1). As a complement to the regional regolith chemistry program, 26 samples of duricrust and bedrock (where available) were collected from five locations (Roadside Hill, Putairta Hill, King Edward River – Kalumburu, north Kimberley, Koolama Bay) in the north of the project area (Fig. 24).

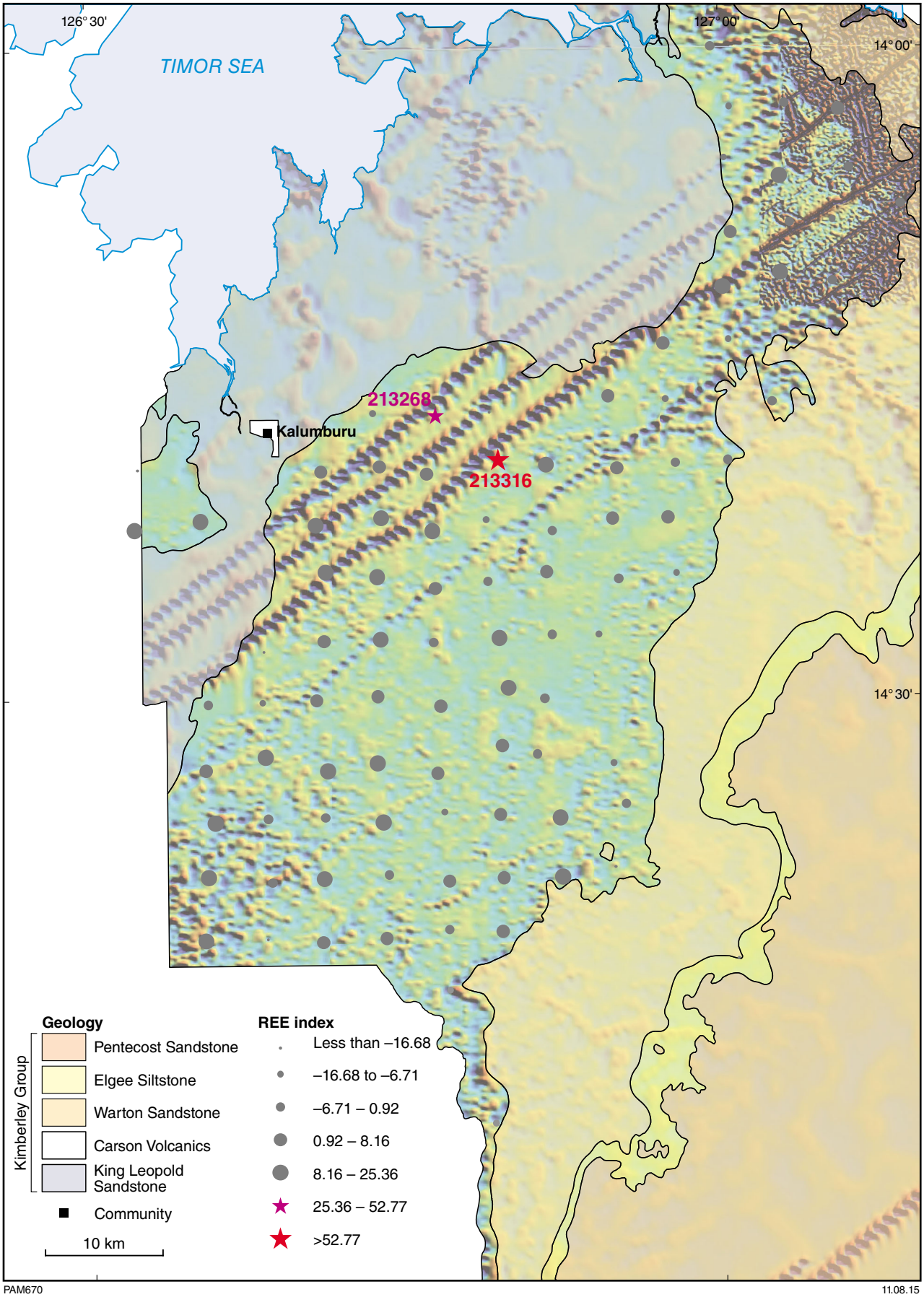

Figure 22. REE index for samples of regolith from the Carson Volcanics (see text for construction of index) shown against aeromagnetic image (first vertical derivative RTP). Northeast-trending linear features have been interpreted as dikes.

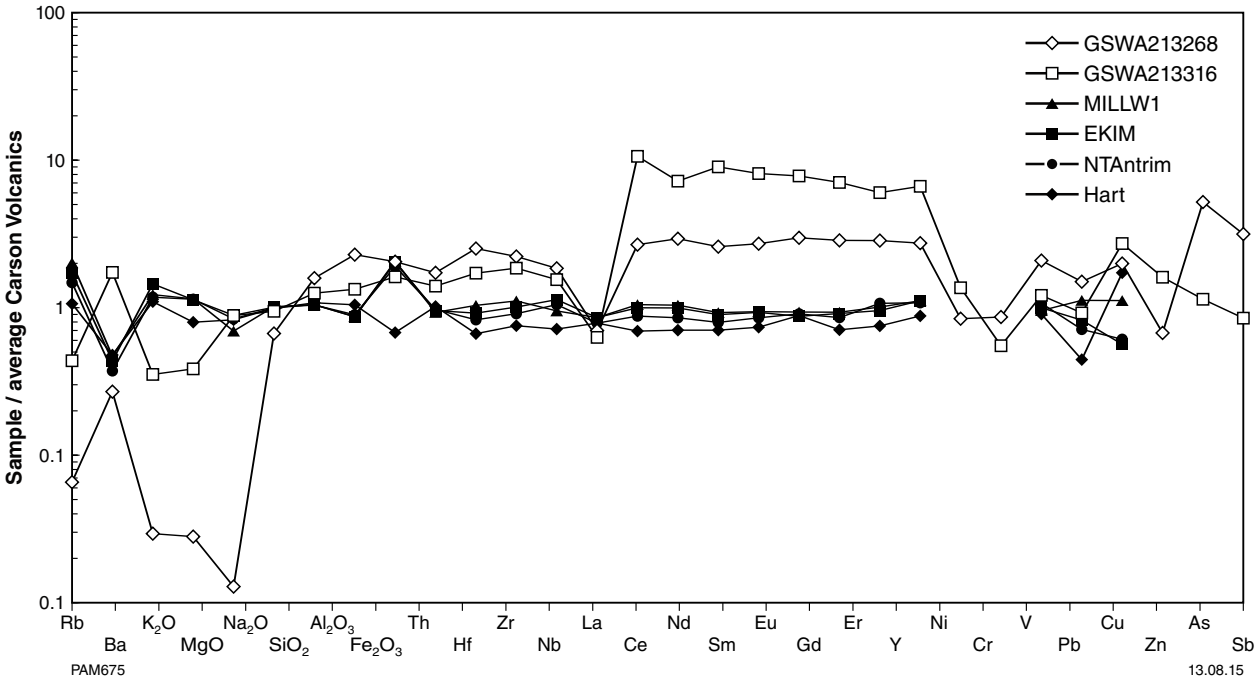

Figure 23. Spider diagram showing the chemistry of regolith samples 213316 and 213268 in relation to representative samples from the c.500 Ma Kalkarinji LIP. MILLW1 (Milliwindi Dike), EKIM (Antrim Plateau Basalt average, East Kimberley), NTAntrim (Antrim Plateau Basalt average, Northern Territory), Hart Dolerite, from Hanley and Wingate (2006). Data normalized to the average of 37 analyses of the Carson Volcanics (K Orth, written communication, 2014; Table 13)

At two locations (Roadside Hill and Putairta Hill), duricrust overlies the Carson Volcanics, whereas at King Edward River – Kalumburu duricrust overlies the King Leopold Sandstone. At Koolama Bay, duricrust is found over part of the Warton Sandstone, whereas the north Kimberley locality includes samples from both the King Leopold Sandstone and the Carson Volcanics (Table 21). At each sample site, between 1 and 3 kg of material was collected. Each sample was crushed in a Boyd jaw crusher to a nominal particle size of 0.5 mm, and a representative part then milled to <75 µm in a low-Cr steel mill. Samples were analysed using the same protocols as regolith.

Duricrust of the Carson Volcanics

Roadside Hill

At this location (Fig. 24), fresh Carson Volcanics and duricrust are exposed in a semicontinuous vertical profile extending over a vertical extent of about 70 m (Fig. 25). The top of the succession forms a plateau, which has been mapped as aluminous duricrust ($R_r x_a v_b$, Fig. 5, Plate 1). Seven samples were collected, comprising one sample of fresh bedrock and six samples of duricrust.

The Carson Volcanics at the base of the succession consists of fine-grained, weakly porphyritic bluish-grey basalt which is locally columnar jointed (213111; Fig. 25a). Overlying the basalt on the west side of the hill are blocks of ferruginized basalt in a crumbly ferruginous matrix (213102, 213110). Approximately 20 m below the top of the hill, angular duricrust fragments are found in an iron-rich matrix (213109). On the top of the hill, the regolith is heterogeneous, including fragments of altered mafic rock in a fine-grained cement (213108), as well as blocks of pisolitic and nodular duricrust with some weathered mafic rock fragments (213450).

The concentrations of some major element oxides normalized to fresh basalt (Fig. 26a) show that SiO_2 and P_2O_5 gradually decrease with stratigraphic height, and this is inversely matched by similar degrees of enrichment of TiO_2 and Al_2O_3. Although Fe_2O_3 also increases with stratigraphic height, the pattern is more erratic, with a rapid increase up to about 250 m above sea level (ASL) and then little enrichment. Loss-on-ignition shows the most dramatic change, with enrichment in samples on the plateau surface almost eight times that of fresh basalt. Elements such as Cr, As and Zr (Fig. 26b) tend to behave incompatibly during chemical weathering. The behaviour of the three elements is broadly similar, becoming more enriched with stratigraphic height, but two of them (Cr and As) show similar but inconsistent behaviour up to about 250 m ASL (cf. Fe_2O_3, Fig. 26a). All three are strongly enriched towards the top of the profile. Rare earth elements and Y show similar behaviour (Fig. 26c), with marked depletion at the base of the regolith profile relative to fresh basalt, and LREE more depleted than Er and Y. Lanthanum shows less variation in levels of enrichment with stratigraphic height. There is a greater level of enrichment for all REE and Y above 270 m, with HREE more enriched than LREE. The LREE are depleted

in the upper most part of the regolith profile (i.e. the most Al_2O_3-rich interval), but HREE continue to be enriched upwards in the profile.

A multi-element plot of fresh basalt and duricrust analyses from Roadside Hill (Fig. 27) shows data normalized to average Carson Volcanics basalt (Table 13). Fresh basalt 213111 shows little deviation from this average, apart from lower MgO, Ni, Cr, As and Sb, which is probably due to weak fractionation and less modal sulfides. The variable depletion in duricrust of Rb, Ba, K, Mg, Na and Ni can be explained by the alteration of phases such as olivine, pyroxene, and feldspar. This has also produced a decrease in SiO_2 with a minimum of 4.0 wt% in 212450. Conversely, Al_2O_3, Fe_2O_3 and TiO_2 are enriched, with the highest Al_2O_3 of 32.8 wt% found in the sample with the lowest SiO_2 (212450). Thorium and the HFSE TiO_2, Hf, Zr, and Nb are enriched relative to fresh basalt, and the duricrust samples can be divided into two groups based on the concentrations of these elements.

Samples found lower in the succession (213104, 213102, 213109, 213110) have lower Al_2O_3 and higher SiO_2 concentrations compared to the two samples on top of the plateau (212450, 213108), which also have higher Fe_2O_3 and LOI. They can also be separated in terms of REE (see also Fig. 26c), and although there is no clear separation of samples in terms of transition elements (Ni, Cr and V), samples on the plateau have higher base metals (Cu, Pb and Zn) and chalcophile elements (As and Sb). This enrichment in Al_2O_3, Th, HFSE, Cr, V and chalcophile elements of these two samples reflects more intense weathering. Chondrite-normalized REE concentrations (Fig. 28) show the overall depletion in most REE in the weathering profile, the development of a positive Ce anomaly, and the flatter REE patterns for the two more aluminous samples on the plateau surface.

Putairta Hill

Three duricrust samples were collected from Putairta Hill, approximately 19 km to the northeast of Roadside Hill. Here, ferruginous and aluminous duricrust is developed on basaltic rocks of the Carson Volcanics (Plate 1). Two of the samples (213128 and 213129; Table 21, Fig. 25g) are from the flat-lying top of the hill, and the third (213127) is from several metres below the top of the plateau (Fig. 25f). The latter comprises friable, ferruginized mafic rock fragments in a ferruginous matrix. On the plateau surface, duricrust is yellow-brown nodular material found as scattered blocks.

The spider diagram patterns for these three samples (Fig. 29) are remarkably similar to those from Roadside Hill (Fig. 27), including the separation of samples according to stratigraphic height. Thus, 213128 and 213129, collected from the plateau surface, have lower SiO_2 (1.49 and 1.53 wt%) and higher Al_2O_3 (40.2 wt% and 35.3 wt%) compared to 213127. This stratigraphic separation is also apparent for Th, HFSE, and REE.

Discussion

With the onset of weathering of basalt, labile components Rb–Na_2O are markedly depleted due to the alteration of phenocryst phases such as pyroxene, olivine and feldspar. The less drastic behaviour of Al_2O_3 is due to the retention of clay after feldspar in the weathering profile. With ongoing chemical weathering, SiO_2 decreases with increasing Al_2O_3 and stratigraphic height (Fig. 26a) due to the alteration of kaolinite to gibbsite (Freyssinet et al., 2005):

$$Al_2Si_2O_5 + 3H_2O + O_2 \rightarrow Al_2O_3{\cdot}3H_2O + 2SiO_2$$

And gibbsite to boehmite:

$$Al_2O_3{\cdot}3H_2O = 2AlO(OH) + 2H_2O$$

During these transformations, elements with high charge or ionic radii (incompatible elements; e.g. Th, HFSE, V and Cr) will become concentrated, as they are found in minerals such as monazite, rutile, zircon and chromite, which are more resistant to chemical weathering. Similarly, work by Smith et al. (1989) and Smith and Singh (2007) has shown that the weathering of Archean greenstones results in the concentration of chalcophile elements. In both areas sampled for duricrust, Pb is weakly enriched relative to average Carson Volcanics, but the other two base metals (Cu and especially Zn) are depleted. Smith and Singh (2007) discussed the distribution of base metals in laterite from the Golden Grove VHMS deposit, and noted that some base metals were hosted in iron pseudomorphs after sulfides. Thus, there is evidence of base metal mobility in the production of lateritic duricrust.

The behaviour of REE and Y in duricrust shows that all REE are strongly depleted relative to fresh basalt (Fig. 26c), and that more strongly weathered, Al-rich duricrust found at the top of the Roadside Hill location and on the plateau surface at Putairta Hill has higher REE concentrations (Figs 27, 29). Thus, within the duricrust profile, the formation of gibbsite results in an increase in REE concentrations. Furthermore, HREE are preferentially enriched relative to LREE, resulting in lower (La/Yb)CN (where 'CN' designates chondrite normalization, using the values of Sun and McDonough, 1989) with increasing Al_2O_3. The breakdown of phenocrysts is unlikely to explain the behaviour of REE because mineral–melt partition coefficients for REE and silicate minerals are usually much less than 1 (Rollinson, 1993). In a discussion of weathering profiles over basalts of the Deccan Traps, Babechuk et al. (2014) noted that weathering produces not only changes in REE concentrations, but also some fractionation. They noted that in the older Bidar weathering profile, REE were depleted relative to fresh bedrock. Babechuk et al. (2014) and Humphris (1984) have suggested that clays, resulting from weathering, retain REE, and that with increasing SiO_2 loss during lateritization, REE were progressively released. Babechuk et al. (2014) also noted an increase in Sm/Nd with increasing alteration, but offered no explanation for this behaviour.

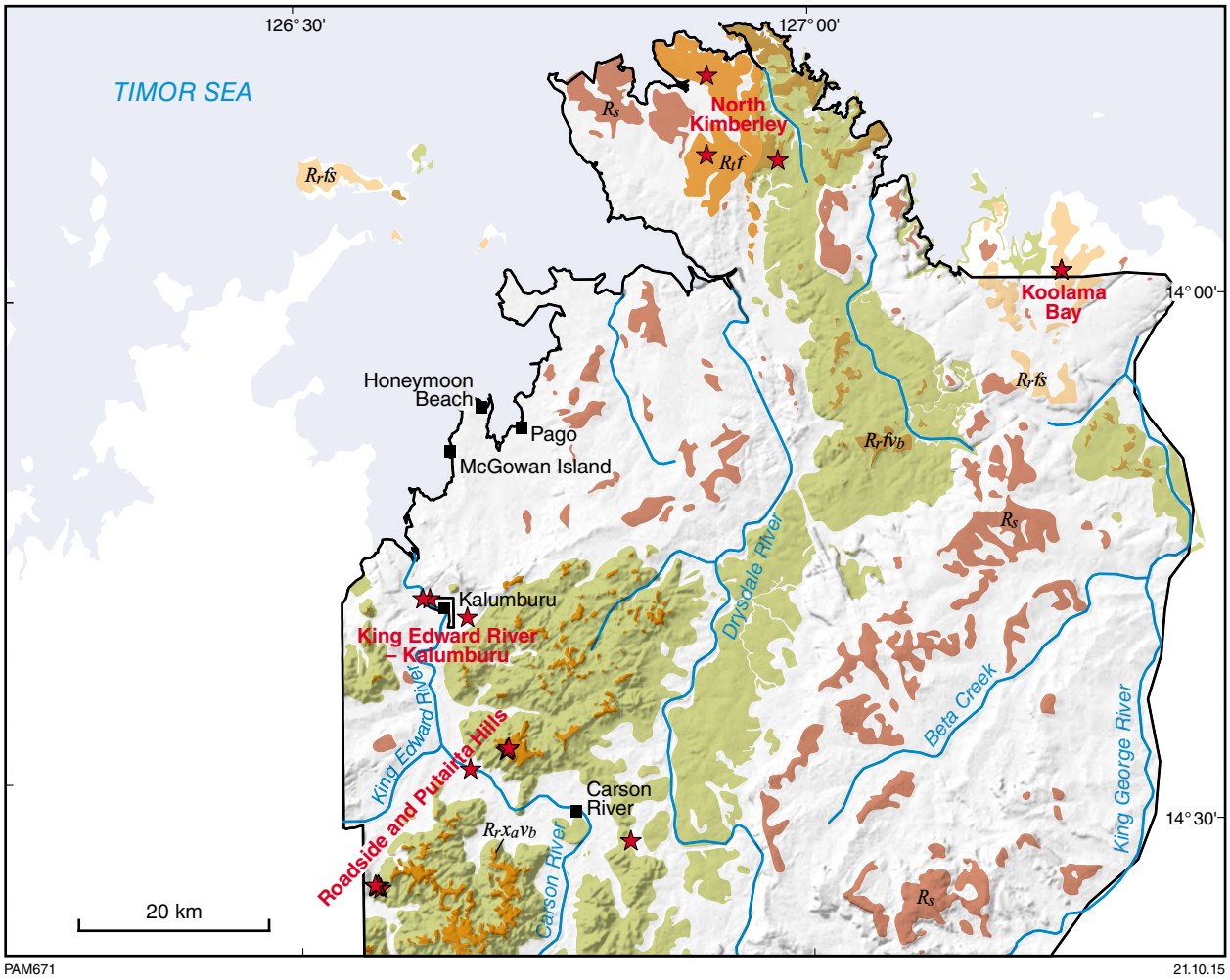

Figure 24. Locations of 26 duricrust samples analysed from the northern part of the Balanggarra project area. See Table 21 for details.

Table 21. Summary of samples and site observations for seven areas of duricrust and related fresh rock from the north of the project area. See Figures 25 and 30 for locations. Heights above sea level (ASL) are from hand-held GPS.

GWSA number	*Elevation (m ASL)*	*Description*
Roadside Hill		
213111	212	Carson Volcanics. **Figure 25a,b**
213104	231	Base of regolith immediately overlying fresh Carson Volcanics. Bleached and clay rich material in a ferruginous matrix. **Figure 25c**
213102	249	Intensely weathered and ferruginized basaltic saprolite
213110	250	Intensely weathered and ferruginized basaltic saprolite, with localized rock fragments in Fe-rich matrix
213109	268	Fragmentary and cemented ferruginous duricrust below the western edge of plateau
213108	284	Sample from plateau. Ferruginous duricrust with altered mafic fragments. **Figure 25d**
212450	284	Similar to 213108. Pisolitic to nodular ferruginous–aluminous duricrust with some weathered mafic fragments. **Figure 25e**
Putairta Hill		
213127	237	Ferruginous duricrust from a small cliff approximately 2 m below plateau. Regolith is friable and contains highly altered mafic fragments. **Figure 25f**
213128	243	Plateau Surface. Scattered blocks of yellow-brown alcrete, less ferruginous than 213127
213129	251	Rubbly exposure. Scattered loose duricrust blocks with yellow-brown cement. **Figure 25g**
North Kimberley		
213122	59	Vicinity of site M3545 (GSWA213473). Low plateau of possibly aluminous ferricrete, although 213122 appears more iron-rich. Scattered sandstone float
213130		
213123	49	Vicinity of site M3544 (GSWA213438). Ferricrete, as low rubbly outcrop
213124		
213125	22	Vicinity of site M3557 (GSWA213241). Sample 213125 is iron rich and exposed as a continuous sheet of ferricrete. Sample 213126 is surface lag, possibly containing lithic fragments
213126		
Koolama Bay		
213121 213131 213118 213119 213120	120	Outcrops of rubbly ferricrete north of site. Ferricrete contains quartz grains in a ferruginous matrix. Some appear buff coloured chemical precipitate on the surface, possibly more limonitic material. Scattered outcrop of quartz-rich sandstone
King Edward River		
213116 213117	4	Fresh sample from low cliff section of King Leopold Sandstone outcrop, eastern bank of King Edward River, dipping 31° in direction 230°. Strong ferruginization in joints of sandstone. On contact with sandstone, alteration is about 3 cm thick, then more brick-red, sandy regolith, either more altered or transported, but without exotic material. The subvertical joints, all about 20 cm thick, show same material. Sample 213117 is from this ferruginised weathered sandstone material
212451	13	Stream containing well-cemented ferricrete with ferruginized weathered sandstone clasts. The area is surrounded by outcropping King Leopold Sandstone and residual, grey quartz sand, which is around 20 cm thick and covers a gravel-rich layer of iron-rich granules and nodules. **Figure 30i**. Field book is 21 x 12.5 cm
212454	24	Ferruginized colluvium or channel fill, containing various quartz-rich sandstone clasts and fragments, cemented by an iron-rich matrix. **Figure 30g,h**

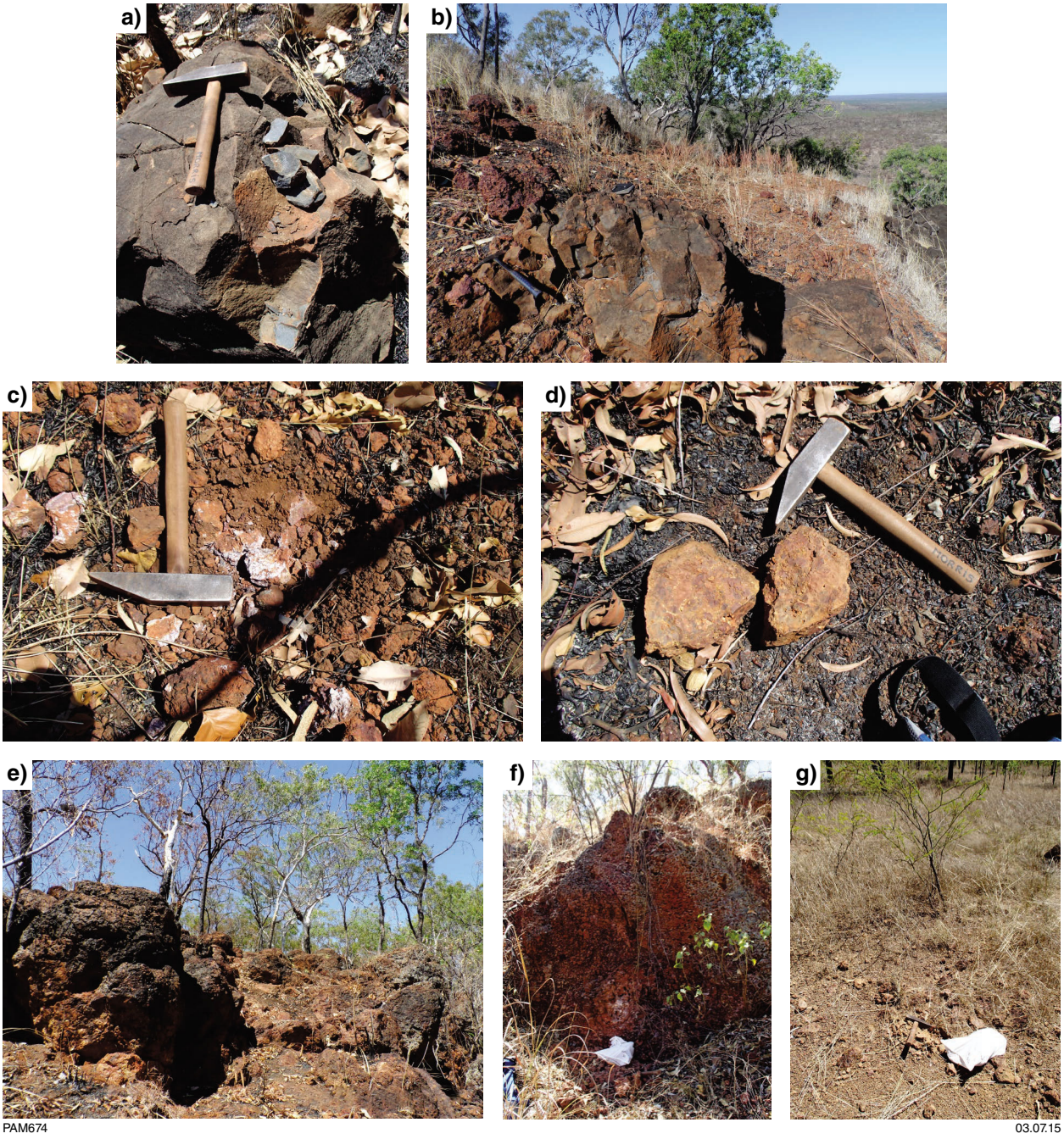

Figure 25. Field photographs, regolith and fresh bedrock, Carson Volcanics: a), b) fresh basalt (GSWA213111; Table 13) of the Carson Volcanics, Roadside Hill (MGA 238378E 8389277N, 212 m ASL). Hammer is 40 cm long; c) weathered mafic volcanic rock, Roadside Hill, GSWA213104 (MGA 238948E 8388942N, 231 m ASL); d) cemented, ferruginized mafic rock fragments, plateau of Roadside Hill, GSWA213108 (MGA 238714E 8289241N, 284 m ASL); e) western edge of plateau, Roadside Hill, GSWA212450 (MGA 238513E 8389145N); f) ferruginous and fragmentary duricrust forming low cliffs immediately below plateau surface, Putairta Hill, GSWA213127 (MGA 252133E 8403441N, 270 m ASL); g) loose blocks forming rubbly surface on plateau, Putairta Hill, GSWA213129 (MGA 252391E 8403748N). Cement is possibly more Al rich

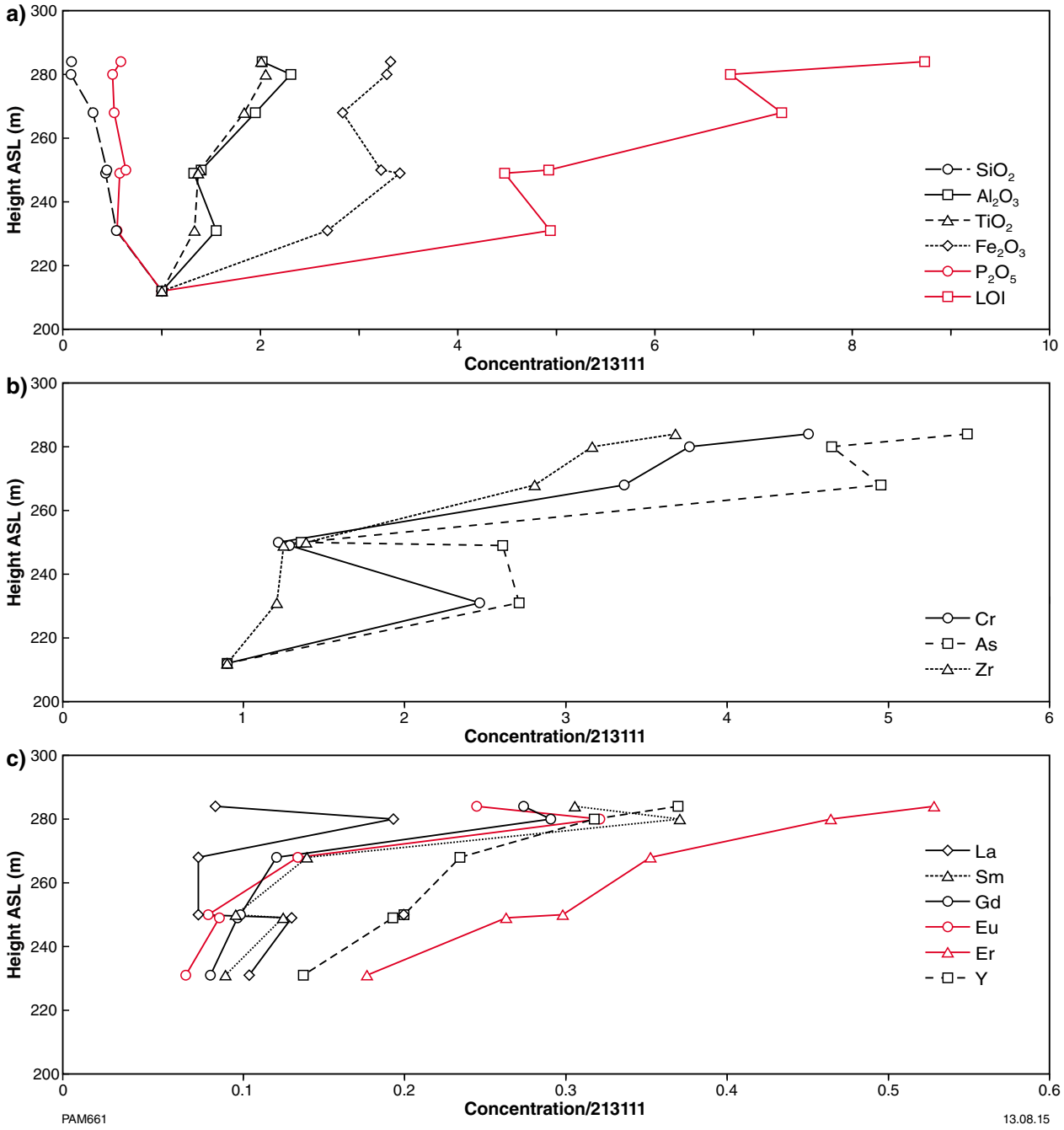

Figure 26. Variations of analytes from duricrust over Carson Volcanics with stratigraphic height, shown relative to fresh Carson Volcanics sample GSWA213111: a) major element oxides and LOI (wt%); b) Cr, As and Zr (ppm); c) selected REE and Y (ppm).

Chondrite-normalized REE profiles from Roadside Hill (Fig. 28) show a pronounced positive Ce anomaly in duricrust samples, with values gradually increasing with stratigraphic height. Braun et al. (1990) discussed Ce anomalies in laterite from Cameroon in terms of leaching of REE in a reducing environment followed by oxidation of Ce^{3+} to Ce^{4+} and precipitation of the Ce phosphate cerianite. Cerium fractionation and precipitation of cerianite under oxidizing conditions was also observed in the B horizon of a recent laterite profile in Madagascar (Berger et al., 2014). Babechuk et al. (2014) noted redox-related Ce anomalies and decoupling from the other REE in weathering profiles over Deccan basalts from India. The most extreme variation and anomalous Ce concentrations were found in the highly lateritized part of an older profile. In the Balanggarra duricrust profiles, precipitation of secondary Ce-bearing minerals under different oxidation conditions may explain positive Ce anomalies (Fig. 28), but P_2O_5 is progressively depleted with stratigraphic height (Fig. 26a), inconsistent with stabilization of REE in secondary phosphate minerals. The enrichment of HREE high in the profile could reflect adsorption of these elements onto clay minerals (Coppin et al., 2002).

Ferruginous duricrust over the King Leopold Sandstone

King Edward River – Kalumburu

Ferruginous duricrust is found as scattered outcrops, and as joint fillings in the King Leopold Sandstone, north of Kalumburu. Three samples of duricrust from this area consist of a joint filling in the King Leopold Sandstone from a location on the King Edward River (213116; Fig. 24), and two samples of ferruginous duricrust are from a surface exposure approximately two kilometres from the King Edward River location (212454, 212451). A fresh sample of King Leopold Sandstone (213117) was also collected at the King Edward River location. This is a well-sorted, quartz-rich siliciclastic rock, with joints dipping 31° towards 230°. Some joints are filled with orange-brown Fe-cemented material (Fig. 30e; 213116), and weak ferruginization of the sandstone is found adjacent to these joints.

Scattered exposures of duricrust in the King Edward River – Kalumburu area consist of variably ferruginized siliciclastic sandstone fragments, and ferruginous nodules and granules in an iron-rich matrix, commonly found in drainage depressions (212454, 212451; Fig. 30g,h).

Koolama Bay and north Kimberley

Koolama Bay, in the northeast part of the project area (Fig. 24), has been mapped as ferruginous duricrust developed on sedimentary rocks of the Warton Sandstone. Here, isolated rubbly exposures of duricrust are interspersed with outcrops of siliciclastic sedimentary rock. Duricrust comprises ferruginous nodules in an iron-cemented matrix with quartz grains. Parts of the matrix are more buff coloured and are probably limonitic. Five duricrust samples were collected within a one kilometre radius (213121, 213131, 213118, 213119, 213120; Table 21).

Six samples, collected from three locations on a low plateau between 29 and 59 m ASL north of Kalumburu (Fig. 24; Table 21), are from areas of iron-rich duricrust derived by weathering of the Carson Volcanics (R_sf_vb; 213122, 213130), or ferricrete (R_lf) overlying siliciclastic sedimentary rocks of the King Leopold Sandstone (213123, 213124, 213125, 213126). Near regolith sample site 213473 on the Carson Volcanics, duricrust samples appear to have different cement types, comprising more aluminous material (213130), and more ferruginous material (213122), along with scattered sandstone blocks. Two ferricrete samples (213123 and 213124) from the King Leopold Sandstone were collected near regolith sampling site 213438, and at a third locality near regolith sampling site 213241, a sample of ferricrete from a well-developed sheet (213125) was collected, as well as a sample of ferruginous lag which has occasional sandstone fragments (213126).

Discussion

The King Leopold Sandstone sample 213117 from the King Edward River has 96.9 wt% SiO_2, and low contents of Fe_2O_3 (1.24 wt%), Al_2O_3 (0.87 wt%) and TiO_2 (0.08 wt%). Ferruginized sandstone from a joint in the sandstone has lower SiO_2 (57.6 wt%), and higher Fe_2O_3 (26.69 wt%), Al_2O_3 (6.99 wt%) and TiO_2 (0.38 wt%). Duricrust sample 212454 has broadly similar SiO_2, TiO_2, Fe_2O_3 and Al_2O_3 contents to ferricrete, but sample 212452 has lower SiO_2 and higher TiO_2, Al_2O_3 and Fe_2O_3 contents.

A multi-element plot of the three duricrust samples is shown in relation to the six duricrust samples from Roadside Hill (Fig. 31), with patterns normalized to Carson Volcanic average. The most striking differences between the two areas is the higher REE contents and steeper REE profiles of the King Edward River – Kalumburu samples, the negative TiO_2 anomaly, and the higher SiO_2 and lower Al_2O_3 contents. The chalcophile elements are also more enriched. One sample has a positive K_2O anomaly. Multi-element patterns for samples from Koolama Bay (Fig. 32) and the north Kimberley (Fig. 33) are similar, and show the same REE and chalcophile profiles as duricrust samples from King Edward River – Kalumburu. However, Koolama Bay (Fig. 32) and the north Kimberley samples (Fig. 33) have SiO_2/Al_2O_3 <1, and Th is more strongly enriched relative to the HFSE, with a steeper Th/TiO_2, indicative of more intense chemical weathering. The two samples from the north Kimberley location over the Carson Volcanics have slightly lower K_2O contents.

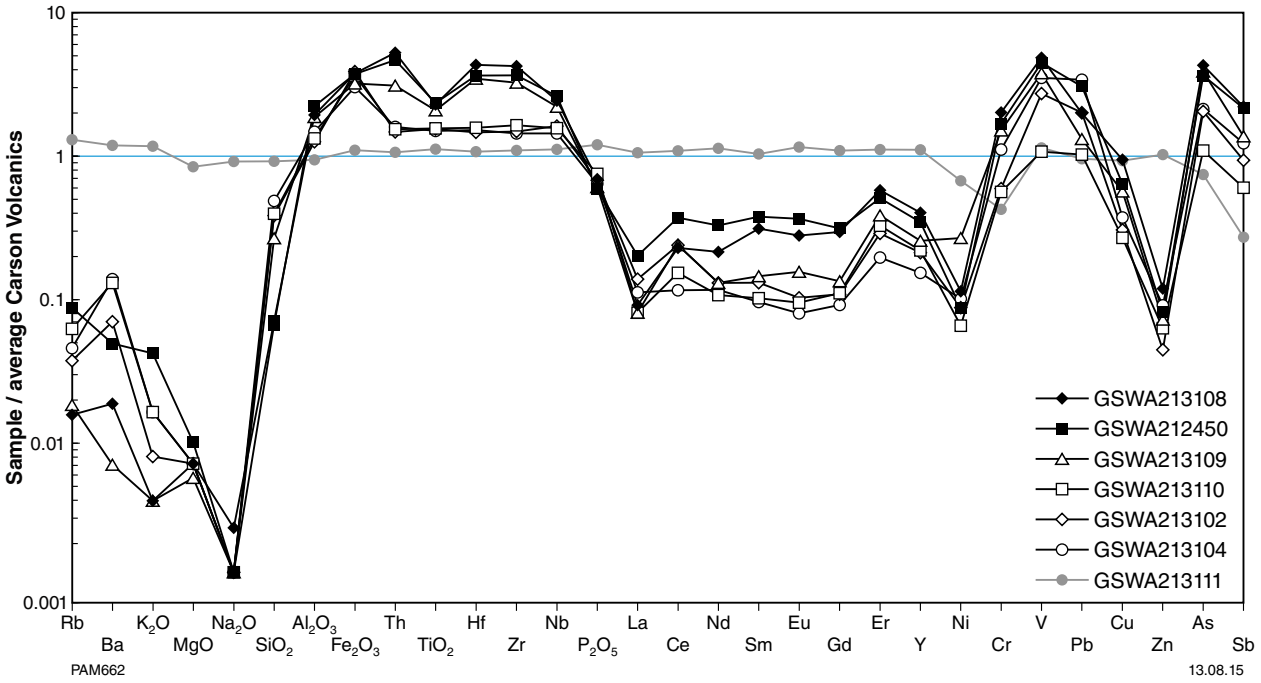

Figure 27. Spider diagram for fresh basalt and duricrust from Roadside Hill (Table 21; Fig. 25) normalized to the average of 37 analyses of fresh Carson Volcanics (Table 13)

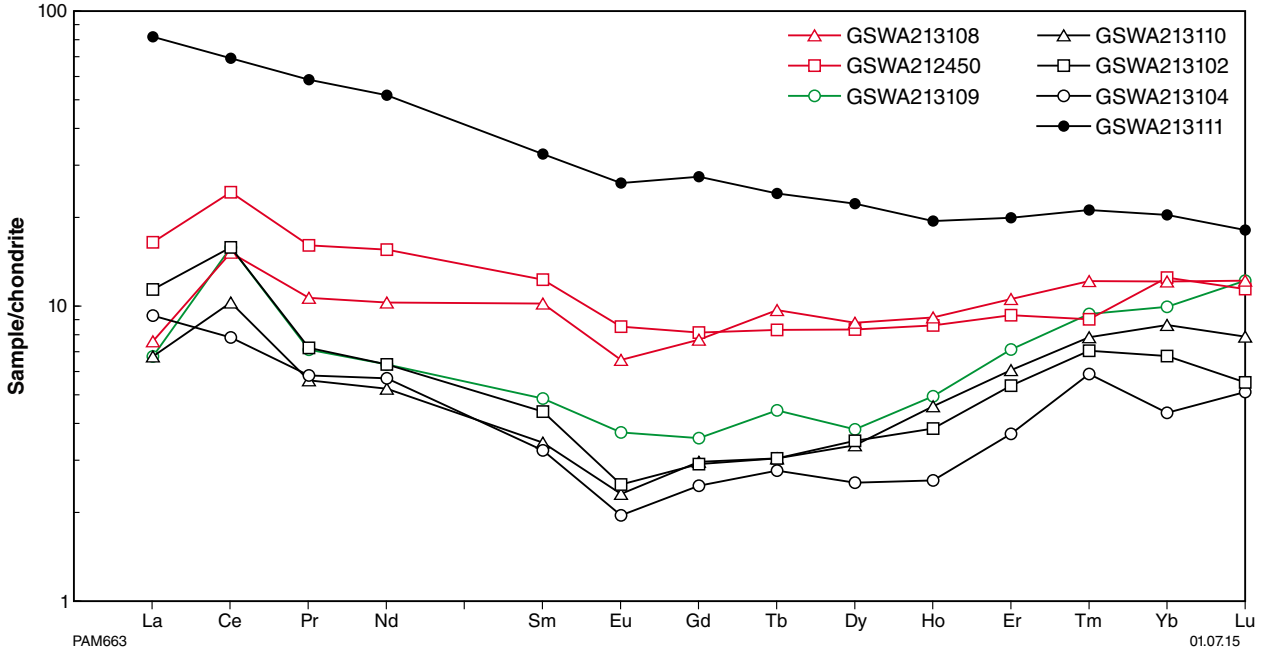

Figure 28. Chondrite-normalized REE profiles for fresh Carson Volcanics basalt and duricrust from Roadside Hill (Table 21; Fig. 25). Chondrite normalizing factors from Sun and McDonough (1989)

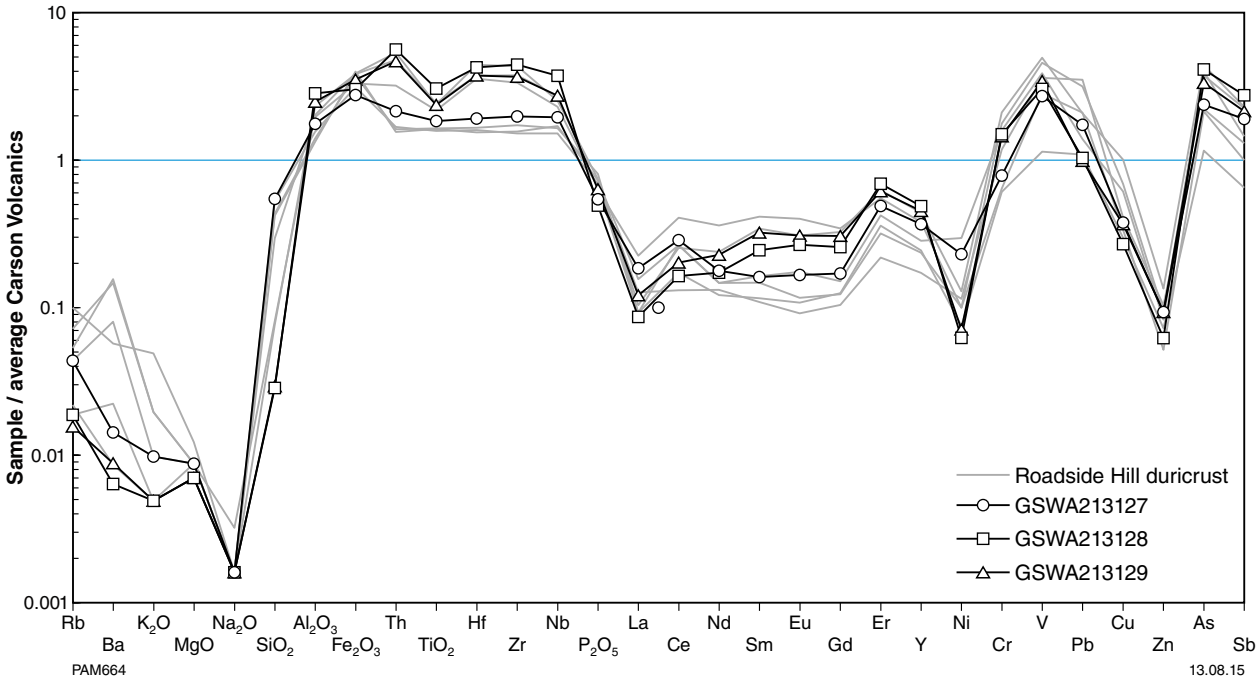

Figure 29. Spider diagram for duricrust from Putairta Hill (Table 21; Fig. 25) normalized to the average of 37 analyses of fresh Carson Volcanics (Table 13). Also shown are six analyses of duricrust from Roadside Hill (Table 21) for comparison.

Although the multi-element patterns for duricrust samples from all five locations are broadly similar, they fall into two groups: (i) Roadside and Putairta Hills; (ii) King Edward River – Kalumburu, Koolama Bay, and north Kimberley. In comparing suites of igneous rocks, it is common practice to separate samples according to their incompatible element contents or ratios (e.g. Th/Nb, Ti/Zr; Rollinson, 1993), as ratios in particular are relatively insensitive to magmatic processes and instead reflect the parent composition. In dealing with duricrust, this approach must take into account the effect of chemical weathering, which can have marked effects on the concentration of elements such as the HFSE and REE. However, a plot of Ti/Zr (Fig. 34) shows a clear separation into high Ti/Zr samples (Roadside and Putairta Hills) and low Ti/Zr samples (King Edward River, Koolama Bay, north Kimberley). Fresh Carson Volcanics plots on the same trend as Roadside and Putairta Hills, whereas King Leopold Sandstone plots with samples from Koolama Bay, north Kimberley and King Edward River.

These groups also show separation in terms of Th/Nb – Ti/Zr (Fig. 35). Also shown on Figure 35 plot are 87 samples of regolith from areas of outcrop on the Carson Volcanics. The variation in Ti/Zr is attributable to the loss of Ti and increase in Zr as opaque oxides are weathered and zircon is concentrated during weathering. This has little effect on either Th or Nb, with correspondingly negligible change in Th/Nb. Samples from Roadside and Putairta Hills plot close to Carson Volcanics regolith samples, whereas samples from Koolama Bay, north Kimberley and the three duricrust samples from King Edward River – Kalumburu plot on a simple mixing line between fresh Carson Volcanics from Roadside Hill and King Leopold Sandstone from the King Edward River. This shows that these regolith samples found over the King Leopold Sandstone are a mixture of locally derived sandstone and eroded, weathered and transported Carson Volcanics. This is consistent with the lower Ti/Zr ratio of these samples (Fig. 34) that lie on a similar trend to the King Leopold Sandstone.

Thus, these duricrust samples are interpreted as the remnants of a once more extensive duricrust sheet. The closest outcrop of mafic volcanic rocks to Koolama Bay is approximately two kilometres to the northwest (Fig. 24), but that exposure is about 60 m below the level of duricrust at Koolama Bay, so it is an unlikely source. The nearest exposure of the Carson Volcanics at a similar stratigraphic level is about 15 km to the south of Koolama Bay (Fig. 24). If this is the source of mafic material for duricrust, and assuming radial dispersion of transported material from this source, the original duricrust sheet could have covered an area of at least 700 km^2.

Similar element ratios (e.g. Ti/Zr, Th/Nb) and multi-element patterns of duricrust at Roadside and Putairta Hills to fresh Carson Volcanics indicate in situ development of regolith. In contrast, there is both field and geochemical evidence that duricrust developed on the King Leopold Sandstone is a mixture of locally derived siliciclastic lithologies and weathered and transported Carson Volcanics. Aluminous duricrust developed in situ at Roadside and Putairta Hills has Al_2O_3 concentrations (27.8 to 42.7 wt%) comparable to bauxite deposits of the Darling Range (Bauxite Resources Ltd, 2013).

Figure 30. Field photographs from the King Edward River location, and near Kalumburu: a) near site M3544, rubbly exposure of ferricrete on plateau surface; GSWA 213123, 213124 (MGA 237237E 8466191N); b), c) near site M3557, semi-continuous ferricrete sheet, with ferruginized lag of lithic fragments; GSWA 213125, 213126 (MGA 273224E 8575499N); d) low cliff section of King Leopold Sandstone, eastern bank of King Edward River (MGA 243384E 8419463N). Unit dips 31° in direction 230°; e) joints in King Leopold Sandstone at King Edward River, infilled with ferricrete (MGA 243384E 8419463N). Sandstone adjacent to joint is weakly ferruginized; f) well-sorted, quartz-rich King Leopold Sandstone at King Edward River (MGA 243364E 8419514N); g), h) nodular ferricrete forming a semi-continuous surface on the King Leopold Sandstone approximately 5 km southeast of King Edward River location; GSWA 212454 (MGA 248055E 8417477N); i) ferruginized and weathered sandstone fragments (on field notebook) from beneath a well-sorted quartz sand near outcrop of the King Leopold Sandstone, approximately 700 m east of the King Edward River location; GSWA 212451 (MGA 244117E 8419456N)

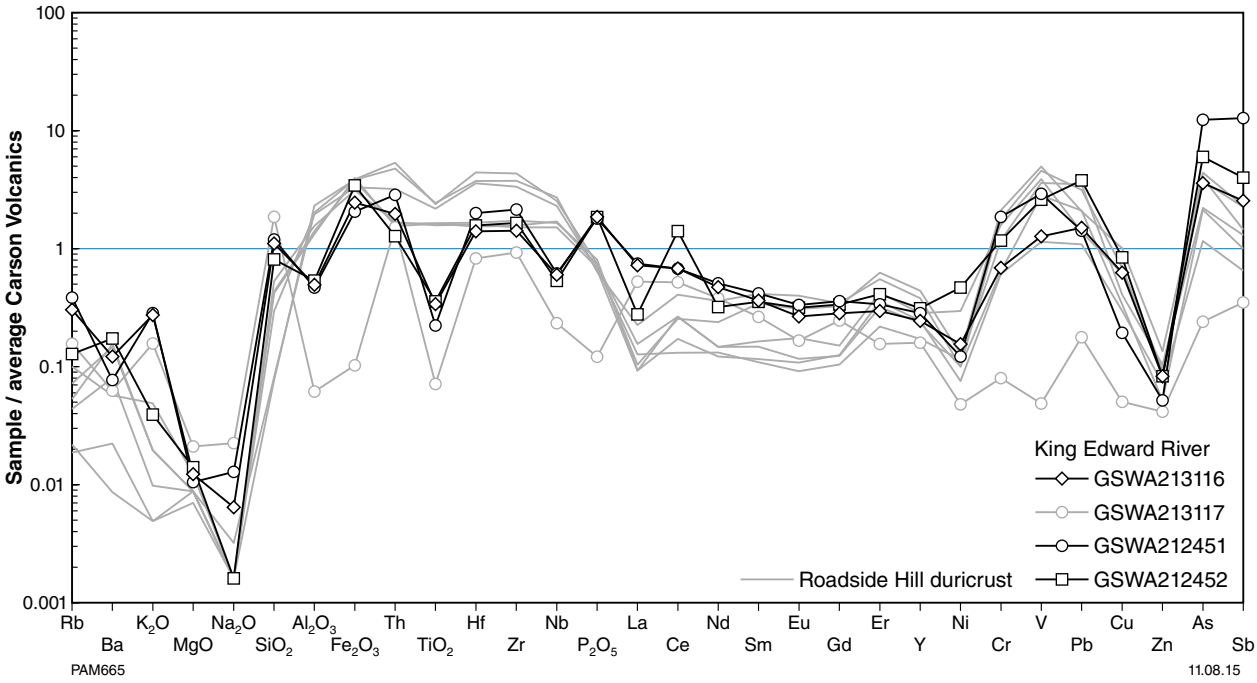

Figure 31. Spider diagram for samples from King Edward River north of Kalumburu (Table 21; Fig. 30) normalized to the average of 37 analyses of fresh Carson Volcanics (Table 13). Also shown are six analyses of duricrust from Roadside Hill for comparison.

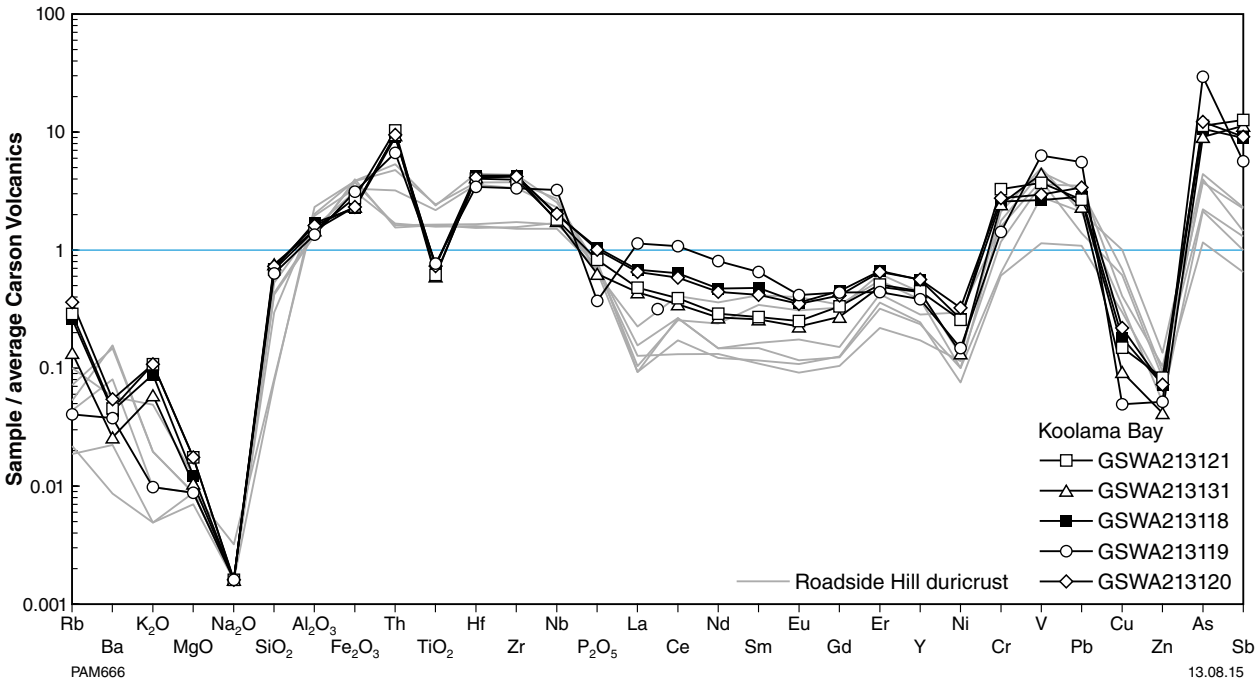

Figure 32. Spider diagram for duricrust from Koolama Bay (Table 21) normalized to the average of 37 analyses of fresh Carson Volcanics (Table 13). Also shown are six analyses of duricrust from Roadside Hill for comparison.

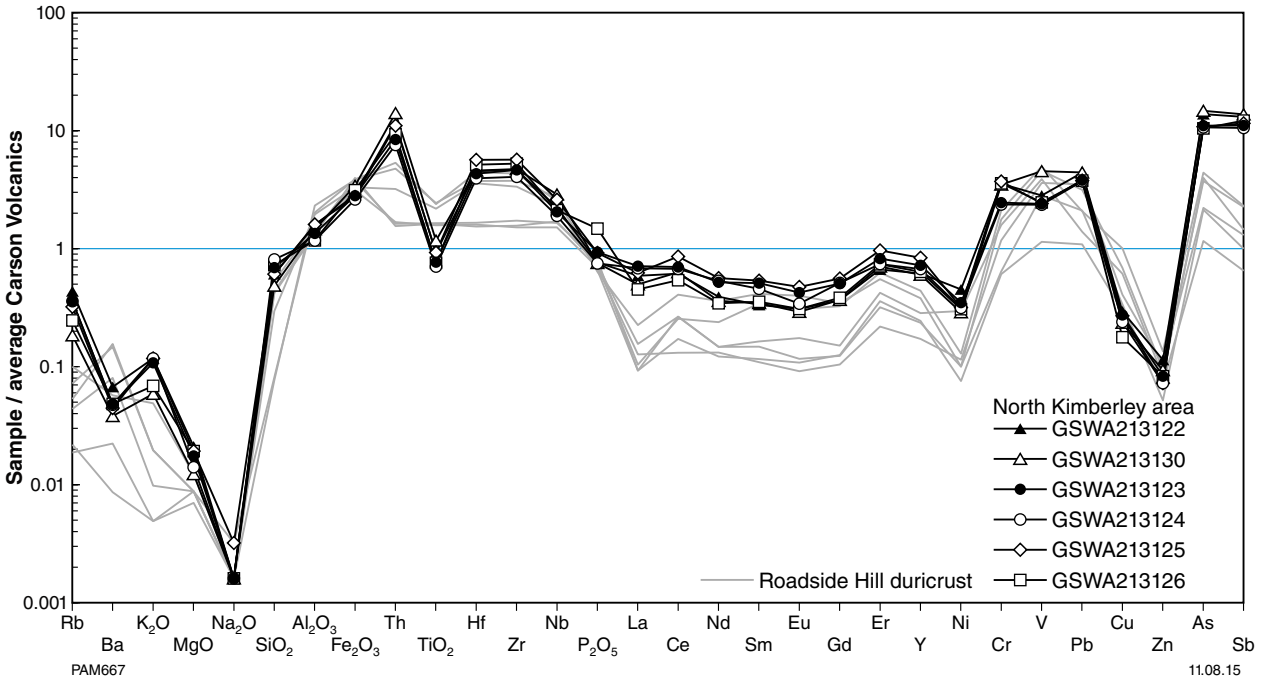

Figure 33. Spider diagram for duricrust from the north Kimberley area (Table 21) normalized to the average of 37 analyses of fresh Carson Volcanics (Table 13). Also shown are six analyses of duricrust from Roadside Hill for comparison.

There, bauxite mineralization is restricted to the duricrust and friable fragmental units of the lateritic profile below which the gibbsite content decreases with an increase of Fe oxide (Hickman et al., 1992). This is also seen at Roadside Hill, where Al_2O_3 and Fe_2O_3 decrease and SiO_2 increases towards the bottom of the profile. Ball and Gilkes (1987) noted a strong depletion in CaO, MnO, Ni, Co, Li, Rb and Cs in bauxite at Mt Saddleback, similar to that seen in the Balanggarra area. Coincidentally, aluminous duricrust at Roadside and Putairta Hills is found at a similar elevation (240–280 m) to the Darling Range bauxite deposits (280–300 m).

Conclusion

The Kimberley Plateau is one of the few areas in Western Australia where the topography, bedrock geology, and climate have resulted in extensive areas of exposed fresh bedrock which exceeds the area of regolith. Of the transported regolith component, about 75% is colluvium, which is found adjacent to or immediately downslope of areas of outcrop. This, and the preservation of about 10% of regolith as in situ residuum, means that the composition of regolith is in large part a reliable proxy for that of bedrock. A complicating factor for this relationship is the effect of chemical weathering. For chemically immature rocks such as basalts of the Carson Volcanics, the topography and climate mean that even regolith found in areas of outcrop is depleted in labile components, as shown by the depletion of Rb, Ba, K_2O, Na_2O MgO and Ni, and enrichment in Th, Fe_2O_3, HFSE, Cr, V, some base metals, and chalcophile elements relative to fresh bedrock. These changes can be accounted for by the early breakdown of phenocrysts (olivine, pyroxene, feldspar), and the concentration of resistate phases (zircon, monazite, chromite, rutile) and secondary iron oxide. In the case of some elements such as Al and Si, the similarity in concentrations between regolith and fresh bedrock reflects the breakdown of primary phases such as feldspar, but the retention of these elements in secondary phases such as clay minerals. During the process, REE are little affected, in part due to their low concentrations and low mineral–melt partition coefficients, coupled with their stabilization in secondary minerals including clays (e.g. Coppin et al., 2002).

The production of depositional regolith (colluvium and alluvium) involves more intense weathering that is affected by transport. The pattern of labile component depletion and resistate phase concentration is again evident, although in alluvium, depletion in HFSE could indicate the effects of mechanical sorting. The most intense phase of chemical weathering of regolith is the production of residual duricrust where, in addition to the behaviour of labile and incompatible elements seen in other regolith types, REE are depleted, and this is attributed to the breakdown of clay minerals. Due to their chemical maturity, the effect of chemical weathering on siliciclastic sedimentary rocks is less obvious, with a similar but more subdued behaviour of labile and incompatible elements compared with Carson Volcanics.

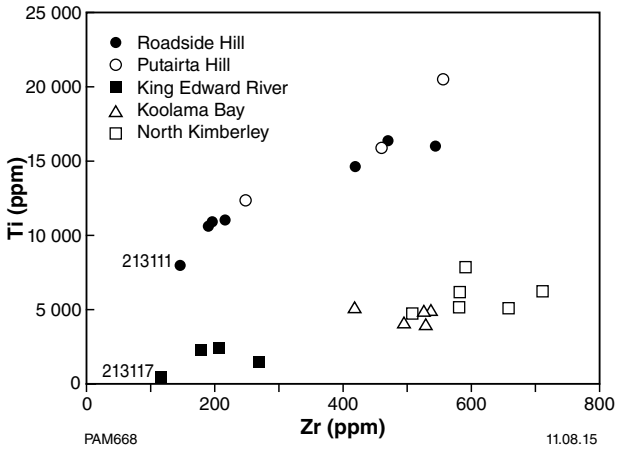

Figure 34. Bivariate plot of Ti (ppm; converted from TiO_2 wt%) versus Zr (ppm) for fresh rock and duricrust samples from the northern part of the project area. Fresh volcanic rock samples: 213111 – Carson Volcanics basalt; 213117 – King Leopold Sandstone

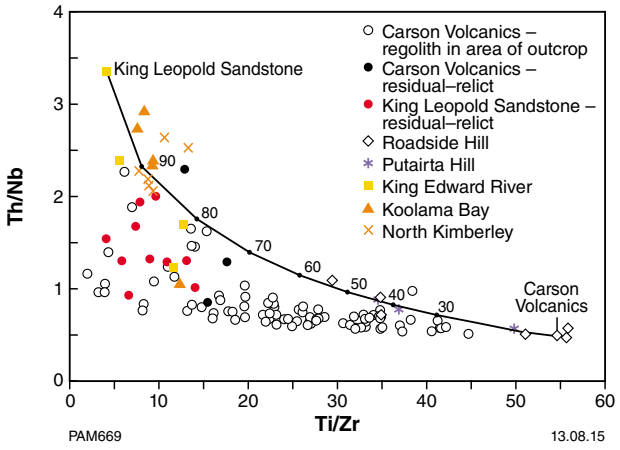

Figure 35. Bivariate plot of Th/Nb versus Ti/Zr showing fresh rock and duricrust samples from the north Kimberley as well as 87 samples of regolith from areas of outcrop on the Carson Volcanics, and relict samples on the King Leopold Sandstone. Also shown is a simple mixing line between fresh Carson Volcanics GSWA213111 and King Leopold Sandstone GSWA213117 (Table 13).

Statistical analysis of regolith shows the strong lithological contrast between mafic volcanic rocks of the Carson Volcanics and quartz-dominated siliciclastic sedimentary rocks of the King Leopold, Warton, and Pentecost Sandstones. Anomalous concentrations of different groups of elements indicate departures from the simple relationship between bedrock and regolith composition, which must be interpreted in conjunction with an assessment of the effects of chemical weathering. Those samples which depart from this relationship may reflect factors such as incorrectly assigning the parent lithology (especially if the sample site is close to the unit contacts), input of regolith from an adjacent lithological unit through erosion and transport, intense in situ weathering of underlying bedrock, or lithological variability within the bedrock.

The high degree of correlation between regolith and bedrock chemistry means that regolith composition can be used to assess bedrock lithology variations. The elevated concentrations of Cr, Ni, MgO, chalcophile elements, Pt and Au in regolith from locations close to the lower contact of the Carson Volcanics with the King Leopold Sandstone show that early in the eruptive cycle, less fractionated, sulfide-rich, and potentially mineralized magma was emplaced. Copper mineralization in lower parts of the Carson Volcanics is well known, although regolith chemistry has not identified any anomalous Cu concentrations lower in the succession. Instead, there is a generally higher Cu background throughout the unit.

In the same unit, two samples show unusually high contents of REE. As these enrichments are decoupled from HFSE, Cr, V and Th, they cannot be explained by concentration of resistate phases. The trace element and REE chemistry is similar to that of altered Cenozoic basalts from southeastern Victoria, which have been linked to hydrothermal alteration. As both regolith samples plot on major northeast-trending crustal structures, this is consistent with these structures acting as conduits for hydrothermal fluids. If this is the case, then alteration associated with hydrothermal activity must have taken place after regolith formation.

In the Pentecost Sandstone, nine strike-oriented regolith samples from areas of outcrop have anomalous concentrations of Zr and Hf, but not other HFSE, Th or REE. Some have anomalous K_2O and Rb, as well as Sr and Tl. The association of Zr and Hf to the exclusion of other incompatible elements is consistent with zircon control, which can be explained by mechanical sorting during deposition of this part of the Pentecost Sandstone excluding lower density heavy minerals. The regolith samples are found over the central part of the sandstone unit, which is more lithic-rich than the overlying and underlying units, consistent with the higher K_2O and Rb contents of regolith.

Statistical comparison of regolith from areas of outcrop for the three major siliciclastic sedimentary units (King Leopold, Warton and Pentecost Sandstones) highlights the higher level of chemical maturity of the older King Leopold Sandstone compared to the younger Warton and Pentecost Sandstones. This indicates a change in the source composition of siliciclastic sedimentary rocks prior to and after eruption of the Carson Volcanics. The composition and sedimentary structures described by Gellatly and Sofoulis (1969) and Derrick (1968) indicate a generally shallower, more locally influenced provenance for the three sedimentary units of the Kimberley Group overlying the Carson Volcanics.

Examination of duricrust from five areas in the north of the project area provide the opportunity to further investigate the process of chemical weathering seen in regional regolith samples. At one location where regolith stratigraphy is well preserved, the pattern of labile element

depletion, incompatible element enrichment, and REE depletion is already seen at the stratigraphically lowest part of a regolith profile over the Carson Volcanics, with the development of aluminous and ferruginous duricrust. With increasing time (i.e. towards stratigraphically higher levels), early-formed clay minerals are transformed into illite and then gibbsite and boehmite, with concomitant loss of SiO_2 and increasing Al_2O_3 and TiO_2. The REE also increase slightly with stratigraphic height, consistent with their release during clay breakdown and their incorporation in secondary minerals. At the top of these regolith profiles, Al_2O_3 reaches concentrations of >40 wt% and SiO_2 is <2 wt% — concentrations similar to those in economic bauxite deposits. Where ferruginous and aluminous duricrust is developed on siliciclastic sedimentary rocks, regolith has different HFSE ratios (e.g. Ti/Zr), Th/Nb and REE patterns, which accord with field observations that these regolith deposits represent eroded and transported mafic volcanic material from the Carson Volcanics that has mixed with sedimentary detritus. The spatial distribution of these relict units indicates the duricrust sheet (of which these deposits are the remnant) extended across least 700 km^2. This shows that regolith–landform mapping in conjunction with regolith chemistry can be used to reconstruct paleogeography.

References

Anand, RR, Churchward, HM, Smith, RE, Smith, K, Gozzard, JR, Craig, MA, and Munday, TJ 1993, Classification and atlas of regolith–landform mapping units, Exploration perspectives for the Yilgarn Craton, Australia: CSIRO Division of Exploration and Mining Restricted Report 440R (unpublished).

Anand, RR and Butt, CRM 2010, A guide for mineral exploration through the regolith in the Yilgarn Craton, Western Australia: Australian Journal of Earth Sciences, v. 57, p. 1015–1114.

Babechuk, MG, Widdowson, M and Kamber, BS 2014, Quantifying chemical weathering intensity and trace element release from two contrasting basalt profiles, Deccan Traps, India: Chemical Geology, v. 363, p. 56–75.

Ball, PJ and Gilkes, RJ 1987, The Mount Saddleback bauxite deposit, southwestern Australia: Chemical Geology, v. 60, p. 215–225.

Bauxite Resources Ltd 2013, 26.8 Mt bauxite resource at BRL's Darling Range Fortuna Project: Report to Australian Securities Exchange, 9 May 2013, 6p.

Berger, A, Janots, E, Gnos, E, Frei, R and Bernier, F 2014, Rare earth element mineralogy and geochemistry in a laterite profile from Madagascar: Applied Geochemistry, v. 41, p. 218–228.

Berkman, DA 1989, Field Geologists' Manual (Third edition): Australasian Institute of Mining and Metallurgy Monograph Series 9, 382p.

Braun, J-J, Pagel, M, Muller, J-P, Bilong, P, Michard, A and Guillet, B 1990, Cerium anomalies in lateritic profiles: Geochimica et Cosmochimica Acta, v. 54, p. 781–795.

Carver, RN, Chenoweth, LM, Mazzucchelli, RH, Oates, CJ and Robbins, TW 1987, "Lag" — a geochemical sampling medium for arid regions: Journal of Geochemical Exploration, v. 23, p. 183–199.

Coppin, F, Berger, G, Bauer, A, Castet, S and Loubet, M 2002, Sorption of lanthanides on smectite and kaolinite: Chemical Geology, v. 182, p. 57–68.

Cornelius, M, Robertson, IDM, Cornelius, AJ and Morris, PA 2008, Geochemical mapping of the deeply weathered western Yilgarn Craton of Western Australia, using laterite geochemistry: Geochemistry: Exploration, Environment, Analysis, v. 8, p. 241–254.

David, TWE 1950, Geology of the Commonwealth of Australia, v. II: Edward Arnold and Co., London, 719p.

Davis, JC 1973, Statistics and data analysis in geology: John Wiley and Sons, New York, 550p.

Derrick, GM (compiler) 1968, Ashton, Western Australia: Geological Survey of Western Australia, 1:250 000 Geological Series Explanatory Notes, 16p.

Eggleton, RA (editor) 2001, The regolith glossary: surficial geology, soils and landscapes: Cooperative Research Centre for Landscape Evolution and Mineral Exploration (CRC LEME), Canberra, Australian Capital Territory, 144p.

Fodor, RV, Bauer, GR, Jacobs, RS and Bornhorst, TJ 1987, Kahoolawe Island, Hawaii: tholeiitic, alkalic, and unusual hydrothermal(?) 'enrichment' characteristics: Journal of Volcanology and Geothermal Research, v. 31, p. 171–176.

Frey, FA, Green, DH and Rof, SD 1978, Integrated models of basalt petrogenesis: a study of quartz tholeiites to olivine melilites from south eastern Australia utilizing geochemical and experimental petrological data: Journal of Petrology, v. 19, p. 463–513.

Freyssinet, PH, Butt, CRM, Morris, RC and Piantone, P 2005, Ore-forming processes related to lateritic weathering: Economic Geology, 100th Anniversary Volume, p. 681–722.

Gellatly, DC and Sofoulis, J (compilers) 1969, Drysdale and Londonderry, Western Australia: Geological Survey of Western Australia, 1:250 000 Geological Series Explanatory Notes, 18p.

Geological Survey of Western Australia 2013, Revised classification system for regolith in Western Australia, and the recommended approach to regolith mapping: Geological Survey of Western Australia, Record 2013/7, 26p.

Geological Survey of Western Australia 2014, Kimberley, 2014: Geological Survey of Western Australia, Geological Information Series.

Glass, LM and Phillips, D 2006, The Kalkarindji continental flood basalt province: a new Cambrian large igneous province in Australia with possible links to faunal extinctions: Geology, v. 34, no. 6, p. 461–464, doi:10.1130/G22122.1.

Grunsky, EC 2010, The interpretation of geochemical survey data: Geochemistry: Exploration, Environment, Analysis, v. 10, p. 27–74.

Hanley, LM and Wingate, MTD 2000, SHRIMP zircon age for an Early Cambrian dolerite dyke: an intrusive phase of the Antrim Plateau Volcanics of northern Australia: Australian Journal of Earth Sciences, v. 47, p. 1029–1040.

Hickman, AH, Smurthwaite, AJ, Brown, IM and Davy, R 1992, Bauxite mineralization in the Darling Range, Western Australia: Geological Survey of Western Australia, Report 33, 82p.

Hollis, JA, Kemp, AIS, Tyler, IM, Kirkland, CL, Wingate, MTD, Phillips, C, Sheppard, S, Belousova, E and Greau, Y 2014, Basin formation by orogenic collapse: zircon U–Pb and Lu–Hf isotope evidence from the Kimberley and Speewah Groups, northern Australia: Geological Survey of Western Australia, Report 137, 46p.

Humphris, SE 1984, The mobility of the rare earth elements in the crust, *in* Rare Earth Element Geochemistry *edited by* P Henderson: Elsevier, Amsterdam, The Netherlands, Developments in Geochemistry 2, p. 317–342.

Kammermann, M 2008, Annual report for M80/492 Ashmore Diamond Project; North Australian Diamonds Limited: Geological Survey of Western Australia, Statutory mineral exploration report, 77111.

Kane, JS 1990, Reference samples for use in analytical geochemistry: their availablity, preparation, and appropriate use: Journal of Geochemical Exploration, v. 44, p. 37–63.

King, LC 1949, The cyclic land surfaces of Australia: Proceedings of the Royal Society of Victoria, v. 62, p. 79–95.

Krauskopf, KB 1967, Introduction to geochemistry: McGraw–Hill Book Company, New York, 721p.

Marston, RJ 1979, Copper mineralization in Western Australia: Geological Survey of Western Australia, Mineral Resources Bulletin 13, 210p.

McDonough, WF, McCulloch, MT and Sun, S-S 1985, Isotopic and geochemical systematics in Tertiary–Recent basalts from southeastern Australia and implications for the evolution of the sub-continental lithosphere: Geochimica et Cosmochimica Acta, v. 49, p. 2051–2067.

McNaughton, NJ, Rasmussen, B and Fletcher, IR 1999, SHRIMP uranium–lead dating of diagenetic xenotime in siliciclastic sedimentary rocks: Science, v. 285, p. 78–80.

Morris, PA 2000, Composition of Geological Survey of Western Australia geochemical reference materials: Geological Survey of Western Australia, Record 2000/11, 33p.

Morris, PA 2007, Composition of the Bunbury Basalt (BB1) and Kerba Monzogranite (KG1) geochemical reference materials, and assessing the contamination effects of mill heads: Geological Survey of Western Australia, Record data package 2007/14.

Morris, PA 2013, Fine-fraction geochemistry of regolith from the east Wongatha area: tracing bedrock and mineralization through cover: Geological Survey of Western Australia, Record 2012/13, 61p.

Morris, PA and Verren, AL 2001, Geochemical mapping of the Byro 1:250 000 sheet: Geological Survey of Western Australia, 1:250 000 Regolith Geochemistry Explanatory Notes data package.

Orth, K 2015, The Carson–Hart Large Igneous Province intrusive complex: implications for Speewah-style vanadium–titanium–iron mineralization in the Kimberley region, *in* GSWA 2015 extended abstracts: promoting the prospectivity of Western Australia: GSWA Record 2015/2, p. 19–22.

Page, RW and Sun, S-S 1994, Evolution of the Kimberley Region, W.A. and adjacent Proterozoic inliers — new geochronological constraints: Geological Society of Australia; Geoscience Australia — 1994 and Beyond, Abstracts v. 37, p. 332–333.

Price, RC, Gray, CM, Wilson, RE, Frey, FA and Taylor, SR 1991, The effects of weathering on rare-earth element, Y and Ba abundances of Tertiary basalts from southeastern Australia: Chemical Geology, v. 93, p. 245–265.

Reimann, C, Filzmoser, P, Garrett, RG and Dutter, R 2008, Statistical data analysis explained: John Wiley and Sons, Ltd, Chichester, UK, 343p.

Rollinson, HR 1993, Using geochemical data: evaluation, presentation, interpretation: Pearson Education Ltd, Harlow, England, 352p.

Ruddock, I 2003, Mineral occurrences and exploration potential of the north Kimberley: Geological Survey of Western Australia, Report data package 85.

Rudnick, RL and Gao, S 2003, Composition of the continental crust: Treatise of Geochemistry, v. 3, p. 1–64.

Scott, KM and Pain, CF (compilers) 2008, Regolith Science: CSIRO Publishing, Collingwood, Victoria, 461p.

Sheppard, S, Page, RW, Griffin, TJ, Rasmussen, B, Fletcher, IR, Tyler, IM, Kirkland, CL, Wingate, MTD, Hollis, J and Thorne, AM 2012, Geochronological and isotopic constraints on the tectonic setting of the c. 1800 Ma Hart Dolerite and the Kimberley and Speewah Basins, northern Western Australia: Geological Survey of Western Australia, Record 2012/7, 28p.

Smith, RE, Birrell, RD and Brigden, JF 1989, The implications to exploration of chalcophile corridors in the Archaean Yilgarn Block, Western Australia, as revealed by laterite geochemistry: Journal of Geochemical Exploration, v. 32, p. 169–184.

Smith, RE, Perdrix, JJ and Davis, JM 1987, Dispersion into pisolitic laterite from the Greenbushes mineralized Sn–Ta pegmatite system, Western Australia: Journal of Geochemical Exploration, v. 29, no. 1–3, p. 251–265.

Smith, RE and Singh, B 2007, Recognizing, in lateritic cover, detritus shed from the Archaean Gossan Hill Cu–Zn–Su volcanic-hosted massive sulphide deposit, Western Australia: Geochemistry: Exploration, Environment, Analysis, v. 7, no. 1, p. 71–86.

Speck, NH 1960, Land systems of the North Kimberley region, Western Australia: CSIRO Land Research Series, v. 4, p. 71–85.

Stewart, GA, Twidale, CR and Bradley, J 1960, Geomorphology of the North Kimberley area, W.A.: CSIRO Land Research Series, v. 4, p. 26–31.

Summers, S 2005, Final surrender report for the period 1/7/2004 to 30/6/2005; Cape Alumina: Geological Survey of Western Australia, Statutory mineral exploration report, 70909 (open file).

Sun, S-S and McDonough, WF 1989, Chemical and isotopic systematics of oceanic basalts: implications for mantle composition and processes, *in* Magmatism in the Ocean Basins *edited by* AD Saunders and MJ Norry: Geological Society, London, Special Publication 42, p. 313–345.

Figures B10–B17

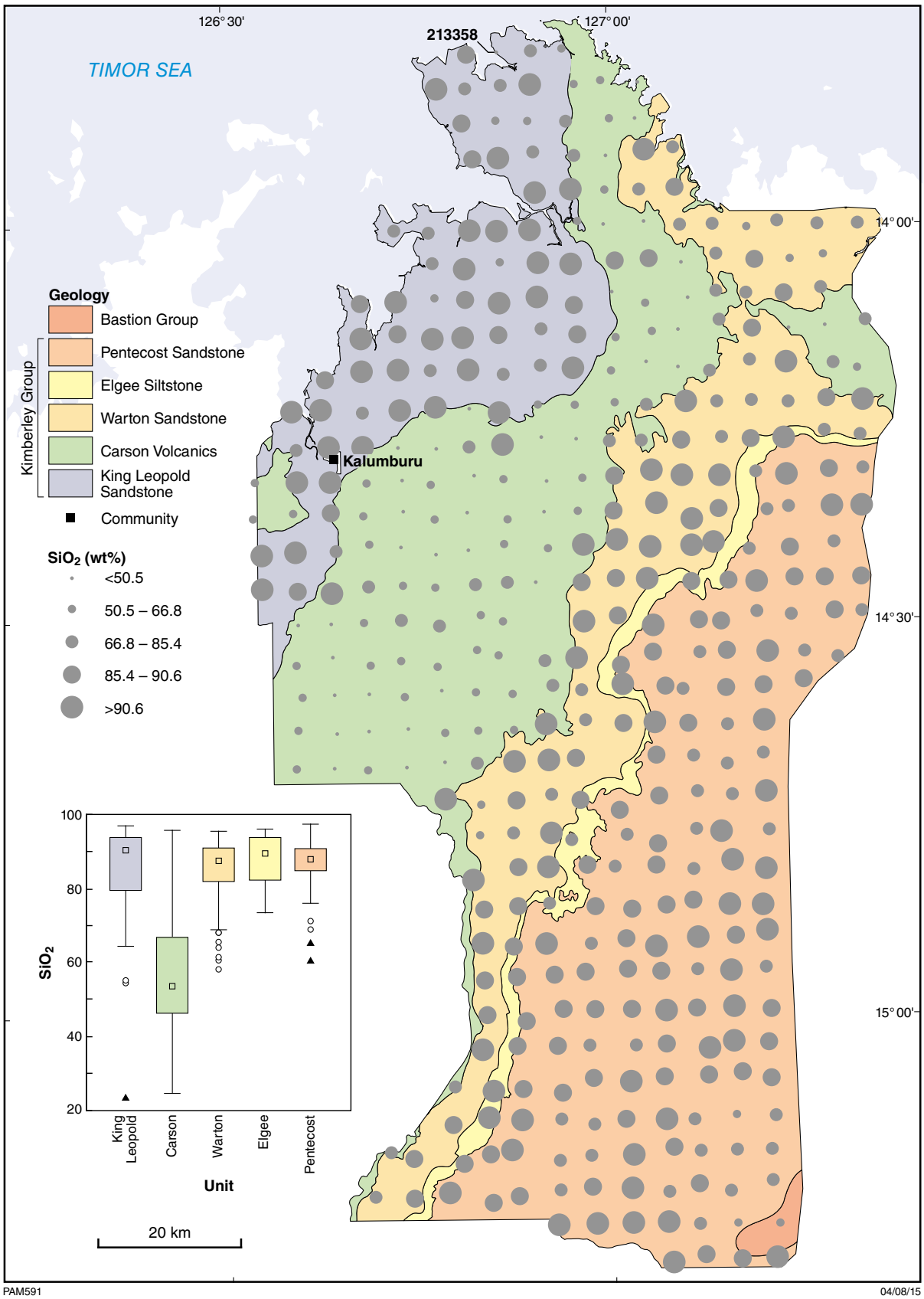

Figure B10. **Bubble plots for major element oxides, LOI, pH and TDS measured in regolith from the Balanggarra project area. Bubble divisions have been determined using box and whisker plots (see p. 21 for explanation), apart from analytes with a high proportion of censored data (MnO, CaO), where bubble divisions use natural breaks, and box and whisker plots have not been compiled. Samples with anomalous concentrations shown by stars (purple – outlier; red – extreme). Also shown is the box and whisker plot according to major lithological units, showing the median, interquartile range (box) and samples with anomalous concentrations (outlier – open circle; extreme – triangle): a) SiO_2 (wt%); b) TiO_2 (wt%); c) Al_2O_3 (wt%); d) Fe_2O_3 (wt%); e) MnO (wt%); f) MgO (wt%); g) CaO (wt%); h) Na_2O (wt%); i) K_2O (wt%); j) P_2O_5 (wt%); k) SO_3 (wt%); l) LOI (wt%); m) pH; n) TDS (mg/kg)**

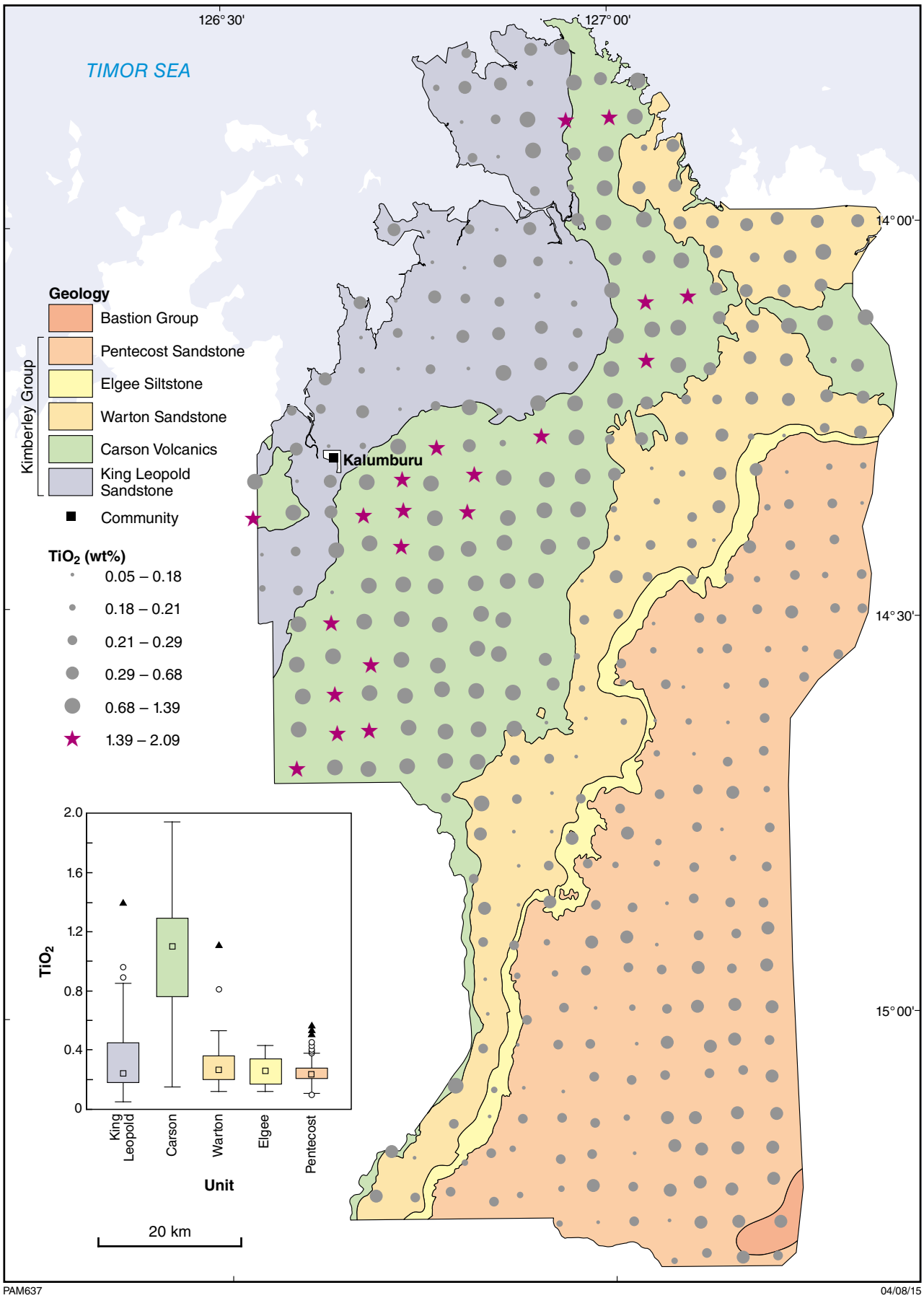
126° 30'
127° 00'
TIMOR SEA
14° 00'
14° 30'
15° 00'
Geology
Kimberley Group
Bastion Group
Pentecost Sandstone
Elgee Siltstone
Warton Sandstone
Carson Volcanics
King Leopold Sandstone
Community
Kalumburu
TiO2 (wt%)
0.05 – 0.18
0.18 – 0.21
0.21 – 0.29
0.29 – 0.68
0.68 – 1.39
1.39 – 2.09
TiO2
2.0
1.6
1.2
0.8
0.4
0
King Leopold
Carson
Warton
Elgee
Pentecost
Unit
20 km
PAM637
04/08/15

Figure B10b.

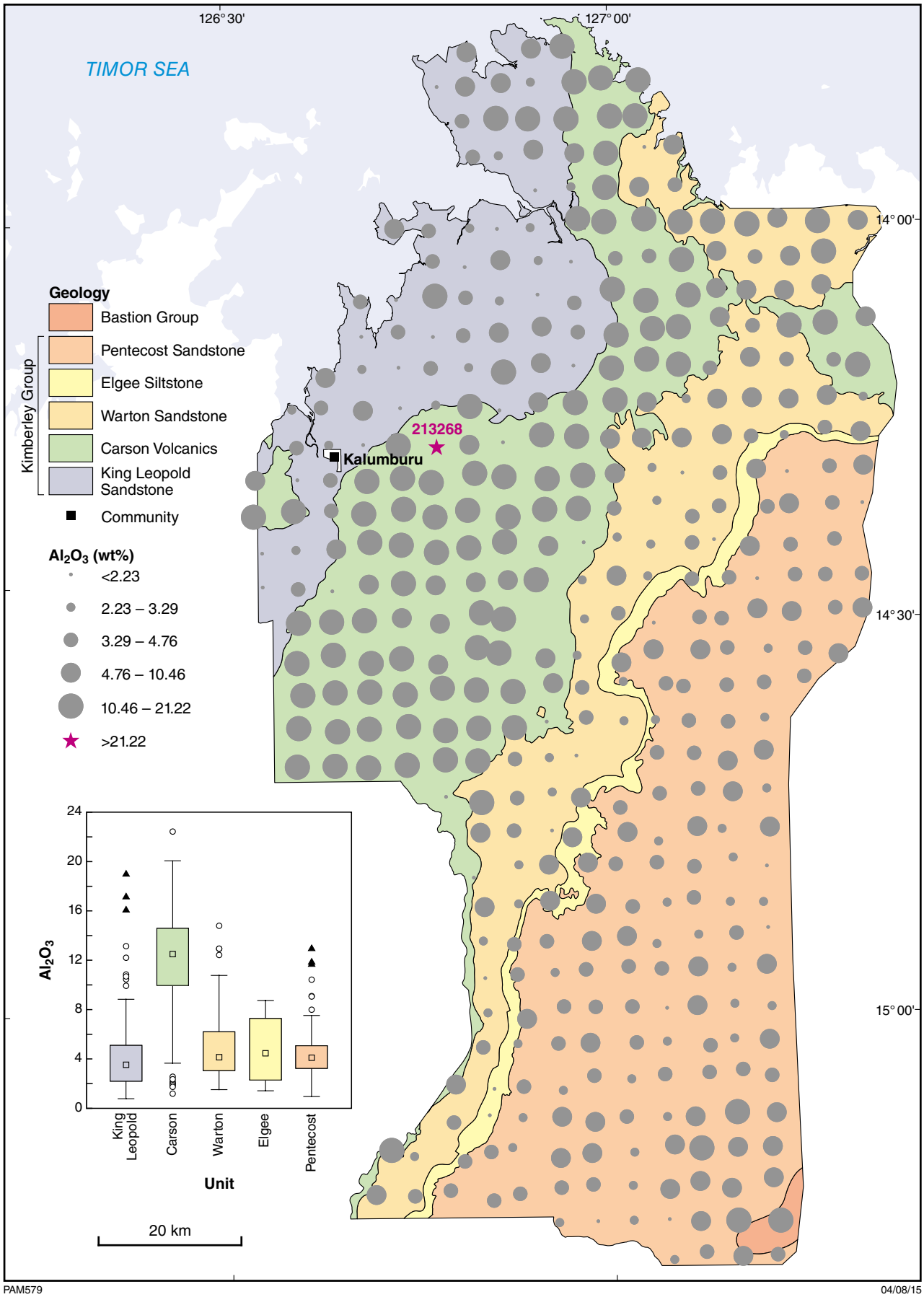
126° 30'
127° 00'
TIMOR SEA
14° 00'
14° 30'
15° 00'
Geology
Bastion Group
Kimberley Group
Pentecost Sandstone
Elgee Siltstone
Warton Sandstone
Carson Volcanics
King Leopold Sandstone
Community
Al2O3 (wt%)
<2.23
2.23 – 3.29
3.29 – 4.76
4.76 – 10.46
10.46 – 21.22
>21.22
213268
Kalumburu
24
20
16
12
8
4
0
Al2O3
King Leopold
Carson
Warton
Elgee
Pentecost
Unit
20 km
PAM579
04/08/15

Figure B10c.

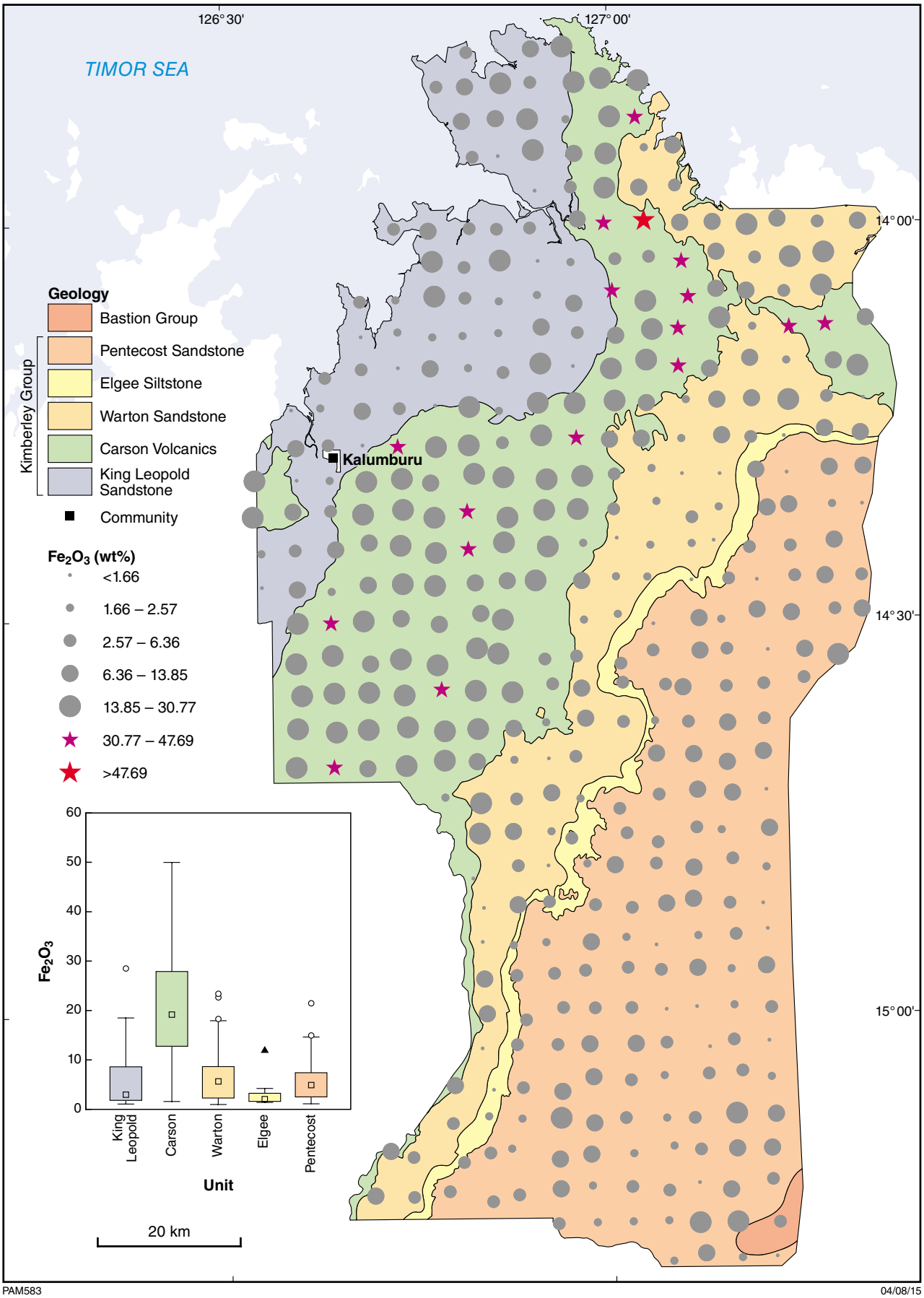
126° 30'
127° 00'
TIMOR SEA
14° 00'
14° 30'
15° 00'
Geology
Kimberley Group
Bastion Group
Pentecost Sandstone
Elgee Siltstone
Warton Sandstone
Carson Volcanics
King Leopold Sandstone
Community
Kalumburu
Fe2O3 (wt%)
<1.66
1.66 – 2.57
2.57 – 6.36
6.36 – 13.85
13.85 – 30.77
30.77 – 47.69
>47.69
Fe2O3
60
50
40
30
20
10
0
King Leopold
Carson
Warton
Elgee
Pentecost
Unit
20 km
PAM583
04/08/15

Figure B10d.

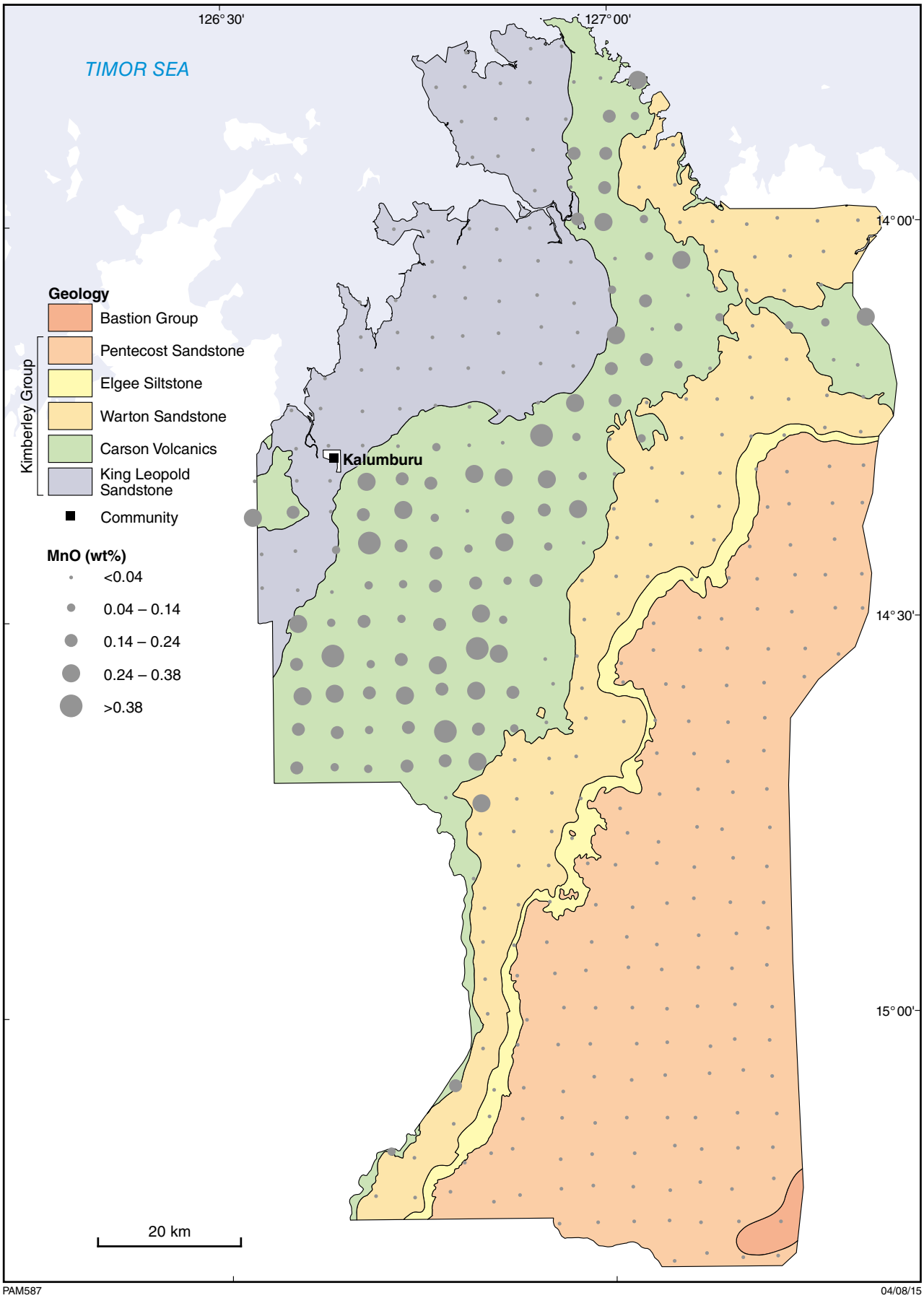
126° 30'
127° 00'
TIMOR SEA
14° 00'
14° 30'
15° 00'
Geology
Bastion Group
Pentecost Sandstone
Elgee Siltstone
Warton Sandstone
Carson Volcanics
King Leopold Sandstone
Kimberley Group
Community
Kalumburu
MnO (wt%)
<0.04
0.04 – 0.14
0.14 – 0.24
0.24 – 0.38
>0.38
20 km
PAM587
04/08/15

Figure B10e.

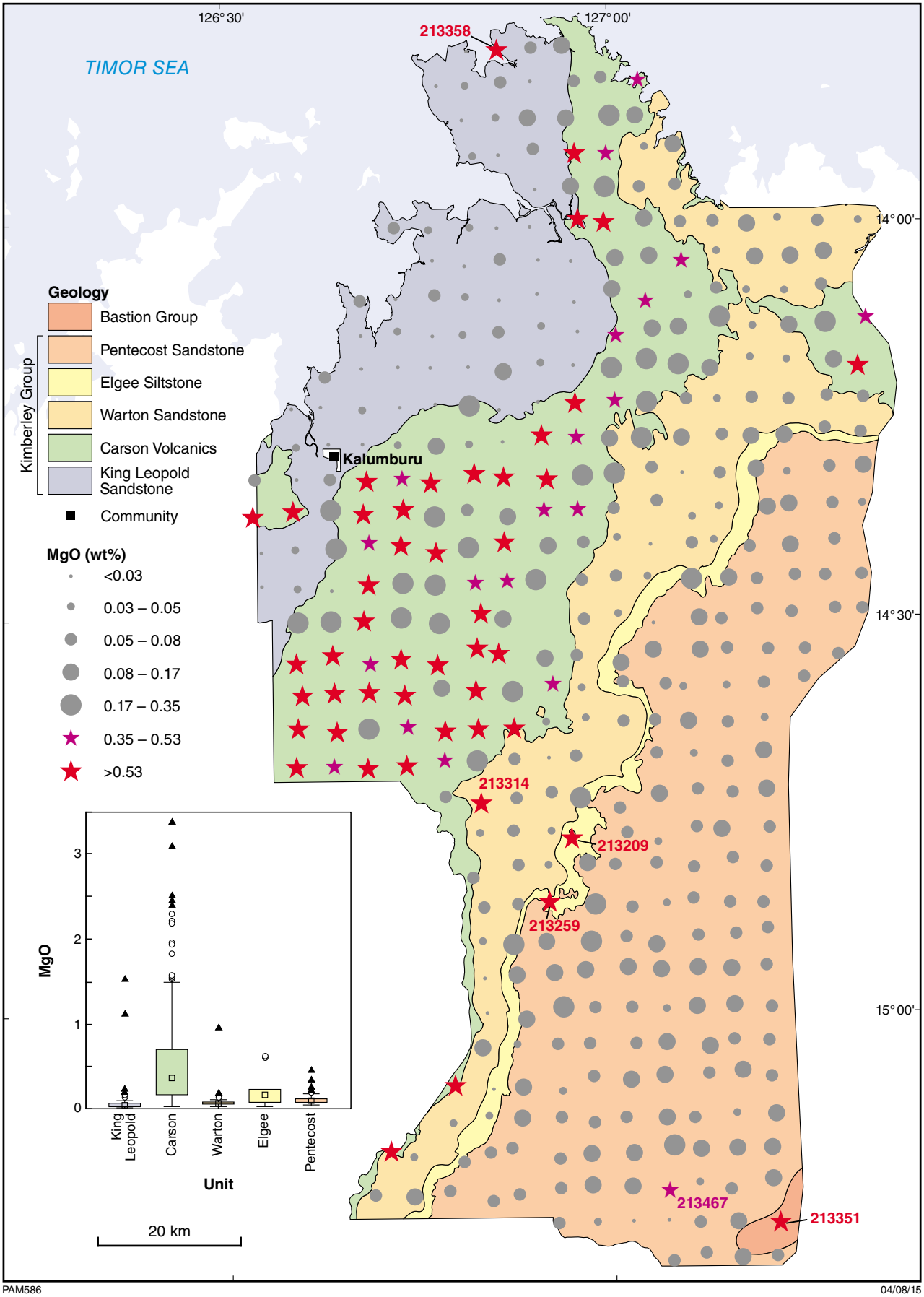
126° 30'
127° 00'
TIMOR SEA
213358
14° 00'
14° 30'
15° 00'
Geology
Kimberley Group
Bastion Group
Pentecost Sandstone
Elgee Siltstone
Warton Sandstone
Carson Volcanics
King Leopold Sandstone
Community
Kalumburu
MgO (wt%)
<0.03
0.03 – 0.05
0.05 – 0.08
0.08 – 0.17
0.17 – 0.35
0.35 – 0.53
>0.53
213314
213209
213259
213467
213351
MgO
Unit
King Leopold
Carson
Warton
Elgee
Pentecost
20 km
PAM586
04/08/15

Figure B10f.

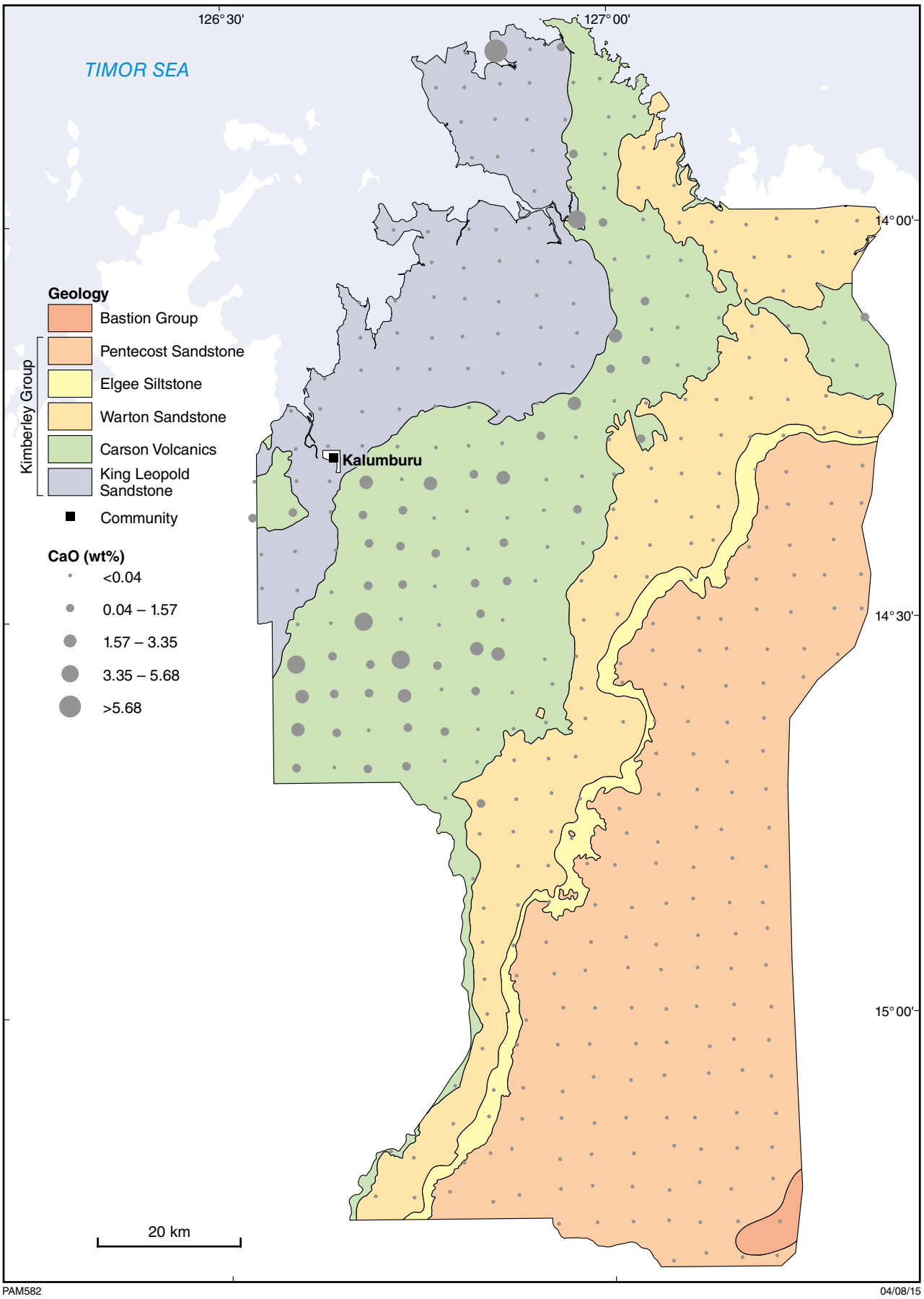
126° 30'
127° 00'
TIMOR SEA
14° 00'
14° 30'
15° 00'
Geology
Bastion Group
Kimberley Group
Pentecost Sandstone
Elgee Siltstone
Warton Sandstone
Carson Volcanics
King Leopold Sandstone
Community
Kalumburu
CaO (wt%)
<0.04
0.04 – 1.57
1.57 – 3.35
3.35 – 5.68
>5.68
20 km
PAM582
04/08/15

Figure B10g.

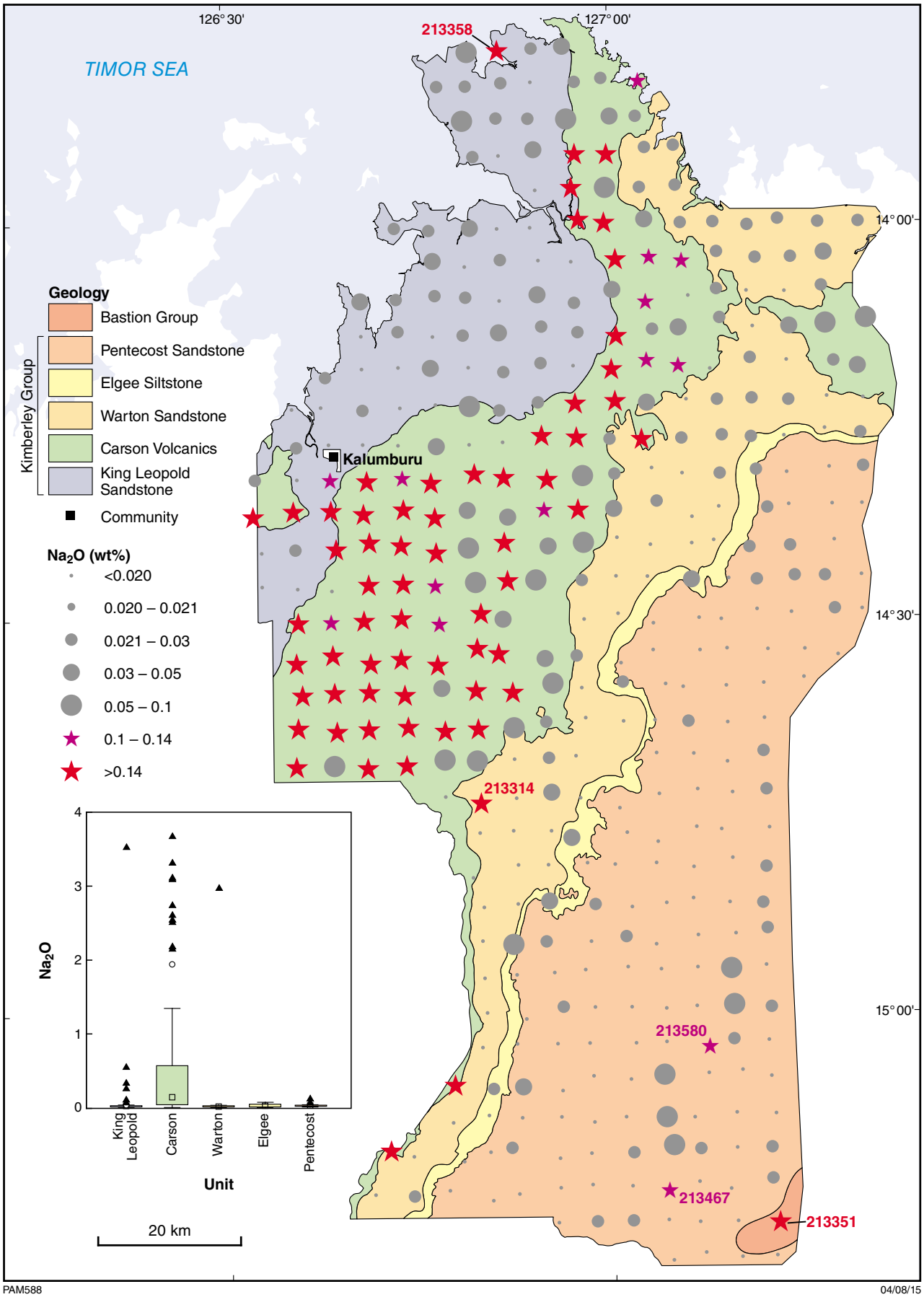
126° 30'
127° 00'
213358
TIMOR SEA
14° 00'
14° 30'
15° 00'
Geology
Bastion Group
Kimberley Group
Pentecost Sandstone
Elgee Siltstone
Warton Sandstone
Carson Volcanics
King Leopold Sandstone
Community
Kalumburu
Na2O (wt%)
<0.020
0.020 – 0.021
0.021 – 0.03
0.03 – 0.05
0.05 – 0.1
0.1 – 0.14
>0.14
213314
213580
213467
213351
Na2O
Unit
King Leopold
Carson
Warton
Elgee
Pentecost
20 km
PAM588
04/08/15

Figure B10h.

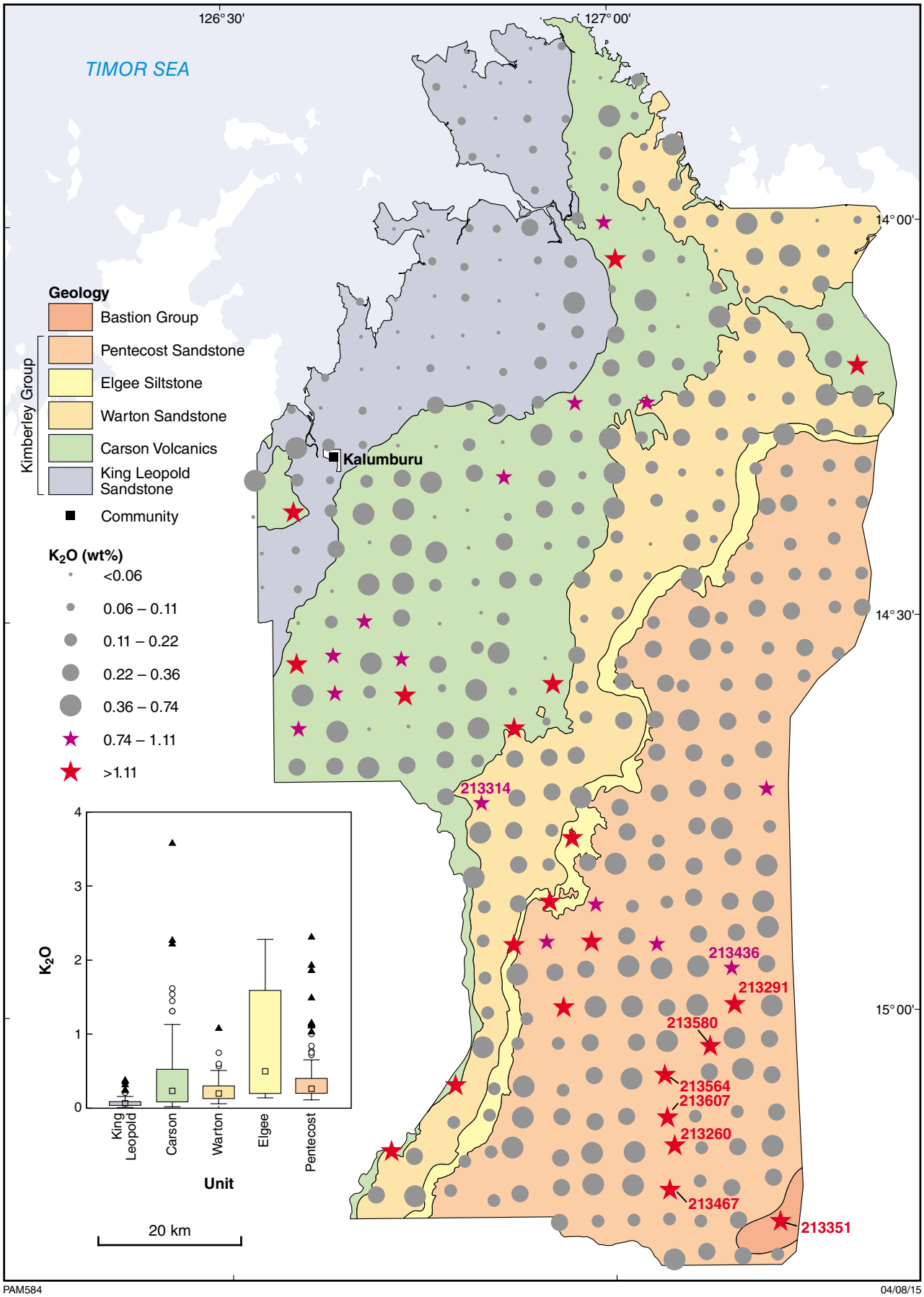
126° 30'
127° 00'
TIMOR SEA
14° 00'
14° 30'
15° 00'
Geology
Bastion Group
Pentecost Sandstone
Elgee Siltstone
Warton Sandstone
Carson Volcanics
King Leopold Sandstone
Kimberley Group
Community
Kalumburu
K2O (wt%)
<0.06
0.06 – 0.11
0.11 – 0.22
0.22 – 0.36
0.36 – 0.74
0.74 – 1.11
>1.11
213314
213436
213291
213580
213564
213607
213260
213467
213351
K2O
Unit
King Leopold
Carson
Warton
Elgee
Pentecost
20 km
PAM584
04/08/15

Figure B10i.

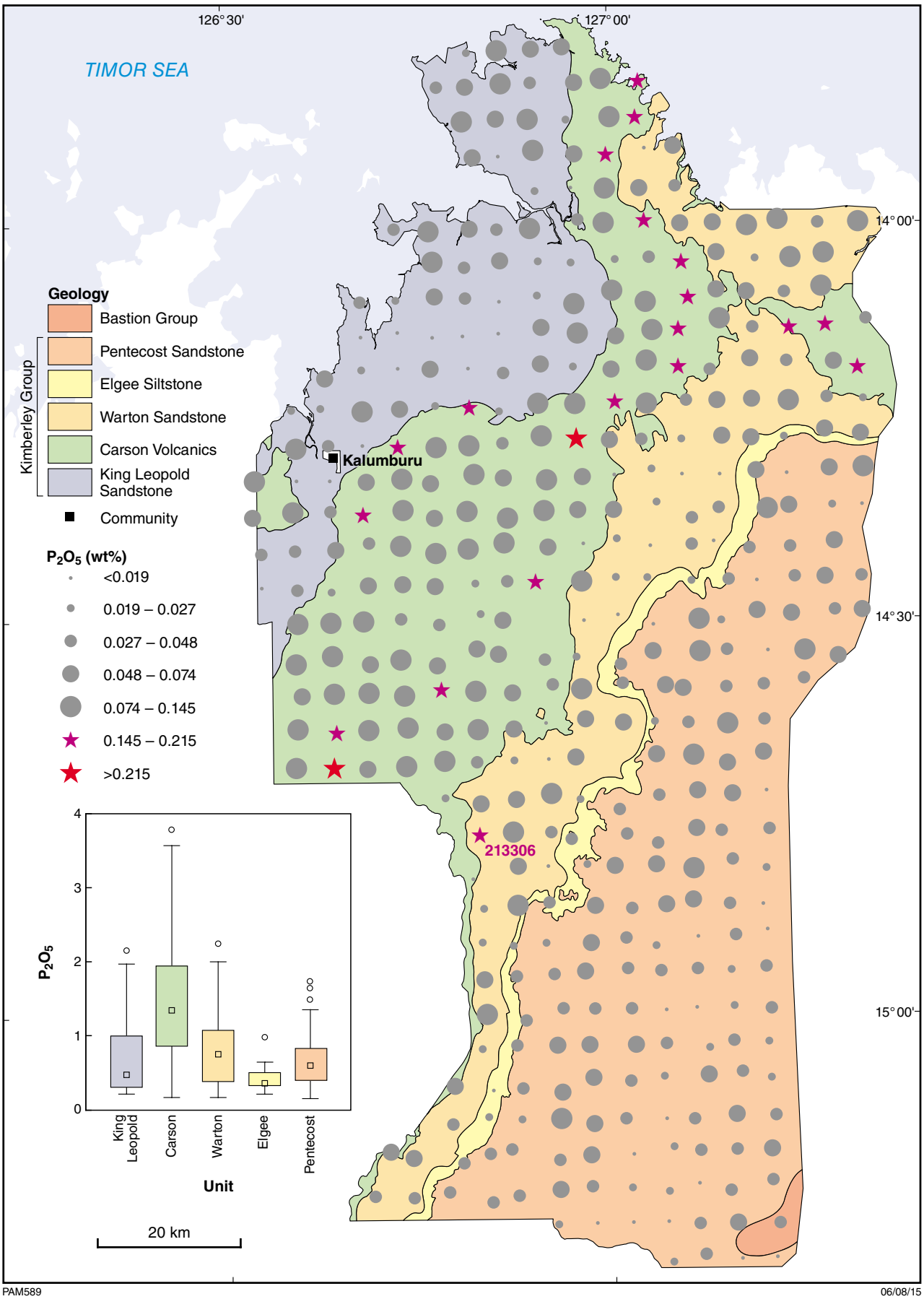
126° 30'
127° 00'
TIMOR SEA
14° 00'
14° 30'
15° 00'
Geology
Kimberley Group
Bastion Group
Pentecost Sandstone
Elgee Siltstone
Warton Sandstone
Carson Volcanics
King Leopold Sandstone
Community
Kalumburu
P2O5 (wt%)
<0.019
0.019 – 0.027
0.027 – 0.048
0.048 – 0.074
0.074 – 0.145
0.145 – 0.215
>0.215
213306
P2O5
0
1
2
3
4
King Leopold
Carson
Warton
Elgee
Pentecost
Unit
20 km
PAM589
06/08/15

Figure B10j.

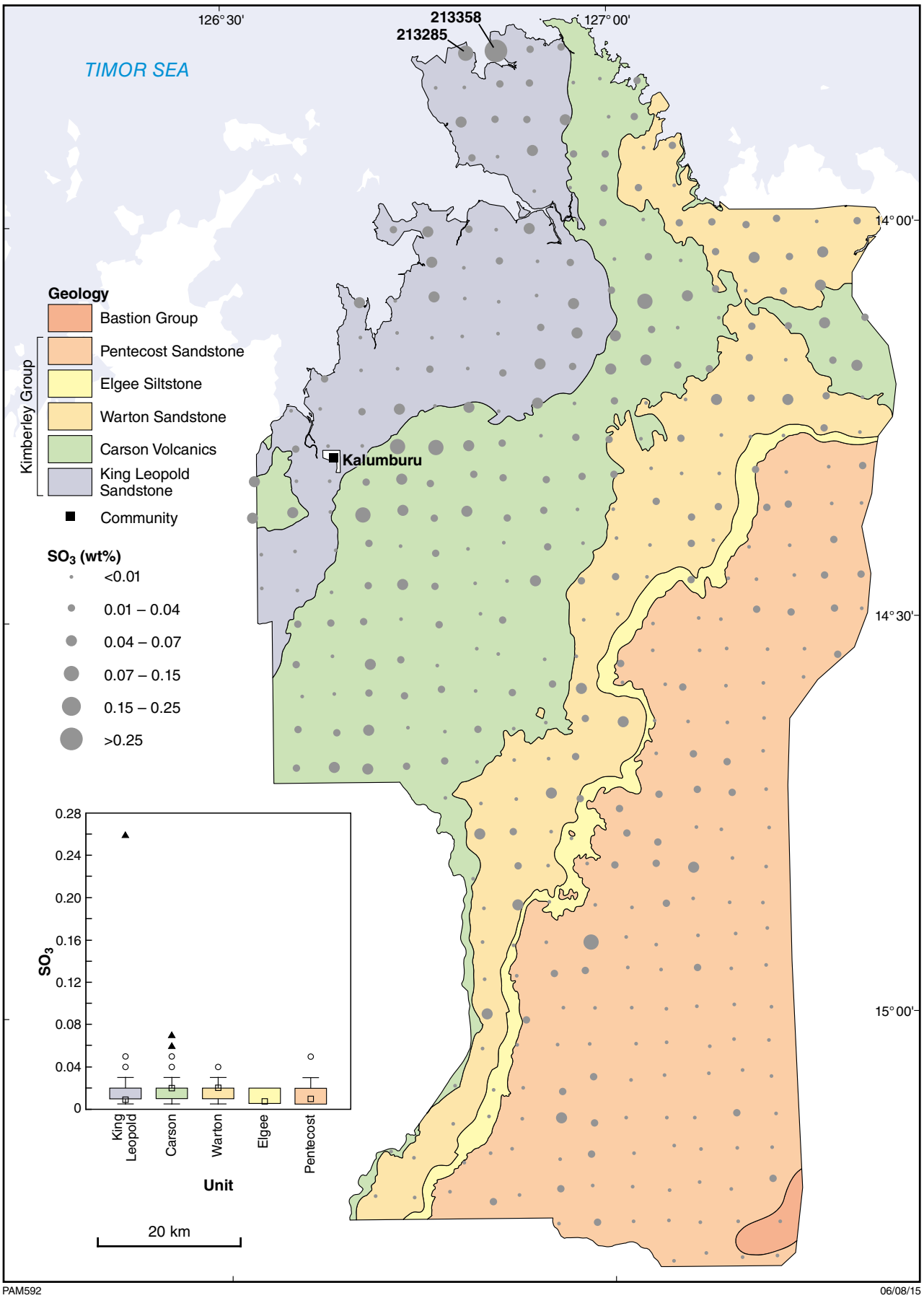
126° 30'
127° 00'
213358
213285
TIMOR SEA
14° 00'
14° 30'
15° 00'
Geology
Bastion Group
Kimberley Group
Pentecost Sandstone
Elgee Siltstone
Warton Sandstone
Carson Volcanics
King Leopold Sandstone
Community
Kalumburu
SO3 (wt%)
<0.01
0.01 – 0.04
0.04 – 0.07
0.07 – 0.15
0.15 – 0.25
>0.25
0.28
0.24
0.20
0.16
0.12
0.08
0.04
0
SO3
King Leopold
Carson
Warton
Elgee
Pentecost
Unit
20 km
PAM592
06/08/15

Figure B10k.

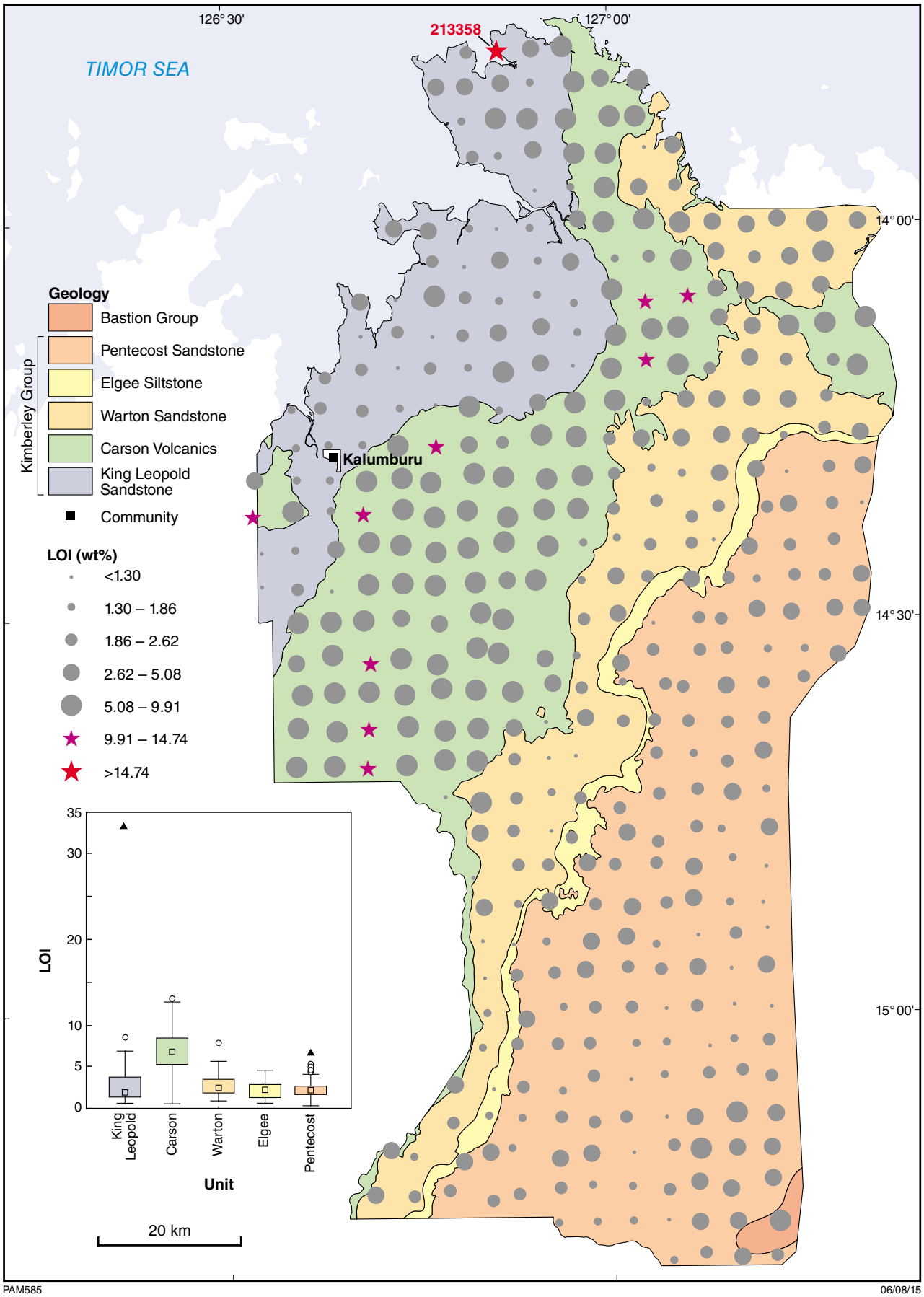
126° 30'
127° 00'
213358
TIMOR SEA
14° 00'
14° 30'
15° 00'
Geology
Bastion Group
Pentecost Sandstone
Elgee Siltstone
Warton Sandstone
Carson Volcanics
King Leopold Sandstone
Kimberley Group
Community
Kalumburu
LOI (wt%)
<1.30
1.30 – 1.86
1.86 – 2.62
2.62 – 5.08
5.08 – 9.91
9.91 – 14.74
>14.74
LOI
35
30
20
10
5
0
King Leopold
Carson
Warton
Elgee
Pentecost
Unit
20 km
PAM585
06/08/15

Figure B10l.

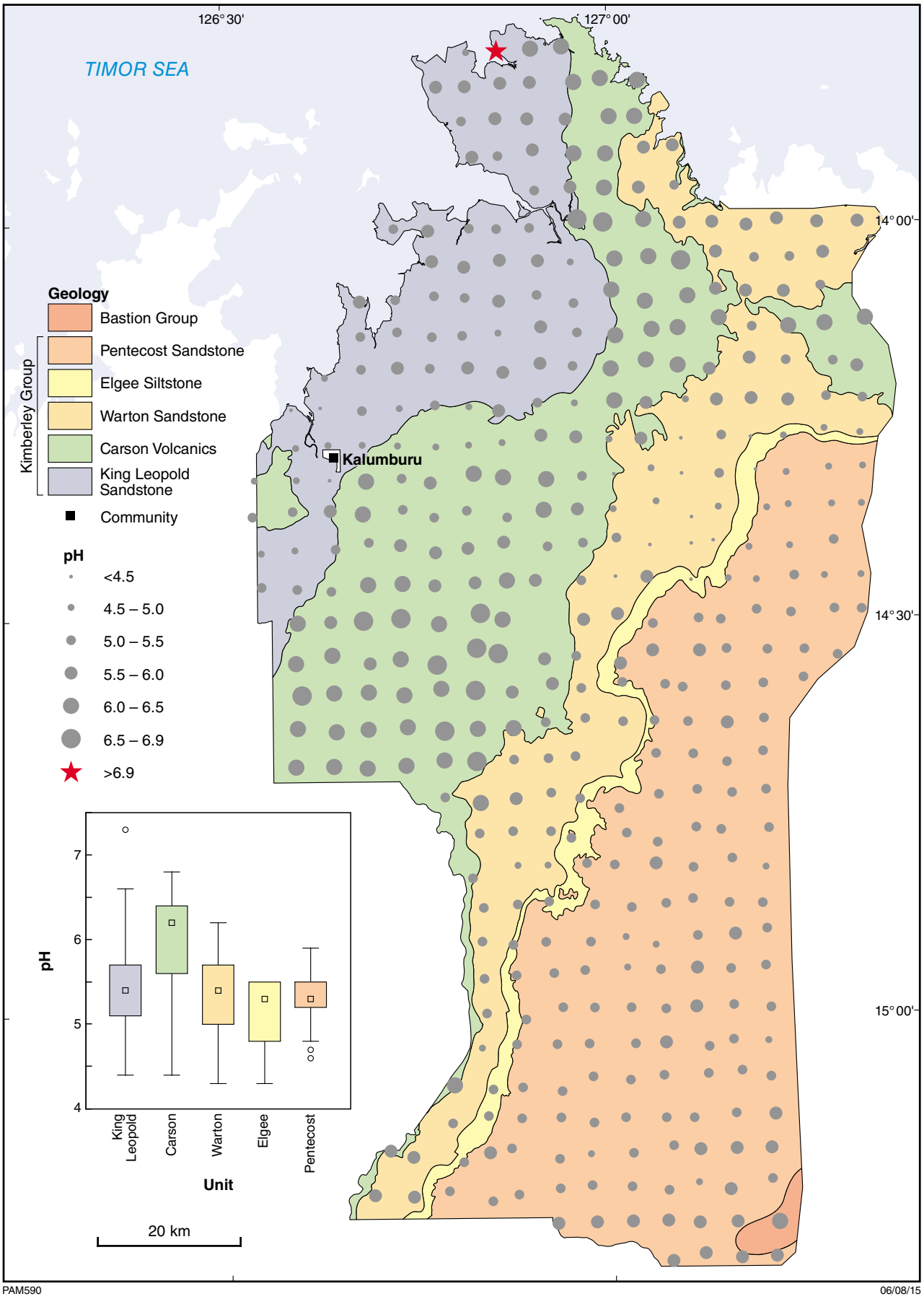
126° 30'
127° 00'
TIMOR SEA
14° 00'
14° 30'
15° 00'
Geology
Kimberley Group
Bastion Group
Pentecost Sandstone
Elgee Siltstone
Warton Sandstone
Carson Volcanics
King Leopold Sandstone
Community
Kalumburu
pH
<4.5
4.5 – 5.0
5.0 – 5.5
5.5 – 6.0
6.0 – 6.5
6.5 – 6.9
>6.9
pH
7
6
5
4
King Leopold
Carson
Warton
Elgee
Pentecost
Unit
20 km
PAM590
06/08/15

Figure B10m.

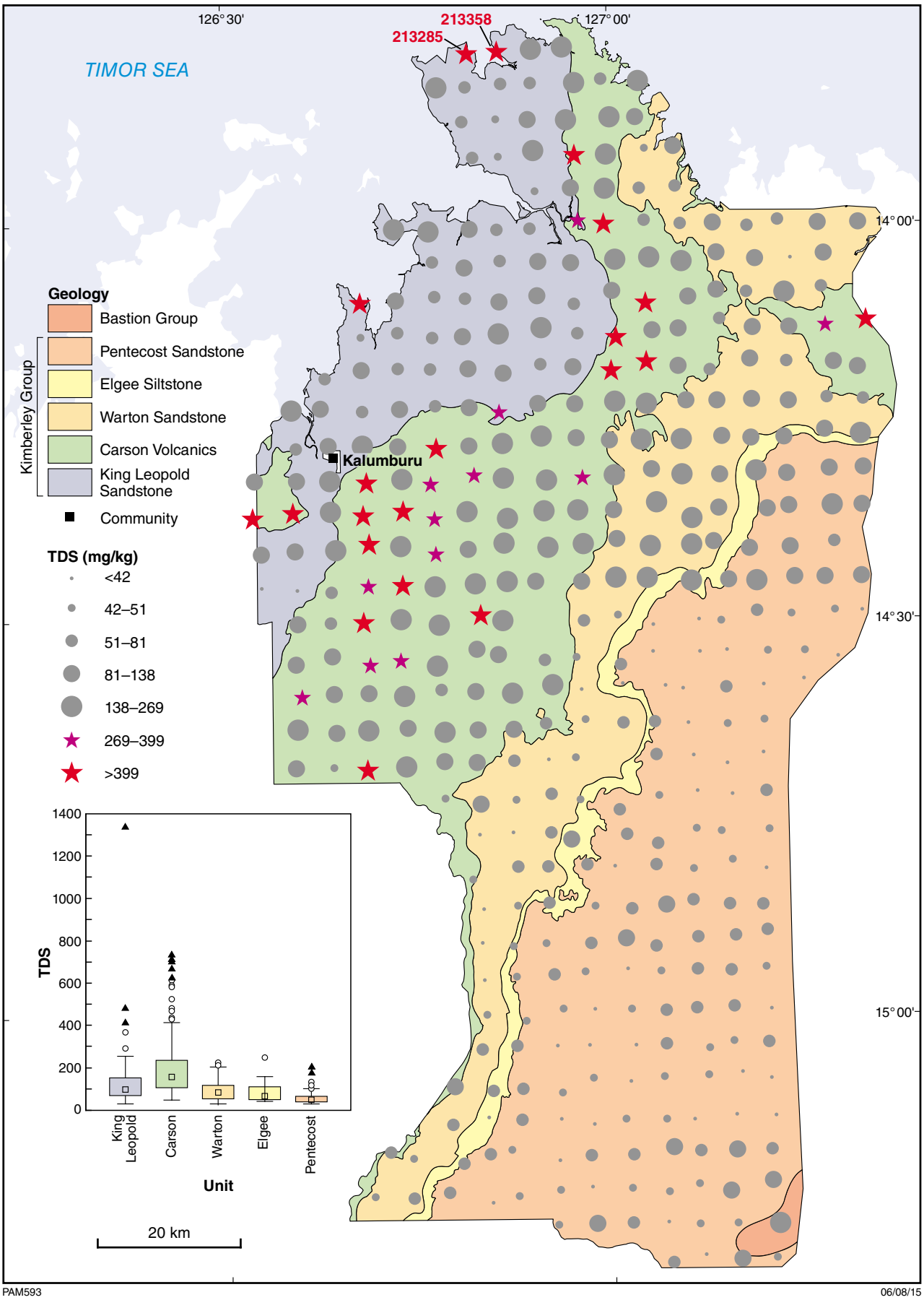
126° 30'
127° 00'
213358
213285
TIMOR SEA
14° 00'
14° 30'
15° 00'
Geology
Kimberley Group
Bastion Group
Pentecost Sandstone
Elgee Siltstone
Warton Sandstone
Carson Volcanics
King Leopold Sandstone
Community
Kalumburu
TDS (mg/kg)
<42
42–51
51–81
81–138
138–269
269–399
>399
TDS
1400
1200
1000
800
600
400
200
0
King Leopold
Carson
Warton
Elgee
Pentecost
Unit
20 km
PAM593
06/08/15

Figure B10n.

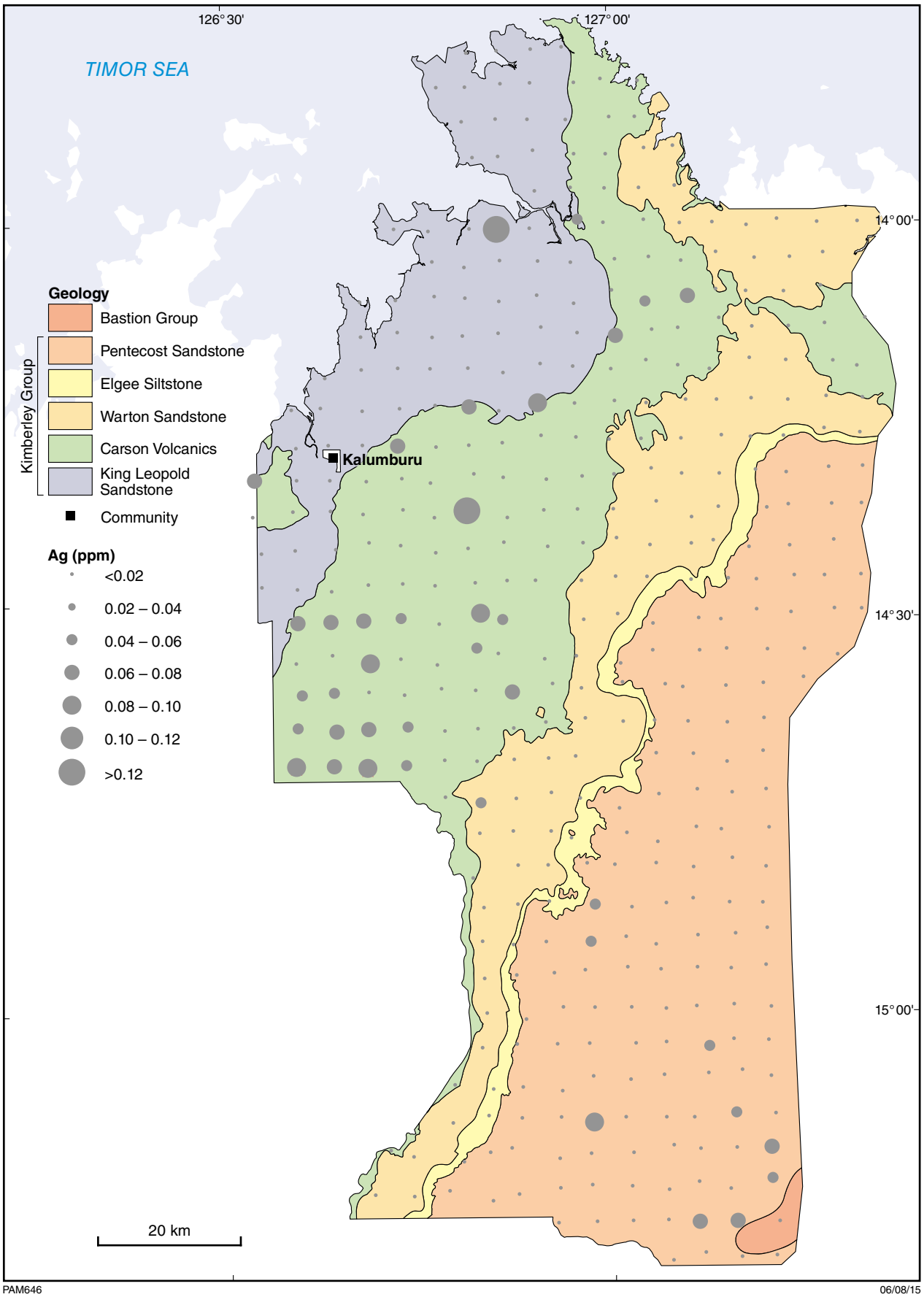

Figure B11. **Bubble plots for precious metals measured in regolith from the Balanggarra project area. Due to the high proportion of censored data, bubble divisions use natural breaks, and box and whisker plots have not been compiled: a) Ag (ppm); b) Au (ppb); c) Pd (ppb); d) Pt (ppb)**

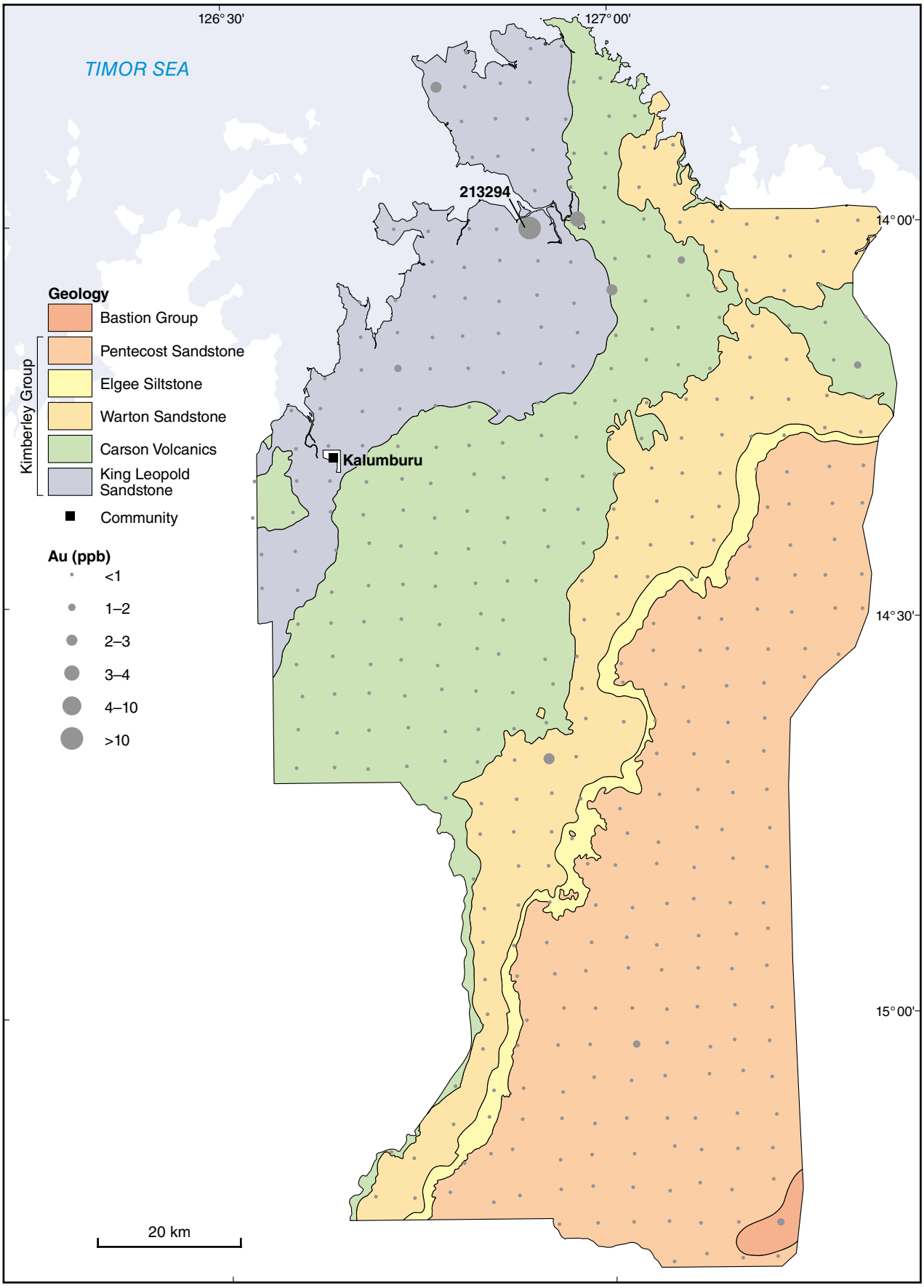
126° 30'
127° 00'
TIMOR SEA
213294
14° 00'
14° 30'
15° 00'
Kalumburu
Geology
Bastion Group
Kimberley Group
Pentecost Sandstone
Elgee Siltstone
Warton Sandstone
Carson Volcanics
King Leopold Sandstone
Community
Au (ppb)
<1
1–2
2–3
3–4
4–10
>10
20 km

Figure B11b.

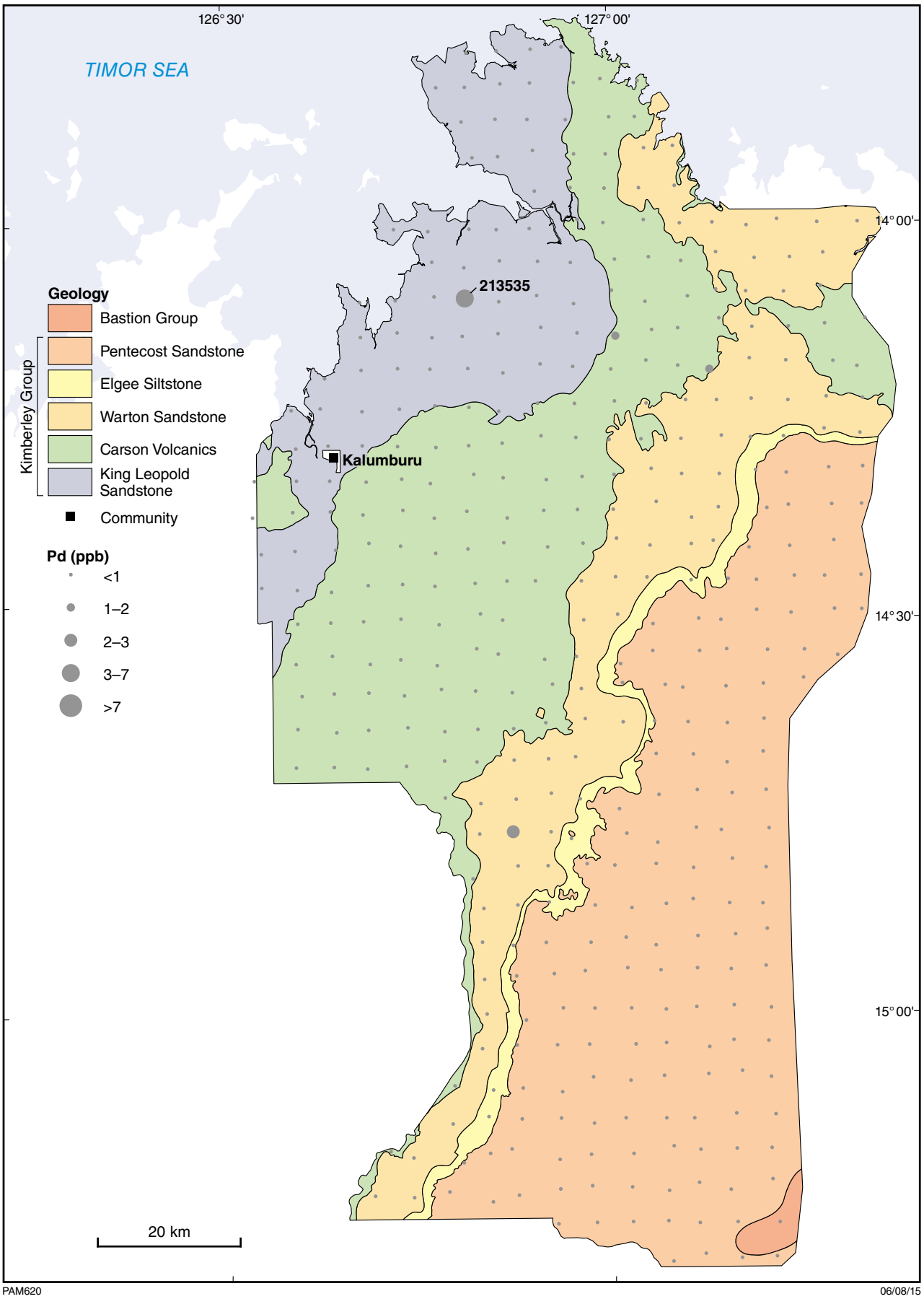
126° 30'
127° 00'
TIMOR SEA
14° 00'
14° 30'
15° 00'
213535
Kalumburu
Geology
Bastion Group
Kimberley Group
Pentecost Sandstone
Elgee Siltstone
Warton Sandstone
Carson Volcanics
King Leopold Sandstone
Community
Pd (ppb)
<1
1–2
2–3
3–7
>7
20 km
PAM620
06/08/15

Figure B11c.

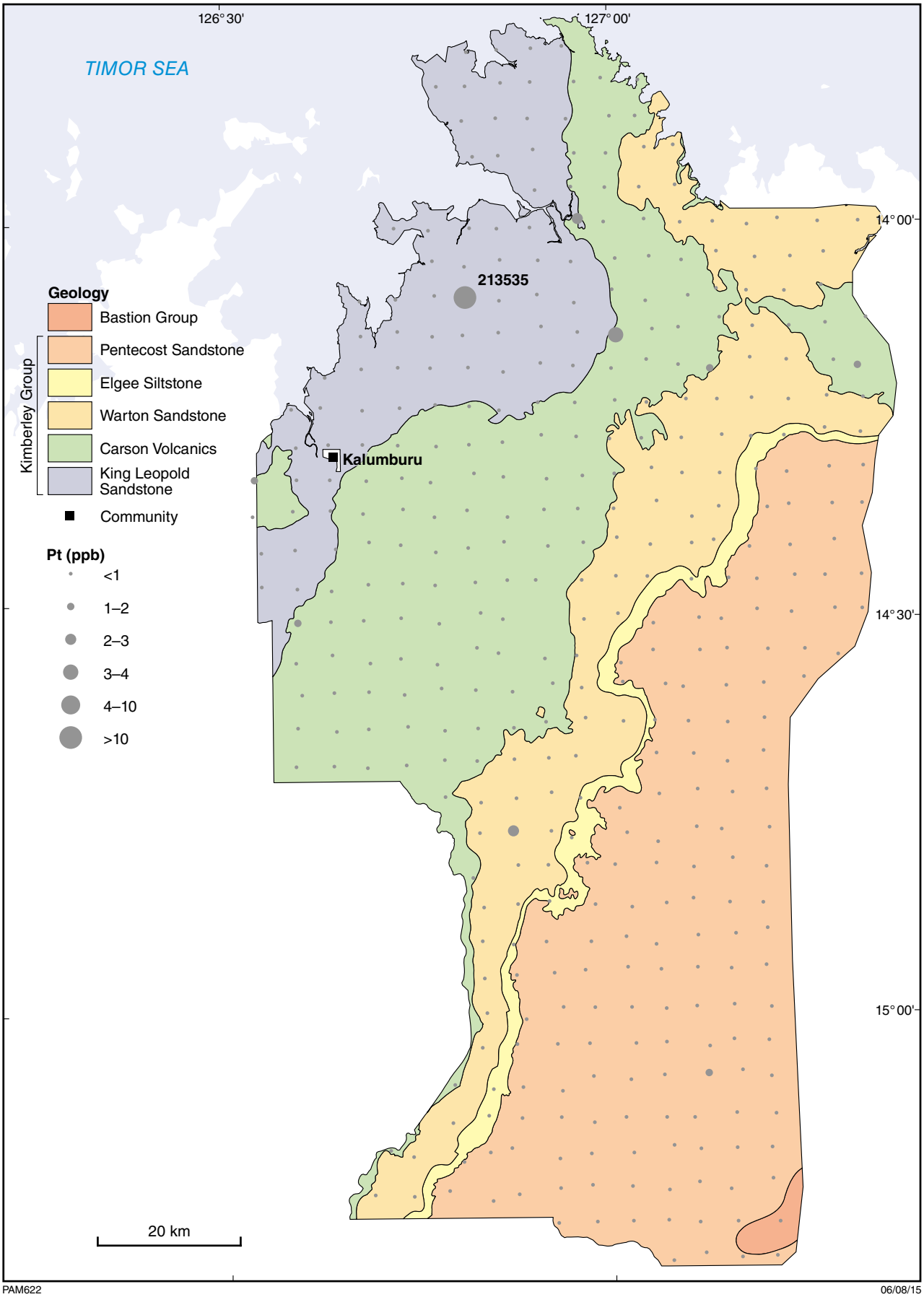
126° 30'
127° 00'
TIMOR SEA
14° 00'
14° 30'
15° 00'
213535
Kalumburu
Geology
Bastion Group
Kimberley Group
Pentecost Sandstone
Elgee Siltstone
Warton Sandstone
Carson Volcanics
King Leopold Sandstone
Community
Pt (ppb)
<1
1–2
2–3
3–4
4–10
>10
20 km
PAM622
06/08/15

Figure B11d.

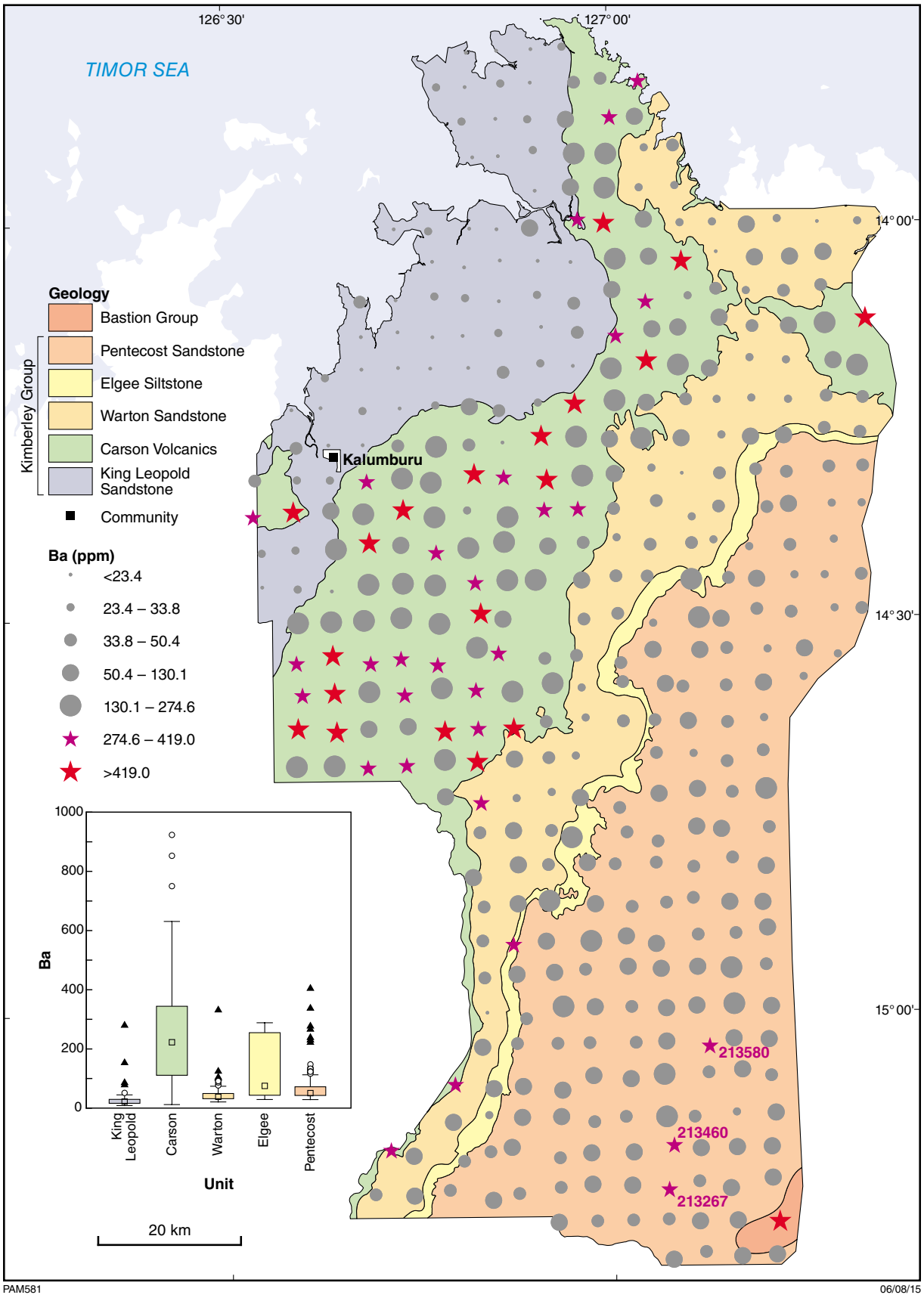

Figure B12. **Bubble plots for lithophile elements measured in regolith from the Balanggarra project area. Bubble divisions have been determined using box and whisker plots (see text for explanation). Samples with anomalous concentrations are shown by stars (purple – outlier; red – extreme). Also shown is the box and whisker plot according to major lithological units, showing the median, interquartile range (box) and samples with anomalous concentrations (outlier – open circle; extreme – triangle): a) Ba (ppm); b) Be (ppm); c) C (wt%); d) Cs (ppm); e) Ga (ppm); f) Ge (ppm); g) In (ppm); h) Li (ppm); i) Rb (ppm); j) Sn (ppm); k) Sr (ppm); l) Th (ppm); m) Tl (ppm); n) U (ppm)**

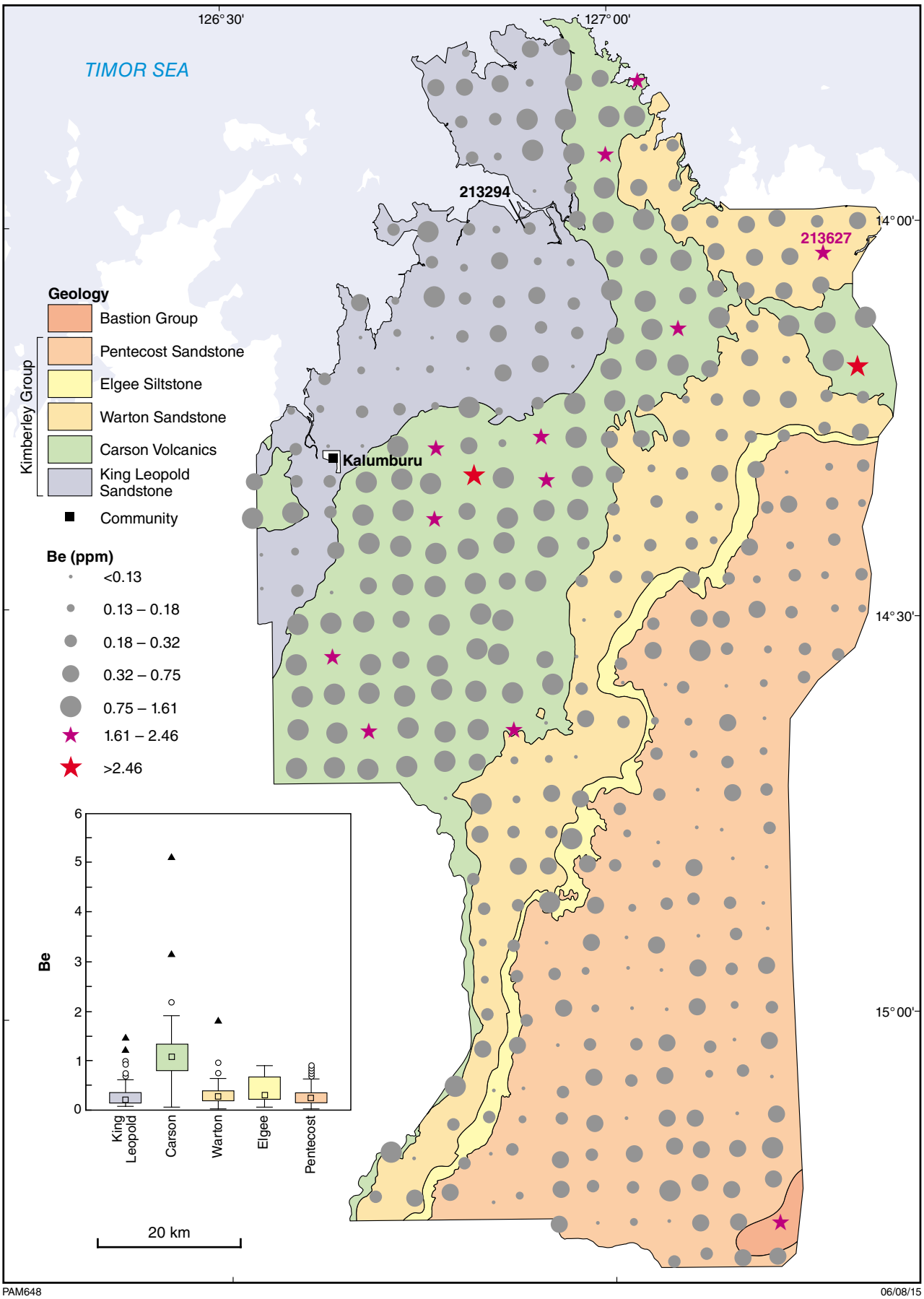
126° 30'
127° 00'
TIMOR SEA
213294
213627
14° 00'
14° 30'
15° 00'
Kalumburu
Geology
Kimberley Group
Bastion Group
Pentecost Sandstone
Elgee Siltstone
Warton Sandstone
Carson Volcanics
King Leopold Sandstone
Community
Be (ppm)
<0.13
0.13 – 0.18
0.18 – 0.32
0.32 – 0.75
0.75 – 1.61
1.61 – 2.46
>2.46
Be
King Leopold
Carson
Warton
Elgee
Pentecost
20 km
PAM648
06/08/15

Figure B12b.

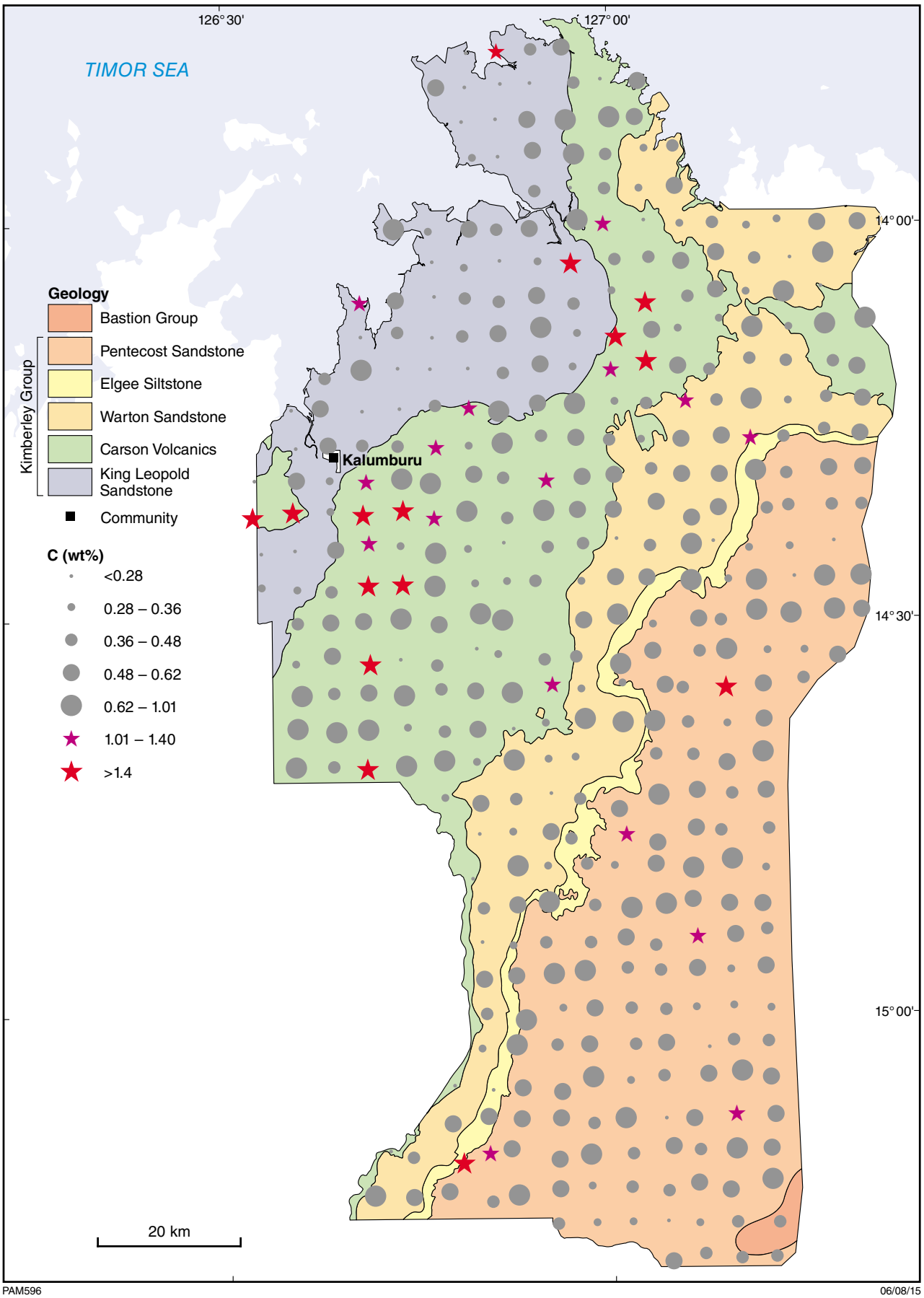
126° 30'
127° 00'
TIMOR SEA
14° 00'
14° 30'
15° 00'
Geology
Kimberley Group
Bastion Group
Pentecost Sandstone
Elgee Siltstone
Warton Sandstone
Carson Volcanics
King Leopold Sandstone
Community
Kalumburu
C (wt%)
<0.28
0.28 – 0.36
0.36 – 0.48
0.48 – 0.62
0.62 – 1.01
1.01 – 1.40
>1.4
20 km
PAM596
06/08/15

Figure B12c.

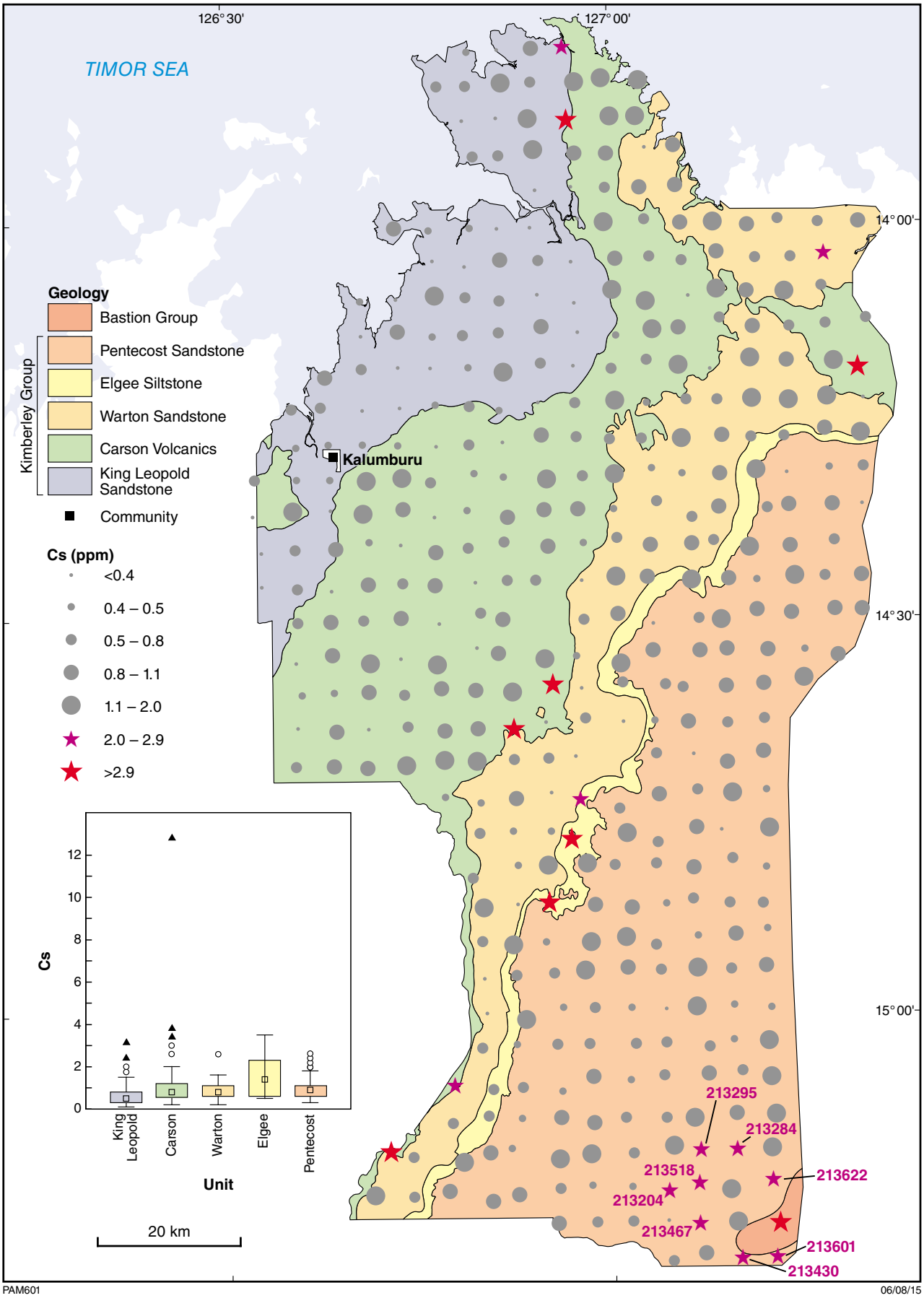
126° 30'
127° 00'
TIMOR SEA
14° 00'
14° 30'
15° 00'
Geology
Kimberley Group
Bastion Group
Pentecost Sandstone
Elgee Siltstone
Warton Sandstone
Carson Volcanics
King Leopold Sandstone
Community
Kalumburu
Cs (ppm)
<0.4
0.4 – 0.5
0.5 – 0.8
0.8 – 1.1
1.1 – 2.0
2.0 – 2.9
>2.9
Cs
Unit
King Leopold
Carson
Warton
Elgee
Pentecost
20 km
213295
213284
213518
213622
213204
213467
213601
213430
PAM601
06/08/15

Figure B12d.

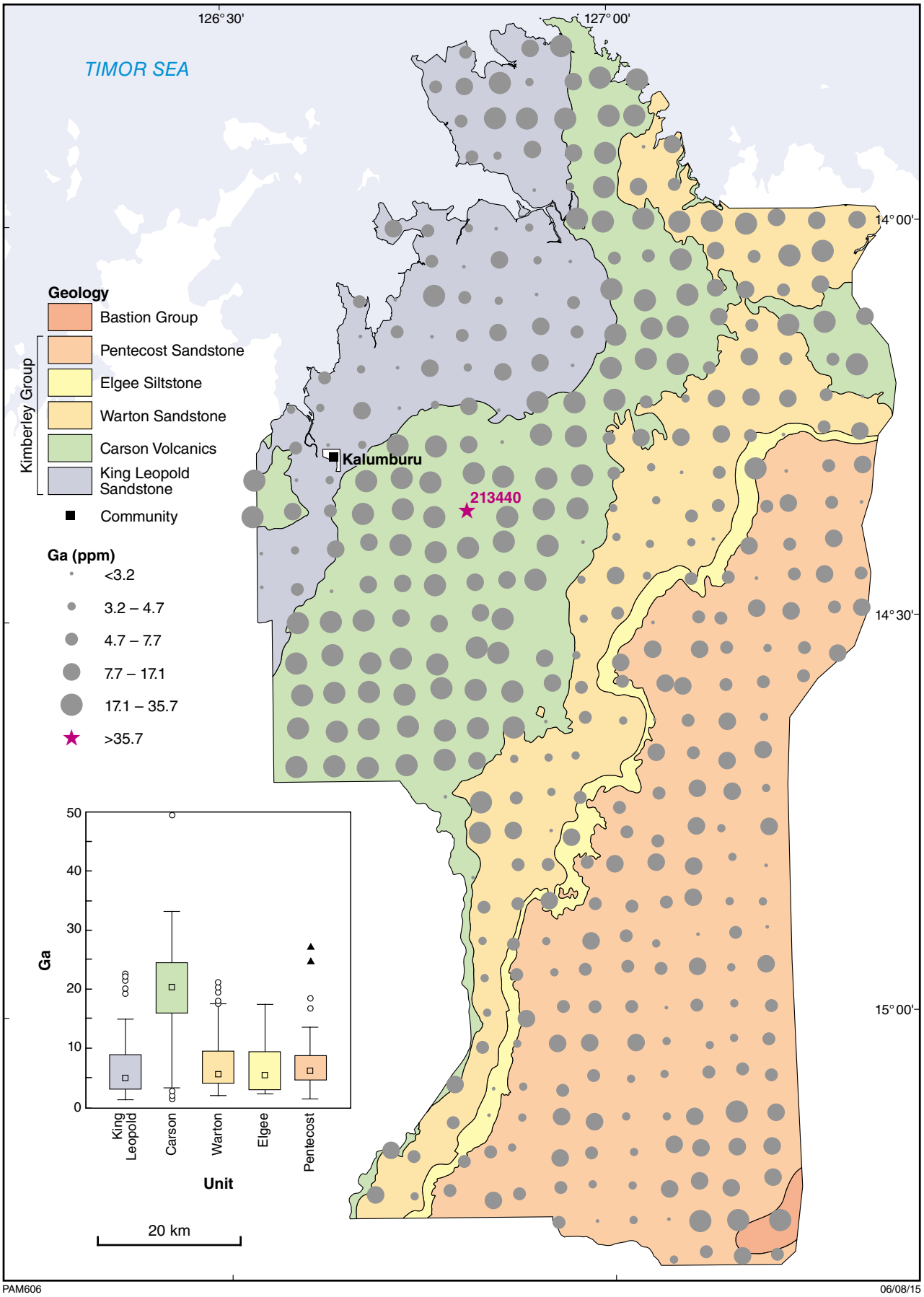
126° 30'
127° 00'
TIMOR SEA
14° 00'
14° 30'
15° 00'
Geology
Kimberley Group
Bastion Group
Pentecost Sandstone
Elgee Siltstone
Warton Sandstone
Carson Volcanics
King Leopold Sandstone
Community
Kalumburu
213440
Ga (ppm)
<3.2
3.2 – 4.7
4.7 – 7.7
7.7 – 17.1
17.1 – 35.7
>35.7
Ga
50
40
30
20
10
0
King Leopold
Carson
Warton
Elgee
Pentecost
Unit
20 km
PAM606
06/08/15

Figure B12e.

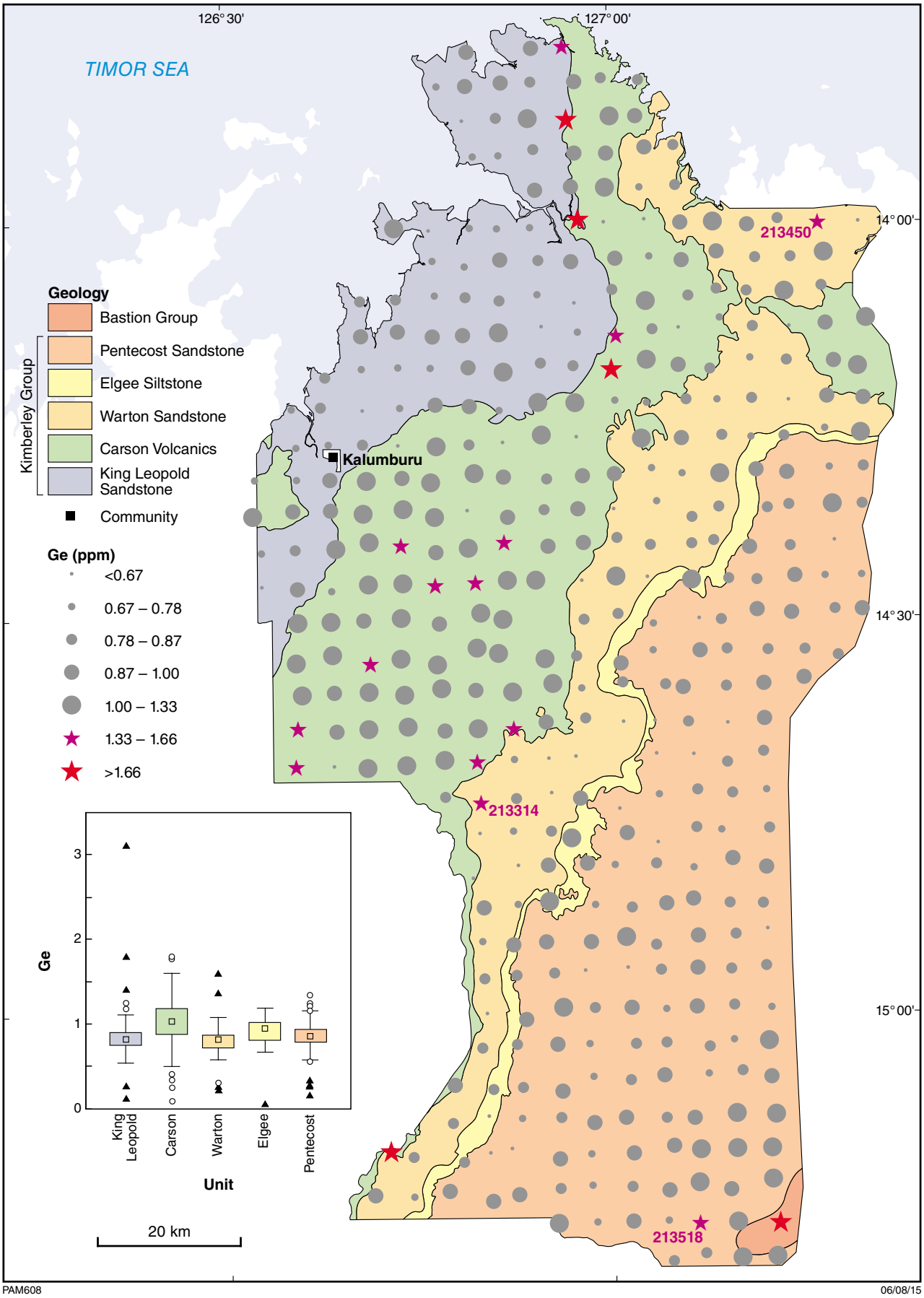
126° 30'
127° 00'
TIMOR SEA
14° 00'
14° 30'
15° 00'
213450
213314
213518
Kalumburu
Geology
Bastion Group
Pentecost Sandstone
Elgee Siltstone
Warton Sandstone
Carson Volcanics
King Leopold Sandstone
Kimberley Group
Community
Ge (ppm)
<0.67
0.67 – 0.78
0.78 – 0.87
0.87 – 1.00
1.00 – 1.33
1.33 – 1.66
>1.66
Ge
0
1
2
3
King Leopold
Carson
Warton
Elgee
Pentecost
Unit
20 km
PAM608
06/08/15

Figure B12f.

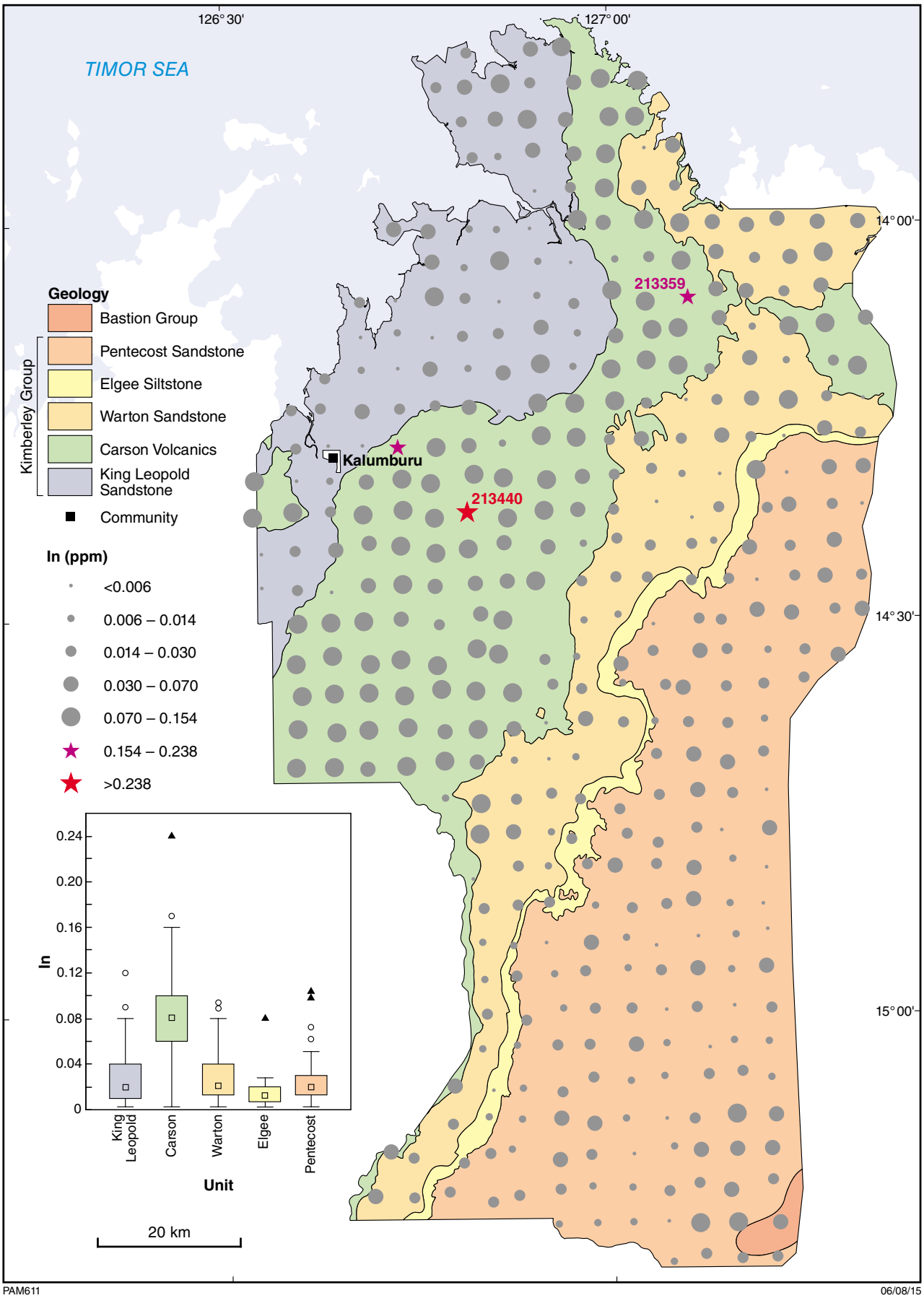
126° 30'
127° 00'
TIMOR SEA
14° 00'
14° 30'
15° 00'
213359
213440
Kalumburu
Geology
Bastion Group
Kimberley Group
Pentecost Sandstone
Elgee Siltstone
Warton Sandstone
Carson Volcanics
King Leopold Sandstone
Community
ln (ppm)
<0.006
0.006 – 0.014
0.014 – 0.030
0.030 – 0.070
0.070 – 0.154
0.154 – 0.238
>0.238
ln
0.24
0.20
0.16
0.12
0.08
0.04
0
King Leopold
Carson
Warton
Elgee
Pentecost
Unit
20 km
PAM611
06/08/15

Figure B12g.

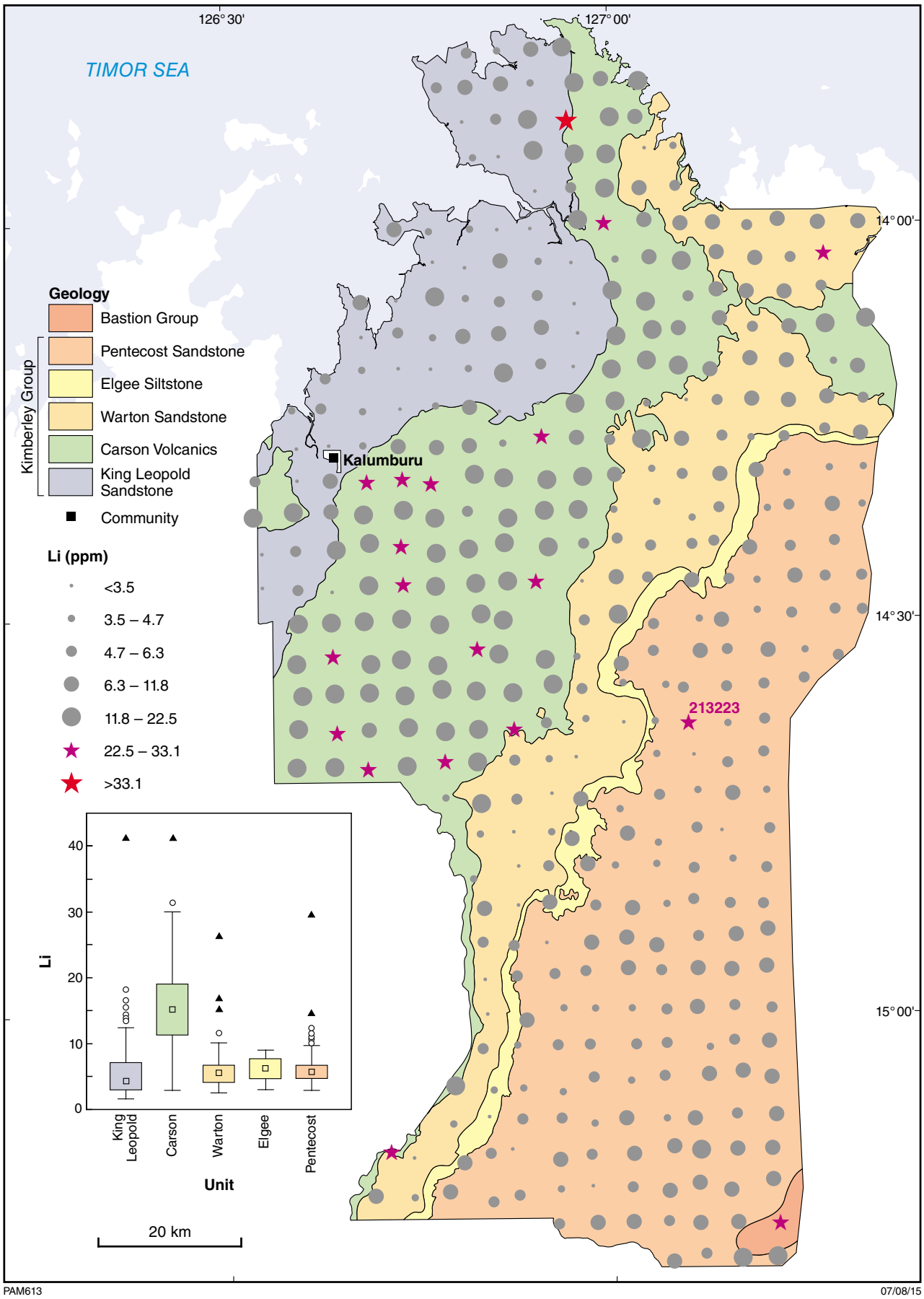
126° 30'
127° 00'
TIMOR SEA
14° 00'
14° 30'
15° 00'
Geology
Bastion Group
Kimberley Group
Pentecost Sandstone
Elgee Siltstone
Warton Sandstone
Carson Volcanics
King Leopold Sandstone
Community
Kalumburu
Li (ppm)
<3.5
3.5 – 4.7
4.7 – 6.3
6.3 – 11.8
11.8 – 22.5
22.5 – 33.1
>33.1
213223
Li
0
10
20
30
40
King Leopold
Carson
Warton
Elgee
Pentecost
Unit
20 km
PAM613
07/08/15

Figure B12h.

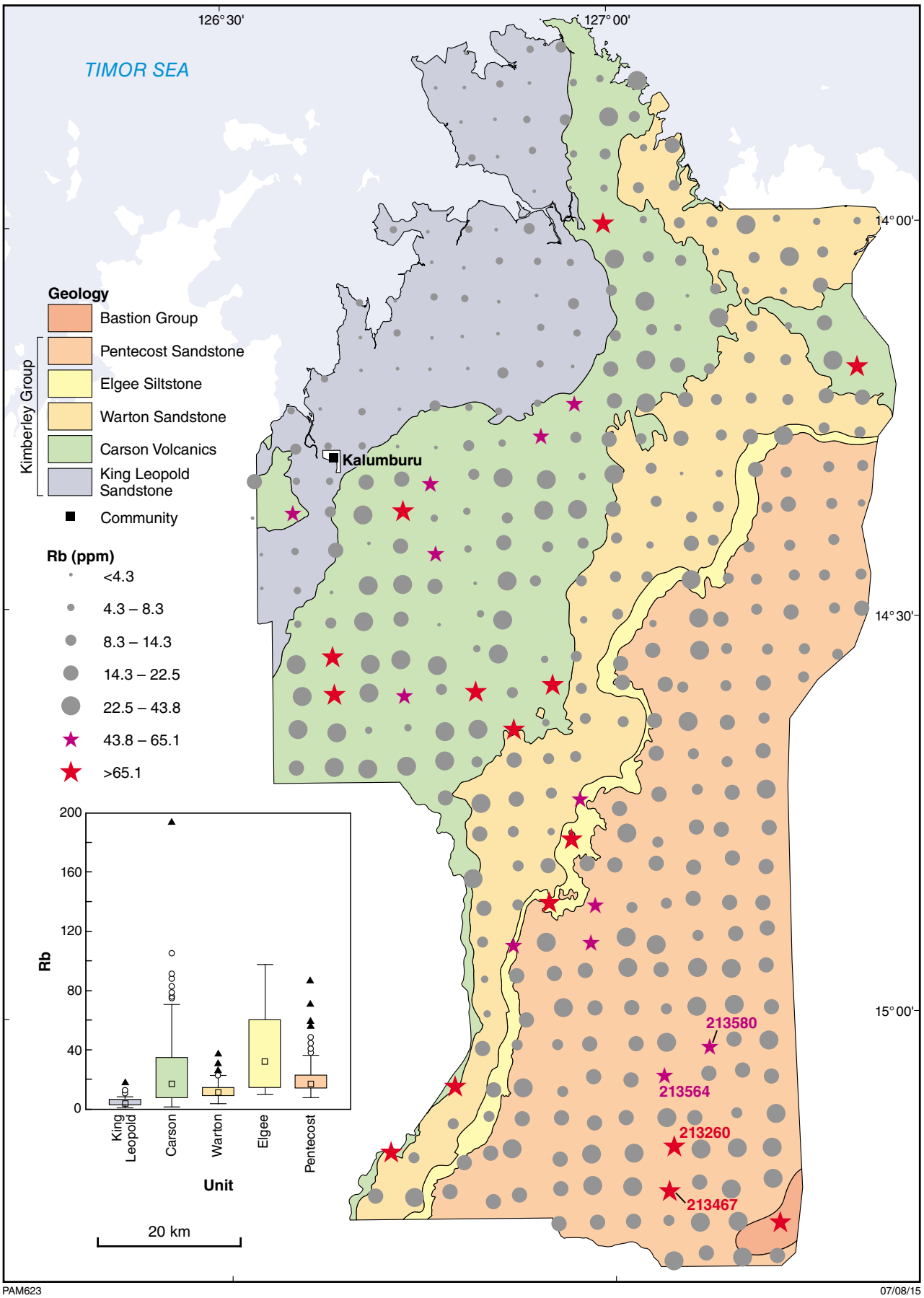
126° 30'
127° 00'
TIMOR SEA
14° 00'
14° 30'
15° 00'
Geology
Kimberley Group
Bastion Group
Pentecost Sandstone
Elgee Siltstone
Warton Sandstone
Carson Volcanics
King Leopold Sandstone
Community
Kalumburu
Rb (ppm)
<4.3
4.3 – 8.3
8.3 – 14.3
14.3 – 22.5
22.5 – 43.8
43.8 – 65.1
>65.1
200
160
120
80
40
0
Rb
King Leopold
Carson
Warton
Elgee
Pentecost
Unit
20 km
213580
213564
213260
213467
PAM623
07/08/15

Figure B12i.

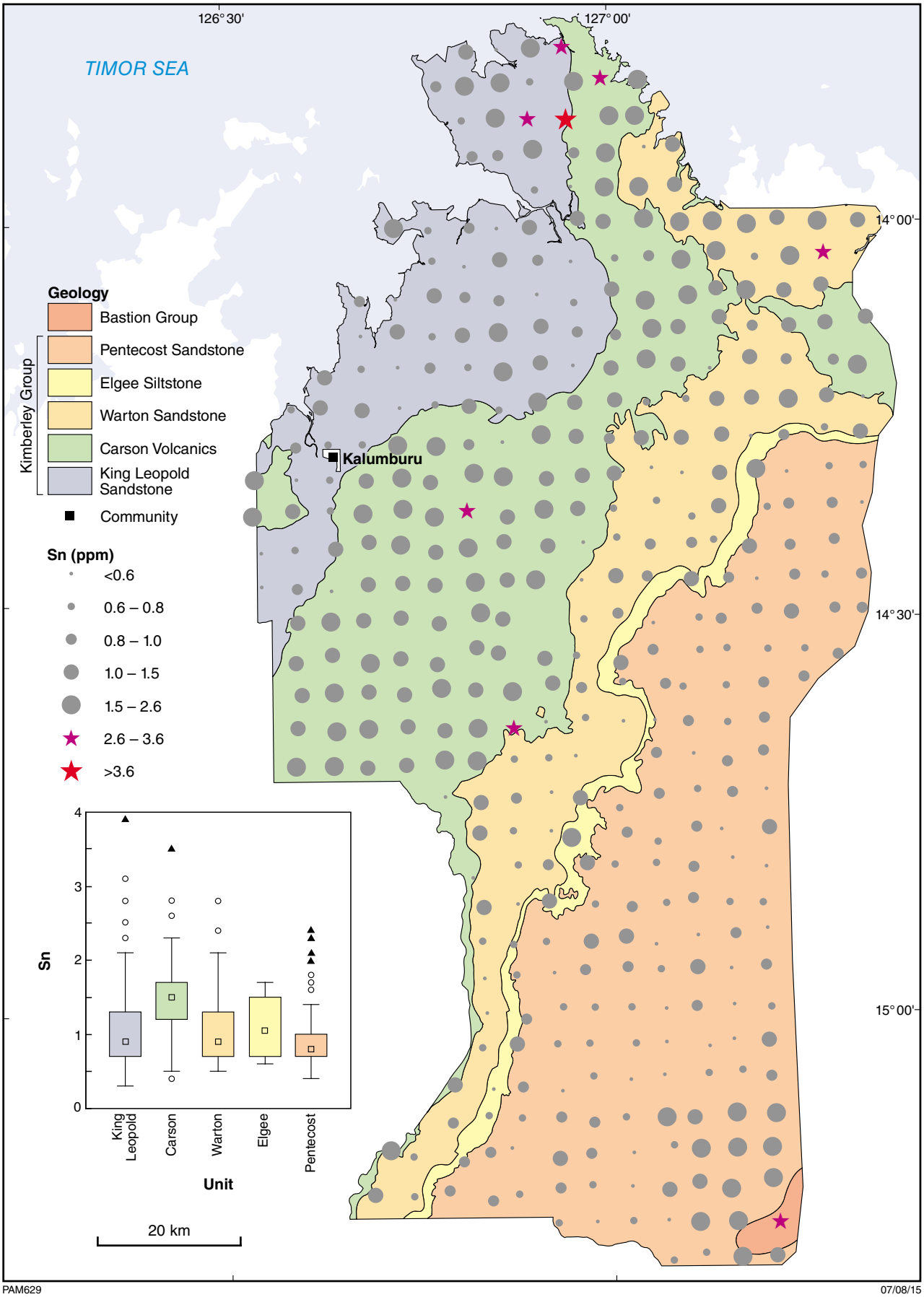
126° 30'
127° 00'
TIMOR SEA
14° 00'
14° 30'
15° 00'
Geology
Kimberley Group
Bastion Group
Pentecost Sandstone
Elgee Siltstone
Warton Sandstone
Carson Volcanics
King Leopold Sandstone
Community
Kalumburu
Sn (ppm)
<0.6
0.6 – 0.8
0.8 – 1.0
1.0 – 1.5
1.5 – 2.6
2.6 – 3.6
>3.6
Sn
0
1
2
3
4
King Leopold
Carson
Warton
Elgee
Pentecost
Unit
20 km
PAM629
07/08/15

Figure B12j.

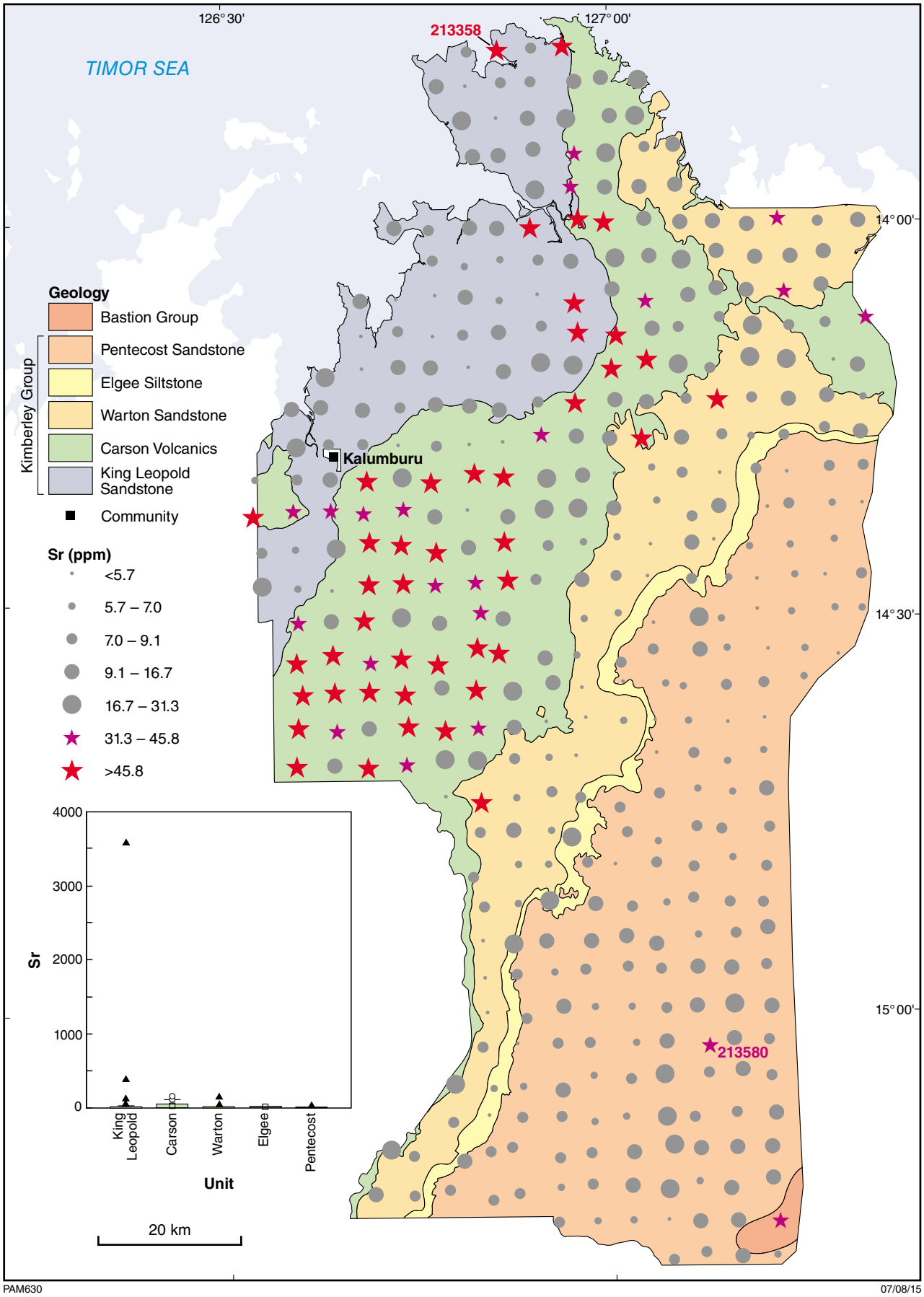
126° 30'
127° 00'
14° 00'
14° 30'
15° 00'
TIMOR SEA
213358
213580
Kalumburu
Geology
Kimberley Group
Bastion Group
Pentecost Sandstone
Elgee Siltstone
Warton Sandstone
Carson Volcanics
King Leopold Sandstone
Community
Sr (ppm)
<5.7
5.7 – 7.0
7.0 – 9.1
9.1 – 16.7
16.7 – 31.3
31.3 – 45.8
>45.8
Sr
4000
3000
2000
1000
0
King Leopold
Carson
Warton
Elgee
Pentecost
Unit
20 km
PAM630
07/08/15

Figure B12k.

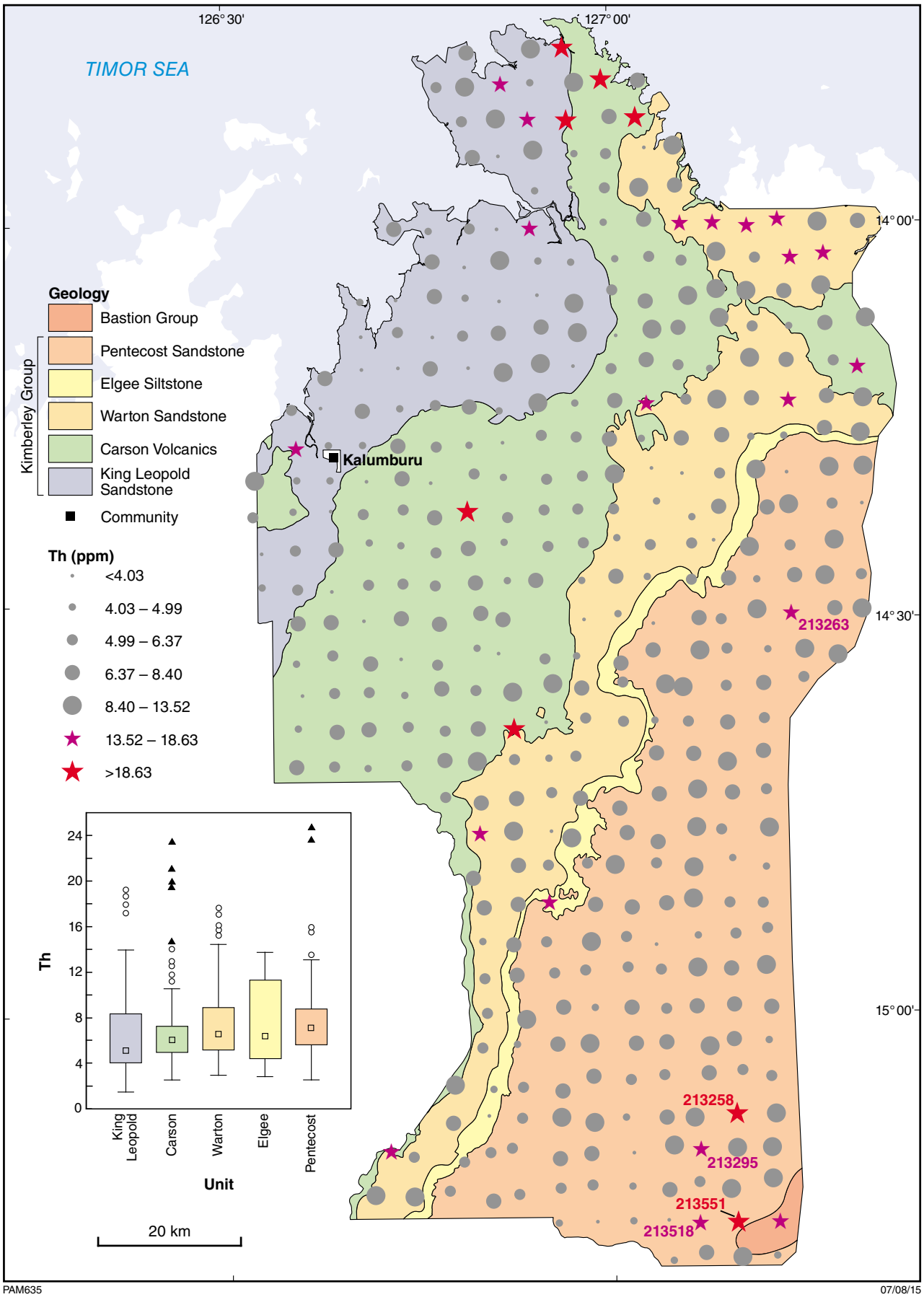
126° 30'
127° 00'
TIMOR SEA
14° 00'
14° 30'
15° 00'
Geology
Kimberley Group
Bastion Group
Pentecost Sandstone
Elgee Siltstone
Warton Sandstone
Carson Volcanics
King Leopold Sandstone
Community
Kalumburu
Th (ppm)
<4.03
4.03 – 4.99
4.99 – 6.37
6.37 – 8.40
8.40 – 13.52
13.52 – 18.63
>18.63
213263
213258
213295
213551
213518
Th
0
4
8
12
16
20
24
King Leopold
Carson
Warton
Elgee
Pentecost
Unit
20 km
PAM635
07/08/15

Figure B12l.

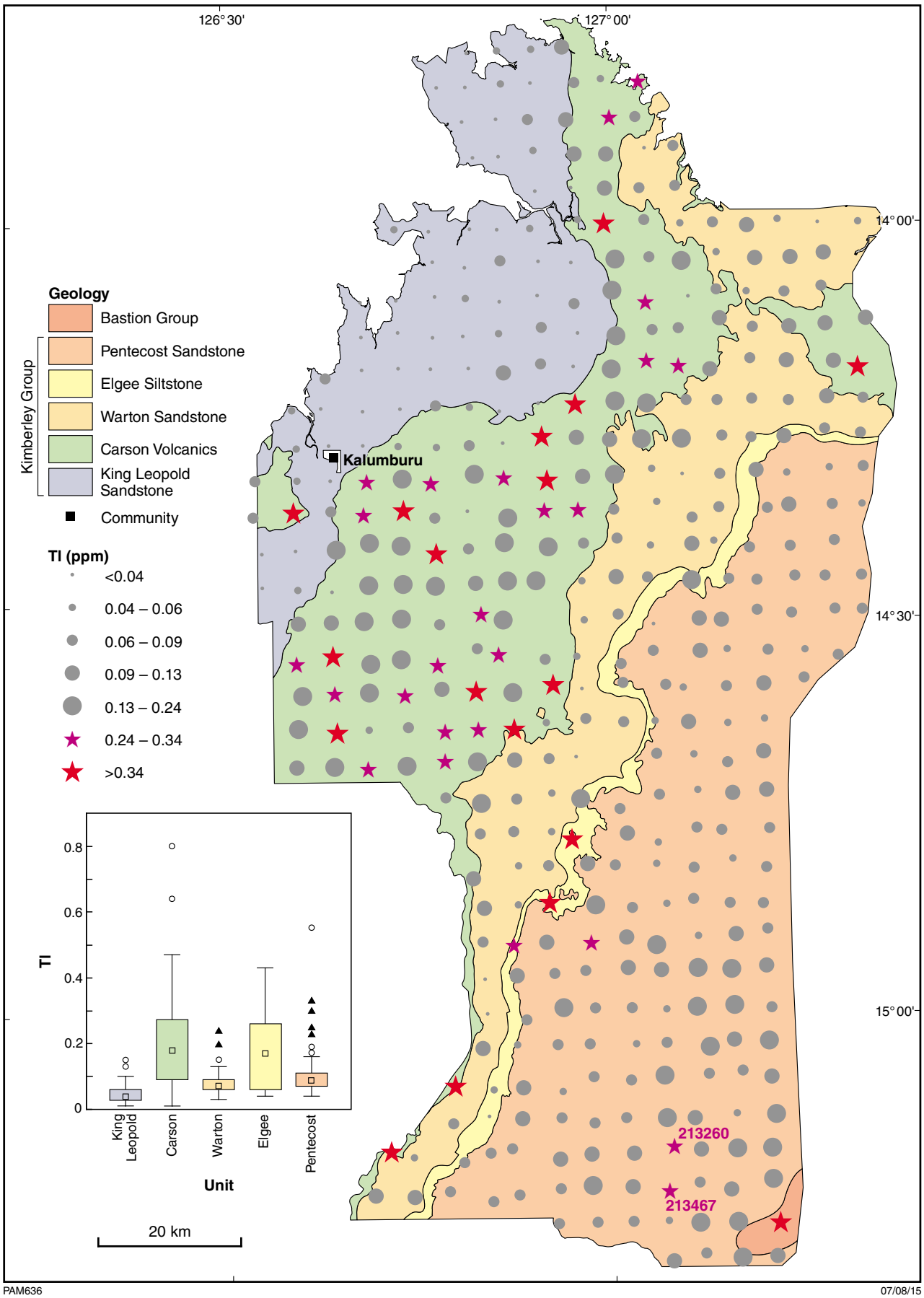
126° 30'
127° 00'
14° 00'
14° 30'
15° 00'
Geology
Kimberley Group
Bastion Group
Pentecost Sandstone
Elgee Siltstone
Warton Sandstone
Carson Volcanics
King Leopold Sandstone
Community
Kalumburu
Tl (ppm)
<0.04
0.04 – 0.06
0.06 – 0.09
0.09 – 0.13
0.13 – 0.24
0.24 – 0.34
>0.34
Tl
0.8
0.6
0.4
0.2
0
King Leopold
Carson
Warton
Elgee
Pentecost
Unit
20 km
213260
213467
PAM636
07/08/15

Figure B12m.

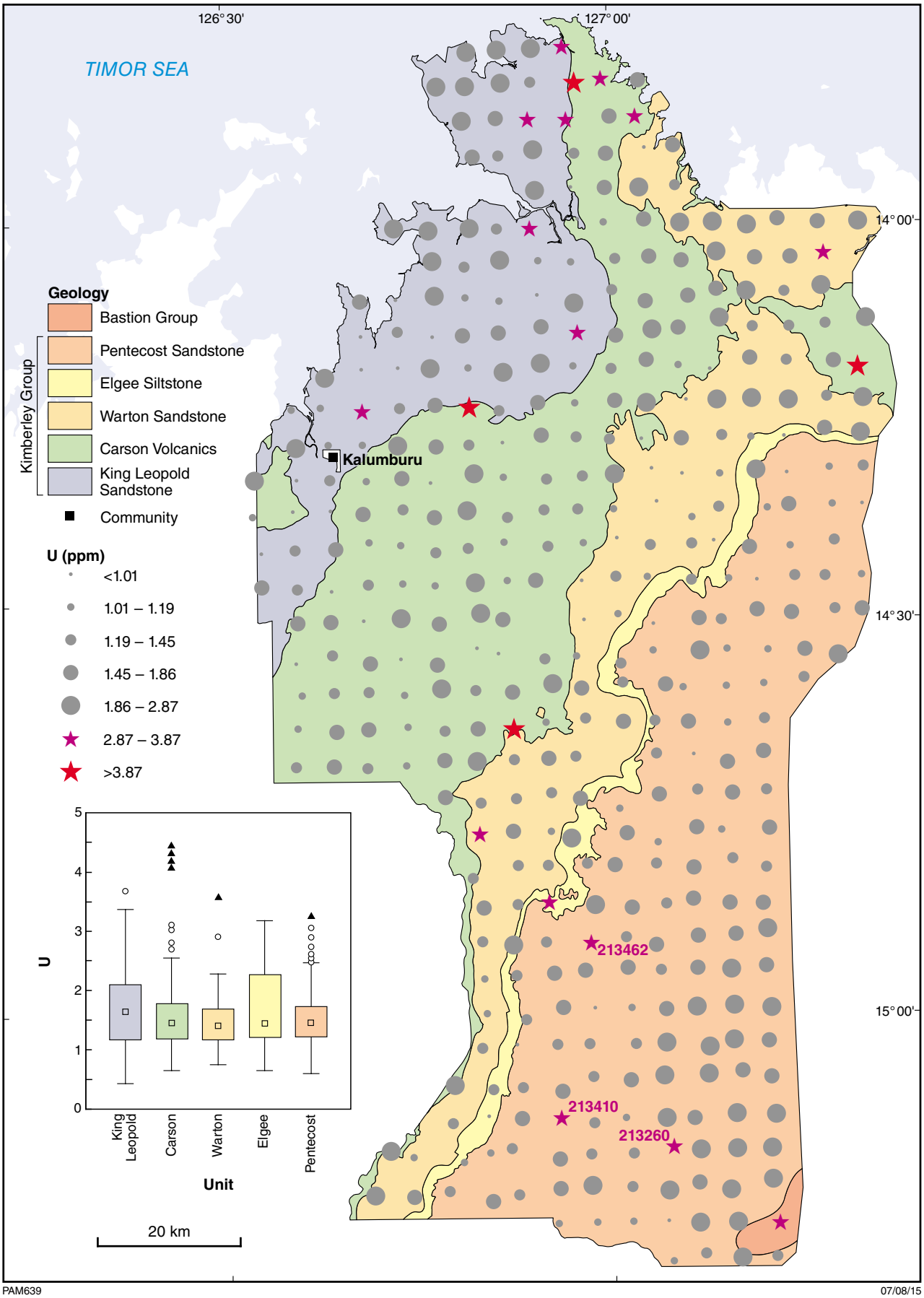
126° 30'
127° 00'
TIMOR SEA
14° 00'
14° 30'
15° 00'
Geology
Bastion Group
Kimberley Group
Pentecost Sandstone
Elgee Siltstone
Warton Sandstone
Carson Volcanics
King Leopold Sandstone
Community
Kalumburu
U (ppm)
<1.01
1.01 – 1.19
1.19 – 1.45
1.45 – 1.86
1.86 – 2.87
2.87 – 3.87
>3.87
213462
213410
213260
U
Unit
King Leopold
Carson
Warton
Elgee
Pentecost
20 km
PAM639
07/08/15

Figure B12n.

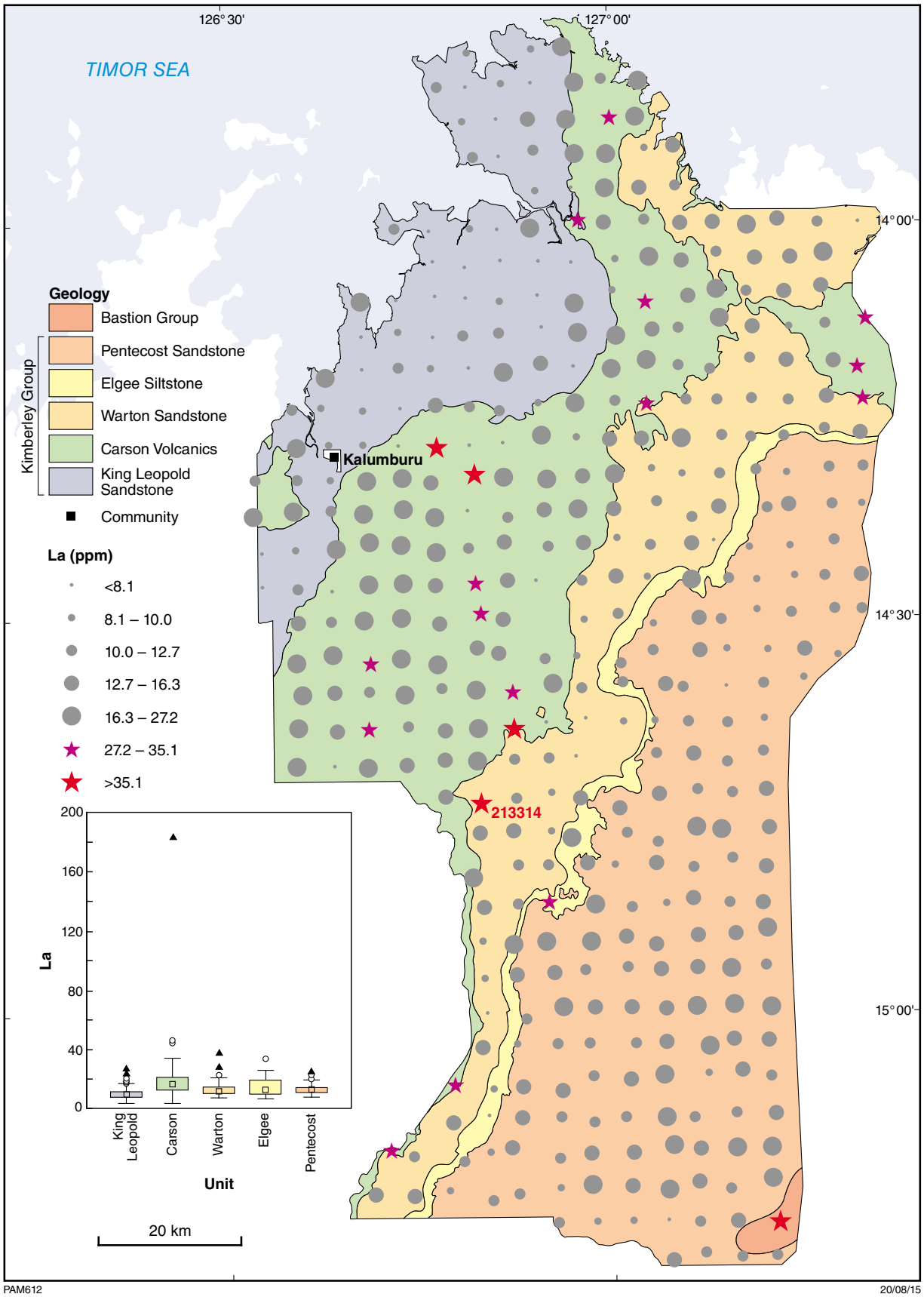

Figure B13. Bubble plots for rare earth elements (REE) measured in regolith from the Balanggarra project area. Bubble divisions have been determined using box and whisker plots (see text for explanation). Samples with anomalous concentrations shown by stars (purple – outlier; red – extreme). Also shown is the box and whisker plot according to major lithological units, showing the median, interquartile range (box) and samples with anomalous concentrations (outlier – open circle; extreme – triangle): a) La (ppm); b) Ce (ppm); c) Pr (ppm); d) Nd (ppm); e) Sm (ppm); f) Eu (ppm); g) Gd (ppm); h) Tb (ppm); i) Dy (ppm); j) Ho (ppm); k) Er (ppm); l) Tm (ppm); m) Yb (ppm); n) Lu (ppm); o) Y (ppm)

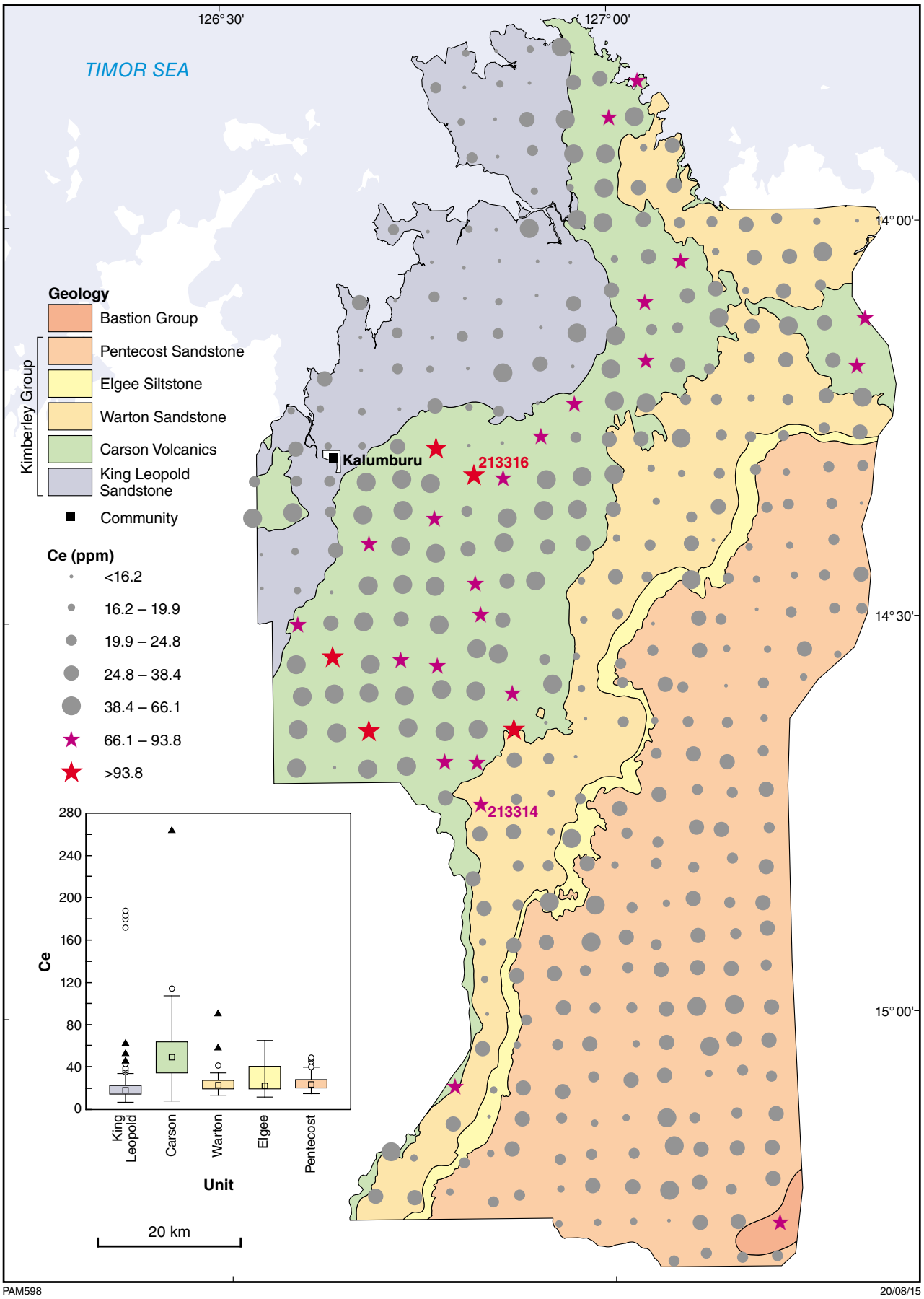
126° 30'
127° 00'
TIMOR SEA
14° 00'
14° 30'
15° 00'
Geology
Bastion Group
Kimberley Group
Pentecost Sandstone
Elgee Siltstone
Warton Sandstone
Carson Volcanics
King Leopold Sandstone
Community
Kalumburu
213316
213314
Ce (ppm)
<16.2
16.2 – 19.9
19.9 – 24.8
24.8 – 38.4
38.4 – 66.1
66.1 – 93.8
>93.8
Ce
280
240
200
160
120
80
40
0
King Leopold
Carson
Warton
Elgee
Pentecost
Unit
20 km
PAM598
20/08/15

Figure B13b.

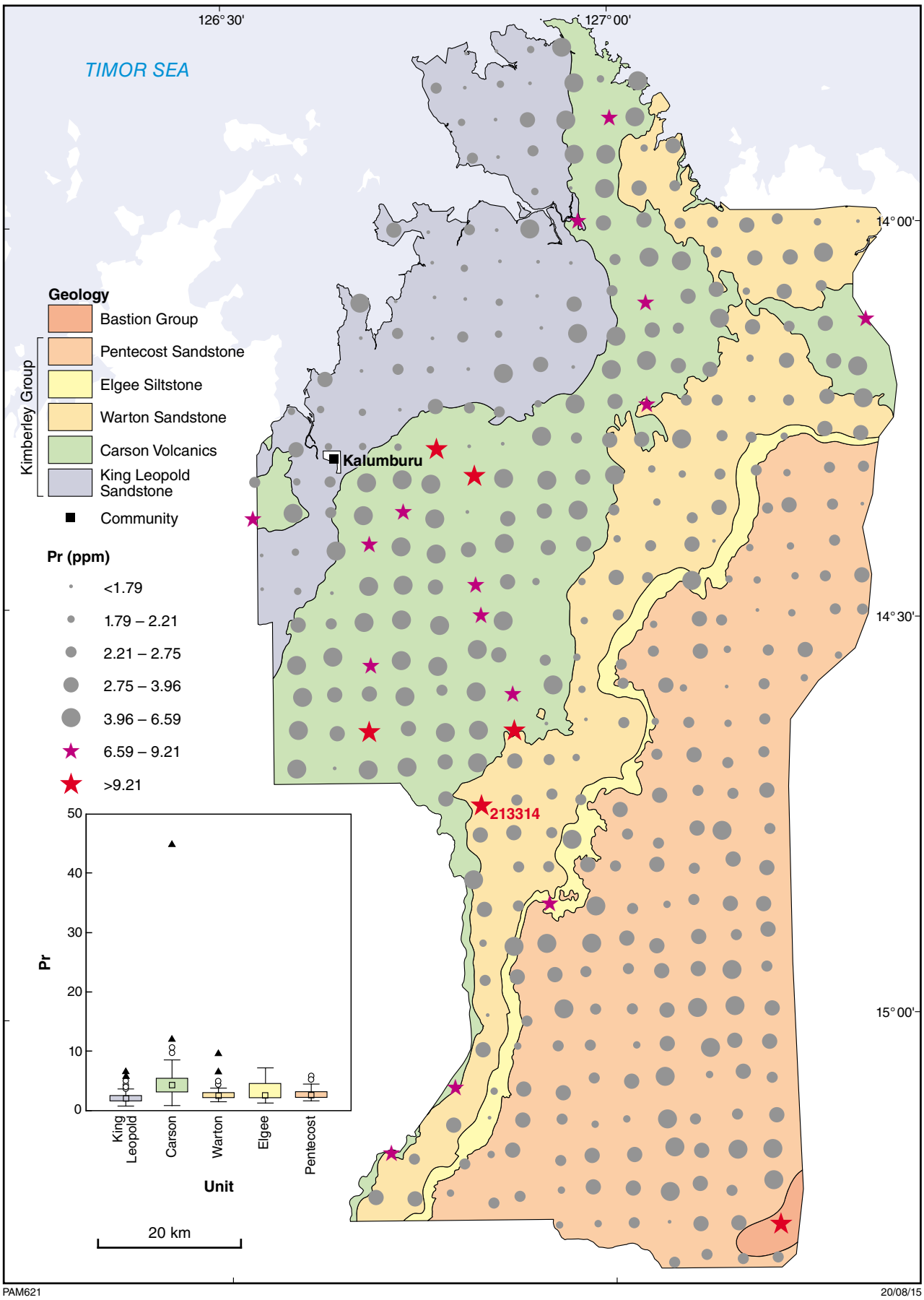
126° 30'
127° 00'
TIMOR SEA
14° 00'
14° 30'
15° 00'
Geology
Kimberley Group
Bastion Group
Pentecost Sandstone
Elgee Siltstone
Warton Sandstone
Carson Volcanics
King Leopold Sandstone
Community
Kalumburu
Pr (ppm)
<1.79
1.79 – 2.21
2.21 – 2.75
2.75 – 3.96
3.96 – 6.59
6.59 – 9.21
>9.21
213314
Pr
50
40
30
20
10
0
King Leopold
Carson
Warton
Elgee
Pentecost
Unit
20 km
PAM621
20/08/15

Figure B13c.

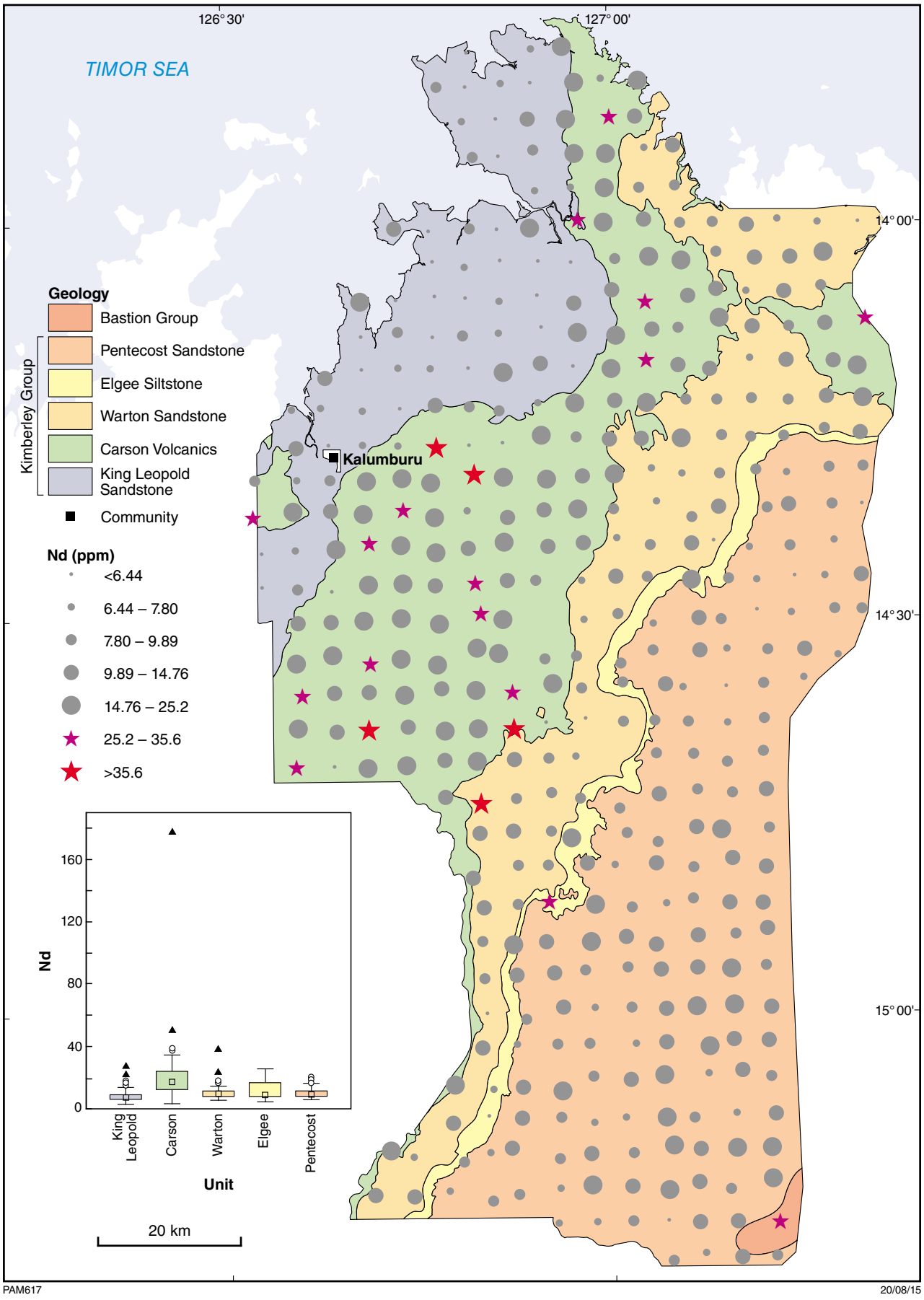
126° 30'
127° 00'
TIMOR SEA
14° 00'
14° 30'
15° 00'
Geology
Bastion Group
Kimberley Group
Pentecost Sandstone
Elgee Siltstone
Warton Sandstone
Carson Volcanics
King Leopold Sandstone
Community
Kalumburu
Nd (ppm)
<6.44
6.44 – 7.80
7.80 – 9.89
9.89 – 14.76
14.76 – 25.2
25.2 – 35.6
>35.6
Nd
0
40
80
120
160
King Leopold
Carson
Warton
Elgee
Pentecost
Unit
20 km
PAM617
20/08/15

Figure B13d.

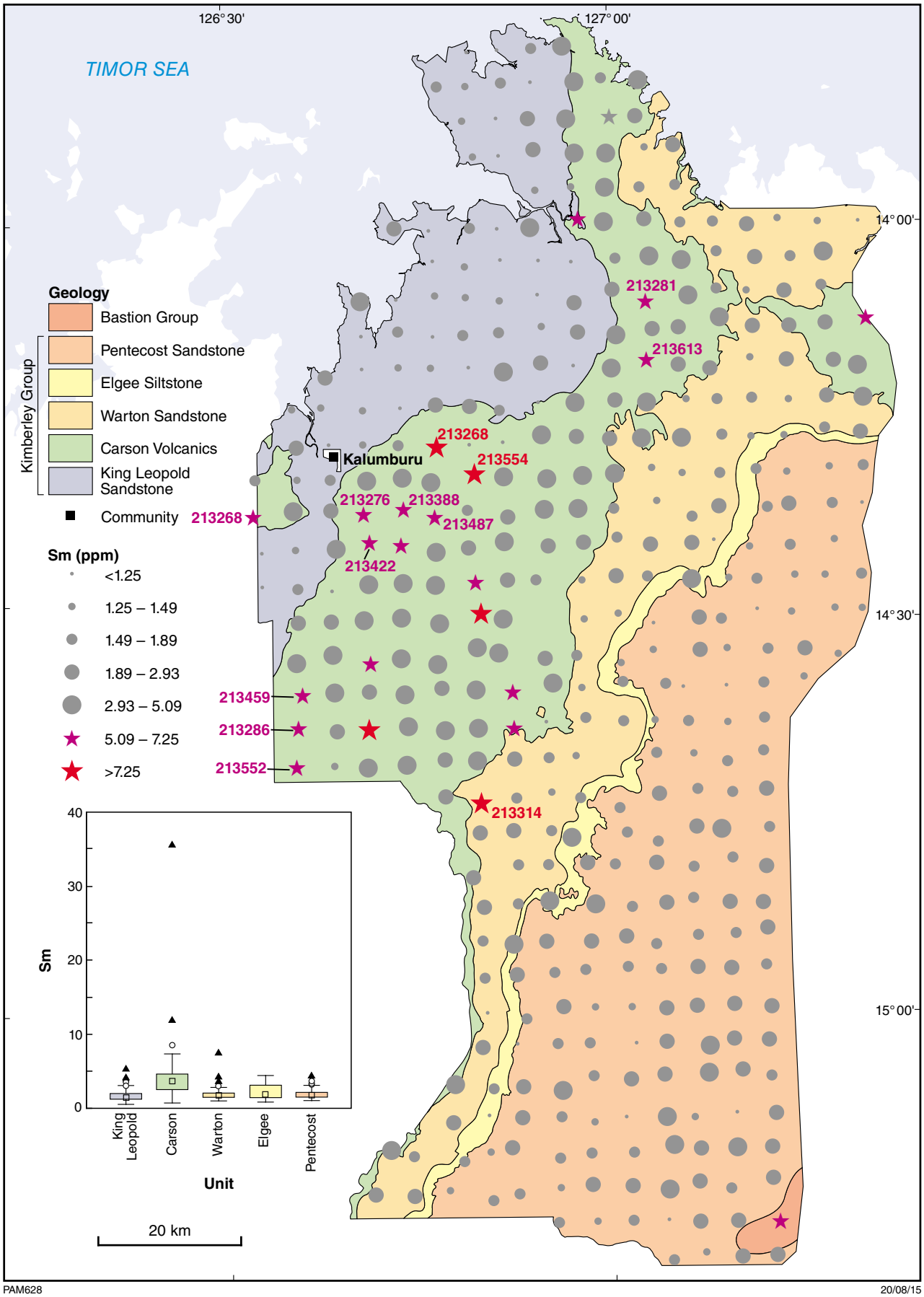
126° 30'
127° 00'
TIMOR SEA
14° 00'
14° 30'
15° 00'
Geology
Kimberley Group
Bastion Group
Pentecost Sandstone
Elgee Siltstone
Warton Sandstone
Carson Volcanics
King Leopold Sandstone
Community
Kalumburu
213268
213281
213613
213554
213276
213388
213487
213422
213459
213286
213552
213314
Sm (ppm)
<1.25
1.25 – 1.49
1.49 – 1.89
1.89 – 2.93
2.93 – 5.09
5.09 – 7.25
>7.25
Sm
Unit
King Leopold
Carson
Warton
Elgee
Pentecost
20 km
PAM628
20/08/15

Figure B13e.

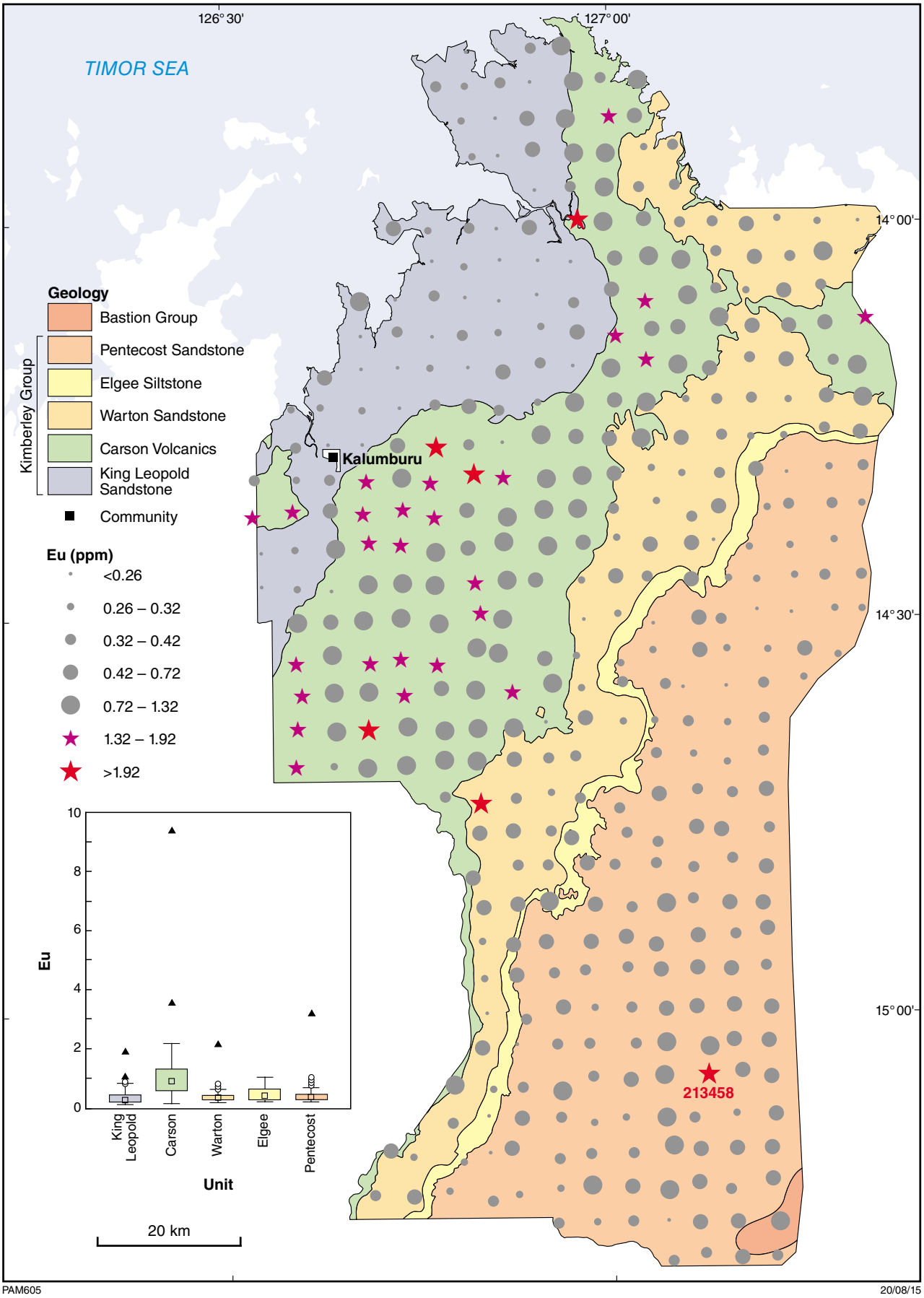
126° 30'
127° 00'
TIMOR SEA
14° 00'
14° 30'
15° 00'
Geology
Bastion Group
Kimberley Group
Pentecost Sandstone
Elgee Siltstone
Warton Sandstone
Carson Volcanics
King Leopold Sandstone
Community
Kalumburu
Eu (ppm)
<0.26
0.26 – 0.32
0.32 – 0.42
0.42 – 0.72
0.72 – 1.32
1.32 – 1.92
>1.92
213458
Eu
10
8
6
4
2
0
King Leopold
Carson
Warton
Elgee
Pentecost
Unit
20 km
PAM605
20/08/15

Figure B13f.

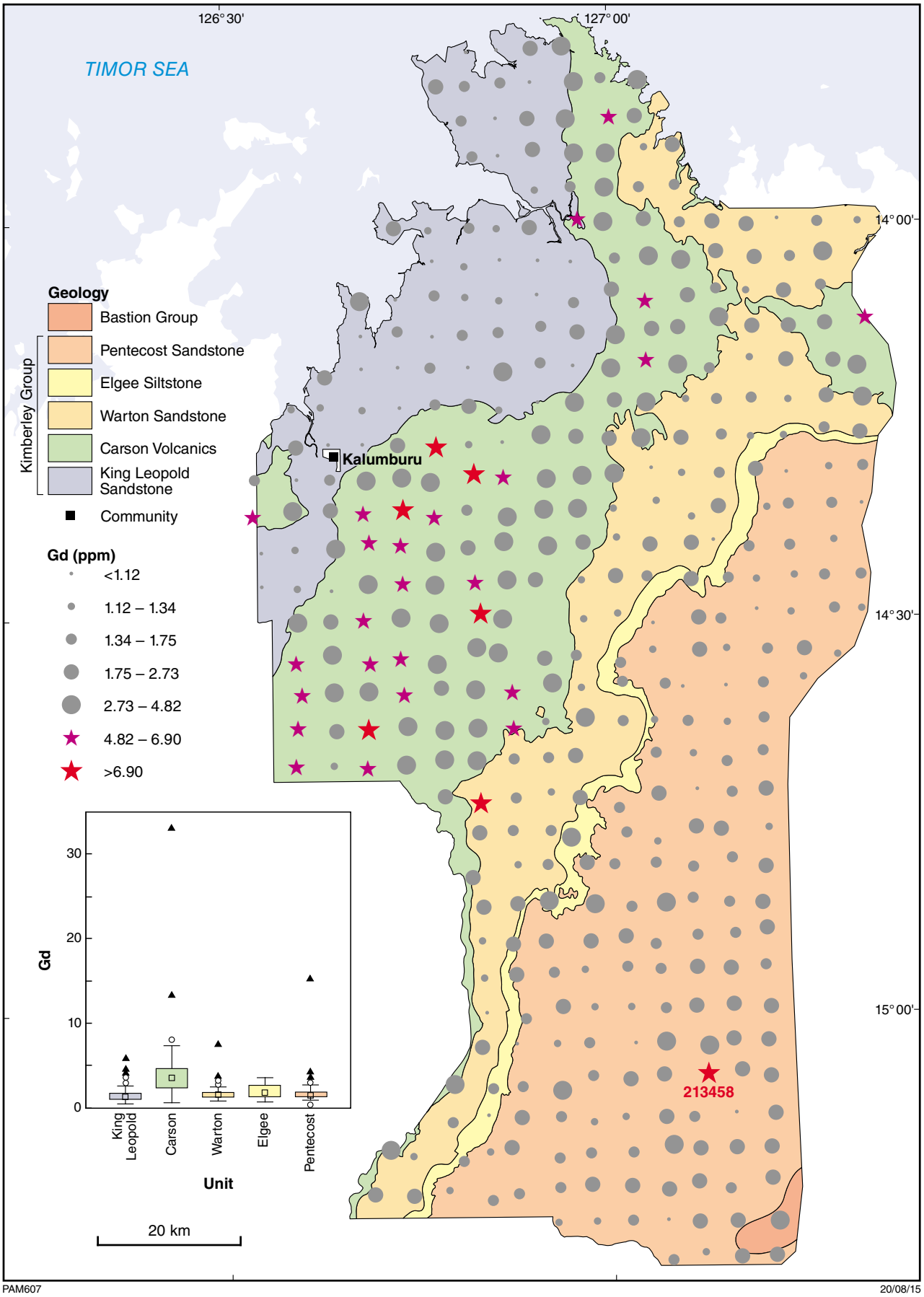
126° 30'
127° 00'
TIMOR SEA
14° 00'
14° 30'
15° 00'
Geology
Kimberley Group
Bastion Group
Pentecost Sandstone
Elgee Siltstone
Warton Sandstone
Carson Volcanics
King Leopold Sandstone
Community
Kalumburu
Gd (ppm)
<1.12
1.12 – 1.34
1.34 – 1.75
1.75 – 2.73
2.73 – 4.82
4.82 – 6.90
>6.90
213458
Gd
30
20
10
0
King Leopold
Carson
Warton
Elgee
Pentecost
Unit
20 km
PAM607
20/08/15

Figure B13g.

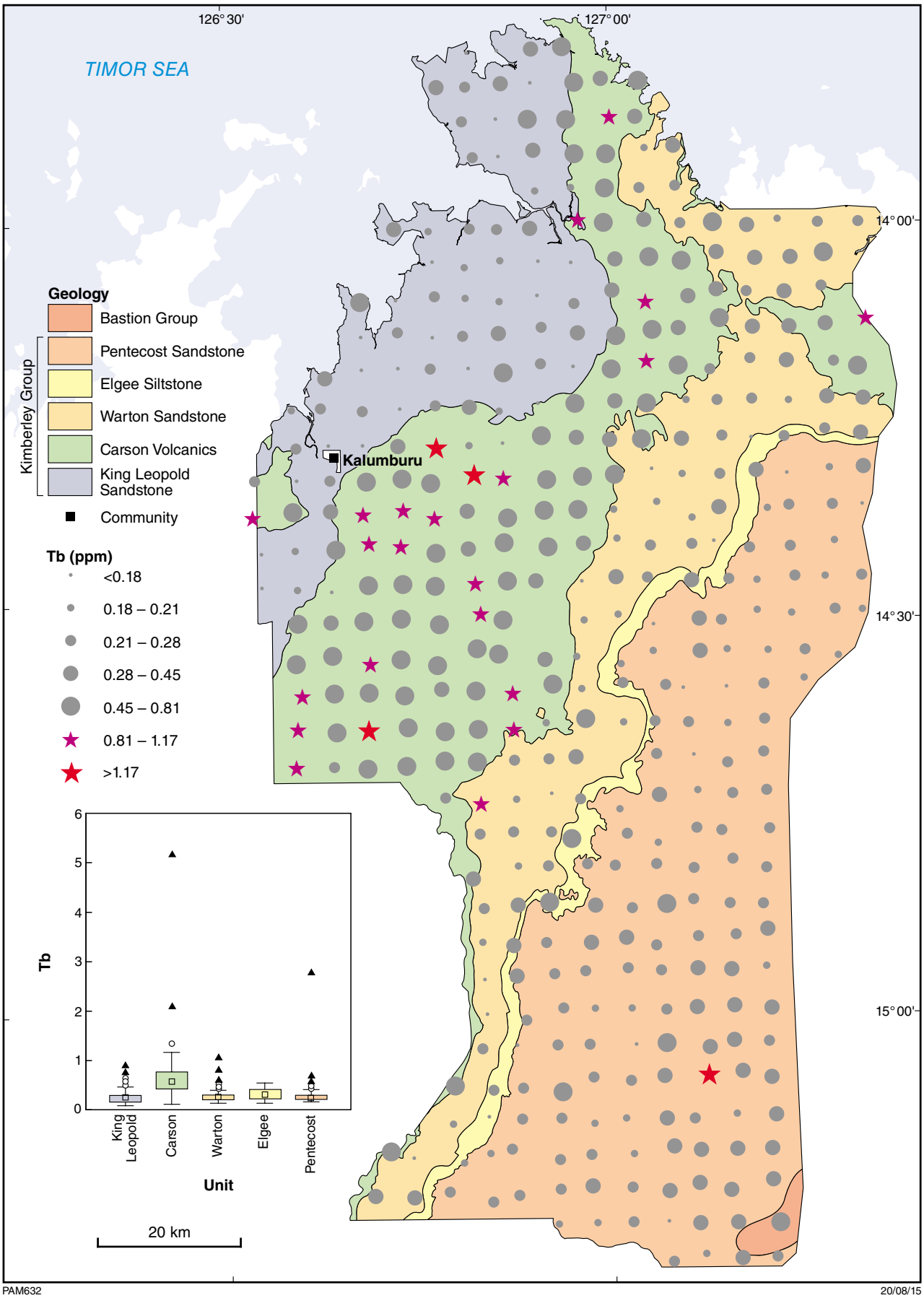
126° 30'
127° 00'
TIMOR SEA
14° 00'
14° 30'
15° 00'
Geology
Kimberley Group
Bastion Group
Pentecost Sandstone
Elgee Siltstone
Warton Sandstone
Carson Volcanics
King Leopold Sandstone
Community
Kalumburu
Tb (ppm)
<0.18
0.18 – 0.21
0.21 – 0.28
0.28 – 0.45
0.45 – 0.81
0.81 – 1.17
>1.17
Tb
0
1
2
3
4
5
6
King Leopold
Carson
Warton
Elgee
Pentecost
Unit
20 km
PAM632
20/08/15

Figure B13h.

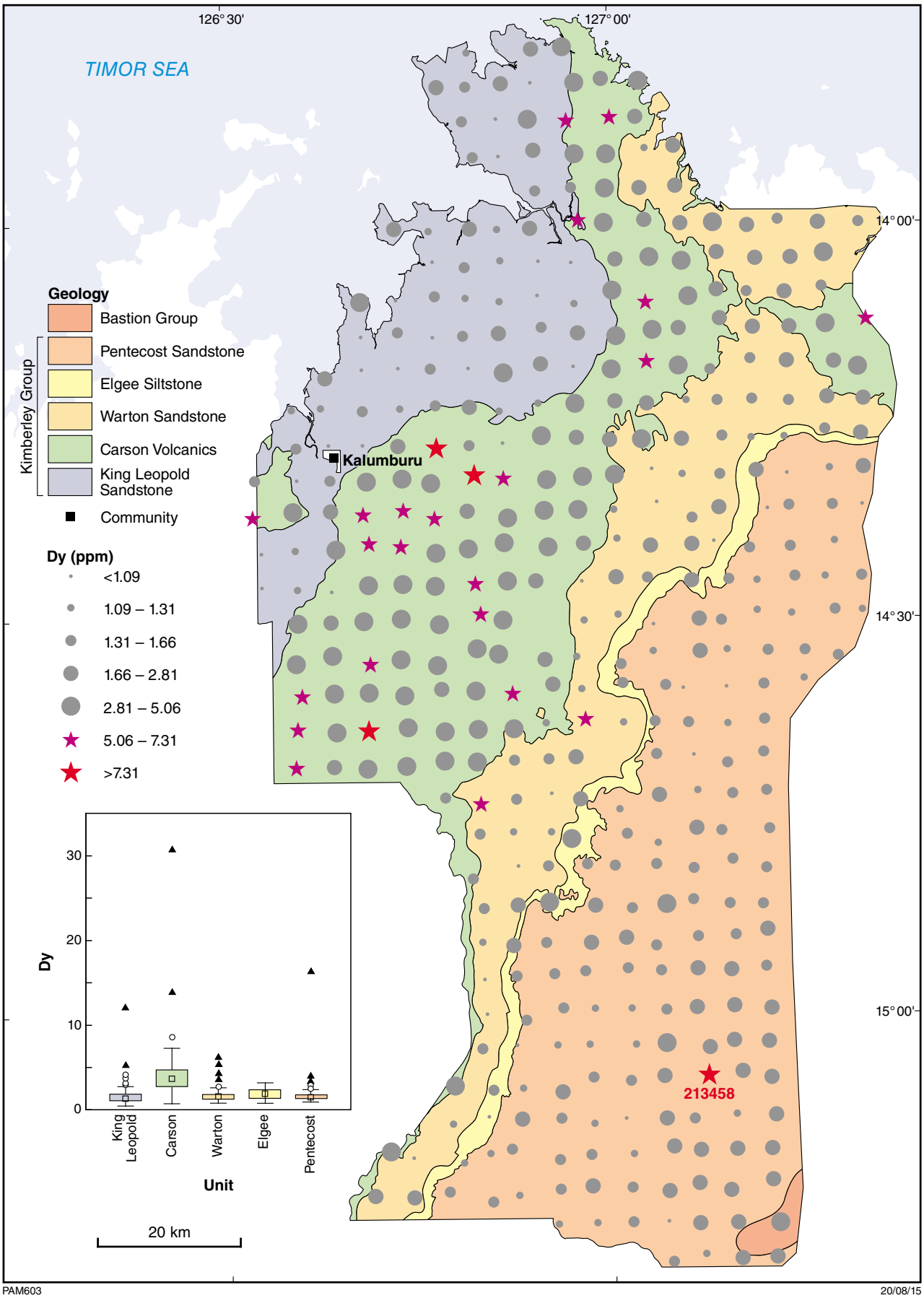
126° 30'
127° 00'
TIMOR SEA
14° 00'
14° 30'
15° 00'
Geology
Kimberley Group
Bastion Group
Pentecost Sandstone
Elgee Siltstone
Warton Sandstone
Carson Volcanics
King Leopold Sandstone
Community
Kalumburu
Dy (ppm)
<1.09
1.09 – 1.31
1.31 – 1.66
1.66 – 2.81
2.81 – 5.06
5.06 – 7.31
>7.31
213458
Dy
30
20
10
0
King Leopold
Carson
Warton
Elgee
Pentecost
Unit
20 km
PAM603
20/08/15

Figure B13i.

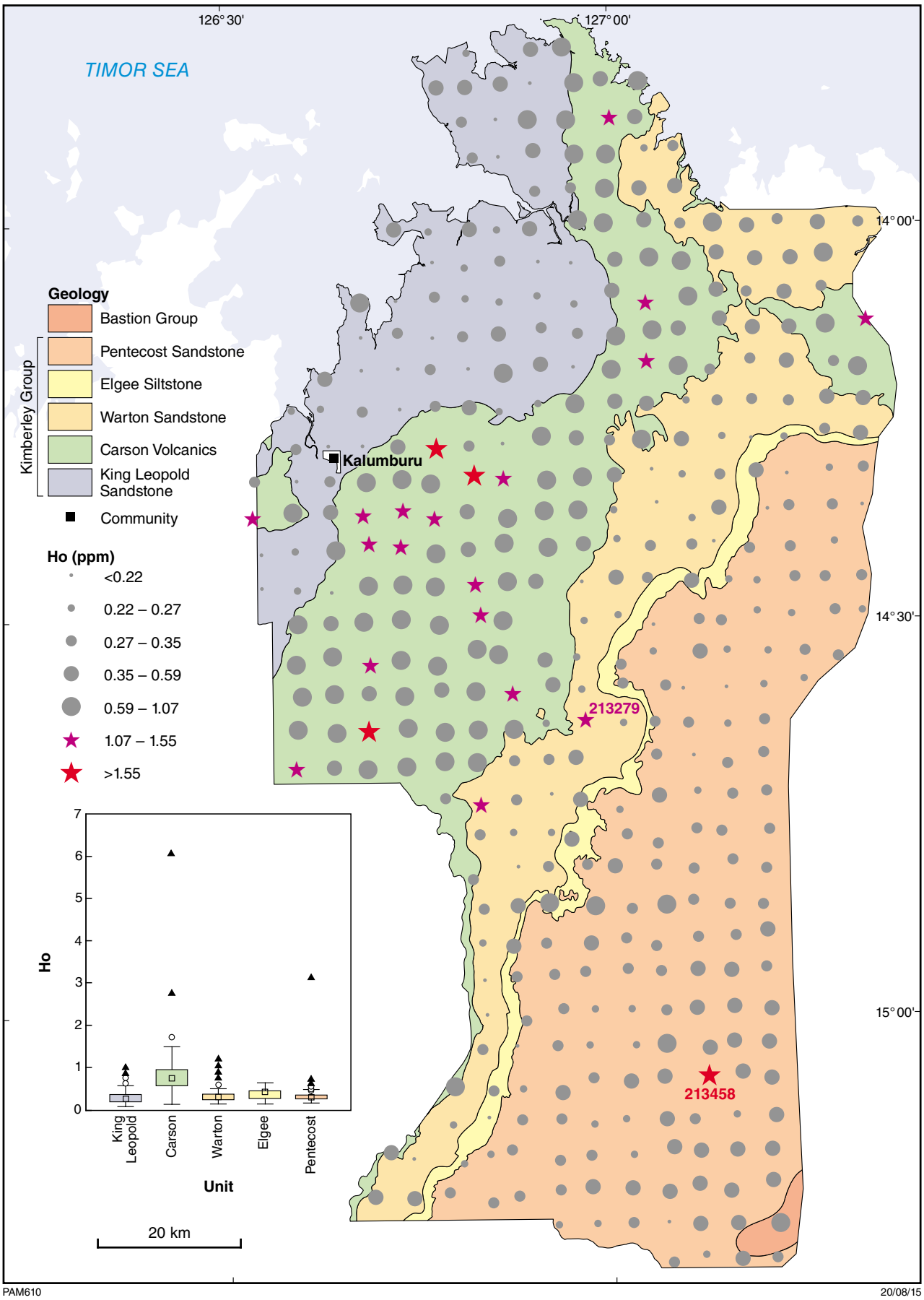
126° 30'
127° 00'
TIMOR SEA
14° 00'
14° 30'
15° 00'
Geology
Kimberley Group
Bastion Group
Pentecost Sandstone
Elgee Siltstone
Warton Sandstone
Carson Volcanics
King Leopold Sandstone
Community
Kalumburu
Ho (ppm)
<0.22
0.22 – 0.27
0.27 – 0.35
0.35 – 0.59
0.59 – 1.07
1.07 – 1.55
>1.55
213279
213458
Ho
Unit
King Leopold
Carson
Warton
Elgee
Pentecost
20 km
PAM610
20/08/15

Figure B13j.

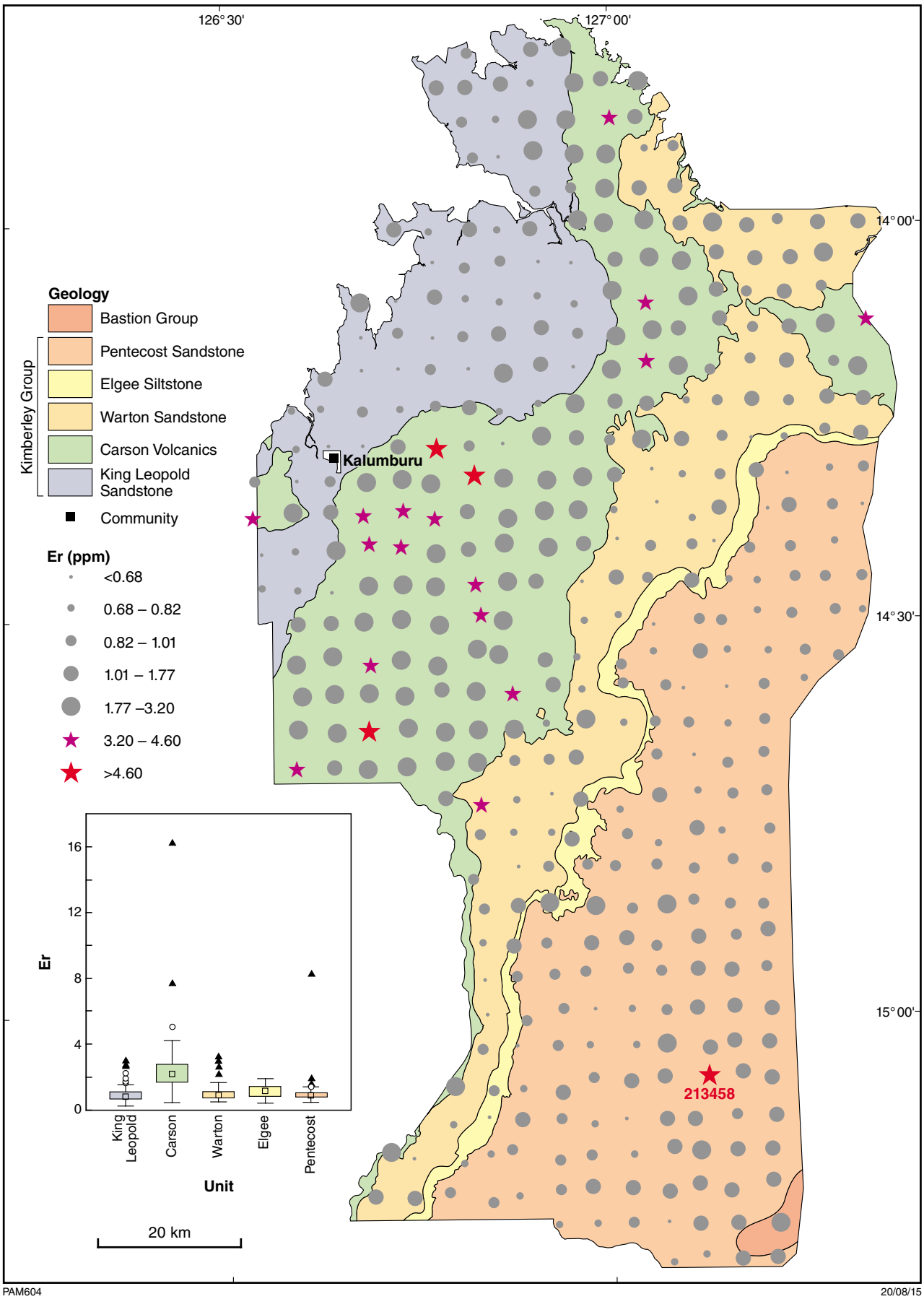
126° 30'
127° 00'
14° 00'
14° 30'
15° 00'
Geology
Kimberley Group
Bastion Group
Pentecost Sandstone
Elgee Siltstone
Warton Sandstone
Carson Volcanics
King Leopold Sandstone
Community
Er (ppm)
<0.68
0.68 – 0.82
0.82 – 1.01
1.01 – 1.77
1.77 –3.20
3.20 – 4.60
>4.60
Kalumburu
213458
Er
16
12
8
4
0
King Leopold
Carson
Warton
Elgee
Pentecost
Unit
20 km
PAM604
20/08/15

Figure B13k.

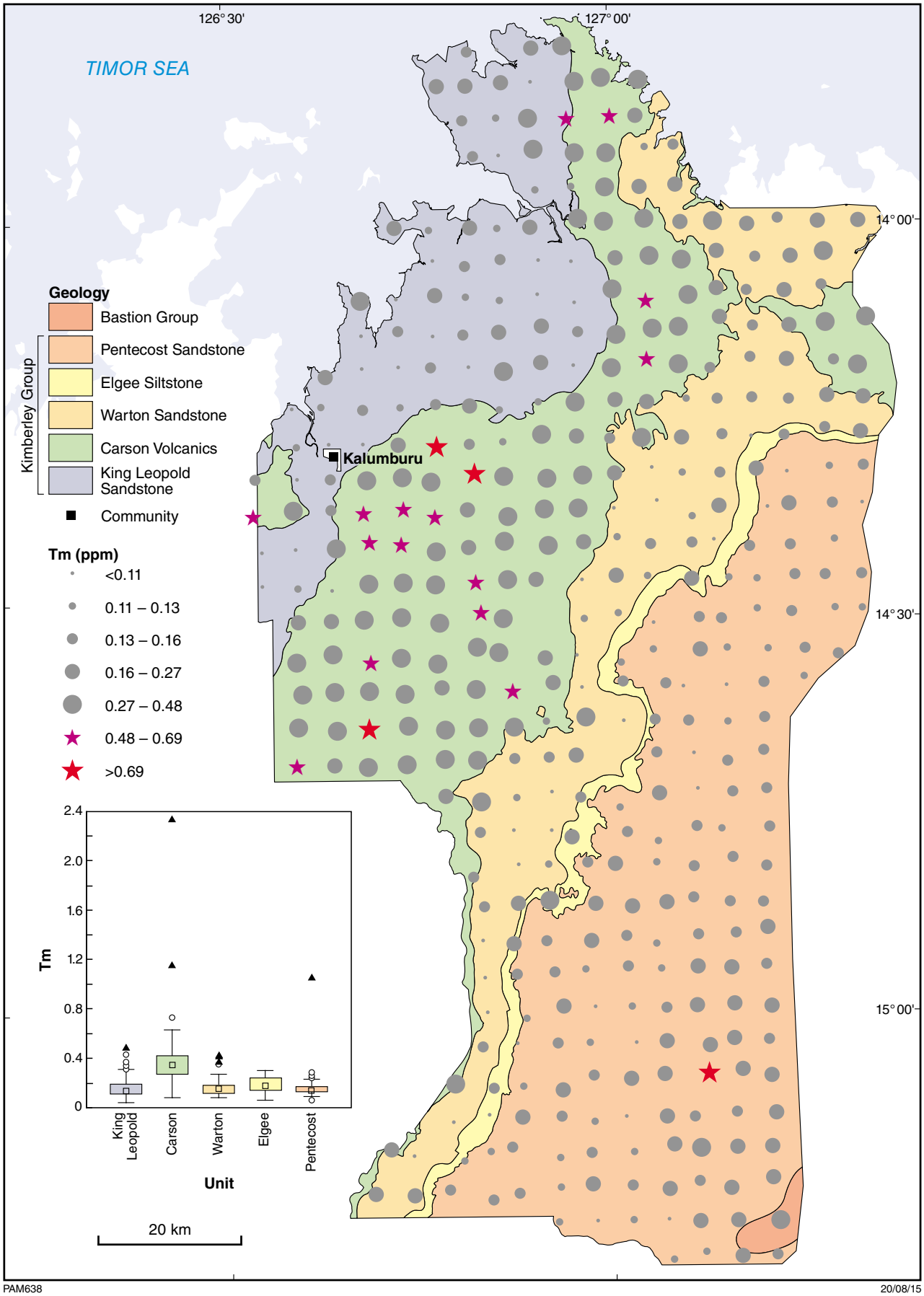
126° 30'
127° 00'
TIMOR SEA
14° 00'
14° 30'
15° 00'
Geology
Bastion Group
Pentecost Sandstone
Elgee Siltstone
Warton Sandstone
Carson Volcanics
King Leopold Sandstone
Kimberley Group
Community
Kalumburu
Tm (ppm)
<0.11
0.11 – 0.13
0.13 – 0.16
0.16 – 0.27
0.27 – 0.48
0.48 – 0.69
>0.69
Tm
2.4
2.0
1.6
1.2
0.8
0.4
0
King Leopold
Carson
Warton
Elgee
Pentecost
Unit
20 km
PAM638
20/08/15

Figure B13l.

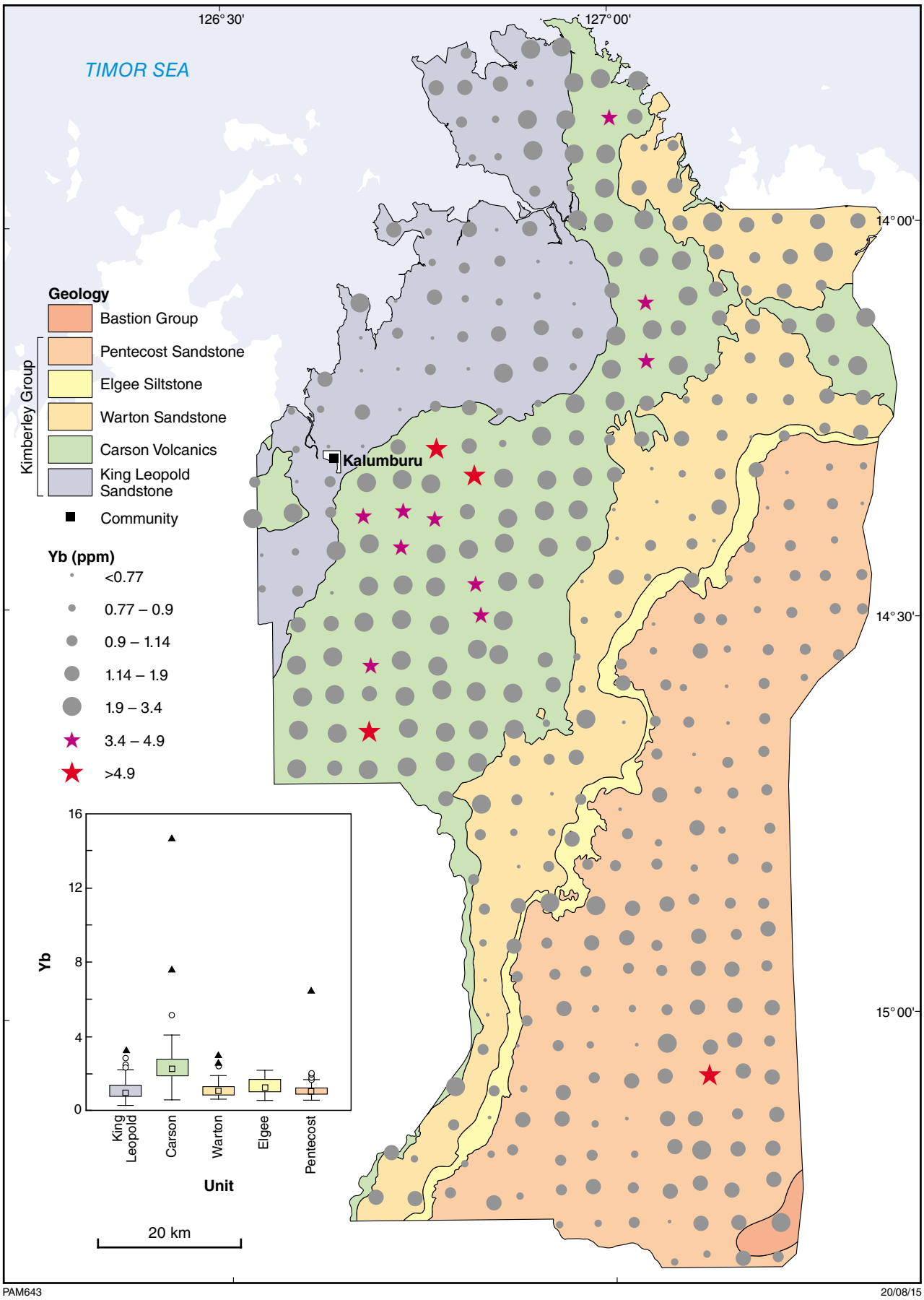
126° 30'
127° 00'
TIMOR SEA
14° 00'
14° 30'
15° 00'
Geology
Kimberley Group
Bastion Group
Pentecost Sandstone
Elgee Siltstone
Warton Sandstone
Carson Volcanics
King Leopold Sandstone
Community
Kalumburu
Yb (ppm)
<0.77
0.77 – 0.9
0.9 – 1.14
1.14 – 1.9
1.9 – 3.4
3.4 – 4.9
>4.9
Yb
16
12
8
4
0
King Leopold
Carson
Warton
Elgee
Pentecost
Unit
20 km
PAM643
20/08/15

Figure B13m.

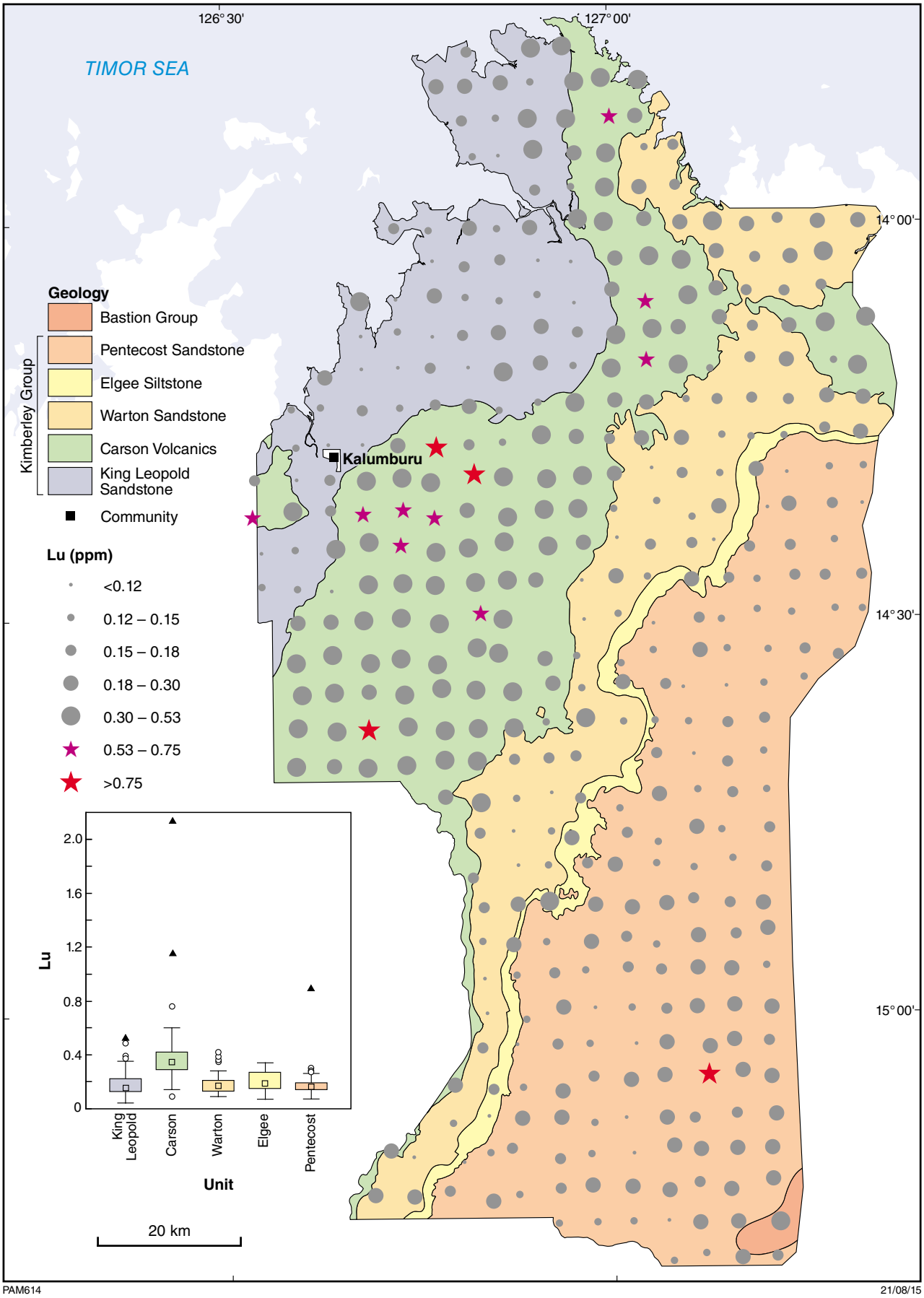
126° 30'
127° 00'
TIMOR SEA
14° 00'
14° 30'
15° 00'
Geology
Kimberley Group
Bastion Group
Pentecost Sandstone
Elgee Siltstone
Warton Sandstone
Carson Volcanics
King Leopold Sandstone
Community
Kalumburu
Lu (ppm)
<0.12
0.12 – 0.15
0.15 – 0.18
0.18 – 0.30
0.30 – 0.53
0.53 – 0.75
>0.75
Lu
2.0
1.6
1.2
0.8
0.4
0
King Leopold
Carson
Warton
Elgee
Pentecost
Unit
20 km
PAM614
21/08/15

Figure B13n.

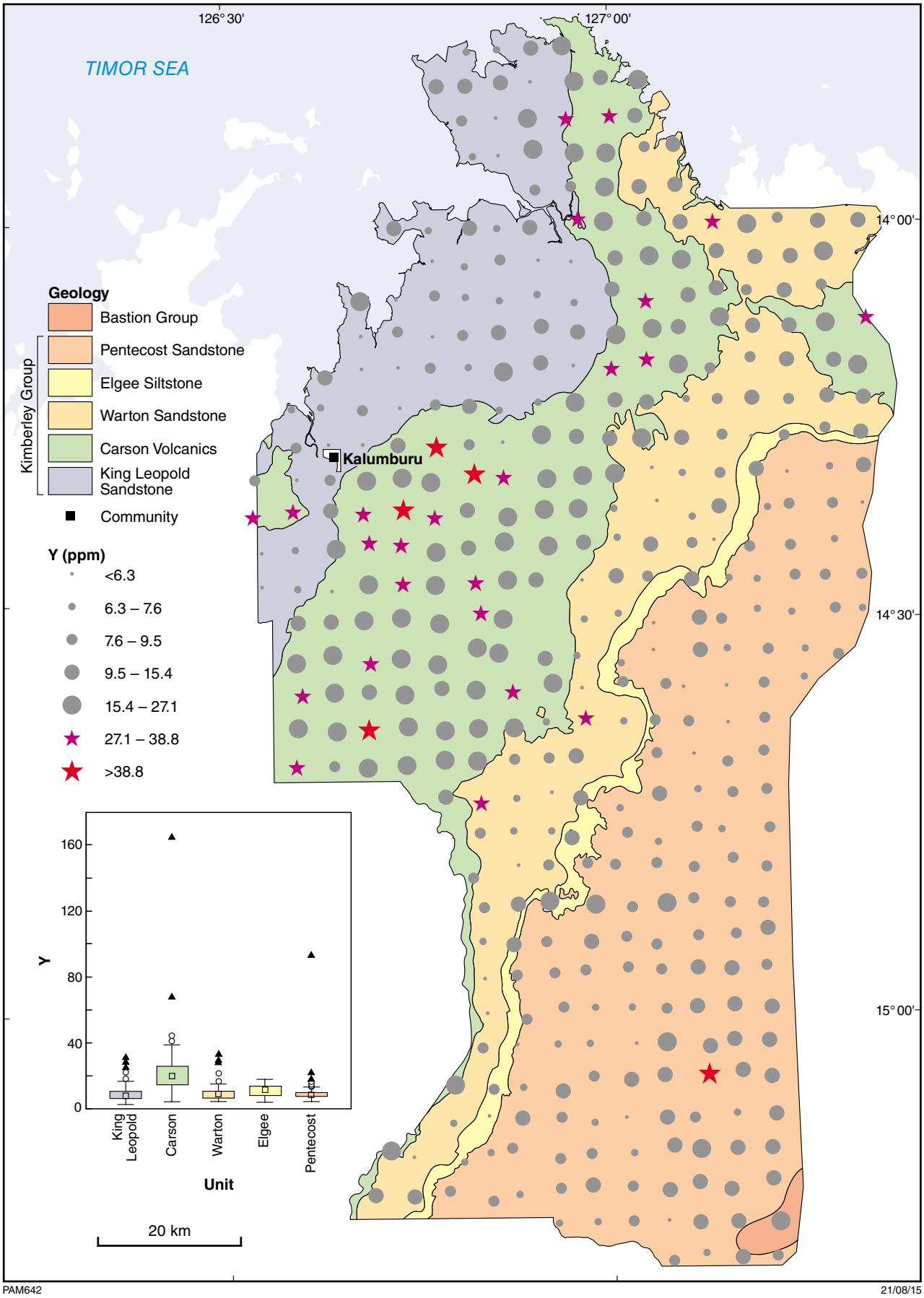
126° 30'
127° 00'
TIMOR SEA
14° 00'
14° 30'
15° 00'
Geology
Kimberley Group
Bastion Group
Pentecost Sandstone
Elgee Siltstone
Warton Sandstone
Carson Volcanics
King Leopold Sandstone
Community
Kalumburu
Y (ppm)
<6.3
6.3 – 7.6
7.6 – 9.5
9.5 – 15.4
15.4 – 27.1
27.1 – 38.8
>38.8
160
120
80
40
0
Y
King Leopold
Carson
Warton
Elgee
Pentecost
Unit
20 km
PAM642
21/08/15

Figure B13o.

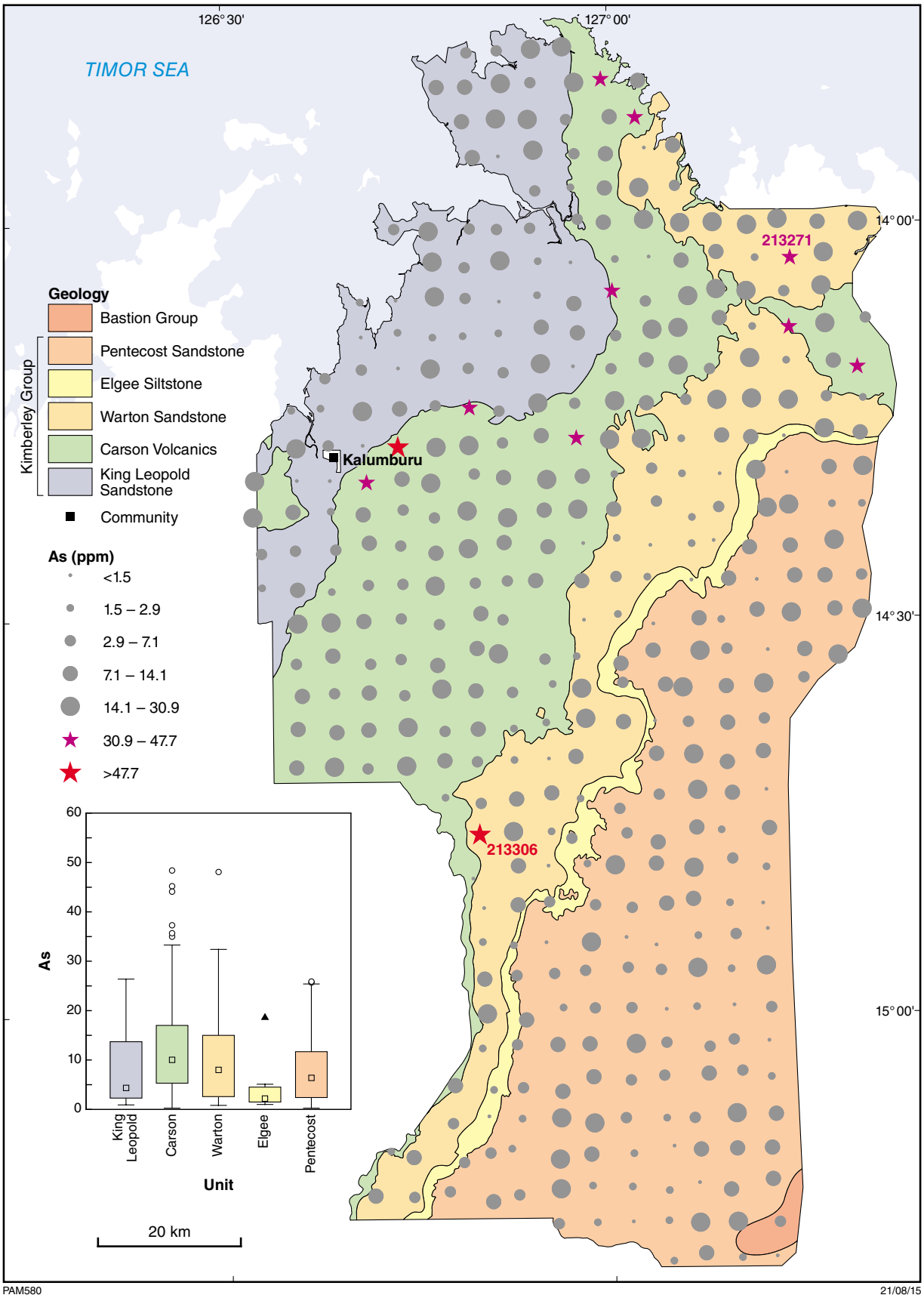

Figure B14. Bubble plots for chalcophile elements measured in regolith from the Balanggarra project area. Bubble divisions have been determined using box and whisker plots (see text for explanation), apart from analytes with a high proportion of censored data (Cd, Se, Te), where bubble divisions use natural breaks, and box and whisker plots have not been compiled. Samples with anomalous concentrations shown by stars (purple – outlier; red – extreme). Also shown is the box and whisker plot according to major lithological units, showing the median, interquartile range (box) and samples with anomalous concentrations (outlier – open circle; extreme – triangle): a) As (ppm); b) Bi (ppm); c) Sb (ppm); d) Cd (ppm); e) Mo (ppm); f) S (wt%); g) Se (ppm); h) Te (ppm); i) W (ppm)

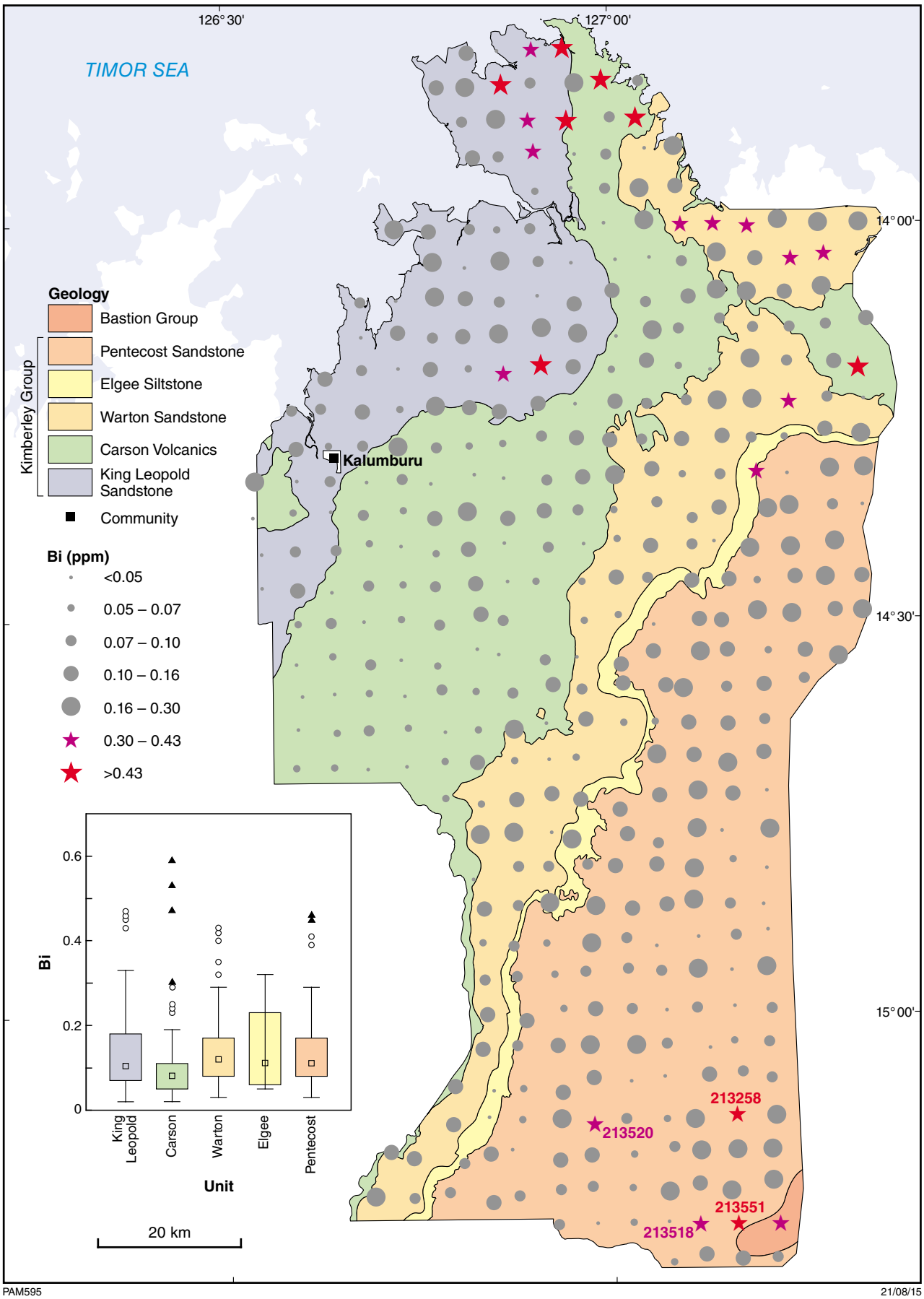
126° 30'
127° 00'
TIMOR SEA
14° 00'
14° 30'
15° 00'
Geology
Kimberley Group
Bastion Group
Pentecost Sandstone
Elgee Siltstone
Warton Sandstone
Carson Volcanics
King Leopold Sandstone
Community
Kalumburu
Bi (ppm)
<0.05
0.05 – 0.07
0.07 – 0.10
0.10 – 0.16
0.16 – 0.30
0.30 – 0.43
>0.43
Bi
0.6
0.4
0.2
0
King Leopold
Carson
Warton
Elgee
Pentecost
Unit
20 km
213258
213520
213551
213518
PAM595
21/08/15

Figure B14b.

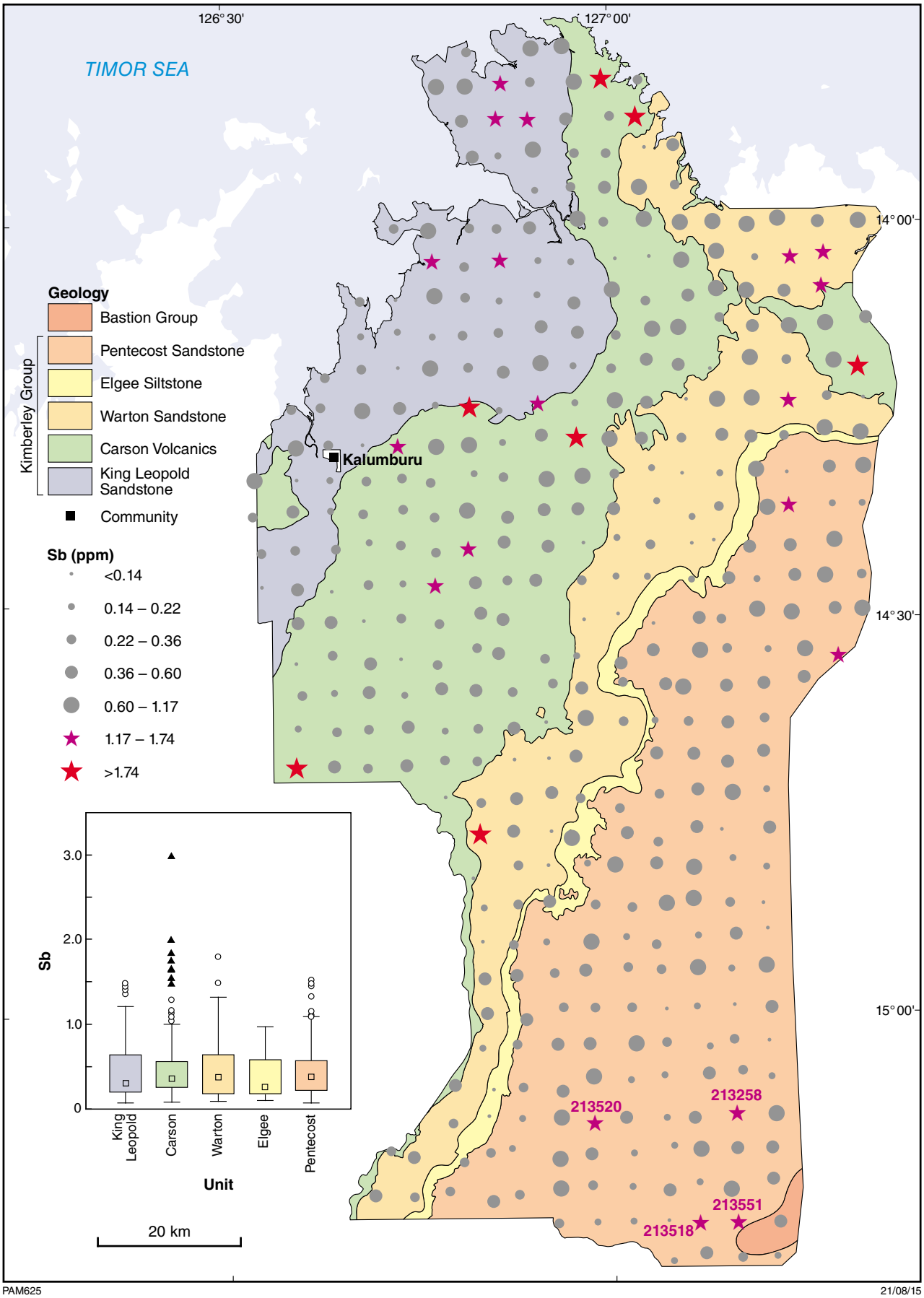
126° 30'
127° 00'
TIMOR SEA
14° 00'
14° 30'
15° 00'
Geology
Kimberley Group
Bastion Group
Pentecost Sandstone
Elgee Siltstone
Warton Sandstone
Carson Volcanics
King Leopold Sandstone
Community
Kalumburu
Sb (ppm)
<0.14
0.14 – 0.22
0.22 – 0.36
0.36 – 0.60
0.60 – 1.17
1.17 – 1.74
>1.74
Sb
3.0
2.0
1.0
0
King Leopold
Carson
Warton
Elgee
Pentecost
Unit
20 km
213520
213258
213551
213518
PAM625
21/08/15

Figure B14c.

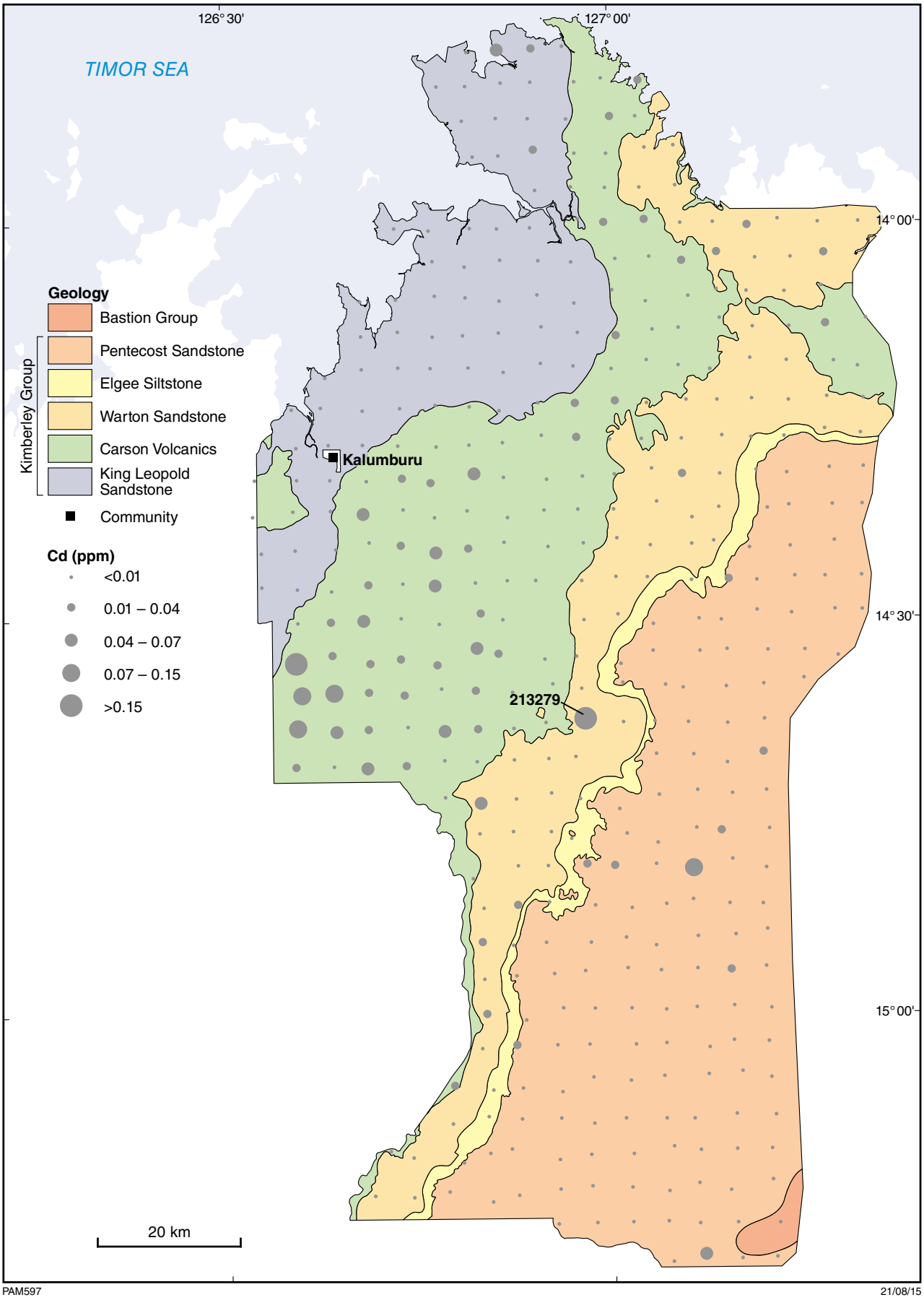
126° 30'
127° 00'
TIMOR SEA
14° 00'
14° 30'
15° 00'
Geology
Bastion Group
Pentecost Sandstone
Elgee Siltstone
Warton Sandstone
Carson Volcanics
King Leopold Sandstone
Kimberley Group
Community
Kalumburu
Cd (ppm)
<0.01
0.01 – 0.04
0.04 – 0.07
0.07 – 0.15
>0.15
213279
20 km
PAM597
21/08/15

Figure B14d.

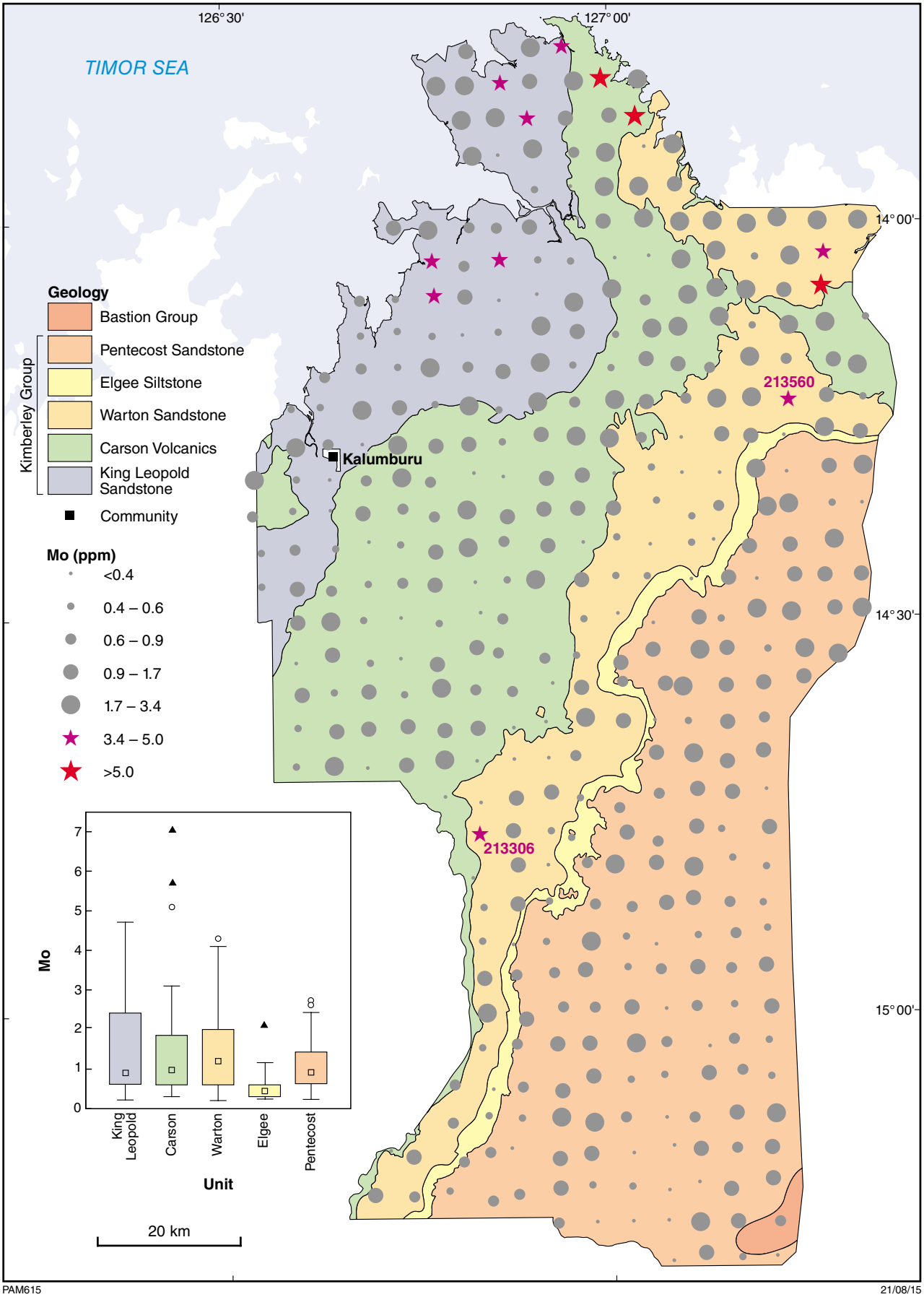
126° 30'
127° 00'
TIMOR SEA
14° 00'
14° 30'
15° 00'
Geology
Bastion Group
Pentecost Sandstone
Elgee Siltstone
Warton Sandstone
Carson Volcanics
King Leopold Sandstone
Kimberley Group
Community
Kalumburu
213560
213306
Mo (ppm)
<0.4
0.4 – 0.6
0.6 – 0.9
0.9 – 1.7
1.7 – 3.4
3.4 – 5.0
>5.0
Mo
0
1
2
3
4
5
6
7
King Leopold
Carson
Warton
Elgee
Pentecost
Unit
20 km
PAM615
21/08/15

Figure B14e.

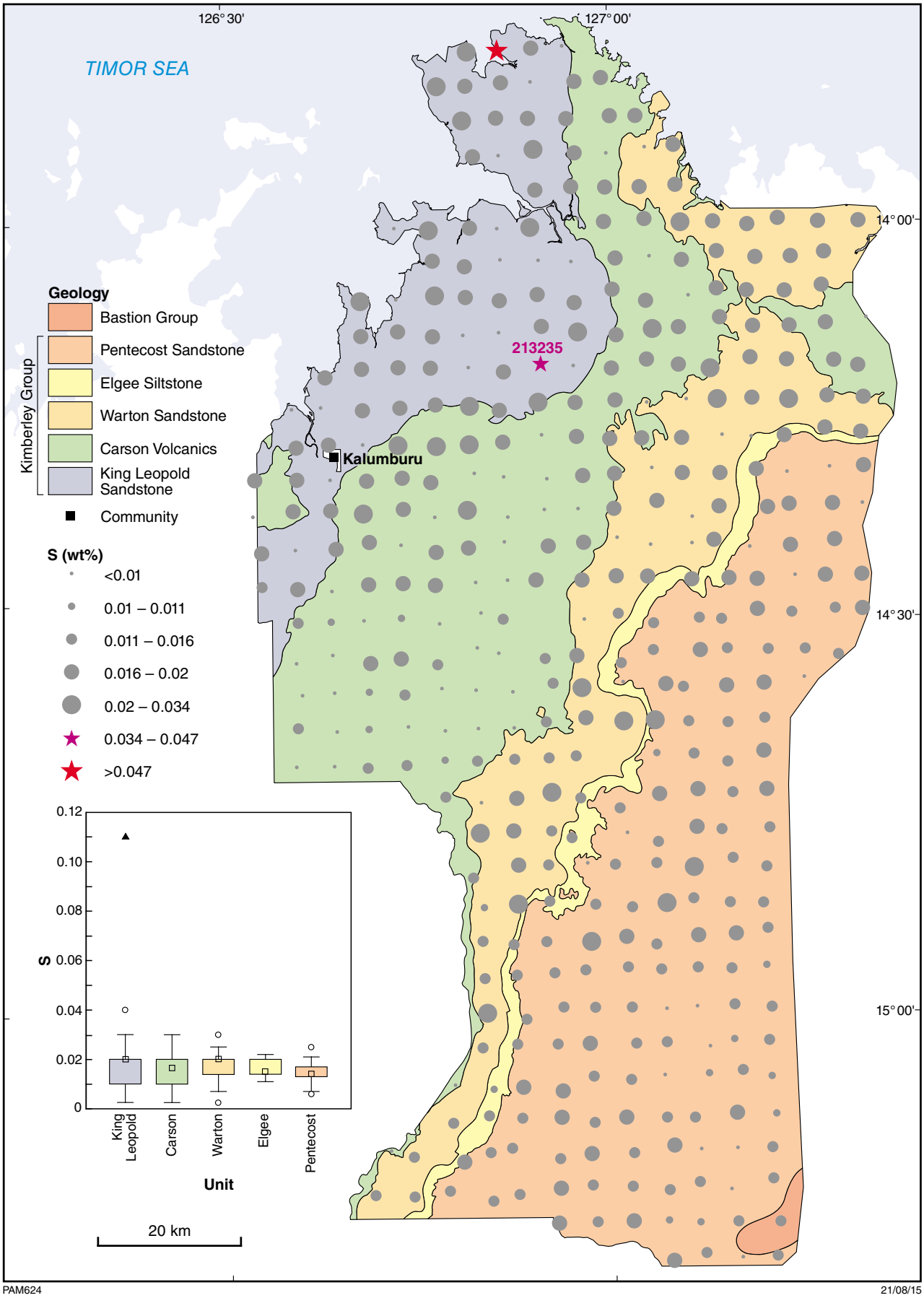
126° 30'
127° 00'
TIMOR SEA
14° 00'
14° 30'
15° 00'
Geology
Bastion Group
Pentecost Sandstone
Elgee Siltstone
Warton Sandstone
Carson Volcanics
King Leopold Sandstone
Kimberley Group
Community
213235
Kalumburu
S (wt%)
<0.01
0.01 – 0.011
0.011 – 0.016
0.016 – 0.02
0.02 – 0.034
0.034 – 0.047
>0.047
0.12
0.10
0.08
0.06
0.04
0.02
0
S
King Leopold
Carson
Warton
Elgee
Pentecost
Unit
20 km
PAM624
21/08/15

Figure B14f.

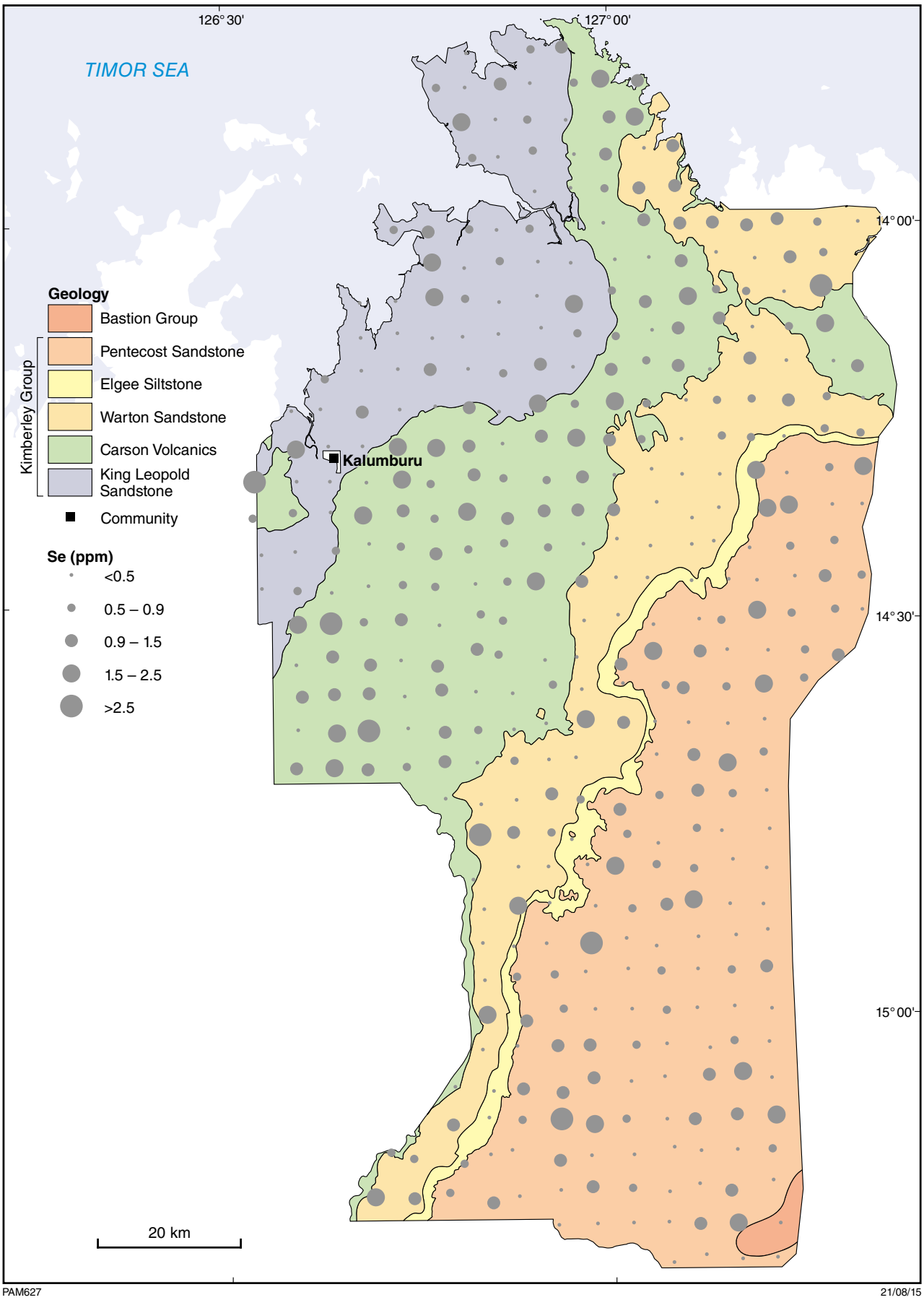
126° 30'
127° 00'
TIMOR SEA
14° 00'
14° 30'
15° 00'
Geology
Bastion Group
Pentecost Sandstone
Elgee Siltstone
Warton Sandstone
Carson Volcanics
King Leopold Sandstone
Kimberley Group
Community
Kalumburu
Se (ppm)
<0.5
0.5 – 0.9
0.9 – 1.5
1.5 – 2.5
>2.5
20 km
PAM627
21/08/15

Figure B14g.

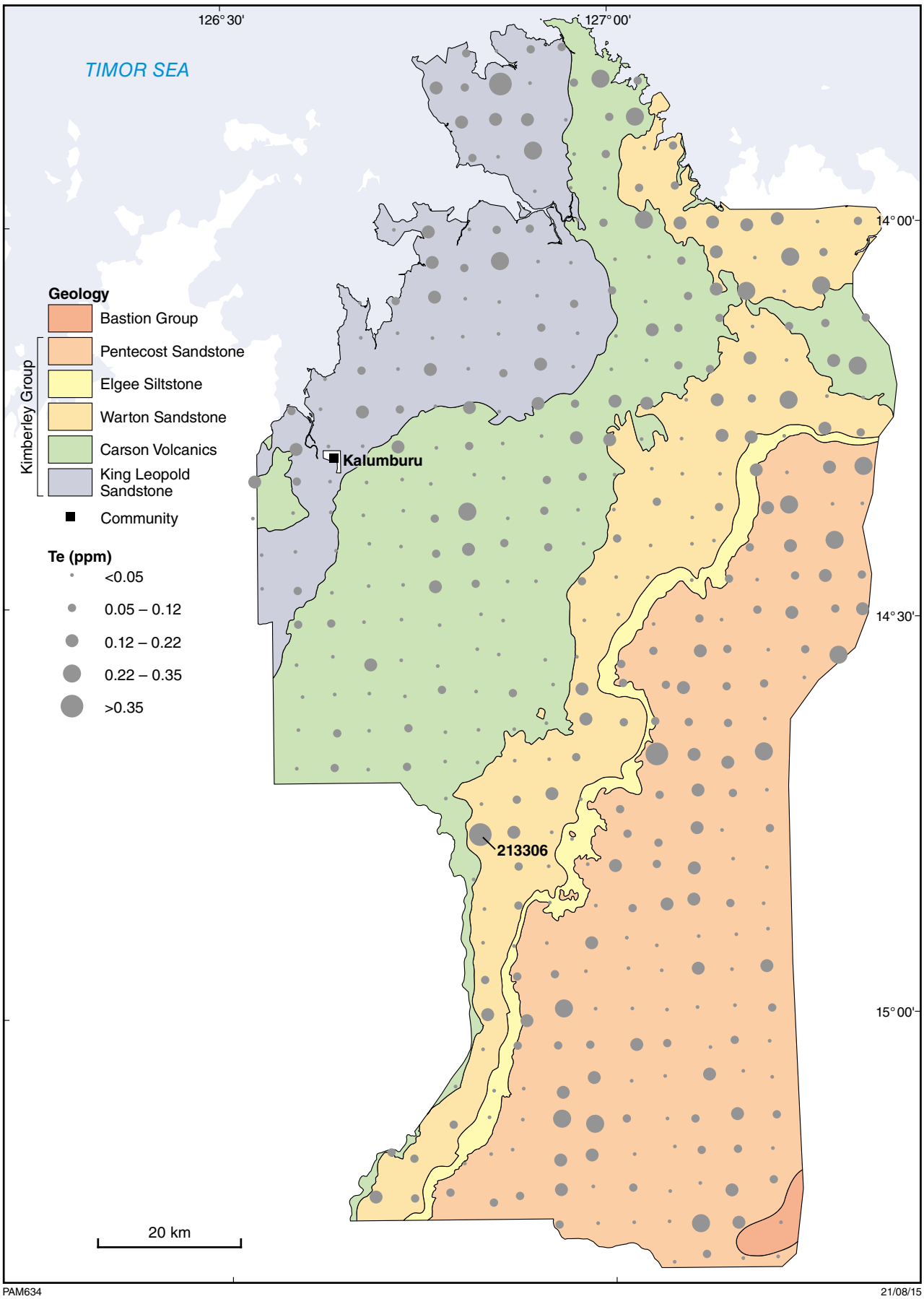
126° 30'
127° 00'
TIMOR SEA
14° 00'
14° 30'
15° 00'
Geology
Bastion Group
Kimberley Group
Pentecost Sandstone
Elgee Siltstone
Warton Sandstone
Carson Volcanics
King Leopold Sandstone
Community
Kalumburu
Te (ppm)
<0.05
0.05 – 0.12
0.12 – 0.22
0.22 – 0.35
>0.35
213306
20 km
PAM634
21/08/15

Figure B14h.

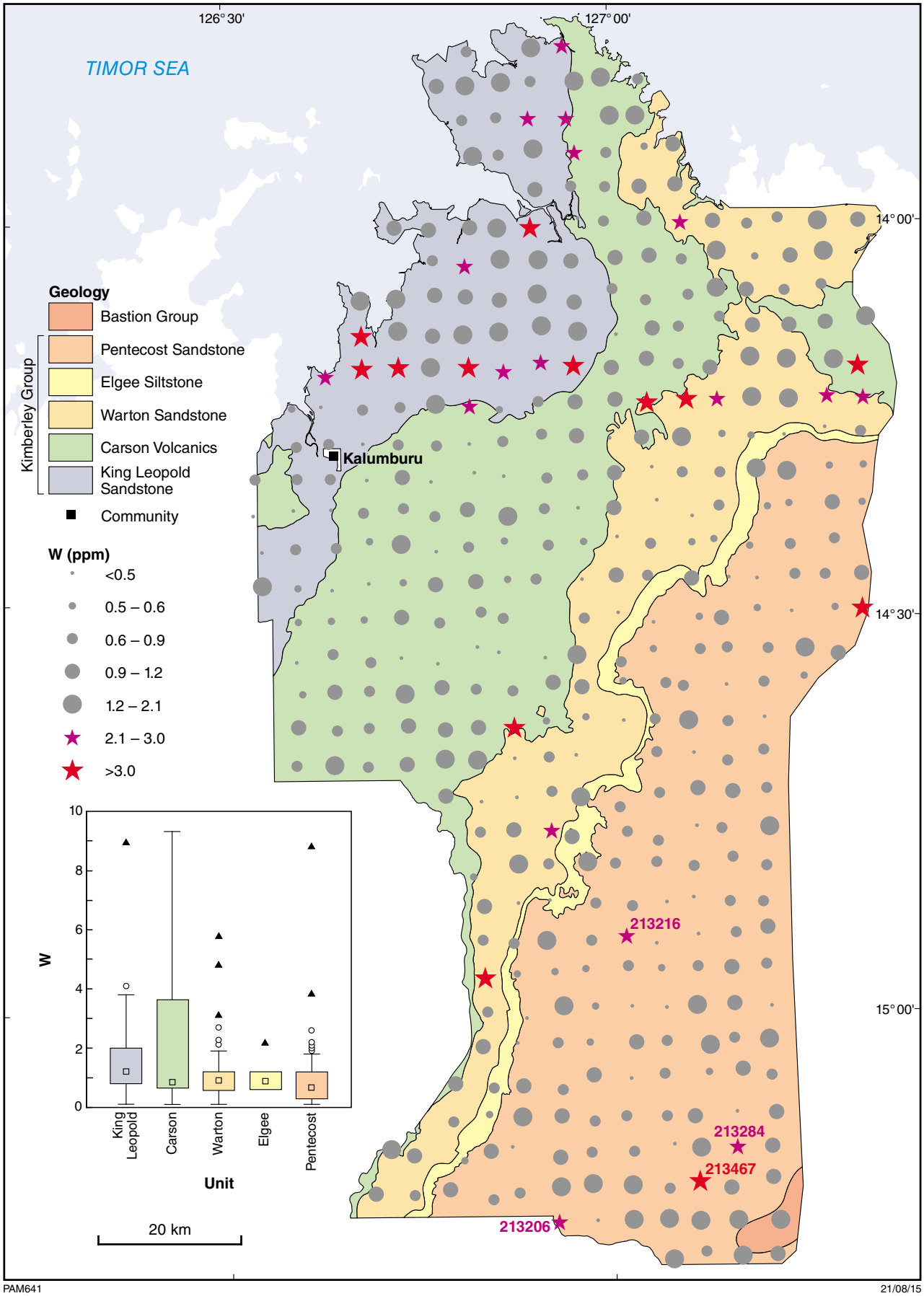
126° 30'
127° 00'
TIMOR SEA
14° 00'
14° 30'
15° 00'
Geology
Bastion Group
Kimberley Group
Pentecost Sandstone
Elgee Siltstone
Warton Sandstone
Carson Volcanics
King Leopold Sandstone
Community
Kalumburu
W (ppm)
<0.5
0.5 – 0.6
0.6 – 0.9
0.9 – 1.2
1.2 – 2.1
2.1 – 3.0
>3.0
213216
213284
213467
213206
W
Unit
King Leopold
Carson
Warton
Elgee
Pentecost
20 km
PAM641
21/08/15

Figure B14i.

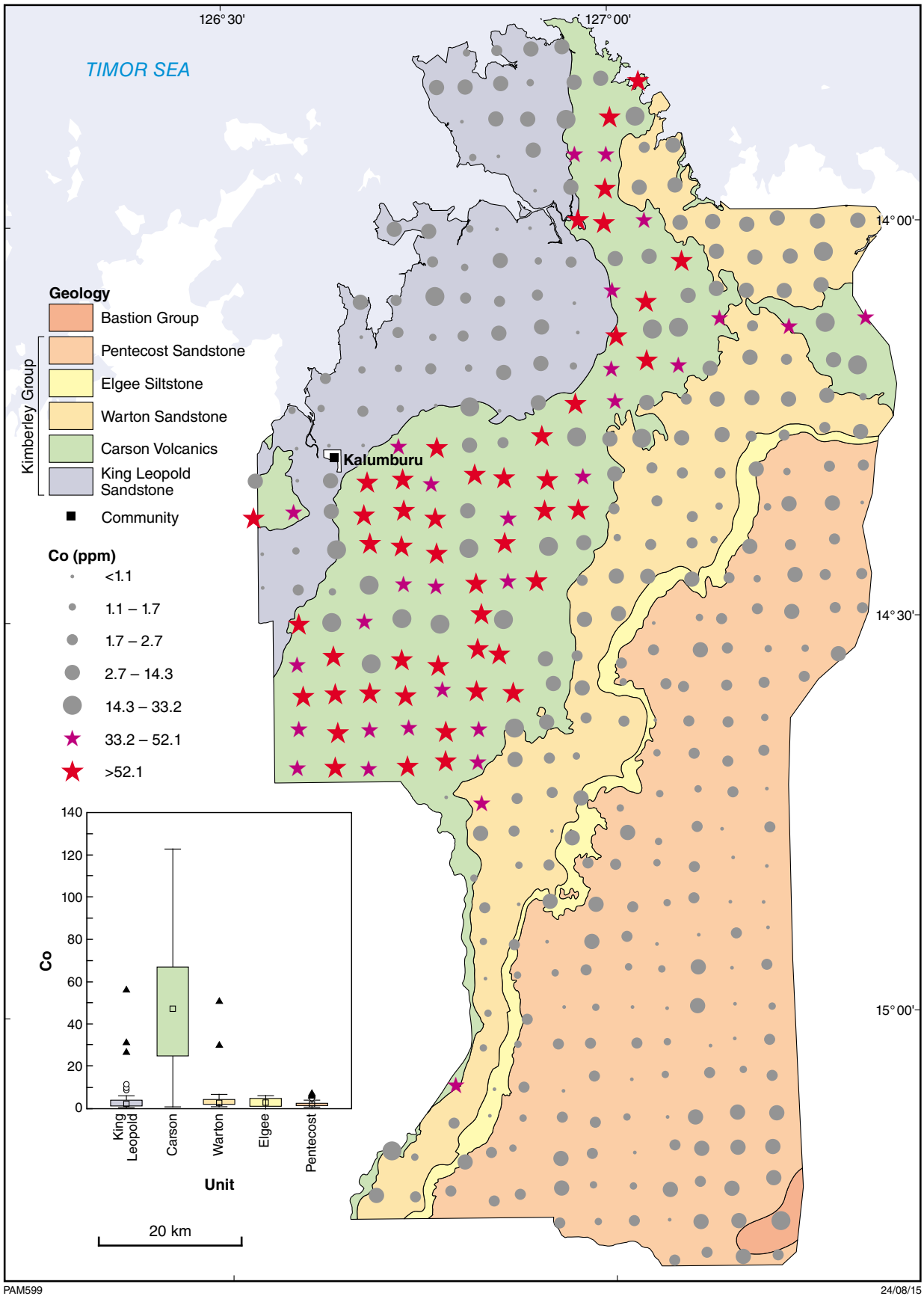

Figure B15. **Bubble plots for transition elements measured in regolith from the Balanggarra project area. Bubble divisions have been determined using box and whisker plots (see text for explanation). Samples with anomalous concentrations shown by stars (purple – outlier; red – extreme). Also shown is the box and whisker plot according to major lithological units, showing the median, interquartile range (box) and samples with anomalous concentrations (outlier – open circle; extreme – triangle): a) Co (ppm); b) Cr (ppm); c) Ni (ppm); d) Sc (ppm); e) V (ppm)**

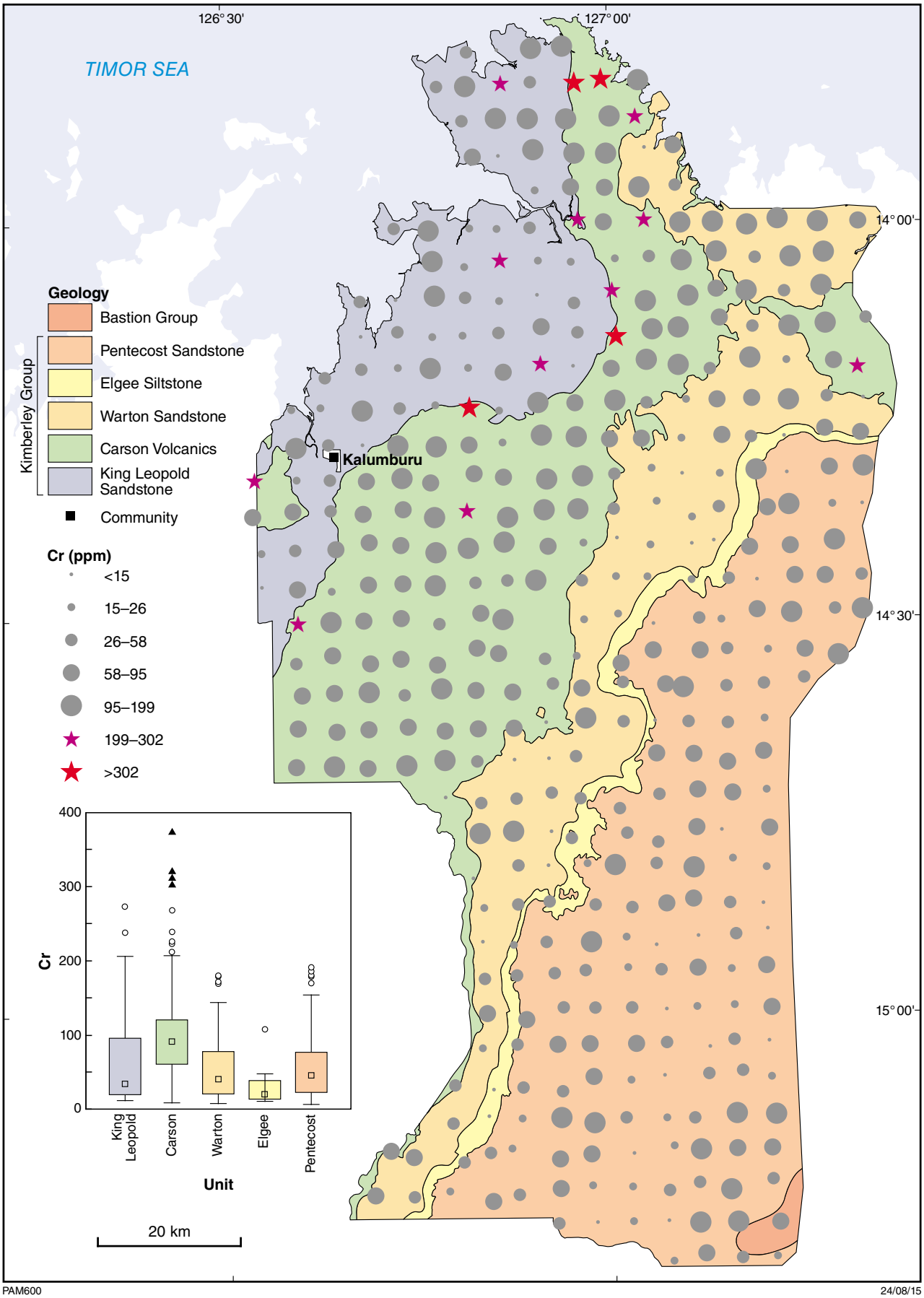
126° 30'
127° 00'
TIMOR SEA
14° 00'
14° 30'
15° 00'
Geology
Bastion Group
Kimberley Group
Pentecost Sandstone
Elgee Siltstone
Warton Sandstone
Carson Volcanics
King Leopold Sandstone
Community
Kalumburu
Cr (ppm)
<15
15–26
26–58
58–95
95–199
199–302
>302
400
300
200
100
0
Cr
King Leopold
Carson
Warton
Elgee
Pentecost
Unit
20 km
PAM600
24/08/15

Figure B15b.

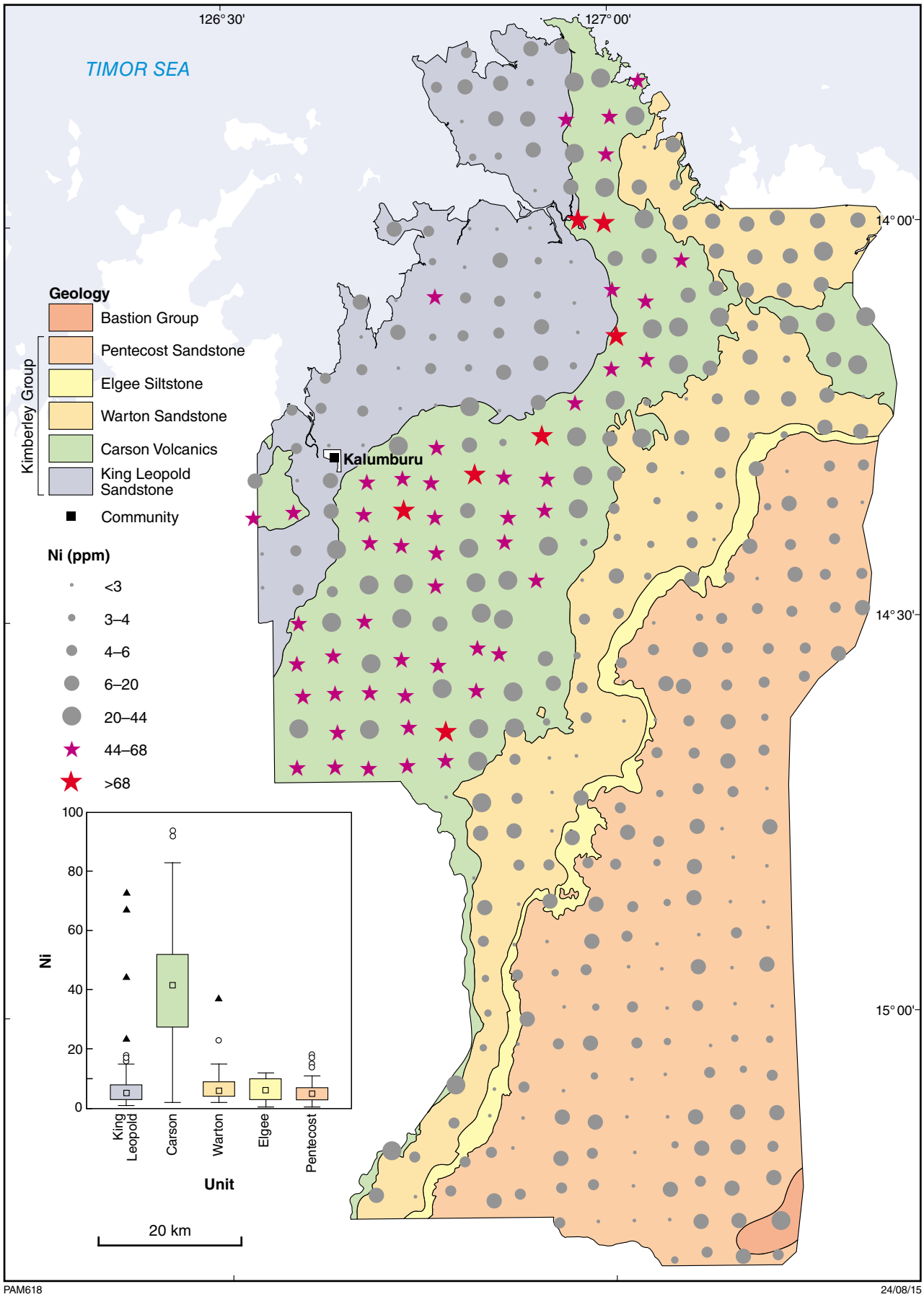
126° 30'
127° 00'
TIMOR SEA
14° 00'
14° 30'
15° 00'
Geology
Bastion Group
Kimberley Group
Pentecost Sandstone
Elgee Siltstone
Warton Sandstone
Carson Volcanics
King Leopold Sandstone
Community
Kalumburu
Ni (ppm)
<3
3–4
4–6
6–20
20–44
44–68
>68
100
80
60
40
20
0
Ni
King Leopold
Carson
Warton
Elgee
Pentecost
Unit
20 km
PAM618
24/08/15

Figure B15c.

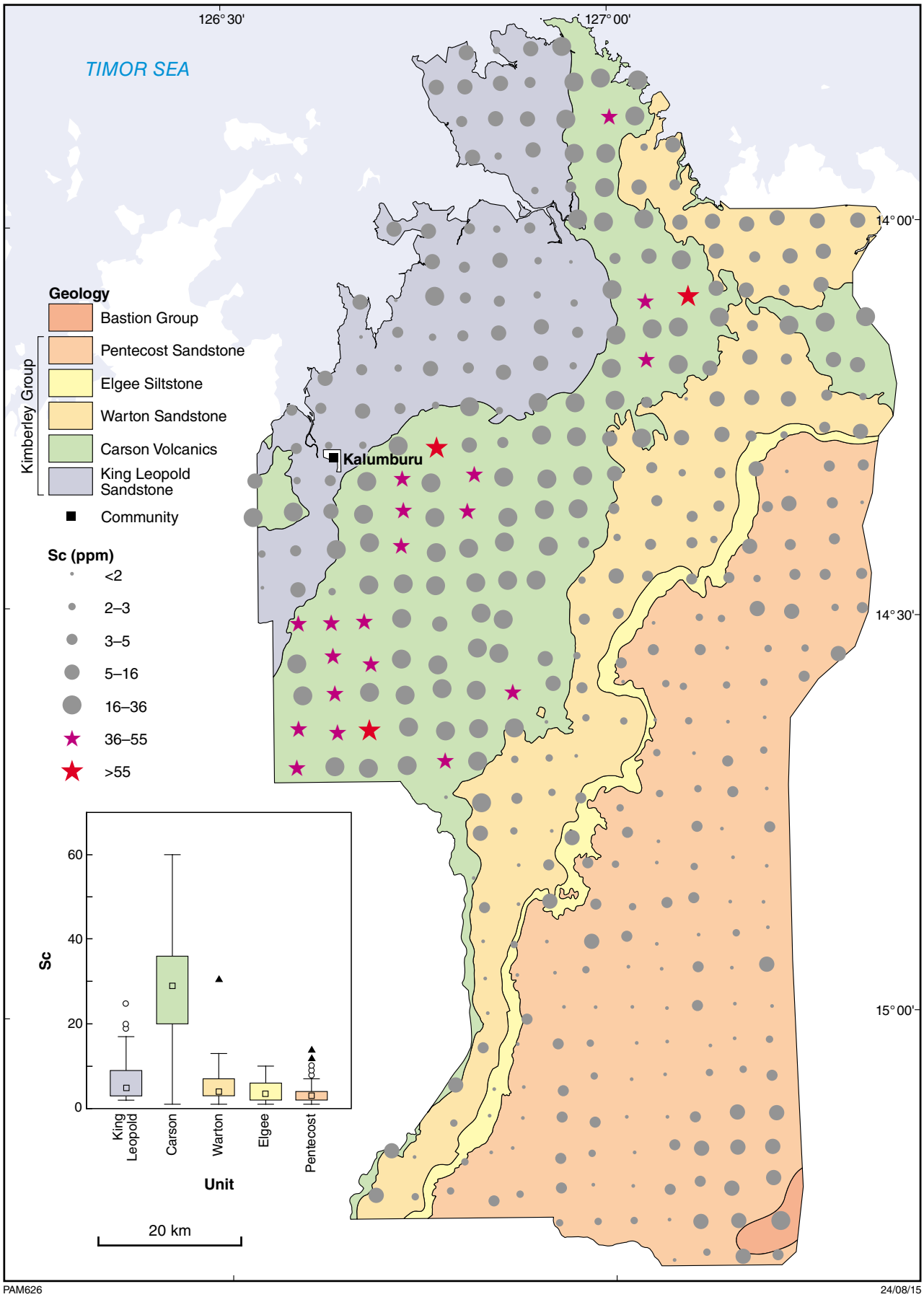
126° 30'
127° 00'
TIMOR SEA
14° 00'
14° 30'
15° 00'
Geology
Kimberley Group
Bastion Group
Pentecost Sandstone
Elgee Siltstone
Warton Sandstone
Carson Volcanics
King Leopold Sandstone
Community
Kalumburu
Sc (ppm)
<2
2–3
3–5
5–16
16–36
36–55
>55
Sc
60
40
20
0
King Leopold
Carson
Warton
Elgee
Pentecost
Unit
20 km
PAM626
24/08/15

Figure B15d.

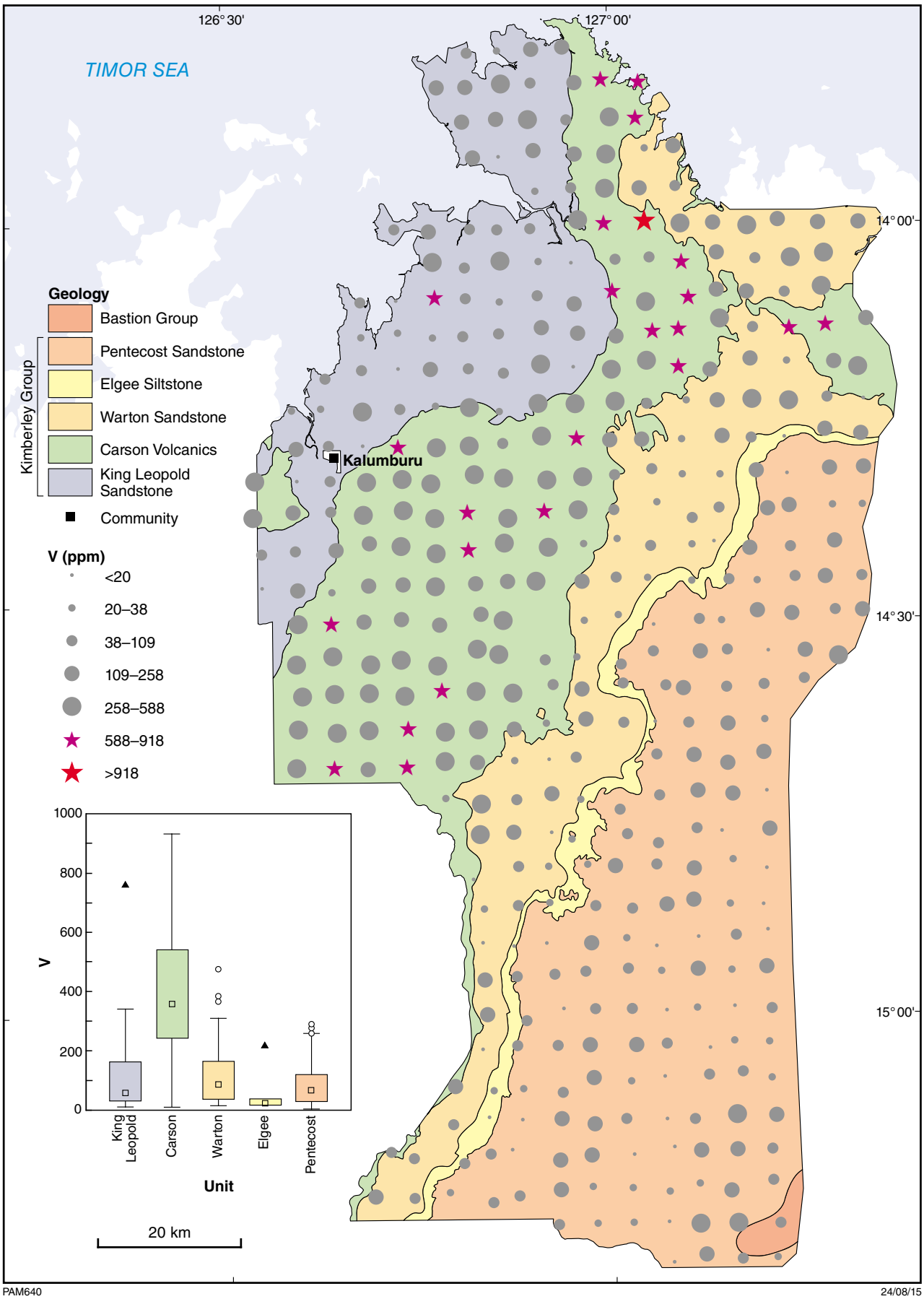
126° 30'
127° 00'
TIMOR SEA
14° 00'
14° 30'
15° 00'
Geology
Bastion Group
Kimberley Group
Pentecost Sandstone
Elgee Siltstone
Warton Sandstone
Carson Volcanics
King Leopold Sandstone
Community
Kalumburu
V (ppm)
<20
20–38
38–109
109–258
258–588
588–918
>918
1000
800
600
400
200
0
V
King Leopold
Carson
Warton
Elgee
Pentecost
Unit
20 km
PAM640
24/08/15

Figure B15e.

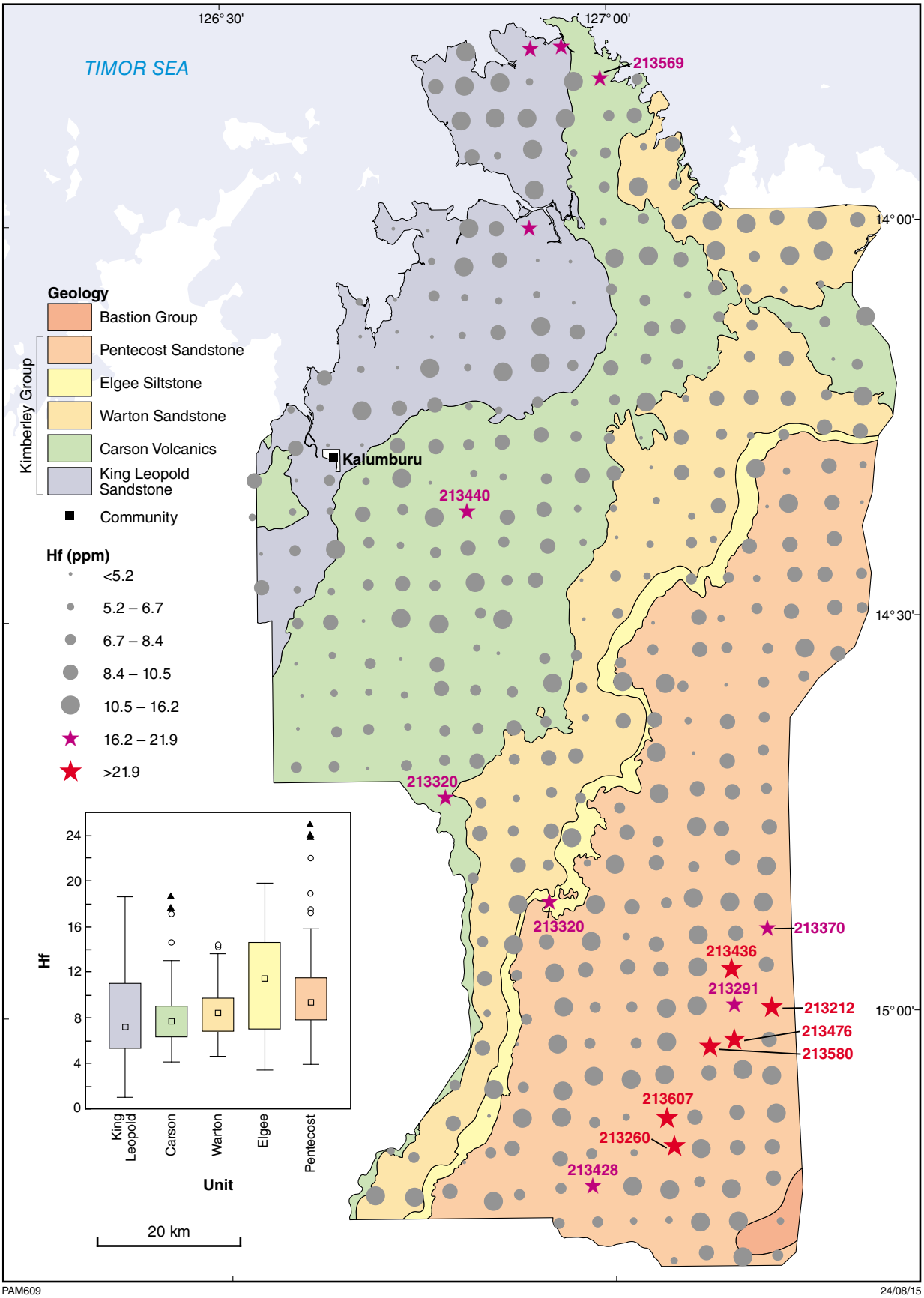

Figure B16. **Bubble plots for high field strength elements (HFSE) measured in regolith from the Balanggarra project area. Bubble divisions have been determined using box and whisker plots (see text for explanation). Samples with anomalous concentrations shown by stars (purple – outlier; red – extreme). Also shown is the box and whisker plot according to major lithological units, showing the median, interquartile range (box) and samples with anomalous concentrations (outlier – open circle; extreme – triangle): a) Hf (ppm); b) Nb (ppm); c) Ta (ppm); d) Zr (ppm)**

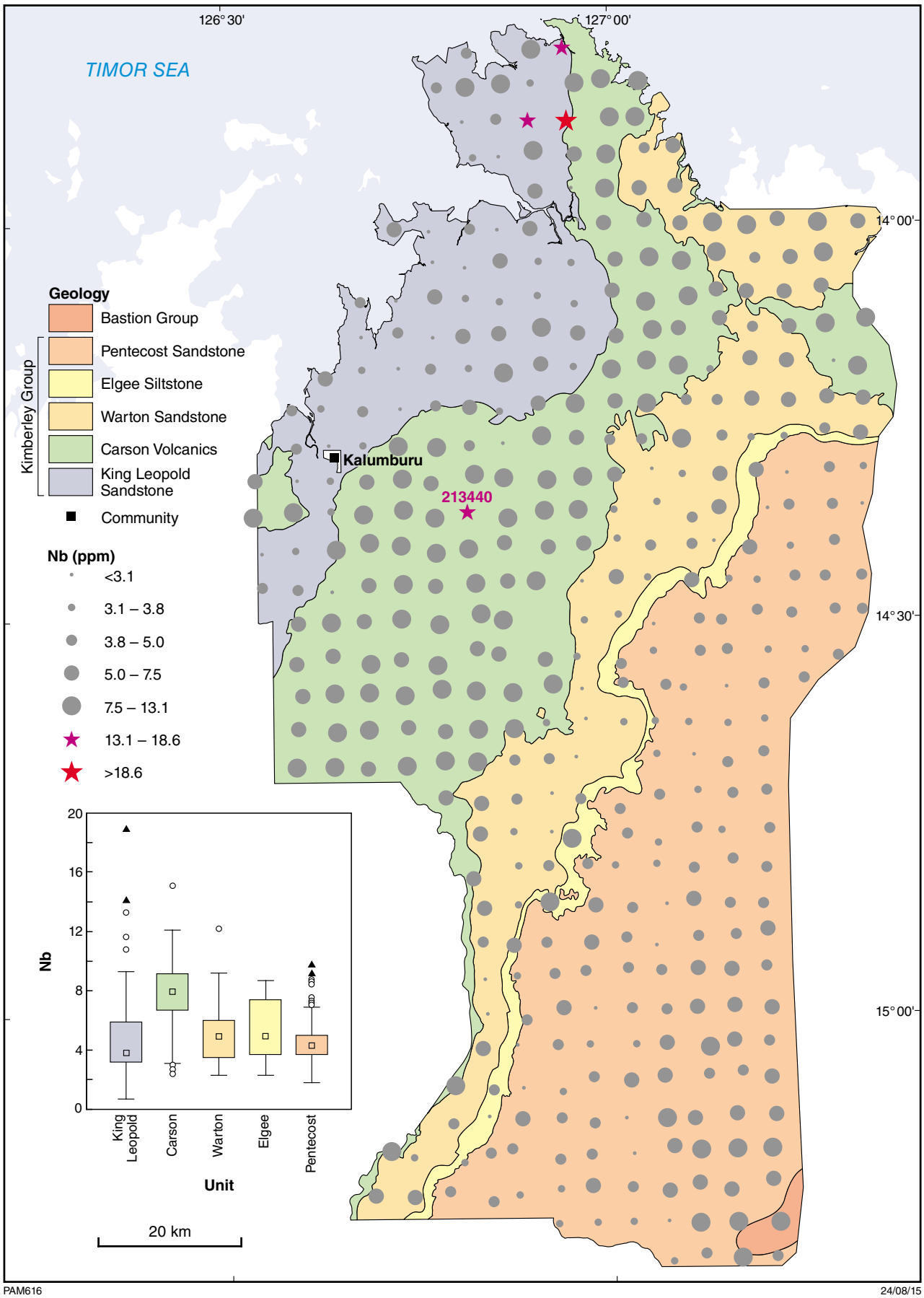
126° 30'
127° 00'
TIMOR SEA
14° 00'
14° 30'
15° 00'
Geology
Kimberley Group
Bastion Group
Pentecost Sandstone
Elgee Siltstone
Warton Sandstone
Carson Volcanics
King Leopold Sandstone
Community
Kalumburu
213440
Nb (ppm)
<3.1
3.1 – 3.8
3.8 – 5.0
5.0 – 7.5
7.5 – 13.1
13.1 – 18.6
>18.6
Nb
20
16
12
8
4
0
King Leopold
Carson
Warton
Elgee
Pentecost
Unit
20 km
PAM616
24/08/15

Figure B16b.

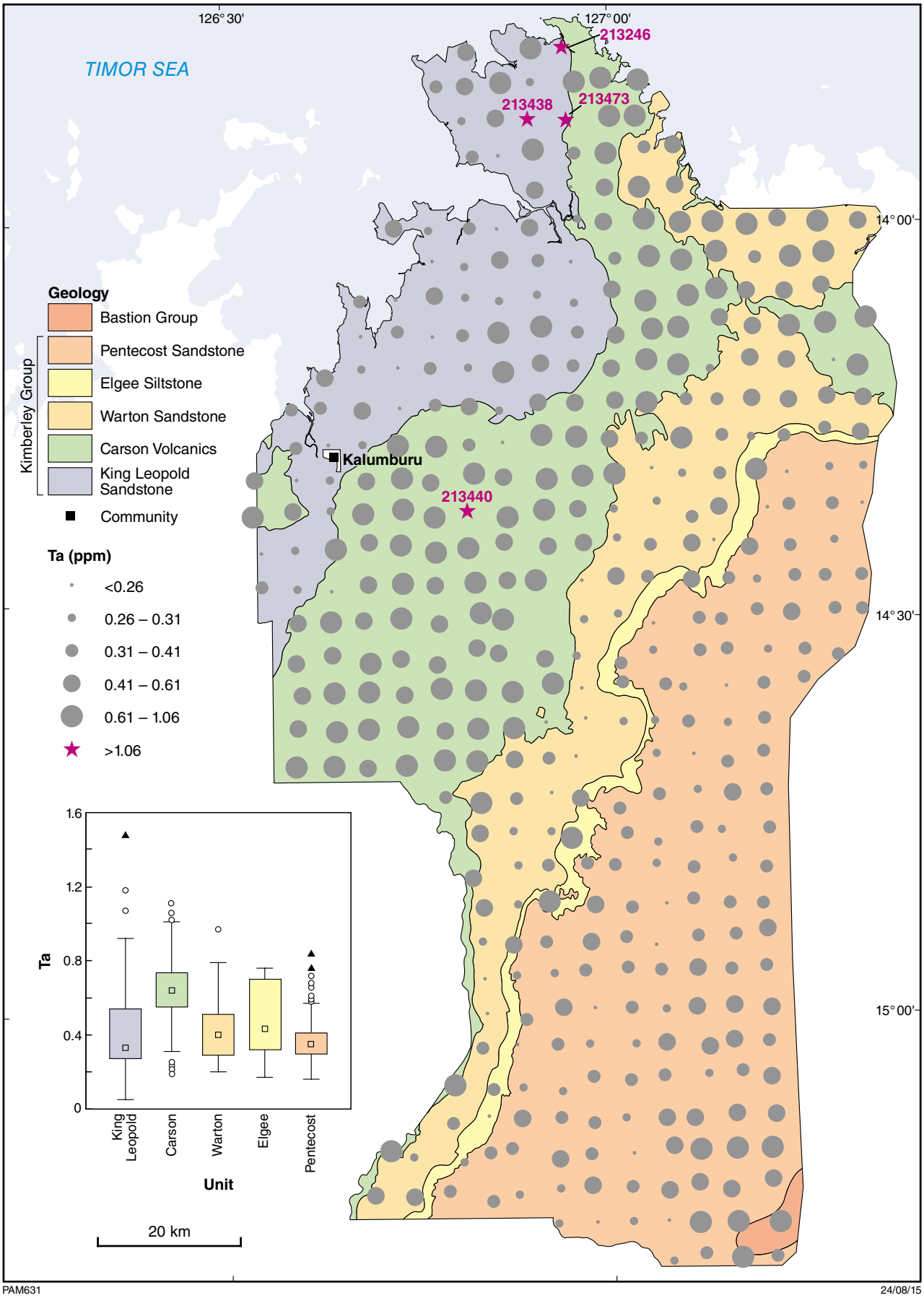
126° 30'
127° 00'
TIMOR SEA
213246
213438
213473
14° 00'
Geology
Bastion Group
Kimberley Group
Pentecost Sandstone
Elgee Siltstone
Warton Sandstone
Carson Volcanics
King Leopold Sandstone
Community
Kalumburu
213440
Ta (ppm)
<0.26
0.26 – 0.31
0.31 – 0.41
0.41 – 0.61
0.61 – 1.06
>1.06
14° 30'
1.6
1.2
0.8
0.4
0
Ta
King Leopold
Carson
Warton
Elgee
Pentecost
Unit
15° 00'
20 km
PAM631
24/08/15

Figure B16c.

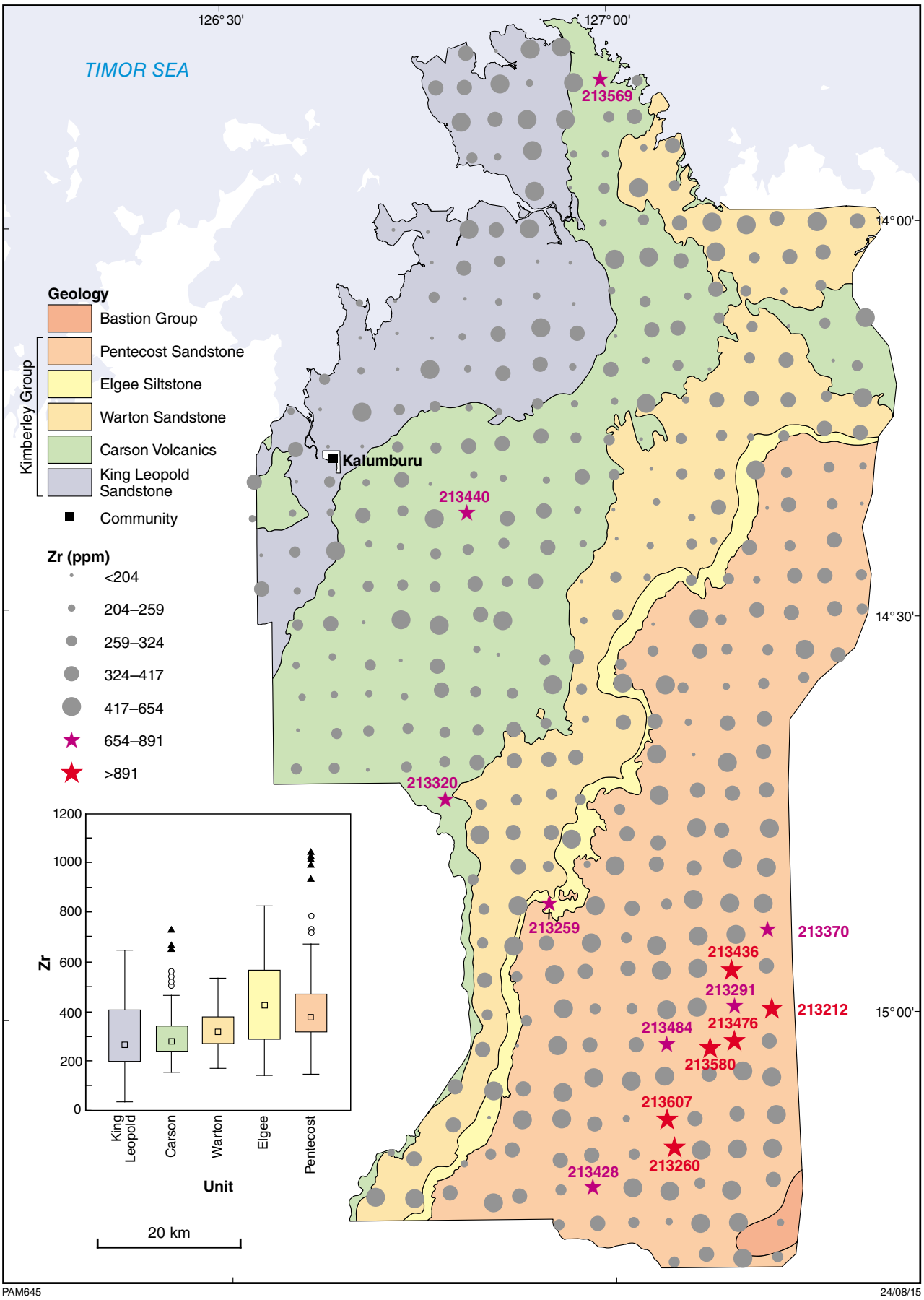
126° 30'
127° 00'
TIMOR SEA
213569
14° 00'
Geology
Bastion Group
Kimberley Group
Pentecost Sandstone
Elgee Siltstone
Warton Sandstone
Carson Volcanics
King Leopold Sandstone
Community
Kalumburu
213440
Zr (ppm)
<204
204–259
259–324
324–417
417–654
654–891
>891
14° 30'
213320
1200
1000
800
600
400
200
0
Zr
King Leopold
Carson
Warton
Elgee
Pentecost
Unit
213259
213370
213436
213291
213212
213484
213476
213580
15° 00'
213607
213260
213428
20 km
PAM645
24/08/15

Figure B16d.

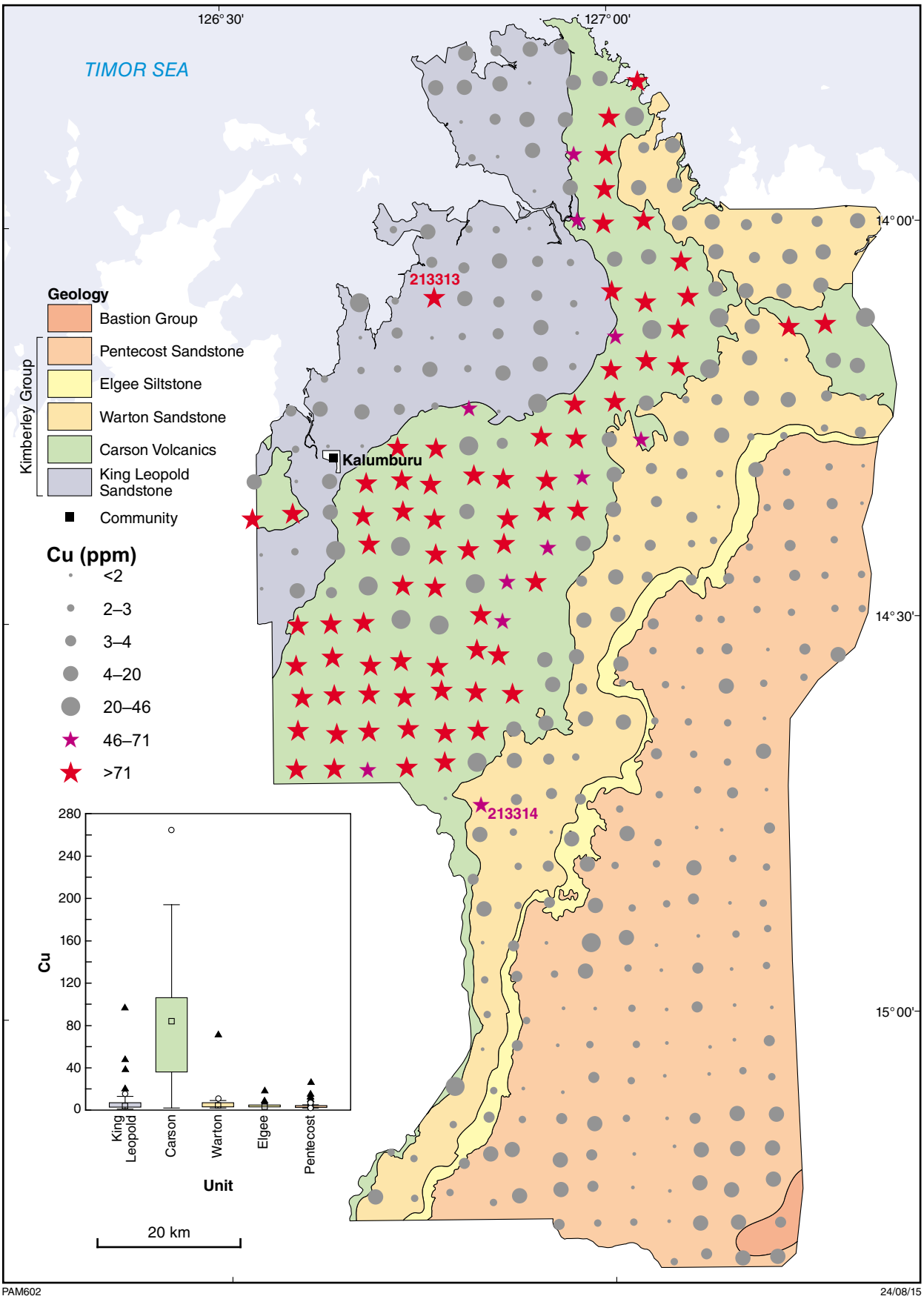

Figure B17. **Bubble plots for base metals measured in regolith from the Balanggarra project area. Bubble divisions have been determined using box and whisker plots (see text for explanation). Samples with anomalous concentrations shown by stars (purple – outlier; red – extreme). Also shown is the box and whisker plot according to major lithological units, showing the median, interquartile range (box) and samples with anomalous concentrations (outlier – open circle; extreme – triangle): a) Cu (ppm); b) Pb (ppm); c) Zn (ppm)**

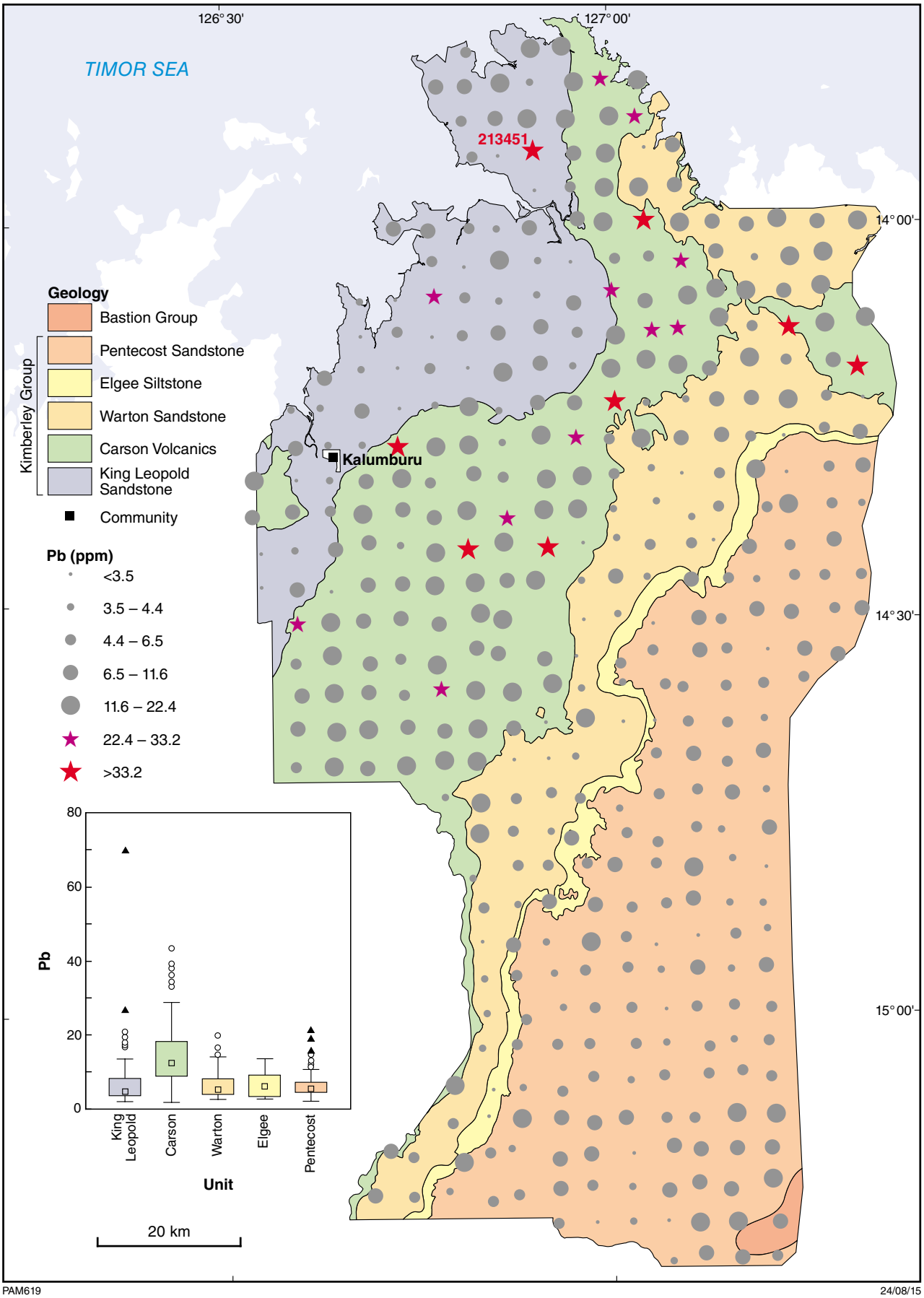
126° 30'
127° 00'
TIMOR SEA
213451
14° 00'
14° 30'
15° 00'
Geology
Bastion Group
Kimberley Group
Pentecost Sandstone
Elgee Siltstone
Warton Sandstone
Carson Volcanics
King Leopold Sandstone
Community
Kalumburu
Pb (ppm)
<3.5
3.5 – 4.4
4.4 – 6.5
6.5 – 11.6
11.6 – 22.4
22.4 – 33.2
>33.2
80
60
40
20
0
Pb
King Leopold
Carson
Warton
Elgee
Pentecost
Unit
20 km
PAM619
24/08/15

Figure B17b.

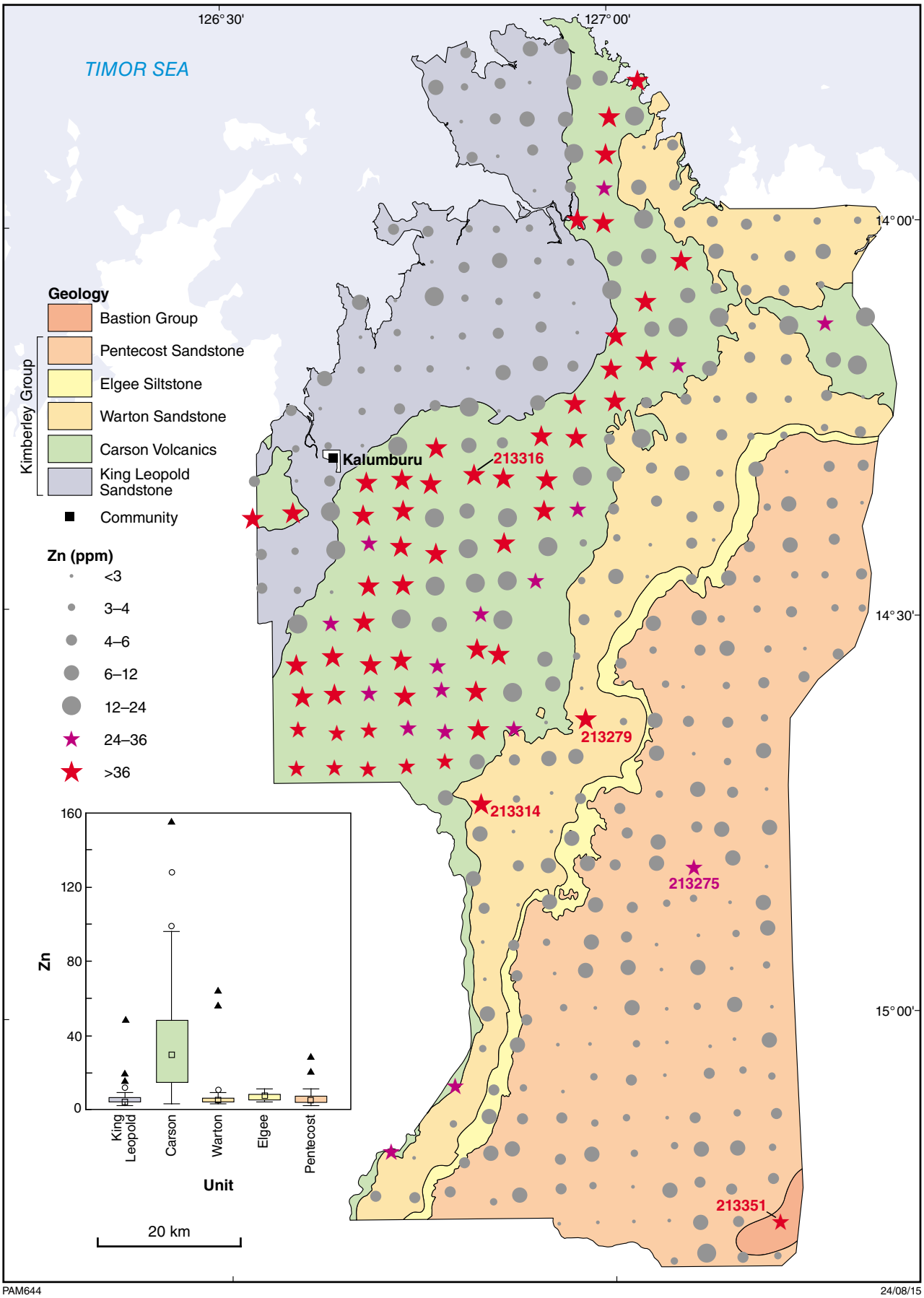
126°30'
127°00'
TIMOR SEA
14°00'
14°30'
15°00'
Geology
Bastion Group
Pentecost Sandstone
Elgee Siltstone
Warton Sandstone
Carson Volcanics
King Leopold Sandstone
Kimberley Group
Community
Kalumburu
213316
213279
213314
213275
213351
Zn (ppm)
<3
3–4
4–6
6–12
12–24
24–36
>36
160
120
80
40
0
Zn
King Leopold
Carson
Warton
Elgee
Pentecost
Unit
20 km
PAM644
24/08/15

Figure B17c.

RECORD 2015/9

REGOLITH CHEMISTRY OF THE BALANGGARRA AREA, NORTH KIMBERLEY

This Record is published in digital format (PDF) and is available as a free download from the DMP website at <www.dmp.wa.gov.au/GSWApublications>.

Further details of geological products produced by the Geological Survey of Western Australia can be obtained by contacting:

Information Centre
Department of Mines and Petroleum
100 Plain Street
EAST PERTH WESTERN AUSTRALIA 6004
Phone: +61 8 9222 3459 Fax: +61 8 9222 3444
www.dmp.wa.gov.au/GSWApublications

Morris et al.

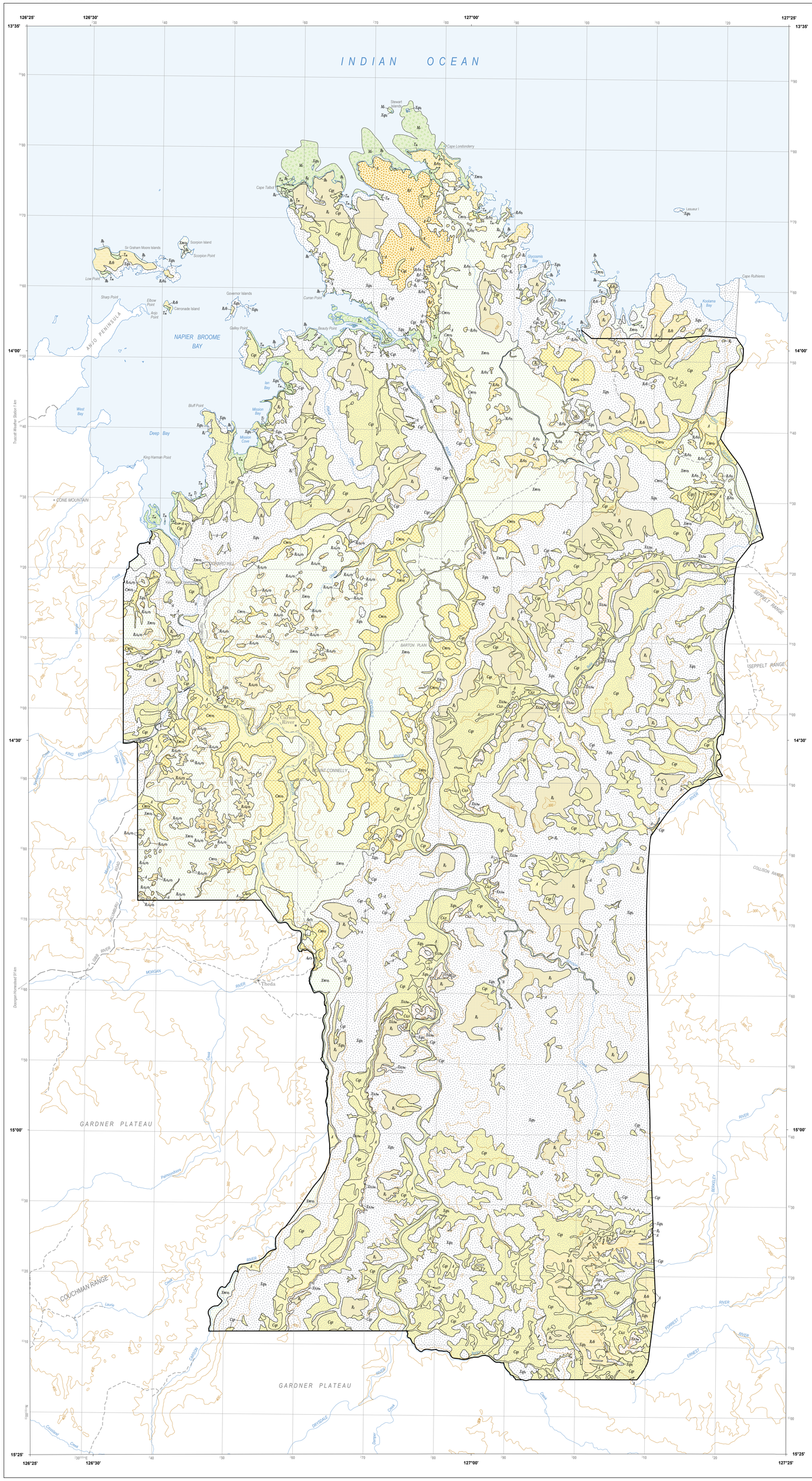

DEPOSITIONAL REGIME

Colluvial units

- *Cmrs* — Ferromagnesian colluvial deposits, red-brown sand and silt, with pisoliths; derived from basalt
- *Cqr* — Quartz-rich sand, silt and gravel in colluvial deposits derived from sedimentary rocks
- *Cmr* — Micaceous colluvium derived from sedimentary rocks

Alluvial units

- *A* — Clay, silt, sand, and gravel in channels and on floodplains
- *Acs* — Black soils (gilgai); grey to black smectitic clays on alluvial plains

Coastal (wave-dominated) units

- *Br* — Beach sand
- *Dr* — Coastal dunes and beach deposits; unconsolidated shelly sand

Coastal (tide-dominated) units

- *Tr* — Sand, silt, and mud on tidal flats; locally with salt crust
- *Tm* — Sand, silt, and mud on mangrove flats
- *Ts* — Sand, silt, and mud on supratidal flats; locally with salt crust

Marine units

- *Mr* — Reef

RESIDUAL REGIME

Residual or relict units

- *Rd* — Ferruginous duricrust, massive to rubbly; derived from siliciclastic sedimentary rocks; includes iron-cemented reworked products
- *Rdvb* — Ferruginous duricrust; pisolitic and locally rubbly; developed on basalt as mesas and caps
- *Rdalvb* — Aluminous duricrust; pisolitic, massive to locally rubbly; developed on basalt as mesas and caps
- *Rr* — Residual sand; locally iron-rich and rubbly; may contain ferruginous pisoliths and nodules
- *Rd* — Transported ferruginous duricrust; iron-cemented sand and gravel

EXPOSED REGIME

- *Xmvs* — Mafic volcanic rocks; basalt
- *Xqs* — Quartz-rich sandstone
- *Xcsltst* — Micaceous mudstone, siltstone, and shale

INTERPRETED BEDROCK GEOLOGY

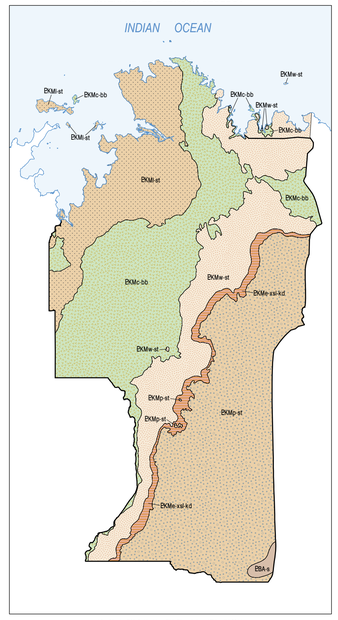

- EBA-s — Bastion Group
- Kimberley Group:
  - EKMp-st — Pentecost Sandstone
  - EKMe-ssl-kd — Elgee Siltstone
  - EKMe-st — Warton Sandstone
  - EKMc-bb — Carson Volcanics
  - EKMl-st — King Leopold Sandstone
- Kimberley Basin, North Australian Craton

After Martin, DMdB, Hocking, RM, Riganti, A and Tyler, IM 2014, 1:500 000 State interpreted bedrock geology of Western Australia, 2014, digital data layer: Geological Survey of Western Australia.

View detailed data at <www.dmp.wa.gov.au/geoview>.

SCALE 1:1 000 000

0 10 20 30 40 50 Kilometres

RADIOMETRIC IMAGE (KTU)

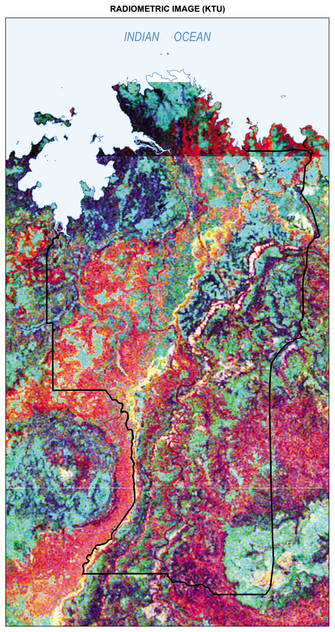

SCALE 1:1 000 000

0 10 20 30 40 50 Kilometres

LANDSAT — AGSO RATIO

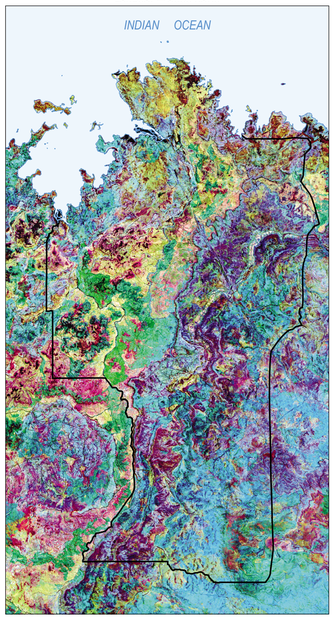

SCALE 1:1 000 000

0 10 20 30 40 50 Kilometres

DEM — SRTM

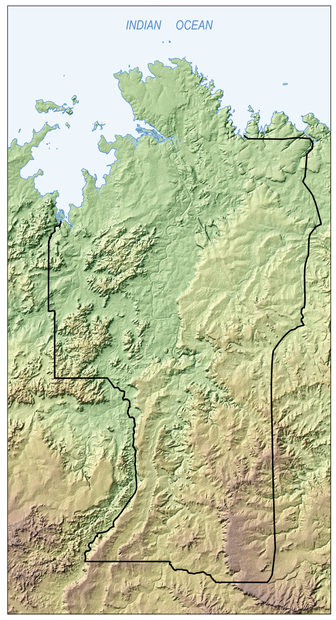

SCALE 1:1 000 000

0 10 20 30 40 50 Kilometres

Geological boundary
exposed
Road, unsealed
Track
Homestead
Aboriginal community
Contour line, 100 metre interval
Watercourse
Extent of project area

DATA SOURCES

Theme	Data Currency	Organization†
Geology *	2015	Geological Survey of Western Australia, Department of Mines and Petroleum
Topographic nomenclature	2015	Landgate
Topography	2015	Landgate
Contours	2006	Geological Survey of Western Australia, Department of Mines and Petroleum

* DMP data can be viewed interactively via GeoVIEW.WA <www.dmp.wa.gov.au/geoview>, and related datasets can be downloaded from the GSWA Data and Software Centre <www.dmp.wa.gov.au/dataworks>

† WA State Government unless otherwise indicated

SHEET INDEX

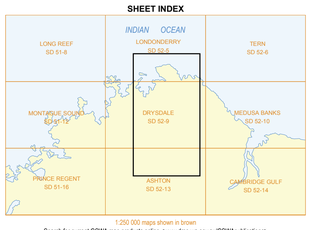

1:250 000 maps shown in brown

Search for current GSWA map products online <www.dmp.wa.gov.au/GSWApublications>

Compiled by N de Souza Kovacs 2015

Geology by N de Souza Kovacs 2015

Cartography by CS Schroder and S Mulligan

Edited by F Eddison and K Greenberg

Published by Geological Survey of Western Australia

This map is published in digital format (PDF) and is available online at <www.dmp.wa.gov.au/GSWApublications>.
Copies are available from:
Information Centre
Department of Mines and Petroleum
100 Plain Street
East Perth, Western Australia 6004
Phone: +61 8 9222 3459 Fax: +61 8 9222 3444
Website: www.dmp.wa.gov.au/gswa Email: geological.survey@dmp.wa.gov.au

The recommended reference for this map is:
de Souza Kovacs N 2015, Interpreted regolith–landform geology of the Balanggarra area, north Kimberley *in* Regolith chemistry of the Balanggarra area, north Kimberley by PA Morris, AJ Scheib, and N de Souza Kovacs: Geological Survey of Western Australia, Record 2015/9, Plate 1.

Government of **Western Australia**
Department of **Mines and Petroleum**

HON. BILL MARMION MLA
MINISTER FOR MINES AND PETROLEUM

Geological Survey of Western Australia

RICK ROGERSON
EXECUTIVE DIRECTOR

SCALE 1 : 250 000

5000 0 5 10 15 20 25 Metres Kilometres

UNIVERSAL TRANSVERSE MERCATOR PROJECTION
HORIZONTAL DATUM: GEOCENTRIC DATUM OF AUSTRALIA 1994
VERTICAL DATUM: AUSTRALIAN HEIGHT DATUM

Grid lines indicate 10 000 metre interval of the Map Grid Australia Zone 52

The Map Grid Australia (MGA) is based on the Geocentric Datum of Australia 1994 (GDA94)
GDA94 positions are compatible within one metre of the datum WGS84 positions

GDA

GEOLOGICAL SURVEY OF WESTERN AUSTRALIA

RECORD 2015/9 PLATE 1

INTERPRETED REGOLITH–LANDFORM GEOLOGY OF THE BALANGGARRA AREA, NORTH KIMBERLEY

December 2015